BioMed Research International

Addressing Peritoneal Dialysis: In vitro PD Models, in vivo Rodent PD Model, Clinical Biobanks, and Underutilization of PD

Guest Editors: Robert H. J. Beelen, Donald J. Fraser, Peter Rutherford, and Janusz Witowski

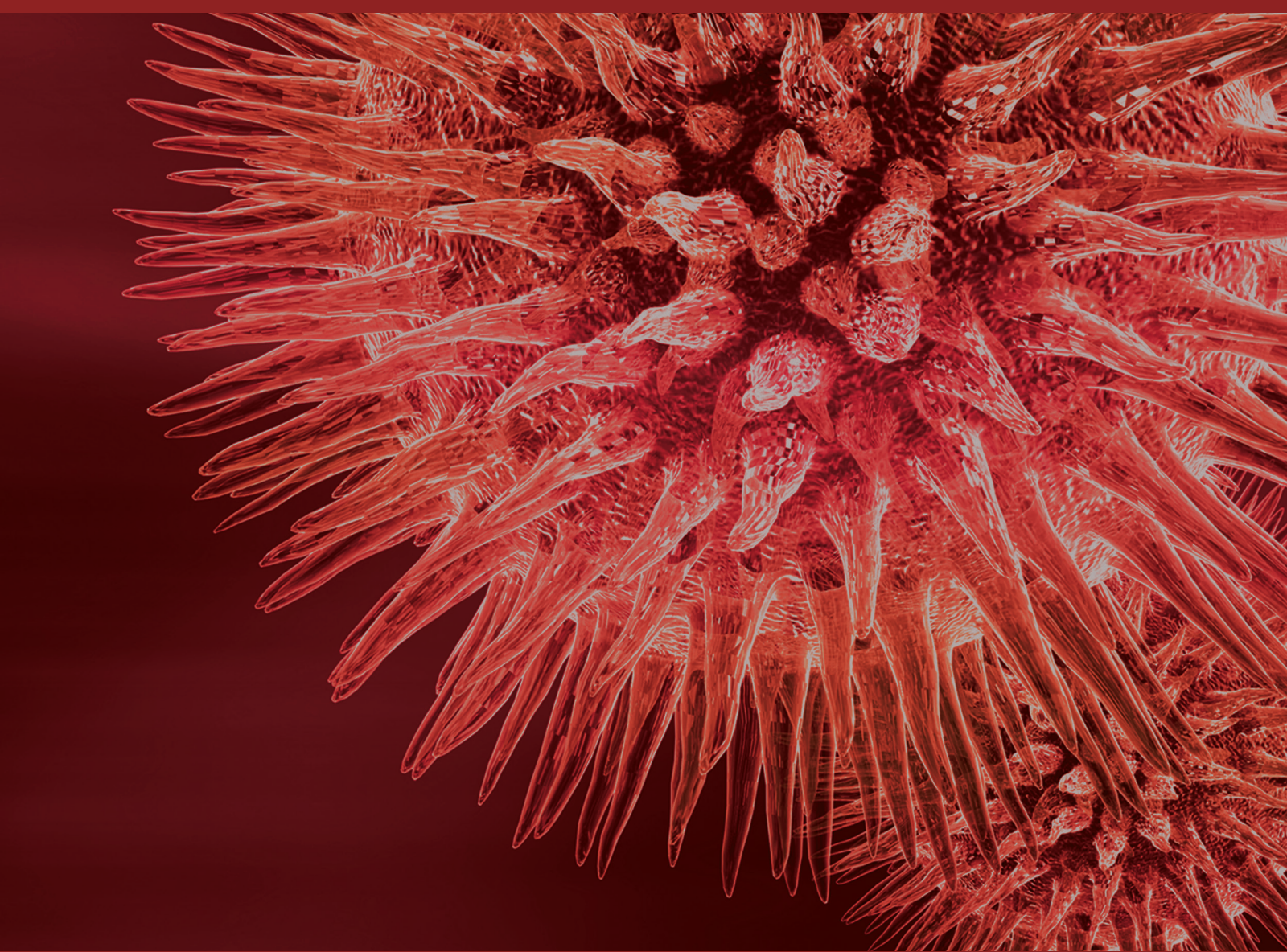

Addressing Peritoneal Dialysis: In vitro PD Models, in vivo Rodent PD Model, Clinical Biobanks, and Underutilization of PD

BioMed Research International

Addressing Peritoneal Dialysis: In vitro PD Models, in vivo Rodent PD Model, Clinical Biobanks, and Underutilization of PD

Guest Editors: Robert H. J. Beelen, Donald J. Fraser, Peter Rutherford, and Janusz Witowski

Contents

Hindawi Publishing Corporation
BioMed Research International
Volume 2016, Article ID 4964316, 2 pages
http://dx.doi.org/10.1155/2016/4964316

Editorial

Addressing Peritoneal Dialysis: In Vitro PD Models, In Vivo Rodent PD Model, Clinical Biobanks, and Underutilization of PD

Robert H. J. Beelen,[1] Donald J. Fraser,[2] Peter Rutherford,[3] and Janusz Witowski[4]

[1]*Department of Molecular Cell Biology and Immunology, VU University Medical Center, 1007 MB Amsterdam, Netherlands*
[2]*Cardiff University School of Medicine, Cardiff, UK*
[3]*Baxter World Trade, Lessines, Belgium, presently Quintiles, Reading, UK*
[4]*Department of Pathophysiology, Poznan University of Medical Science, Poznan, Poland*

Correspondence should be addressed to Robert H. J. Beelen; rhj.beelen@vumc.nl

Received 26 November 2015; Accepted 26 November 2015

Renal replacement therapy (RRT) is necessary for the survival of patients with end-stage renal disease (ESRD) both prior to kidney transplantation or in patients where kidney transplantation is not available. Peritoneal dialysis (PD) and hemodialysis (HD) are lifesaving RRTs for more than 2 million patients with ESRD worldwide [1]. As the incidence of chronic renal disease has doubled over the past decade, the number of patients with ESRD is expected to increase by 5–8% annually [2]. Although long-term morbidity and mortality are comparable between PD and HD, there is an early patient survival advantage for PD and a better quality of life [3]. Moreover PD is cost-effective as compared to hospital-based HD [4]. Nevertheless only one out of 10 patients is treated with PD, which suggests a general underutilization [5]. PD is a simple therapy in which PD fluid is exchanged several times a day; the major limitations are peritoneal membrane damage on the long-term and infection [6]. PD could be largely enhanced if one can identify diagnostic and therapeutic tools to improve PD outcome that promote function of the peritoneal membrane and prevent infectious complications [7]. European Training and Research in Peritoneal Dialysis (EuTRiPD) is an EU funded training programme, in which exactly these goals are targeted [8].

In this special issue of BMRI, we present a number of articles prepared in part (but also by other contributors) with a support from the EuTRiPD initiative. These are both original research papers and review papers that (i) analyze basic aspects of peritoneal cell biology using in vitro methods, (ii) mimic clinical situations in relevant PD models in rodents, and (iii) describe the outcomes of clinical studies using new biomarkers or new interventions.

In the following papers, firstly studies apply in vitro models to investigate the senescence-associated proteome in mesothelial cells, the effect of differently sterilized PD fluids on mesothelial stress responses, and the contribution of mesothelial-to-mesenchymal transition to peritoneal fibroblast expansion. Secondly with respect to papers in rodent PD models a new mouse uremic model is presented, the effect of rapamycin in a mouse model is shown, and moreover clear indications are described in protective effect of paricalcitol in a PD model and another PD-fibrosis-like model. Thirdly clinical material was used in studies showing the importance of, respectively, HA, microRNA, osmolarity of fluid, and tenascin-C levels reflecting peritoneal patient status. Finally underutilization of PD is discussed as originating from less education and referral pattern and moreover it is discussed that new biomarkers in PD could contribute significantly to making choices for the future as shown by EuTRiPD. The editors feel that all these papers give a good overview of the state of art in addressing all aspects of PD.

Robert H. J. Beelen
Donald J. Fraser
Peter Rutherford
Janusz Witowski

References

[1] A. K. Jain, P. Blake, P. Cordy, and A. X. Garg, "Global trends in rates of peritoneal dialysis," *Journal of the American Society of Nephrology*, vol. 23, no. 3, pp. 533–544, 2012.

[2] M. W. M. van de Luijtgaarden, K. J. Jager, M. Segelmark et al., "Trends in dialysis modality choice and related patient survival in the ERA-EDTA Registry over a 20-year period," *Nephrology Dialysis Transplantation*, Article ID gfv295, pp. 1–9, 2015.

[3] K. Chaudhary, H. Sangha, and R. Khanna, "Peritoneal dialysis first: rationale," *Clinical Journal of the American Society of Nephrology*, vol. 6, no. 2, pp. 447–456, 2011.

[4] G. Abraham, S. Varughese, M. Mathew, and M. Vijayan, "A review of acute and chronic peritoneal dialysis in developing countries," *Clinical Kidney Journal*, vol. 8, no. 3, pp. 310–317, 2015.

[5] J. Hingwala, J. Diamond, N. Tangri et al., "Underutilization of peritoneal dialysis: the role of the nephrologist's referral pattern," *Nephrology Dialysis Transplantation*, vol. 28, no. 3, pp. 732–740, 2013.

[6] R. Sinnakirouchenan and J. L. Holley, "Peritoneal dialysis versus hemodialysis: risks, benefits, and access issues," *Advances in Chronic Kidney Disease*, vol. 18, no. 6, pp. 428–432, 2011.

[7] M. N. Schilte, J. W. A. M. Celie, P. M. Ter Wee, R. H. J. Beelen, and J. van den Born, "Factors contributing to peritoneal tissue remodeling in peritoneal dialysis," *Peritoneal Dialysis International*, vol. 29, no. 6, pp. 605–617, 2009.

[8] T. L. Foster, E. Ferrantelli, T. V. W.-V. der Schaaf, and R. H. J. Beelen, "European training and research in peritoneal dialysis: scientific objectives, training, implementation and impact of the programme," *Journal of Renal Care*, vol. 40, no. 1, pp. 34–39, 2014.

Hindawi Publishing Corporation
BioMed Research International
Volume 2015, Article ID 241098, 9 pages
http://dx.doi.org/10.1155/2015/241098

Clinical Study

Effluent Tenascin-C Levels Reflect Peritoneal Deterioration in Peritoneal Dialysis: MAJOR IN PD Study

Ichiro Hirahara, Eiji Kusano, Toshimi Imai, Yoshiyuki Morishita, Makoto Inoue, Tetsu Akimoto, Osamu Saito, Shigeaki Muto, and Daisuke Nagata

Division of Nephrology, Department of Internal Medicine, Jichi Medical University, 3311-1 Yakushiji, Shimotsuke, Tochigi 329-0498, Japan

Correspondence should be addressed to Ichiro Hirahara; hirahara@rpf.jp

Received 22 May 2015; Revised 4 September 2015; Accepted 29 October 2015

Academic Editor: Robert Beelen

Peritoneal deterioration causing structural changes and functional decline is a major complication of peritoneal dialysis (PD). The aim of this study was to explore effluent biomarkers reflecting peritoneal deterioration. In an animal study, rats were intraperitoneally administered with PD fluids adding 20 mM methylglyoxal (MGO) or 20 mM formaldehyde (FA) every day for 21 days. In the MGO-treated rats, tenascin-C (TN-C) levels in the peritoneal effluents were remarkably high and a cluster of TN-C-positive mesothelial cells with epithelial-to-mesenchymal transition- (EMT-) like change excessively proliferated at the peritoneal surface, but not in the FA-treated rats. Effluent matrix metalloproteinase-2 (MMP-2) levels increased in both the MGO- and FA-treated rats. In a clinical study at 18 centers between 2006 and 2013, effluent TN-C and MMP-2 levels were quantified in 182 PD patients with end-stage renal disease. Peritoneal function was estimated using the peritoneal equilibration test (PET). From the PET results, the D/P Cr ratio was correlated with effluent levels of TN-C ($\rho = 0.57$, $p < 0.001$) and MMP-2 ($\rho = 0.73$, $p < 0.001$). We suggest that TN-C in the effluents may be a diagnostic marker for peritoneal deterioration with EMT-like change in mesothelial cells in PD.

1. Introduction

Peritoneal dialysis (PD) is a treatment for patients with severely reduced or absent renal function. Long-term PD results in peritoneal deterioration, causing structural changes and functional decline such as increased peritoneal solute transport; this leads to ultrafiltration failure of the peritoneal membrane. Peritoneal deterioration may result in the cessation of PD treatment; this complication leads to encapsulating peritoneal sclerosis (EPS) in patients with long-term history of PD for renal failure. EPS is associated with an extremely high mortality rate [1–4]. Safe and effective PD requires monitoring of peritoneal deterioration developing to EPS.

Functional decline of the peritoneum, such as increasing peritoneal transport rate, can be assessed with the peritoneal equilibration test (PET) [4–6]. The transport rate increases with peritoneal deterioration and a higher transporter membrane state is a factor contributing to the occurrence of EPS in patients who have experienced PD treatment [5]. Structural changes of the peritoneum can be examined by biopsy of peritoneal tissue; however, because it is invasive, this method is inappropriate for continuous testing. Only exceptionally skilled clinical pathologists perform cytodiagnosis of mesothelial cells in peritoneal effluents [4]. Easy and noninvasive methods are required to evaluate peritoneal structural changes for diagnosis of peritoneal deterioration.

Some effluent biomarkers, such as matrix metalloproteinase-2 (MMP-2), interleukin-6 (IL-6), hyaluronan, and cancer antigen-125 (CA125), are measured to estimate peritoneal deterioration or progression to EPS during PD [2, 4, 7–11]. Kaku et al. demonstrated that the correlation coefficient between the peritoneal solute transport rate estimated by the PET and the effluent levels of MMP-2 was higher than those of IL-6, hyaluronate, and CA125 [11]. We also reported that effluent MMP-2 levels were high in the patients with peritoneal deterioration and strongly correlated with the results of the PET [8]. MMP-2 degrades components of the extracellular matrix, such as fibronectin and type IV collagen,

which comprise the basement membrane. MMP-2 is produced by mesenchymal cells, macrophages, and endothelial cells in the peritoneum; it plays important roles in angiogenesis, epithelial-to-mesenchymal transition (EMT) of mesothelial cells, and migration of cells that promote inflammation or fibroplasia [2, 7, 9–15]. Because they reflect peritoneal deterioration with structural changes and functional decline, effluent MMP-2 levels may be valuable in predicting the occurrence of EPS. Thus, MMP-2 may be the best available indicator of peritoneal deterioration.

Morphologically, mesothelial cells change from polygonal cobblestone-like appearance to a spindle-shaped form in PD [16]. Aguilera et al. reported that the EMT of mesothelial cells may be involved in triggering peritoneal injury with fibrosis in PD patients [17]. In addition, high solute transport of peritoneal membrane is associated with EMT of mesothelial cells [18]. These reports suggest that monitoring EMT of mesothelial cells may enable early diagnosis of peritoneal deterioration.

Tenascin-C (TN-C) is an extracellular matrix glycoprotein formed by hexamers of approximately 300 kDa subunits. Although expression of TN-C is rare in normal adult tissues, high levels are observed in pathological states featuring tissue remodeling, such as inflammation, wound healing, and cancer progression. In particular, TN-C is expected as a biomarker for myocarditis or aortic aneurism [19]. In addition, TN-C induces EMT-like change in cancer cells [20, 21]. As mentioned above, EMT-like change in mesothelial cells is induced at early stage of peritoneal deterioration. TN-C may have potential as an indicator of tissue injury; however, to the best of our knowledge, there are no reports concerning TN-C in PD.

This study aimed to investigate simple and noninvasive methods, to evaluate indicators of peritoneal deterioration used to diagnose early peritoneal deterioration with structural changes and functional decline, such as high solute transport of the peritoneal membrane. Therefore, we examined whether TN-C and MMP-2 in the peritoneal effluents have potential as indicators of peritoneal deterioration.

2. Methods and Patients

2.1. Preparation of Animal Models of Peritoneal Injury. Animals used in this study were 5-6-week-old male Sprague-Dawley (SD) rats weighing approximately 200–250 g (Charles River Japan, Kanagawa, Japan). They were housed in cages in an air-conditioned room, which was maintained at a constant temperature of 23 ± 2°C and relative humidity of 50 ± 10%. The animals were kept under a 12-hour light/dark cycle and had free access to sufficient pellet food and water.

The PD fluids were prepared by adding 20 mM methylglyoxal (MGO) or 20 mM formaldehyde (FA) to a solution (2.5% glucose, 100 mM NaCl, 35 mM sodium lactate, 2 mM $CaCl_2$, and 0.7 mM $MgCl_2$, pH 5.0), which were then daily sterilized by filtration just before injection. Rats were divided into three groups ($n = 6$/group) and intraperitoneally administered with the following solutions for 21 days: group 1, 100 mL/kg PD fluid without adding MGO or FA; group 2, 100 mL/kg PD fluid containing 20 mM MGO; group 3, 100 mL/kg PD fluid containing 20 mM FA. MGO and FA concentrations were determined based on previous reports [12–14]. If any solution remained in the peritoneal cavity, it was drained prior to injection. On day 22 after the start of the experiment, 50 mL/kg of PD fluid containing 2.5% glucose (Midperiq L250, Terumo Co., Tokyo, Japan) was intraperitoneally injected and the drained dialysate was collected 90 minutes later to analyze TN-C and MMP-2 in the effluents. The parietal peritoneum was also sampled for histological analysis.

Adequate attention was paid to maintaining a hygienic environment and to preventing infectious peritonitis in the animals. Furthermore, a sterility test was performed using the dialysate drained on day 22 to check for the presence of aerobic bacteria, anaerobic bacteria, and fungi. All rats were confirmed to be uninfected.

The Institutional Animal Experiment Committee of Jichi Medical University approved the protocol of this animal study. The animal experiments were conducted in accordance with the Institutional Regulations for Animal Experiments and Fundamental Guidelines for the Proper Conduct of Animal Experiments and Related Activities in Academic Research Institutions under the jurisdiction of Japan's Ministry of Education, Culture, Sports, Science and Technology.

2.2. Immunohistological Analysis of Peritoneum in Animal Study. The parietal peritoneum was sampled from the corresponding sites of each rat and fixed with 10% FA/0.1 M phosphate buffer (pH 7.2). The peritoneal specimens were embedded in paraffin to prepare tissue sections with a thickness of 2-3 μm. To analyze the thickness of the peritoneum, the sections were sliced perpendicular to the peritoneal surface. The peritoneal tissue sections prepared from a paraffin block were dewaxed with xylene. The sections were treated with 0.4% pepsin/0.01 N HCl for 10 minutes at 37°C, followed by treatment with 0.3% H_2O_2/methanol for 30 minutes at room temperature. After blocking with 1% bovine serum albumin for 20 minutes at room temperature, these sections were treated overnight at 7°C with a monoclonal antibody against TN-C (Immuno-Biological Laboratories Co., Ltd., Gunma, Japan) at a dilution of 1 : 500, followed by staining with biotinylated anti-mouse IgG (Dako Cytomation Denmark A/S, Glostrup, Denmark) for 30 minutes at room temperature. The sections were treated with peroxidase-labeled streptavidin (Dako) at a dilution of 1 : 700 for 30 minutes at room temperature and then peroxidase activity was detected with 3,3′-diaminobenzidine tetrahydrochloride (Sigma, St. Louis, MO, USA). Sections were also counterstained with Meyer's hematoxylin. Negative staining was confirmed by incubation without primary antibody for immunohistochemical staining.

2.3. Analysis of the Drained Dialysate in Animal Study. To explore markers for peritoneal deterioration, TN-C levels in the drained dialysate were quantitatively determined by enzyme-linked immunosorbent assay (ELISA) (Immuno-Biological Laboratories Co., Ltd.). MMP-2 in the dialysate was analyzed by gelatin zymography [7, 12, 13]. In brief, after electrophoresis under nonreducing conditions on 8%

polyacrylamide gels containing 1 mg/mL gelatin, the gels were treated with 2.5% Triton-100/0.1 M NaCl/50 mM Tris-HCl (pH 7.5) for 2 hours and incubated for 18 hours at 37°C in 50 mM Tris-HCl (pH 7.5)/10 mM $CaCl_2$. The gels were then stained with 0.1% Coomassie Brilliant Blue. MMP-2 was detected as unstained 64 kDa proteolytic bands in the stained gels. The relative concentrations of MMP-2 in the dialysate were quantified by scanning proteolytic bands on the zymograms using the ImageJ quantitation software program (National Institutes of Health, Bethesda, MD, USA).

2.4. Patients in Multicenter Clinical Study. PD patients with end-stage renal disease at 18 centers in Japan were analyzed during the period from January 2007 to March 2013. Patients treated with PD for less than 3 months were excluded from the present study, as were those with bacterial peritonitis at the time of the analysis or in the 4 preceding weeks.

Clinical analysis was conducted after receiving approval from the Ethics Committee of Jichi Medical University, and informed consent was obtained from each patient. TN-C in the serum was analyzed in 20 patients from whom informed consent for analysis of the serum had been obtained.

This study was registered as the MAJOR IN PD study (Multicenter Analysis in Japan, ORiginal INdicator of Peritoneal Deterioration) in the University Hospital Medical Information Network-Clinical Trials Registry (UMIN-CTR), which was approved by the International Committee of Medical Journal Editors (number UMIN000010572).

2.5. Peritoneal Equilibration Test (PET) for Human. The peritoneal solute transport rate was assessed by the PET [4, 6]. Intra-abdominal fluid was drained and PD fluid containing 2.27–2.5% glucose was intraperitoneally injected. Creatinine (Cr) level of the drained dialysate obtained 4 hours after injection (D) was divided by that of the patient's blood (P) to calculate the D/P Cr ratio. The glucose level of the dialysate obtained 4 hours after injection (D) was divided by that obtained immediately after injection (D0) to calculate the D/D0 glucose ratio. The drained dialysate was aliquoted and stored at −80°C. It was confirmed that TN-C and MMP-2 were stable at −80°C and were not decomposed by several repeated freeze-thaw cycles.

2.6. Analysis of Biomarker Levels in the Drained Dialysate in Multicenter Clinical Study. The concentrations of TN-C and MMP-2 in the drained dialysate obtained at the PET were measured by EIA (TN-C: Immuno-Biological Laboratories Co., Ltd.; MMP-2: GE Healthcare, Piscataway, NJ, USA).

Serum TN-C levels were analyzed and regression lines were calculated based on the power relationship between the molecular weights of β2-microglobulin (MW: 11,800 Da), MMP-3 (MW: 59,000 Da), albumin (MW: 69,000 Da), transferrin (MW: 85,000 Da), and IgG (MW: 150,000 Da) and their measured dialysate/serum (D/S) ratios when plotted on a double-logarithmic scale [8–10]. These proteins were transported from the circulation to the peritoneal cavity by the osmotic pressure of the PD fluid. By interpolation of the molecular weights of TN-C (MW: 1,800,000 Da) in the regression equation, the expected D/S ratios were calculated, assuming that their concentration in the drained dialysate would be determined by transport only from the circulation.

2.7. Statistical Analysis. Statistical analyses were performed using R statistical software version 2.15.1 (R Foundation for Statistical Computing). Receiver operating characteristic (ROC) curve analyses were performed to evaluate the diagnostic accuracy of MMP-2 and TN-C. Comparisons between groups were performed by Wilcoxon's test. Relationships between clinical variables and effluent biomarker levels were analyzed by Spearman's correlation coefficient test. Clinical data are expressed as medians with the spread from the 25th to 75th percentiles. In the animal experiment, statistical comparisons were conducted by analysis of variance (ANOVA). Animal experimental data are presented as the mean ± SD. A p value of less than 0.05 was considered to be statistically significant.

3. Results

3.1. Animal Experiments. In rats receiving PD fluids containing 20 mM MGO or 20 mM FA, peritoneal thickening significantly increased (Figure 1). These results confirmed that both the MGO- and FA-treated rats had induced peritoneal deterioration with structural changes.

In control rats, a monolayer of mesothelial cells was observed on the surface of the thin peritoneum (Figure 1(a)). In the MGO-treated rats, TN-C was abundant at the surface of the peritoneum where cells excessively proliferated (Figure 1(b)). In the FA-treated rats, there was slight deposition of TN-C at the surface of the peritoneum where cells were lost (Figure 1(c)).

The effluent TN-C levels of the MGO- or FA-treated rats increased approximately 3000 times and 300 times, respectively (Figure 2(a)). The effluent MMP-2 levels of the MGO- and FA-treated rats increased 5 and 3.7 times, respectively (Figure 2(b)).

3.2. Relationships between the Peritoneal Solute Transport Rate and TN-C or MMP-2 Levels in the Drained Dialysate Prepared from Patients. A total of 182 PD patients at 18 centers in Japan were analyzed. Patient characteristics are summarized in Table 1. TN-C and MMP-2 levels in the drained dialysate are shown as median (interquartile range) of 7.1 ng/mL (4.0–12.4 ng/mL) and 150 ng/mL (103–221 ng/mL), respectively. The levels of TN-C and MMP-2 in the drained dialysate highly correlated with the peritoneal solute transport rate determined by the PET (Table 2). The correlation coefficient between effluent TN-C and MMP-2 levels ($\rho = 0.75$, $p < 0.001$) was higher than that between these biomarker levels and the results of the PET (Figure 3 and Table 2). These biomarker levels significantly correlated with the numbers of peritonitis episodes, but not PD duration (Figure 4 and Table 3). The relationships between the effluent biomarker levels and the characteristics of the patients are shown in Table 3.

The proportion of high-PET-category patients in the present study was 8% of PD patients. TN-C and MMP-2 levels in the drained dialysate from high-PET-category

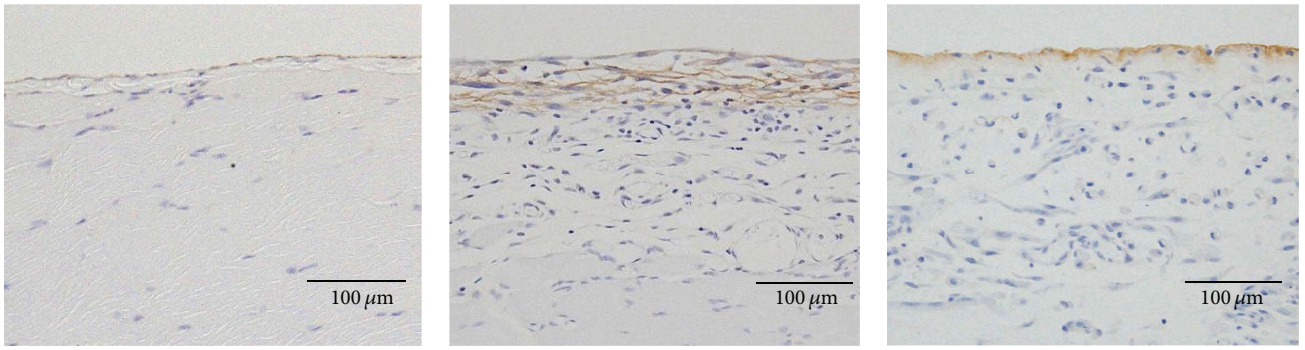

Figure 1: Immunohistopathological findings of peritoneum of the MGO- or FA-treated rats. The parietal peritoneum was analyzed histologically by immune staining with anti-TN-C antibody. (a) Control rat. (b) MGO-treated rat. (c) FA-treated rat. ×200.

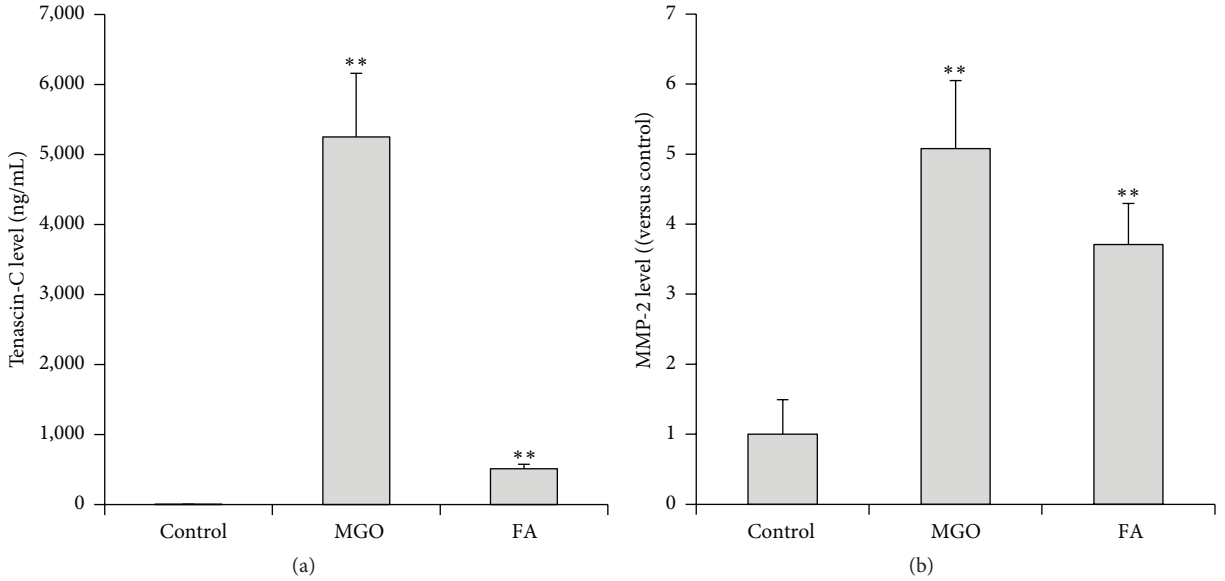

Figure 2: Effluent levels of TN-C and MMP-2 in the MGO- or FA-treated rats. (a) TN-C levels in the drained dialysate. (b) MMP-2 levels in the drained dialysate. Each column represents the mean ± SD of 6 rats. $^{**}p < 0.01$ compared with control.

patients were significantly higher than those from non-high-PET-category patients (Figure 5). To assess the ability of the biomarkers to diagnose the high category of the PET, ROC curves were constructed. On the ROC curves, the cut-off points of TN-C and MMP-2 for the high category of the PET were 5.7 ng/mL and 213 ng/mL, respectively (Table 4). The areas under the ROC curve (AUC) for effluent TN-C and MMP-2 levels against the high category of the PET were 0.71 and 0.91, respectively (Table 4).

Serum TN-C levels were analyzed in 20 patients (median age: 58 years, median PD duration: 15 months, 75% males, 20% with diabetes). The levels of TN-C in the serum were higher than those in the drained dialysate. The regression line was calculated based on least squares regression analysis between the measured D/S ratios of the serum proteins, such as beta 2-microglobulin, MMP-3, albumin, transferrin, and IgG, and their molecular weights. The measured D/S ratio of TN-C was also plotted in relation to the molecular weight. The slope of the regression line represented the size selectivity of the peritoneal membrane; however, the measured D/S ratio of TN-C considerably exceeded the regression line ($p < 0.01$). Regression lines for each individual patient were also calculated. Based on each regression line, the expected D/S ratios of TN-C were predicted assuming that their levels in the dialysate would be determined by transport only from the circulation. In all patients, the measured D/S ratios of TN-C considerably exceeded the expected D/S ratios calculated based on the regression line of each individual patient (data not shown).

4. Discussion

It is important to monitor peritoneal deterioration with structure changes and functional decline, such as an increase of the peritoneal solute transport rate. Functional decline of the peritoneum can be assessed with the PET, but there

Table 1: Characteristics of patients.

Sex (male/female)	104/78 (57% male)
Etiology (nondiabetes/diabetes)	147/35 (19% diabetes)
Age (years)	58 years (47–66 years)
PD duration (months)	33 months (13–59 months)
Peritonitis episode (times)	0 times (0-1 time)
D/P Cr	0.65 (0.59–0.71)
D/D0 glucose	0.40 (0.34–0.44)
Effluent tenascin-C level	7.1 ng/mL (4.0–12.4 ng/mL)
Effluent matrix metalloproteinase-2 level	150 ng/mL (103–221 ng/mL)

Data except sex and etiology of renal failure are expressed as medians with interquartile ranges.

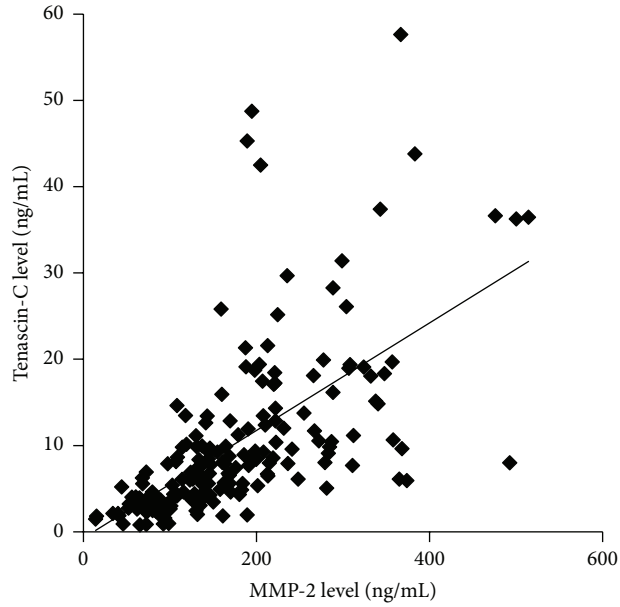

Figure 3: The relationship between TN-C and MMP-2 levels in the drained dialysate.

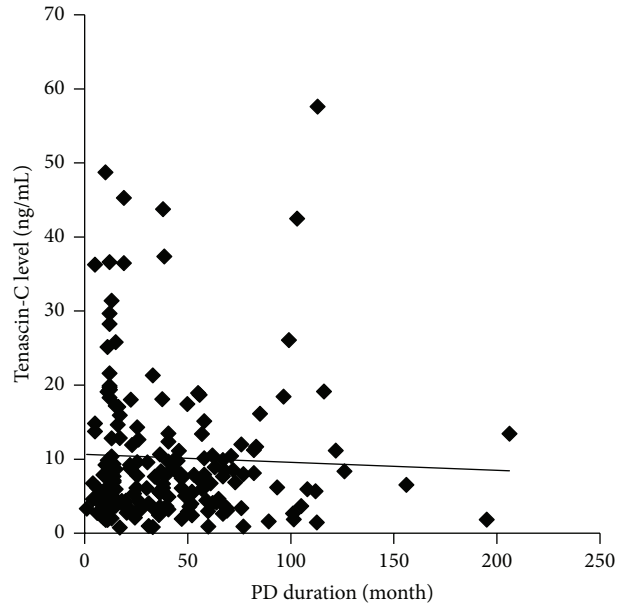

Figure 4: The relationship between PD duration and TN-C levels in the drained dialysate.

Table 2: Spearman's correlation coefficients between effluent biomarker levels and results of the PET.

	Tenascin-C	Matrix metalloproteinase-2
D/P Cr	$\rho = 0.57$	$\rho = 0.73$
	$p < 0.001$	$p < 0.001$
D/D0 glucose	$\rho = -0.43$	$\rho = -0.63$
	$p < 0.001$	$p < 0.001$

ρ values indicate relationships between effluent biomarker levels and results of the PET by Spearman's correlation coefficient.

is no current method to evaluate noninvasively structure changes of the peritoneum. Peritoneal deterioration, whose mechanism is not well known, may develop through multiple factors, such as infectious peritonitis and continuous exposure to unphysiologic PD fluid with low pH, high osmolarity, high concentration of glucose, and glucose degradation products (GDPs), such as MGO, glyoxal, FA, 3-deoxyglucosone (3-DG), and 3,4-dideoxyglucosone-3-ene (3,4-DGE) [2, 3, 12]. Therefore, we explored the biomarkers for peritoneal deterioration using the GDPs-treated rats [12–14]. In the present study, the PD fluids containing 20 mM MGO or FA were injected to rat. On the other hand, the concentrations of MGO and FA are 2 to 33 μM and 6 to 11 μM, respectively, in conventional commercial PD fluids [22–24]. The MGO and FA concentrations administered to rats were 1,000–10,000 times higher than those found in commercial PD fluids. We previously confirmed the permitted daily exposure for GDPs concentrations administered to rats in the recommended guideline by the International Conference on Harmonisation (Guideline for Residual Solvents Q3C, 1997) [12, 13]. Moreover, conventional commercial PD fluids contain various toxic GDPs, such as glyoxal, 3-DG, and 3,4-DGE, in addition to MGO and FA. Oh et al. showed in a cell culture experiment with human peritoneal mesothelial cells that 15 μM MGO changed the expression of EMT markers, E-cadherin and α-smooth muscle actin, and in rat animal models that 27.3 μM MGO in combination with other GDPs, such as glyoxal, FA, and 3-DG, induced EMT-like change in mesothelial cells [25]. These findings suggest that the morphological

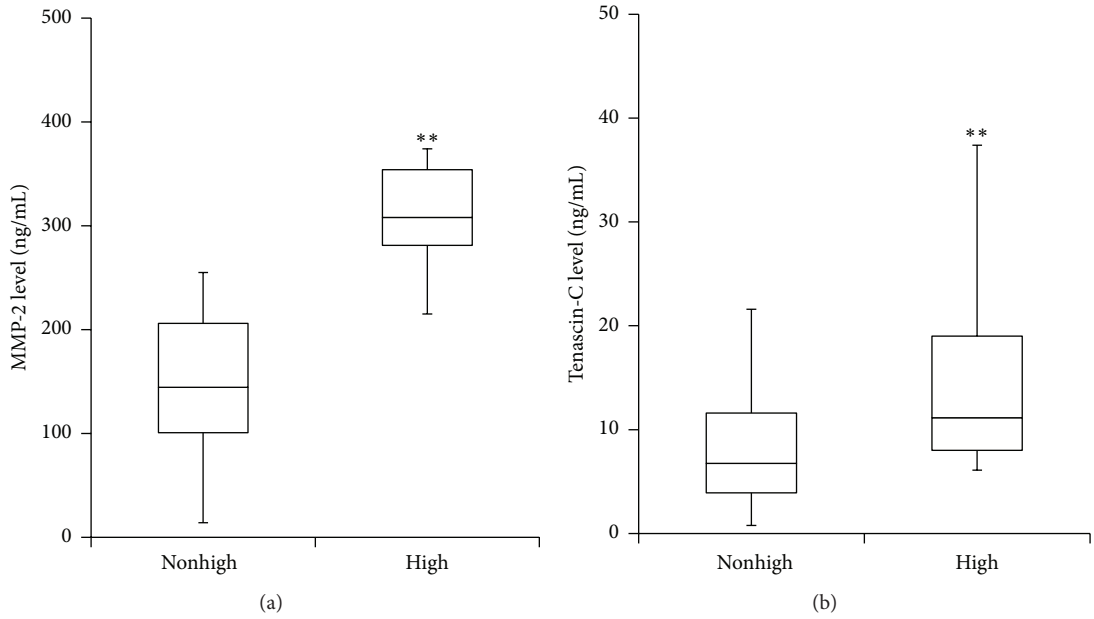

Figure 5: The effluent biomarker levels of patients in the high category of the PET. (a) Effluent TN-C levels. (b) Effluent MMP-2 levels. Data are shown as medians with the spread from 25th to 75th percentile (box). $^{**}p < 0.01$ compared with the nonhigh category group.

Table 3: The correlation coefficients between patient characteristics and effluent biomarker levels.

	Biomarker levels in the peritoneal effluents	
	Tenascin-C	Matrix metalloproteinase-2
Sex (male/female)	$p = 0.62$	$p = 0.50$
Etiology (nondiabetes/diabetes)	$p = 0.12$	$p = 0.30$
Age (years)	$\rho = 0.048$, $p = 0.51$	$\rho = 0.026$, $p = 0.73$
PD duration (months)	$\rho = -0.070$, $p = 0.34$	$\rho = 0.017$, $p = 0.82$
Peritonitis episode (times)	$\rho = 0.15$, $p < 0.05$	$\rho = 0.21$, $p < 0.01$

ρ values: Spearman's correlation coefficient.

Table 4: Test performance of effluent biomarker cut-off levels to diagnose the high category of the PET.

Biomarker	Cut-off level	Sensitivity	Specificity	False negative	AUC
Tenascin-C	5.7 ng/mL	100%	42%	0%	0.71
	6.0 ng/mL	92%	43%	1.3%	
	6.5 ng/mL	85%	48%	3.6%	
Matrix metalloproteinase-2	213 ng/mL	93%	79%	0.8%	0.91
	250 ng/mL	86%	87%	1.4%	
	270 ng/mL	79%	88%	2.0%	

AUC: area under curve.

changes induced in the present animal experiment can be extrapolated to clinical settings.

In the present and our previous animal studies, MGO and FA resulted in peritoneal deterioration with structural changes and functional decline [12–14]. In the MGO-treated rats, effluent TN-C levels were extremely high and, at the surface of the peritoneum where collagen was scarce, TN-C-positive mesenchymal-like cells markedly proliferated. We previously reported the possibility that these cells were transformed from mesothelial cells, such as by EMT-like change via TGF-β1 [13]. Liu et al. showed that miR-30b is involved in MGO-induced EMT of peritoneal mesothelial cells in rats; miR-30b directly inhibited bone morphogenetic protein-7 (BMP-7) by binding to its 3′-untranslated region, causing unavailability of BMP-7 that might be the antagonist of TGF-β1-induced EMT [26]. From these reports, MGO may induce EMT-like change in mesothelial cells via TGF-β1. Che et al. reported that MGO and 3-DG, reactive dicarbonyl metabolites in the glyoxalase system and glycation reaction, respectively, selectively induced heparin-binding epidermal growth

factor-like growth factor (HB-EGF) in a dose- and time-dependent manner by increasing the intracellular peroxide levels in rat aortic smooth muscle cells (SMC) [27]. However, platelet-derived growth factor, another known growth factor of SMC, was not induced by both dicarbonyls. In addition, the signal transduction by MGO and 3-DG was not mediated by protein kinase C. Stoll et al. demonstrated that expression of HB-EGF increased keratinocyte migration and invasiveness in monolayer culture [28]. Coincident with these changes, HB-EGF significantly decreased several epithelial markers including keratins 1, 5, 10, and 14 while increasing expression of markers of cellular motility including SNAI1, ZEB1, COX-2, and MMP-1. HB-EGF induced expression of the mesenchymal protein vimentin and decreased expression of E-cadherin, as well as nuclear translocation of β-catenin. They also showed that HB-EGF was strongly induced in regenerating the epidermis after partial-thickness wounding of human skin [28]. Taken together, their data suggested that expression of HB-EGF in human keratinocytes triggered a migratory and invasive phenotype with many features of EMT. From these reports, MGO may induce EMT-like change in mesothelial cells via HB-EGF.

MGO is a potent promoter of the production of advanced glycation end-products (AGEs). In a previous study using rats, the administration of 20 mM MGO resulted in the accumulation of AGEs, such as imidazolone and carboxyethyl lysine, in the peritoneum [29]. AGEs and MGO induced the expression of the receptor for AGE (RAGE), and then AGE-RAGE interaction induced EMT-like change in mesothelial cells via upregulation of expression of transforming growth factor-β (TGF-β) and vascular endothelial growth factor (VEGF) [24, 30, 31]. We have previously showed that, in 20 mM MGO-treated rats, AGE was detected in mesothelial cells with EMT-like change at the surface of the peritoneum and the gene expressions of RAGE, TGF-β, and VEGF were enhanced in the peritoneum [12, 13]. Thus, EMT-like change in mesothelial cells was induced in response to signals from RAGE binding with AGE. These reports suggest that MGO induces EMT-like change in mesothelial cells not only directly but also indirectly via formation of AGEs.

In the FA-treated rats, peritoneal injury with cellular infiltration was induced; however, cells were lost at the surface of the peritoneum. The peritoneum was fibrous thickening with dense collagen fibers [12–14]. The pathological picture of the peritoneum of the FA-treated rats resembles that of the chlorhexidine gluconate-treated rats [13, 14]. These peritoneal changes may be generally induced by toxic agents.

Effluent TN-C levels in the FA-treated rats increased but were only approximately one-tenth of the levels of the MGO-treated rats. In contrast, effluent levels of MMP-2, a biomarker of peritoneal injury, were extremely high in both MGO- and FA-treated rats. From these results, the effluent TN-C levels reflected not only peritoneal deterioration but also especially EMT-like change in mesothelial cells in the animal study.

In the present clinical study, the measured D/S ratio of TN-C was significantly higher than the expected ratio if TN-C in the effluent was transported only from the circulation. The difference between the measured D/S ratio and the expected ratio may be attributable to the local production of TN-C in the peritoneal tissue rather than the transport of TN-C from the circulation [8–10]. In addition, in the present animal study, mesothelial cells with EMT-like change that proliferated at the surface of the peritoneum showed positive signals on immunohistochemical analysis using the anti-TN-C antibody. Most TN-C in the drained dialysate may be produced from these cells in the peritoneum and effluent TN-C levels may reflect EMT-like change in mesothelial cells. From these results, effluent TN-C could be an effective diagnostic indicator of peritoneal deterioration with structural changes, particularly of mesothelial cells with EMT-like change. To confirm this hypothesis, in a clinical study we should examine the correlation between the effluent TN-C levels and EMT-like change in mesothelial cells by cytopathological analysis using biopsy of peritoneum. However, this would have been difficult to conduct in the present study because of invasive sampling.

In the present multicenter clinical study, the peritoneal transport rate estimated by the PET closely correlated with effluent TN-C levels; however, the correlation coefficient of the TN-C levels was lower than that with the MMP-2 levels. Effluent MMP-2 levels were able to predict, with high sensitivity and specificity, the high category of the PET, which is a risk factor for EPS [5]. In our previous clinical studies, effluent MMP-2 levels were high in patients with peritoneal injury [7]. In many animal studies, effluent MMP-2 levels increased in various peritoneal injury animal models with or without EMT-like change in mesothelial cells [9, 12, 13, 25]. We suggest that MMP-2 should serve as a superior indicator of general peritoneal deterioration.

In the present clinical study, the correlation coefficient between the effluent levels of TN-C and MMP-2 was high. MMP-2 and the degradation of TN-C are associated with tumor recurrence in early-stage non-small cell lung cancer [32]. TN-C deposition into the extracellular matrix requires the participation of MMP-2 and the resulting deposited TN-C promotes pancreatic cancer progression [33]. In peritoneal deterioration, TN-C may promote tissue injury in concert with MMP-2.

Effluent TN-C levels correlated with the peritoneal solute transport rate, but not PD duration in the present cross-sectional study. Confirmation that the change in effluent TN-C levels reflects increased peritoneal solute transport or EMT-like change in mesothelial cells is necessary to reach the conclusion that TN-C is a useful biomarker for early-stage peritoneal deterioration. In our longitudinal analysis, peritoneal solute transport did not develop significantly faster during the period of the present study. Further longitudinal analysis is needed.

5. Conclusion

Effluent TN-C levels correlated with the peritoneal solute transport rate. Most TN-C in the drained dialysate is thought to be produced by mesothelial cell-derived mesenchymal cells at the surface of the peritoneum. Therefore, effluent TN-C has a possibility of biomarker for EMT-like change in mesothelial cells in PD. Because EMT-like change in mesothelial cells is thought to be a trigger of peritoneal injury, TN-C may be

useful as an indicator for early-stage peritoneal deterioration, whereas effluent MMP-2 levels reflect general peritoneal deterioration. To test this hypothesis, further longitudinal studies are necessary to examine the change in effluent TN-C levels during the progression of peritoneal deterioration with increased peritoneal solute transport.

Disclosure

Part of this study was presented at the 18th annual meeting of the Japanese Society for Peritoneal Dialysis held at Osaka, Japan (September 2013).

Conflict of Interests

Ichirou Hirahara is affiliated with Terumo Core Technology Center (Kanagawa, Japan).

Acknowledgments

The collaborators in the multicenter clinical study were as follows: Fumihiko Hatafuku (Department of Urology, Onoda Hospital), Hideki Takizawa (Department of Nephrology, Teine Keijinkai Hospital), Makoto Nishina (Metabolism, Department of Internal Medicine, Tokai University, School of Medicine), Masanobu Horie (Department of Urology, Daiyukaidaiichi Hospital), Morihiro Kondou (Department of Nephrology, Otowa Hospital), Naomi Yoshimune (Department of Internal Medicine, Kinashi Obayashi Hospital), Noriaki Yorioka (Department of Advanced Nephrology, Graduate School of Biomedical Sciences, Hiroshima University), Ryoichi Miyazaki (Department of Internal Medicine, Fujita Memorial Hospital), Ryouji Wakamatsu (Nishikatakai Clinic), Sukenari Koyabu (Department of Internal Medicine, Owase General Hospital), Tadashi Yamamoto (Kidney Center, Shirasagi Hospital), Takeyuki Hiramatsu (Department of Internal Medicine, Aihoku Hospital), Tetsurou Yanase (Dr. Yanase Internal Medicine Office), Tohru Mizumasa (Department of Nephrology, Fukuoka Red Cross Hospital), Tomoyoshi Kimura (Department of Nephrology, Sendai Social Insurance Hospital), Toyonori Saiki (Department of Nephrology, Saiki Jin Clinic), and Yumiko Ikeda (Department of Nephrology, Yokohama Minami Kyousai Hospital). The authors would like to thank them for their help with the preparation of clinical samples and valuable discussions. This study was supported by Terumo Core Technology Center (Kanagawa, Japan). The authors would like to thank Ms. Yuka Shouji (Terumo Core Technology Center) for her assistance with the preparation of pathological tissue, Dr. Taizo Iwasaki (Terumo Core Technology Center) for his help with statistical analysis, and Professor Toshimichi Yoshida (Departments of Pathology and Matrix Biology, Mie University, Mie, Japan) for valuable discussions.

References

[1] V. C. Gandhi, H. M. Humayun, T. S. Ing et al., "Sclerotic thickening of the peritoneal membrane in maintenance peritoneal dialysis patients," *Archives of Internal Medicine*, vol. 140, no. 9, pp. 1201–1203, 1980.

[2] D. W. Schmidt and M. F. Flessner, "Pathogenesis and treatment of encapsulating peritoneal sclerosis: basic and translational research," *Peritoneal Dialysis International*, vol. 28, supplement 5, pp. S10–S15, 2008.

[3] Y. Kawaguchi, A. Saito, H. Kawanishi et al., "Recommendations on the management of encapsulating peritoneal sclerosis in Japan, 2005: diagnosis, predictive markers, treatment, and preventive measures," *Peritoneal Dialysis International*, vol. 25, supplement 4, pp. S83–S95, 2005.

[4] Working Group Committee for the Preparation of Guidelines for Peritoneal Dialysis, "Japanese Society for Dialysis Therapy. 2009 Japanese society for dialysis therapy guidelines for peritoneal dialysis," *Therapeutic Apheresis Dialysis*, vol. 14, no. 6, pp. 489–504, 2010.

[5] R. Yamamoto, Y. Otsuka, M. Nakayama et al., "Risk factors for encapsulating peritoneal sclerosis in patients who have experienced peritoneal dialysis treatment," *Clinical & Experimental Nephrology*, vol. 9, no. 2, pp. 148–152, 2005.

[6] Z. J. Twardowski, K. D. Nolph, R. Khanna et al., "Peritoneal equilibration test," *Peritoneal Dialysis Bulletin*, vol. 7, no. 3, pp. 138–147, 1987.

[7] I. Hirahara, M. Inoue, K. Okuda, Y. Ando, S. Muto, and E. Kusano, "The potential of matrix metalloproteinase-2 as a marker of peritoneal injury, increased solute transport, or progression to encapsulating peritoneal sclerosis during peritoneal dialysis—a multicentre study in Japan," *Nephrology Dialysis Transplantation*, vol. 22, no. 2, pp. 560–567, 2007.

[8] I. Hirahara, M. Inoue, T. Umino, O. Saito, S. Muto, and E. Kusano, "Matrix metalloproteinase levels in the drained dialysate reflect the peritoneal solute transport rate: a multicentre study in Japan," *Nephrology Dialysis Transplantation*, vol. 26, no. 5, pp. 1695–1701, 2011.

[9] D. L. Barreto, A. M. Coester, D. G. Struijk, and R. T. Krediet, "Can effluent matrix metalloproteinase 2 and plasminogen activator inhibitor 1 be used as biomarkers of peritoneal membrane alterations in peritoneal dialysis patients?" *Peritoneal Dialysis International*, vol. 33, no. 5, pp. 529–537, 2013.

[10] M. M. Zweers, D. R. de Waart, W. Smit, D. G. Struijk, and R. T. Krediet, "Growth factors VEGF and TGF-β1 in peritoneal dialysis," *The Journal of Laboratory and Clinical Medicine*, vol. 134, no. 2, pp. 124–132, 1999.

[11] Y. Kaku, K. Nohara, Y. Tsutsumi et al., "The relationship among the markers of peritoneal function such as PET, MMP-2, IL-6 etc, in pediatric and adolescent PD patients," *Jin To Touseki*, vol. 57, supplement, pp. 296–298, 2004.

[12] I. Hirahara, E. Kusano, S. Yanagiba et al., "Peritoneal injury by methylglyoxal in peritoneal dialysis," *Peritoneal Dialysis International*, vol. 26, no. 3, pp. 380–392, 2006.

[13] I. Hirahara, Y. Ishibashi, S. Kaname, E. Kusano, and T. Fujita, "Methylglyoxal induces peritoneal thickening by mesenchymal-like mesothelial cells in rats," *Nephrology Dialysis Transplantation*, vol. 24, no. 2, pp. 437–447, 2009.

[14] I. Hirahara, H. Sato, T. Imai et al., "Methylglyoxal induced basophilic spindle cells with podoplanin at the surface of peritoneum in rat peritoneal dialysis model," *BioMed Research International*, vol. 2015, Article ID 289751, 7 pages, 2015.

[15] S. Osada, C. Hamada, T. Shimaoka, K. Kaneko, S. Horikoshi, and Y. Tomino, "Alterations in proteoglycan components and histopathology of the peritoneum in uraemic and peritoneal

dialysis (PD) patients," *Nephrology Dialysis Transplantation*, vol. 24, no. 11, pp. 3504–3512, 2009.

[16] M. Yáñez-Mó, E. Lara-Pezzi, R. Selgas et al., "Peritoneal dialysis and epithelial-to-mesenchymal transition of mesothelial cells," *The New England Journal of Medicine*, vol. 348, no. 5, pp. 403–413, 2003.

[17] A. Aguilera, M. Yáñez-Mo, R. Selgas, F. Sánchez-Madrid, and M. López-Cabrera, "Epithelial to mesenchymal transition as a triggering factor of peritoneal membrane fibrosis and angiogenesis in peritoneal dialysis patients," *Current Opinion in Investigational Drugs*, vol. 6, no. 3, pp. 262–268, 2005.

[18] G. del Peso, J. A. Jiménez-Heffernan, M. A. Bajo et al., "Epithelial-to-mesenchymal transition of mesothelial cells is an early event during peritoneal dialysis and is associated with high peritoneal transport," *Kidney International*, vol. 73, supplement, pp. S26–S33, 2008.

[19] K. Imanaka-Yoshida, M. Hiroe, Y. Yasutomi et al., "Tenascin-C is a useful marker for disease activity in myocarditis," *The Journal of Pathology*, vol. 197, no. 3, pp. 388–394, 2002.

[20] K. Nagaharu, X. Zhang, T. Yoshida et al., "Tenascin C induces epithelial-mesenchymal transition-like change accompanied by SRC activation and focal adhesion kinase phosphorylation in human breast cancer cells," *American Journal of Pathology*, vol. 178, no. 2, pp. 754–763, 2011.

[21] D. Katoh, K. Nagaharu, N. Shimojo et al., "Binding of $\alpha v\beta 1$ and $\alpha v\beta 6$ integrins to tenascin-C induces EMT like change of breast cancer cell," *Oncogenesis*, vol. 19, no. 2, p. e65, 2013.

[22] C. B. Nilsson-Thorell, N. Muscalu, A. H. G. Andren, P. T. T. Kjellstrand, and A. P. Wieslander, "Heat sterilization of fluids for peritoneal dialysis gives rise to aldehydes," *Peritoneal Dialysis International*, vol. 13, no. 3, pp. 208–213, 1993.

[23] A. P. Wieslander, R. Deppisch, E. Svensson, G. Forsback, R. Speidel, and B. Rippe, "In vitro biocompatibility of a heat-sterilized, low-toxic, and less acidic fluid for peritoneal dialysis," *Peritoneal Dialysis International*, vol. 15, no. 3, pp. 158–164, 1995.

[24] K. N. Lai, J. C. K. Leung, L. Y. Y. Chan et al., "Differential expression of receptors for advanced glycation end-products in peritoneal mesothelial cells exposed to glucose degradation products," *Clinical & Experimental Immunology*, vol. 138, no. 3, pp. 466–475, 2004.

[25] E.-J. Oh, H.-M. Ryu, S.-Y. Choi et al., "Impact of low glucose degradation product bicarbonate/lactate-buffered dialysis solution on the epithelial-mesenchymal transition of peritoneum," *American Journal of Nephrology*, vol. 31, no. 1, pp. 58–67, 2009.

[26] H. Liu, N. Zhang, and D. Tian, "MiR-30b is involved in methylglyoxal-induced epithelial-mesenchymal transition of peritoneal mesothelial cells in rats," *Cellular & Molecular Biology Letters*, vol. 19, no. 2, pp. 315–329, 2014.

[27] W. Che, M. Asahi, M. Takahashi et al., "Selective induction of heparin-binding epidermal growth factor-like growth factor by methylglyoxal and 3-deoxyglucosone in rat aortic smooth muscle cells: the involvement of reactive oxygen species formation and a possible implication for atherogenesis in diabetes," *The Journal of Biological Chemistry*, vol. 272, no. 29, pp. 18453–18459, 1997.

[28] S. W. Stoll, L. Rittié, J. L. Johnson, and J. T. Elder, "Heparin-binding EGF-like growth factor promotes epithelial-mesenchymal transition in human keratinocytes," *Journal of Investigative Dermatology*, vol. 132, no. 9, pp. 2148–2157, 2012.

[29] M. Nakayama, A. Sakai, M. Numata, and T. Hosoya, "Hypervascular change and formation of advanced glycation end-products in the peritoneum caused by methylglyoxal and the effect of an anti-oxidant, sodium sulfite," *American Journal of Nephrology*, vol. 23, no. 6, pp. 390–394, 2003.

[30] V. Schwenger, C. Morath, A. Salava et al., "Damage to the peritoneal membrane by glucose degradation products is mediated by the receptor for advanced glycation end-products," *Journal of the American Society of Nephrology*, vol. 17, no. 1, pp. 199–207, 2006.

[31] A. S. De Vriese, R. G. Tilton, S. Mortier, and N. H. Lameire, "Myofibroblast transdifferentiation of mesothelial cells is mediated by RAGE and contributes to peritoneal fibrosis in uraemia," *Nephrology Dialysis Transplantation*, vol. 21, no. 9, pp. 2549–2555, 2006.

[32] M. Cai, K. Onoda, M. Takao et al., "Degradation of tenascin-C and activity of matrix metalloproteinase-2 are associated with tumor recurrence in early stage non-small cell lung cancer," *Clinical Cancer Research*, vol. 8, no. 4, pp. 1152–1156, 2002.

[33] J. Chen, Z. Chen, M. Chen et al., "Role of fibrillar tenascin-C in metastatic pancreatic cancer," *International Journal of Oncology*, vol. 34, no. 4, pp. 1029–1036, 2009.

Hindawi Publishing Corporation
BioMed Research International
Volume 2015, Article ID 989560, 15 pages
http://dx.doi.org/10.1155/2015/989560

Research Article

Rapamycin Protects from Type-I Peritoneal Membrane Failure Inhibiting the Angiogenesis, Lymphangiogenesis, and Endo-MT

Guadalupe Tirma González-Mateo,[1] Anna Rita Aguirre,[2] Jesús Loureiro,[3] Hugo Abensur,[2] Pilar Sandoval,[1] José Antonio Sánchez-Tomero,[4] Gloria del Peso,[5] José Antonio Jiménez-Heffernan,[6] Vicente Ruiz-Carpio,[1] Rafael Selgas,[5] Manuel López-Cabrera,[1] Abelardo Aguilera,[7] and Georgios Liappas[1]

[1]*Centro de Biología Molecular-Severo Ochoa (CBMSO), Consejo Superior de Investigaciones Científicas (CSIC), Cantoblanco, 28049 Madrid, Spain*
[2]*Departamento de Nefrologia, Hospital das Clínicas da Faculdade de Medicina da Universidade de São Paulo, 05403-000 São Paulo, Brazil*
[3]*Aging and Inflammation Group, Instituto de Investigación Biomédica (INIBIC), 15006 A Coruña, Spain*
[4]*Departamento de Nefrología, Hospital Universitario de la Princesa, Instituto de Investigación Sanitaria Princesa (IP), 28006 Madrid, Spain*
[5]*Departamento de Nefrología, Hospital Universitario La Paz & Instituto de Investigación Sanitaria la Paz (IdiPAZ), 28046 Madrid, Spain*
[6]*Departamento de Patología, Hospital Universitario de la Princesa, Instituto de Investigación Sanitaria Princesa (IP), 28006 Madrid, Spain*
[7]*Unidad de Biología Molecular y Departamento de Nefrología, Hospital Universitario de la Princesa, Instituto de Investigación Sanitaria Princesa (IP), 28006 Madrid, Spain*

Correspondence should be addressed to Abelardo Aguilera; abelardo.aguilera@salud.madrid.org

Received 23 May 2015; Revised 27 August 2015; Accepted 13 October 2015

Academic Editor: Janusz Witowski

Preservation of peritoneal membrane (PM) is essential for long-term survival in peritoneal dialysis (PD). Continuous presence of PD fluids (PDF) in the peritoneal cavity generates chronic inflammation and promotes changes of the PM, such as fibrosis, angiogenesis, and lymphangiogenesis. Mesothelial-to-mesenchymal transition (MMT) and endothelial-to-mesenchymal transition (Endo-MT) seem to play a central role in this pathogenesis. We speculated that Rapamycin, a potent immunosuppressor, could be beneficial by regulating blood and lymphatic vessels proliferation. We demonstrate that mice undergoing a combined PD and Rapamycin treatment (PDF + Rapa group) presented a reduced PM thickness and lower number of submesothelial blood and lymphatic vessels, as well as decreased MMT and Endo-MT, comparing with their counterparts exposed to PD alone (PDF group). Peritoneal water transport in the PDF + Rapa group remained at control level, whereas PD effluent levels of VEGF, TGF-β, and TNF-α were lower than in the PDF group. Moreover, the treatment of mesothelial cells with Rapamycin *in vitro* significantly decreased VEGF synthesis and selectively inhibited the VEGF-C and VEGF-D release when compared with control cells. Thus, Rapamycin has a protective effect on PM in PD through an antifibrotic and antiproliferative effect on blood and lymphatic vessels. Moreover, it inhibits Endo-MT and, at least partially, MMT.

1. Introduction

Peritoneal dialysis (PD) is a form of renal replacement therapy based on the ability of the peritoneal membrane (PM) to perform diffusive and convective transport, in order to maintain solute and fluid equilibrium in uremic patients. Ultrafiltration (UF) failure and the consequent extracellular volume overload are one of the major causes of PD abandonment [1].

In early stages, membrane damage may manifest itself as an increase in water and solute transport, but, as the lesion progresses, transport decreases and underdialysis may take place. The main factors involved in UF failure are peritoneal chronic and acute inflammation, which may lead to progressive deterioration of PM function (type-I PM failure).

Glucose degradation products (GDPs), formation of advanced glycation end-products (AGEs), uremic toxins, and low pH in PD fluids (PDF) play important roles in PM deterioration [2]. These bioincompatible features of PDFs induce an immunological response in PM, involving mesothelial cells (MCs), macrophages, lymphocytes, and neutrophils. They are stimulated to produce a variety of cytokines and growth factors, such as tumor necrosis factor- (TNF-) α, interleukin- (IL-) 1, IL-8, transforming growth factor- (TGF-) β, vascular endothelial growth factor (VEGF), and fibroblast growth factor- (FGF-) 2, which amplify the inflammation, with structural and functional consequences [3]. One important consequence of PDFs bioincompatibility is the induction of MCs transdifferentiation, a phenomenon known as mesothelial-to-mesenchymal transition (MMT) [4]. Transdifferentiated cells have been detected in PM even before the onset of fibrosis [5], a second consequence of PD. They are also major contributors to VEGF and TGF-β production in the peritoneum, providing more stimuli for extracellular matrix (ECM) production (fibrosis) and enhancement of the local vascular networks [6], leading to angiogenesis, a third consequence of PD. The result is a thickened and hypervascularized PM, which leads to the changes in fluid and solute transport observed in patients in the long term of PD [5, 6]. Another important process involved in peritoneal pathogenesis is the endothelial-mesenchymal transdifferentiation (Endo-MT). Its importance has been recently recognized and between 3 to 5% of submesothelial PD fibroblasts seem to derive from this process [7]. MMT and Endo-MT share common triggering mechanisms. Both begin with TGF-β overproduction and activation of Smads cascade, leading to VEGF hyperproduction [8, 9]. But VEGF production is not only regulated by TGF-β; glucose from PDFs *per se* also induces VEGF upregulation, as well as vascular hyperpermeability and PD dysfunction, as has been demonstrated [10]. The implication of VEGF in both, early and late stages of PM failure (inducing high vascular permeability and hypervascularization, resp.), leads us to hypothesize that VEGF may be considered a therapeutic target. In addition, VEGF hyperproduction leads to another of the consequences of PD: peritoneal lymphangiogenesis, which is mainly regulated by VEGF-C and VEGF-D and is closely linked to MMT [6, 11]. Although poorly studied, lymphangiogenesis is one of the most decisive factor implied in peritoneal water transport disorders [1].

Rapamycin is a macrolide antibiotic produced by *Streptomyces hygroscopicus* that shows antifungal, immunosuppressant, and antitumor properties. Its therapeutic effects are derived from its ability to inhibit the so-called mammalian target of rapamycin (mTOR) complex and include antifibrotic, cytostatic, antiangiogenic, and anti-lymphangiogenic effects [12] as has been demonstrated in tumors, especially carcinomas and hematologic cancers, as well as in retinal and corneal diseases [13–15]. The same anti-VEGF effect could also explain the inhibition of lymphangiogenesis showed by Rapamycin in kidneys [16]. We wondered if this drug could have an effect over Endo-MT, which may be involved in tissue fibrosis.

Recently, two articles analyzed the antifibrotic effect of Rapamycin on the PM in a rat PD model [17, 18]. Xu et al. focused their discussion on the capacity of Rapamycin to inhibit the extracellular matrix production and to improve the peritoneal transport [17]. Ceri et al. [18] studied the regression of peritoneal sclerosis in a rat model of encapsulating peritoneal sclerosis (EPS) treated with Rapamycin. Unfortunately, none of them analyzed the intraperitoneal antilymphangiogenic effect of this drug.

According to the aforementioned data, we suggest that the PM deterioration might be treated with Rapamycin, given its pleotropic effects including antiangiogenic, antilymphangiogenic, antifibrotic, and anti-inflammatory properties. The goal of this study was to analyze the effects of Rapamycin on PM damage in a mice PD model. We also analyzed its effect on MCs viability, cytokine production, and wound healing capacity. Herein, we demonstrated that Rapamycin protects the PM in PD, modulating the tissue fibrosis, MMT, Endo-MT, and especially angiogenesis and lymphangiogenesis.

2. Materials and Methods

2.1. Peritoneal Dialysis Fluid Exposure Model in Mice. A total of 21 female C57BL/6 mice aged between 12 and 16 weeks were used in this study (Harlan Interfauna Iberica, Barcelona, Spain). The experimental protocol used was in accordance with the National Institutes of Health Guide for Care and Use of Laboratory Animals and was approved by the Animal Ethics Committee of the "Unidad de Cirugía Experimental" of "Hospital Universitario la Paz." Food and water were provided ad libitum to the animals.

PDF or saline was instilled via a peritoneal catheter connected to a subcutaneous mini access port (Access Technologies, Skokie, IL, USA) as previously described [7, 19]. During the first week after surgery, the animals received 0.2 mL of saline with 1 IU/mL heparin. Thereafter, during a 4-week period, 6 mice did not receive any treatment (control group), 7 mice were daily instilled with 2 mL of standard PD fluid (PDF group) composed of 4.25% glucose and buffered with lactate (Stay Safe; Fresenius, Bad Homburg, Germany), and 7 mice were treated with oral Rapamycin diluted in water (2 mg/kg/day in 15 μL of volume administered to mice using a pipette and a gastric tube) and daily instilled with 2 mL of standard PD fluid (PDF + Rapamycin group).

Two animals of the PDF group and one from PDF + Rapamycin group were not used in the final analysis, because of catheter port infections related to skin wounds (control group, $n = 6$; PDF group, $n = 5$; and PDF + Rapamycin group, $n = 6$). A peritoneal equilibrium test was performed in the last day of experiment. For this purpose, all mice were instilled with 2 mL of PD solution (dextrose 4.25%). After 30 min, they were anaesthetized with isoflurane (MTC Pharmaceuticals, Cambridge, ON, Canada) and sacrificed, so that all the peritoneal fluid volume that remained in the cavity could be recovered, as previously described [7, 19, 20]. Briefly,

this method consists of opening the peritoneal cavity through an incision in the muscle and extracting all the fluid with a pipette. There is always a minimum percentage of remaining volume that is not possible to extract.

Diaphragmatic and parietal peritoneum samples were obtained from the contralateral side of the implanted catheter.

2.2. Histological Analyses of Peritoneal Samples and Effluent Growth Factors Measurements. For histological analysis, parietal peritoneum from the opposite side to the catheter insertion site was divided into several pieces, avoiding the *linea alba*. One piece was directly frozen in OCT (optimal cutting temperature) compound for immunofluorescence analysis and two other pieces were routinely fixed in Bouin or neutral buffered 3.7% formalin and embedded in paraffin to obtain 5 μm tissue sections.

Deparaffinized sections from Bouin fixed samples were stained with Masson's trichrome. The submesothelial thickness was determined in a blinded manner, by microscope analysis and the mean of independent measures every 60 μm was considered for each animal.

For immunohistochemical studies, diaphragmatic and peritoneal tissue samples previously fixed in neutral buffered 3.7% formalin were cut into 3 μm sections and heated to expose the hidden antigens using Real Target Retrieval Solution containing citrate buffer, pH 6.0 (Dako, Glostrup, Denmark). Samples were also pretreated with Real Peroxidase-Blocking Solution (Dako) to block endogenous peroxidase. A biotinylated goat IgG (H + L) (Vector Laboratories, Burlingame, CA, USA) was applied to detect primary antibodies CD31 (Abcam, Cambridge, UK) and podoplanin (PA2.26, a gift from Dr. Gamallo, Laboratory of Pathology, Hospital de La Princesa, Madrid, Spain). Complexes were visualized by R.T.U Vectastain Elite ABC Kit (Vector Laboratories) and using DAB (Dako) as chromogen. Finally, all cases were counterstained with haematoxylin. In order to estimate the vessel density, 6 arbitrary 20x fields in the submesothelial peritoneal area were analyzed and quantified using the scale bar method (numbers of $CD31^+$ cells/μm^2). Images were analyzed by computerized digital image analysis (AnalySIS, Soft Imaging System). Number of cells with single or double positive staining was counted and was expressed as the mean of 10 independent measurements for each animal. Podoplanin positive lymphatic vessels in the diaphragms of 6 arbitrary 10x fields for each animal were quantified using the analysis program Image-J 1.37c (National Institute of Health, Bethesda, Maryland).

For immunofluorescence analysis, cryostat sections (5 μm) from frozen samples were stained with antibodies to visualize vasculature (CD31; Serotec, Oxford, UK), MCs (Pan-Cytokeratin; Sigma-Aldrich), and pathologic fibroblasts (FSP1; Dako). The sections were fixed for 15 minutes in 4% formaldehyde in PBS and blocked with 10% horse serum for 1 hour in PBS with 0.3% Triton X-100. First antibodies were incubated in PBS with 0.1% Triton X-100 overnight at 4°C. After 3 washing steps, secondary Alexa-labelled antibodies were incubated for 90 minutes at room temperature. After another washing process, the preparations were mounted with a 4,6-diamidino-2-phenylindole (DAPI) nuclear stain (Vectashield; Vector Laboratories). Negative controls for immunofluorescence staining were conducted using 10% rabbit serum instead of primary antibody. The cytokeratin and FSP-1 costaining defined the MMT and the CD31 and FSP1 costaining defined the Endo-MT.

The amounts of VEGF-A, TGFβ1, and TNF-α in peritoneal effluent were obtained the last day of experiment (PET day) and determined by ELISA-based assays, according to manufacturers' instructions (BMS619, Bender MedSystems, Vienne, Austria; DY1679, R&D Systems, Minneapolis, USA; and 560478, BD Company, BS, San José, CA, USA, resp.).

2.3. Differences in Peritoneal UF Rate among Mice Exposed to PD versus Controls. In order to analyze the changes in water peritoneal transport between peritoneum exposed to PD and virgin peritoneums, a separate study was performed: twenty mice with virgin peritoneum (control group) received an intraperitoneal injection of 2 mL of Stay Safe 4.25% (Fresenius Medical Care). These mice were sacrificed extracting the total water volume from peritoneal cavity at 20, 30, 40, and 60 minutes after intraperitoneal injection (UF test). Another twenty mice were subjected to PD receiving and intraperitoneal infusion of Stay Safe 4.25%, 2 mL per day, during 30 days. At the end of the experiment we performed the same UF test. Five mice were analyzed in each time point (20, 30, 40, and 60 min) for both groups.

2.4. Culture of Omentum and Effluent-Derived MCs and Treatments. MCs were obtained from omental samples of patients undergoing elective abdominal surgery and from peritoneal effluents of PD patients as previously described [21]. These cells were cultured in Earle's M199 medium supplemented with 20% fetal calf serum, 50 U/mL penicillin, 50 μg/mL streptomycin, and 2% Biogro-2 (containing insulin, transferrin, ethanolamine, and putrescine: Biological Industries, Beit Haemek, Israel). The purity of omentum- and effluent-derived MCs cultures was determined by the expression of standard mesothelial markers: intercellular adhesion molecule- (ICAM-) 1, calretinin, and cytokeratins. These MCs cultures were negative for von-Willebrand factor and CD45, ruling out any contamination by endothelial cells or macrophages [21]. To induce MMT *in vitro*, omentum-derived MCs were initially seeded in bottle flash (25 or 100 mL) and then plated at P6 (50.000 cells/mL in M199 medium, Bauer Chamber). When they reached subconfluence, MCs seeded on wells coated with collagen I (50 μg/mL, Roche Diagnostics GmbH, Mannheim, Germany) and treated in different time points (6 to 48 hours) with human-recombinant TGF-β1 (1 ng/mL, R&D Systems Inc., Minneapolis, MN, USA), a commonly used *in vitro* model of MMT [21]. Where indicated, Rapamycin (Wyeth Laboratories, Madison, NJ, USA) was administered at concentrations of 2 and 4 nM. Effluent-derived MCs that had undergone MMT (as determined by nonepithelioid morphology, by low expression of E-cadherin, and by upregulated expression of mesenchymal markers) were also treated with different doses of Rapamycin (2, 4, and 20 nM) and analyzed at 6, 24, and 48 hours. In order to establish a correction factor we measured the total protein in each well at the end of the experiment.

The present study adjusts to the Declaration of Helsinki and it was approved by the Ethics Committee of "Hospital Universitario de la Princesa" (Madrid, Spain). Informed written consent to use effluent samples was obtained from all the PD patients included in this study and oral informed consent was obtained from omentum donors subjected to elective surgeries.

2.5. Western Blot, Quantitative RT-PCR, and Enzyme-Linked Immunoassays. For western blotting, MCs cultures were lysed in a buffer containing 1% sodium deoxycholate and 0.1% sodium dodecyl sulfate (SDS). Total protein was quantified using a protein assay kit (Bio-Rad, Hercules, CA). Total cell protein (50 μg) was resolved on 8–10% SDS-polyacrylamide gels and transferred to nitrocellulose membranes, which were then blocked with fat-free milk and probed with specific antibodies against E-cadherin, α-SMA, collagen I, fibronectin, and tubulin (Sigma-Aldrich, Inc., St. Louis, MO). These antibodies were detected with peroxidase conjugated goat anti-mouse IgG antibody (BD Biosciences, Franklin Lakes, NJ) and visualized by enhanced chemiluminescence (ECL detection kit, Amersham Biosciences, Freiburg, Germany). Images of the blots were acquired with an LAS-1000 Charge Coupled Device camera (Fujifilm, Cedex, France).

For quantitative RT-PCR analysis, MCs were lysed in TRI Reagent (Ambion Inc., Austin, TX), and RNA was extracted as fabricant instructions. Complementary-DNA was synthesized from 2 μg of total RNA by reverse transcription (RNA PCR Core Kit, Applied Biosystems Inc., New Jersey). Quantitative PCR was carried out in a Light Cycler 2.0 using a SYBR Green Kit (Roche Diagnostics GmbH) and specific primers sets for Snail, E-cadherin, and histone H3. Samples were normalized with respect to the value obtained for H3. The primer sets employed for Snail, E-cadherin, and H3 have been previously described [7].

VEGF-A, VEGF-C, and VEGF-D were measured in the culture supernatants by ELISA kits (R&D Systems Inc., USA): VEGF-A, catalog number DVE00 and sensitivity 9 pg/mL; VEGF-C, catalog number DVEC00 and sensitivity 48.4 pg/mL; VEGF-D, catalog number DVED00 and sensitivity 31.3 pg/mL. For all of them, the cross-reactivity observed with available related molecules was <0.5%.

2.6. Proliferation Assays. For proliferation assays, 10^4 cells/well of omentum derived MCs with epithelioid phenotype (semiconfluent) were seeded into 96-well plates and cultured at 37°C, 5% CO_2 and incubated with Rapamycin 2, 4, and 20 nM for 48 hours. Cells were then pulsed with [3H]-thymidine (1 mCi per well) for 16–18 hours and lysed with Filter Mate Cell Harvester (Perkin Elmer, Turku, Finland). Radioactivity was determined for 1 minute in a basic beta liquid scintillation counter (Perkin Elmer).

As a complementary cell proliferation test and using the same experimental conditions as the previous assay, we also measured total protein synthesis (μg/mL) using Pierce, BCA protein assay kit (Life Technologies, USA).

2.7. Cell Cycle and Wound Healing. To analyze the effect of Rapamycin on cell cycle profile, omentum MCs were grown in fetal calf serum and treated with different doses of Rapamycin (2, 4, and 20 nM) for 48 h. Cells were trypsinized, pelleted, and fixed with 70% cold ethanol for 30 min. After washing, samples were suspended in PBS and an equal volume of propidium iodide solution, containing 200 μg/mL RNase (Sigma Aldrich), 20 μg/mL propidium iodide (Sigma Aldrich), and 0.1% Triton X-100 in PBS, was added to the cell suspension for 30 min at room temperature. A FACS Calibur flow cytometer (BD Bioscience) was used to analyze DNA content; emitted light was measured at 675 nm.

To test the effect of Rapamycin on MCs wound repair capacity, a wound healing experiment was performed with cells treated or not with different doses of Rapamycin. Briefly, MCs from omentum, treated or not with Rapamycin, were subjected to mechanical injury with an adapted cell scraper approximately 1500 μm in width and photographed every eight hours during 72 hours. MCs treated with high doses of Rapamycin showed a slight delay at 24 and 48 hours in wound closure.

2.8. Statistical Analysis. Data from animal experiments and effluent parameters were compared with one-way ANOVA test and nonparametric Mann–Whitney rank sum U test (Figures 1–5). *In vitro* experiments were performed in triplicate. One representative WB picture was taken from each case and quantified using bar graphics (Figures 6 and 7). The cell proliferation and cell cycle experiments were repeated in five occasions (Figures 7(b) and 7(c)). We used the SPSS statistic package version 14.5 (Chicago, IL) and GraphPad Prism version 4.0 (La Jolla, CA). $p < 0.05$ was considered statistically significant. Box plot graphics represent the 25th and 75th percentiles and median, minimum, and maximum values (Figures 1–5 and 7).

3. Results

3.1. Rapamycin Ameliorated Peritoneal Membrane Thickening, Fibrosis, and MMT Induced by Dialysis Fluid Exposure in a Mouse PD Model. We analyzed whether Rapamycin, an mTOR inhibitor with recognized antifibrotic effect [12], might prevent the deterioration of the PM in a mouse model of PDF exposure. Histological analysis of parietal peritoneum biopsies from animals exposed to PDF (PDF group, $n = 5$) showed a loss of MCs monolayer and increased PM thickness when compared to control mice, which preserved the MCs monolayer (control group, $n = 6$). Oral administration of Rapamycin (2 mg/kg/day) to PDF-treated mice (PDF + Rapamycin group, $n = 6$) significantly reduced the peritoneal thickness (Figure 1(a)). Then, we analyzed the contribution of MMT to the number of submesothelial fibroblasts and fibrosis during PD. Figure 1(b) shows the immunofluorescence staining of cytokeratin (red) and FSP-1 (green) (counterstained with DAPI in blue). The PDF exposure-promoted MMT (cells coexpressing cytokeratin and FSP-1 with double positive staining, yellow) is reduced by Rapamycin administration. Importantly, PDF group shows many costained MCs (yellow) in superficial areas (arrows) suggesting that MMT occurs at early stages of MCs transdifferentiation before invading the submesothelial area. PM thickness (μm)

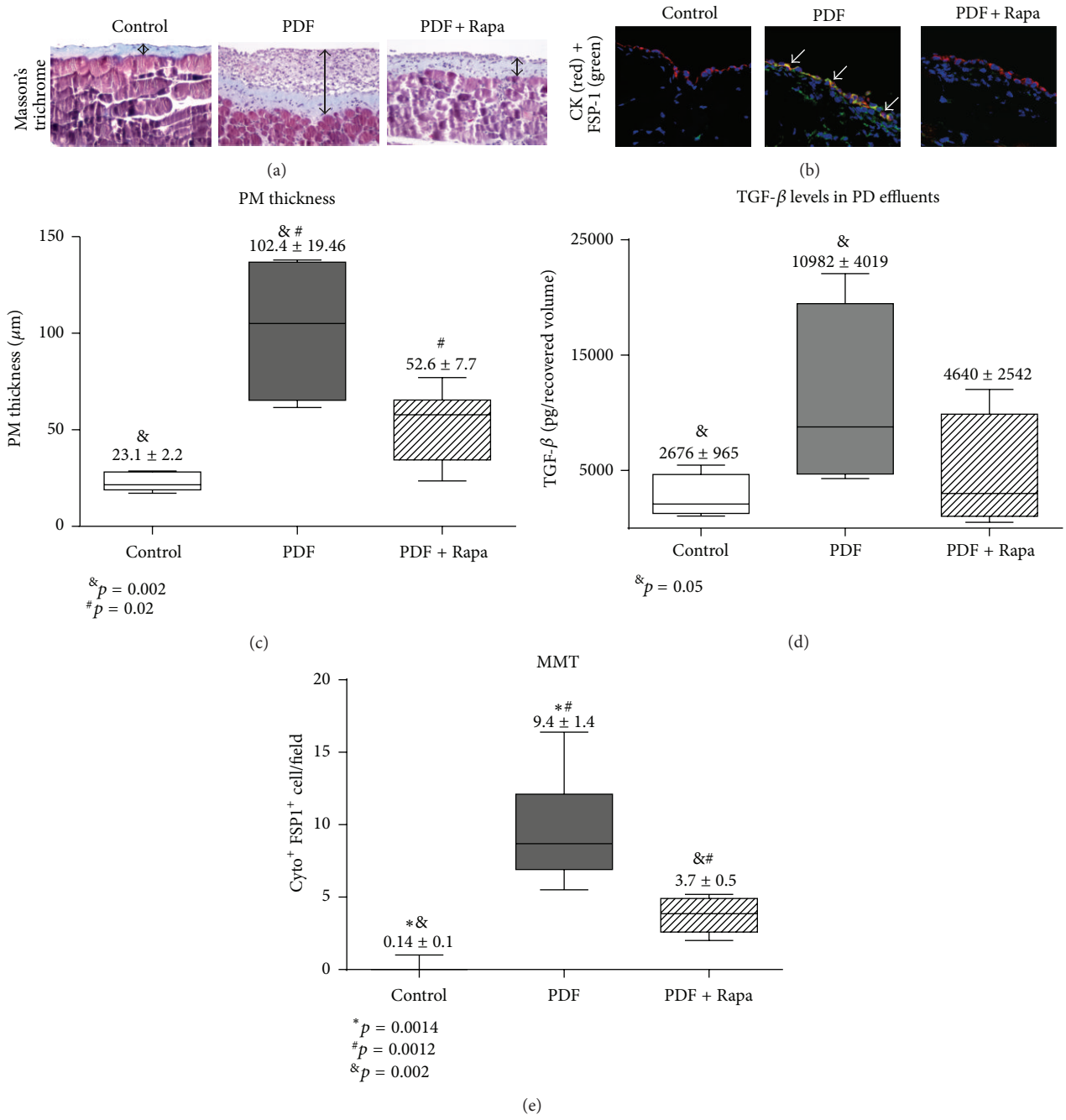

Figure 1: Rapamycin decreases the PM deterioration in a PD mouse model. Mice received a daily instillation of standard PD fluid (2 mL per day) through a intraperitoneal catheter during 4 weeks with or without the oral administration of Rapamycin (2 mg/kg/day: PDF, $n = 5$, and PDF + Rapamycin, $n = 6$). A control group of mice that were only exposed to the presence of the catheter was also included (control; $n = 6$). Peritoneal samples were prepared and analyzed as described in Materials and Methods section. (a) Standard PD fluid exposure increases matrix deposition (blue stained zones) and the thickness of the PM (black lines), while Rapamycin administration significantly reduces these effects when measured in Masson's trichrome staining (sections representative slides). Magnification 200x. (b) As shown in immunofluorescence staining of cytokeratin (red) and FSP-1 (green) (counterstained with DAPI in blue), PDF exposure-promoted MMT (cells coexpressing cytokeratin and FSP-1 with double positive staining, yellow) is reduced by Rapamycin administration. Magnification 400x. (c) The peritoneal thickness (μm) is increased in PDF group compared with control mice, and the group PDF with Rapamycin shows a significant reduction of thickness when compared with PDF group. Analysis of variance results in a significance of $p = 0.001$ (one-way ANOVA test). (d) Measurement of TGF-β1 (pg/mL) in the drained volumes shows a gentle increase (although not statistically significant) of this growth factor in PD fluid-instilled animals while Rapamycin administration tends to reduce TGF-β1 production. The analysis of variance results in a p value of 0.146 (one-way ANOVA test). (e) Numbers of mesothelial cells per field suffering MMT increase during PDF exposition, while Rapamycin is able to reduce the occurrence of this pathological process. The analysis of variance results in a significance of $p < 0.0001$ (one-way ANOVA test). Box plots graphics represent the median, minimum, and maximum values, as well as the 25th and 75th percentiles. Numbers above boxes depict means ± SE. Symbols represent the statistical differences between groups analyzed by Mann-Whitney U test.

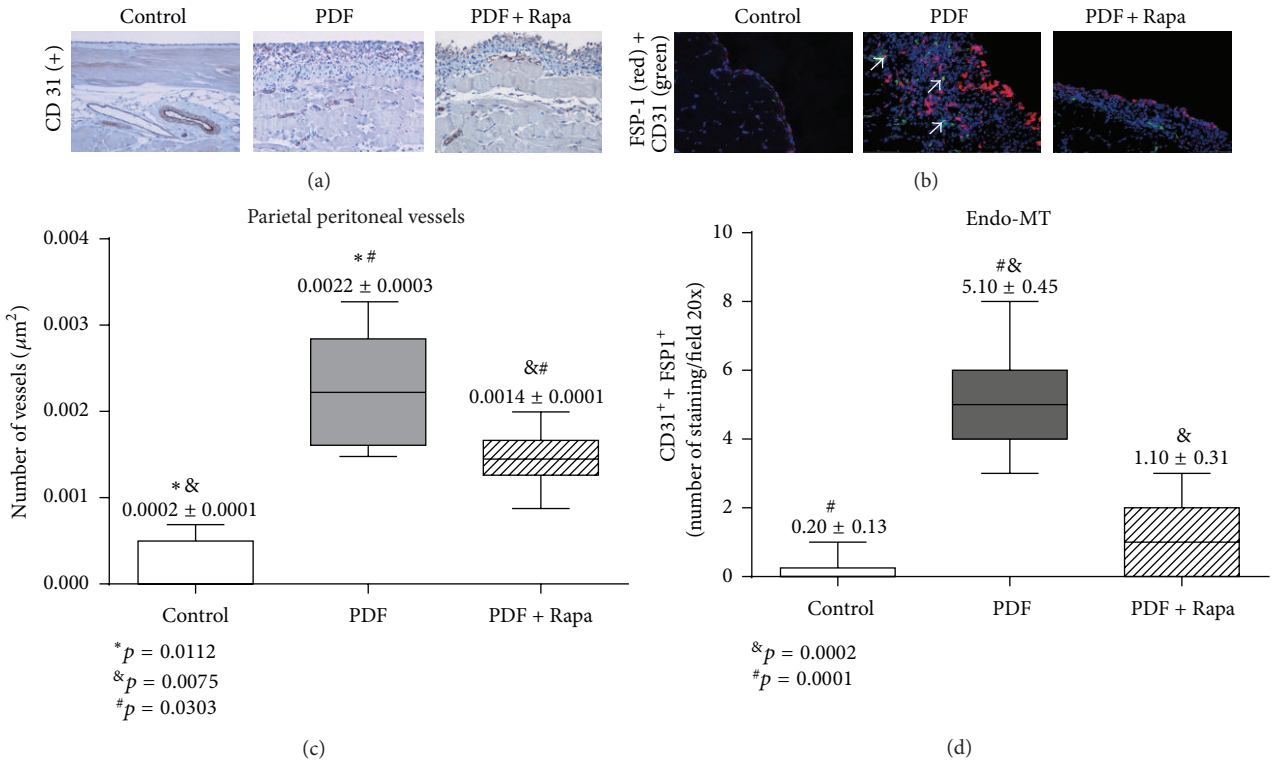

Figure 2: Treatment with Rapamycin decreases PD-induced angiogenesis and Endo-MT. Mice received a daily instillation of standard PD fluid with or without the oral administration of Rapamycin (PDF; $n = 5$ and PDF + Rapamycin; $n = 6$). A control group of mice was also included (control; $n = 6$). (a) Standard PD fluid exposure increases peritoneal angiogenesis and Rapamycin administration significantly reduces the number of submesothelial blood vessels, as determined by CD31 staining (number of $CD31^+$ cells/μm^2). Magnification 200x. (b) Standard PD fluid exposure also increases the presence of endo-MMT, measured as double positive immunofluorescence staining (white arrows) of CD31 (green) and FSP-1 (red) (counterstained with DAPI, in blue), which is reduced by Rapamycin administration. Magnification 200x. (c) Box plots represent the number of submesothelial $CD31^+$ vessels stained cells per field in the different experimental groups and show a decrease of angiogenesis in the Rapamycin-treated animals. The analysis of variance results in a significance of $p < 0.0001$ (one-way ANOVA test). (d) The numbers of double stained $CD31^+/FSP\text{-}1^+$ cells per field increase in the PDF-exposed group and show a decrease in the Rapamycin-treated animals. The one-way ANOVA test resulted in a significance of $p < 0.0001$. Box plots graphics represent 25th and 75th percentiles and median, minimum, and maximum values. Numbers above boxes depict means ± SE. Symbols represent the statistic differences between groups.

increased in PDF group compared with control mice and PDF + Rapamycin group. Figure 1(c) shows the statistic differences between the groups after a double blind count of PM thickness in ten arbitrarily chosen fields of optical microscopy. Since TGF-β is the major inducer of MMT and tissue fibrosis, we measured its levels in PD effluent. We found statistically significant differences between control group and PDF group, which showed maximum levels. Rapamycin group showed low TGF-β, which did not reach statistical significance (Figure 1(d)). Figure 1(e) shows the count of MCs, which have suffered MMT. Given that PM thickness usually runs parallel to the MMT, Rapamycin showed less transdifferentiated MCs, as expected. These differences were statistically significant.

3.2. Rapamycin Decreased PD-Induced Angiogenesis and Endo-MT. Angiogenesis is an important process that occurs in the PM during PD [22], and a robust antiangiogenic effect of Rapamycin has been described in other tissues [12]. This drug acts by decreasing VEGF production or blocking its receptors [23]. To test the effect of Rapamycin on PD-induced angiogenesis, blood vessels of the parietal peritoneum were stained with an anti-CD31 antibody. In the peritoneum from control mice, CD31 expression was confined to deeper vessels located in the muscular tissue (Figure 2(a)) while the PDF group showed a significant increase in the number of submesothelial vessels in comparison with PDF + Rapamycin group.

Although Endo-MT is a poorly known phenomenon in PD, it may contribute to PM fibrosis. Figure 2(b) shows CD31 and FSP1 costaining in the submesothelial compact zone. Again, the PDF group showed more costained cells (yellow, see arrows) than the other groups. Figure 2(c) shows the statistically significant differences between the groups in angiogenesis rate (submesothelial $CD31^+$ vessels) and Figure 2(d) shows the number of endothelial cells suffering Endo-MT ($CD31^+$ and $FSP1^+$). Rapamycin group showed less MCs transdifferentiation than PDF group but similar to controls.

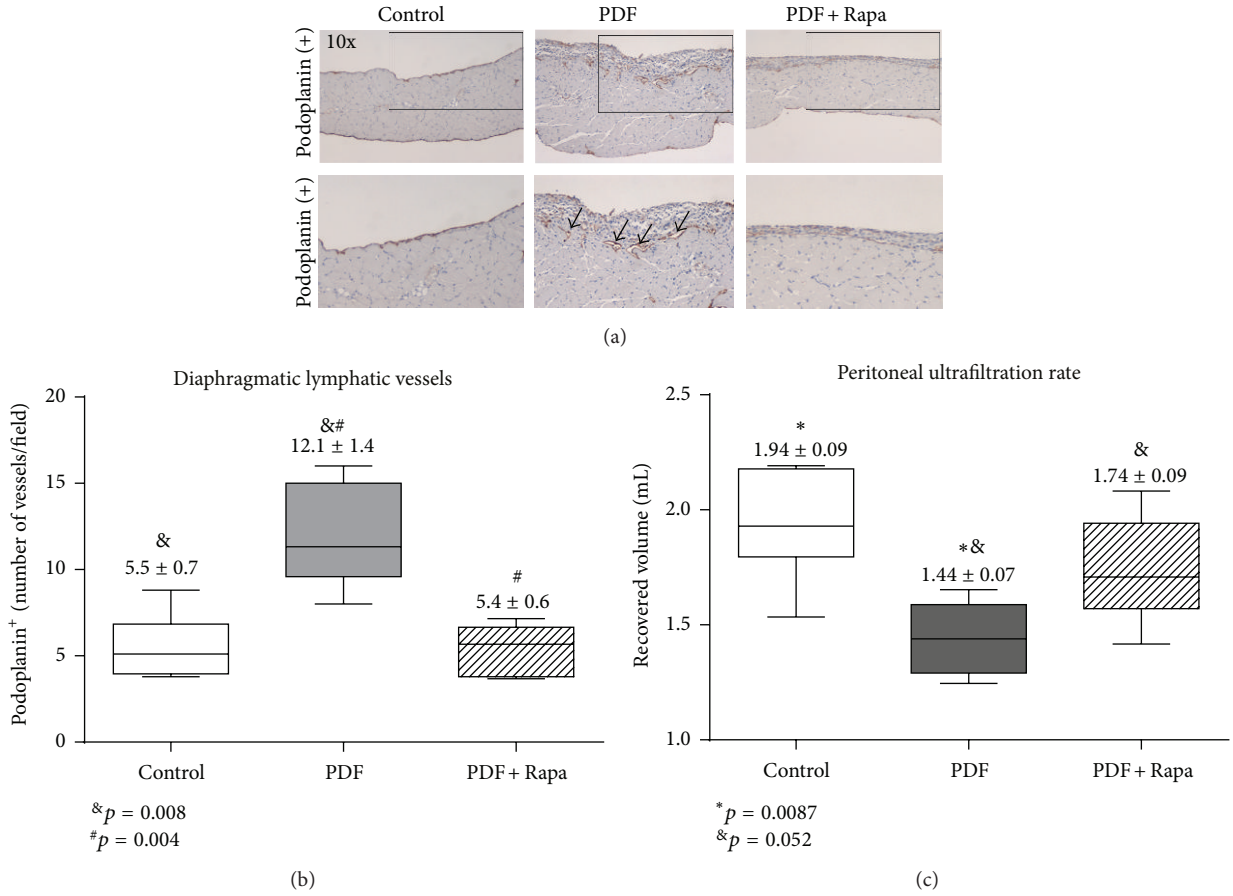

FIGURE 3: Treatment with Rapamycin diminished lymphangiogenesis, improving peritoneal ultrafiltration rate. (a) The diaphragm was stained with podoplanin to analyze the side of the peritoneal cavity. Immunohistochemical staining of podoplanin reveals an increase of submesothelial lymphatic vessels during PDF exposition, while this lymphangiogenesis is reduced with Rapamycin. Images were taken with a 10x objective. Insets below show a detail of the part selected with a square in each picture. (b) Submesothelial count of lymphatic vessels (podoplanin positive staining). Rapamycin showed significantly lower number of lymphatic vessels than the PDF group and similar to controls ($p = 0.0002$, one-way ANOVA test). (c) A 30-minute UF test was performed on the last day of treatments. The volumes recovered from animals exposed to PD fluid are lower than those from control mice and an increase of net UF is obtained in mice exposed to PD fluid that were administrated Rapamycin. A significance of $p = 0.0064$ was obtained with the analysis of variance test.

3.3. Rapamycin Decreased PD-Induced Lymphangiogenesis and Improved Peritoneal Ultrafiltration Rate. Lymphangiogenesis is another anatomical change associated with type-I PM failure. In PD, this process is poorly studied and seems to be closely related to the peritoneal water transport. In renal cancer, Rapamycin has been able to inhibit lymphangiogenesis, thus delaying the progression of this neoformative process [16]. Herein, we explore the effect of Rapamycin on lymphatic vessels formation in a PD mice model. Figure 3(a) shows the immunohistochemical staining of podoplanin, revealing an increase of diaphragmatic lymphatic vessels during PDF exposition. Podoplanin stains MCs, so we can see two MC layers, one in contact with the pleura and the other thickened, facing the peritoneal cavity (magnification 10x). Amplifying the picture, we can see in the PDF group a dramatic increase in lymphatic vessels number (arrows). The number of these lymphatic vessels in Rapamycin-treated mice was similar to controls (Figure 3(b)). At the end of the experiment, we measured the UF rate. The PDF group presented an altered UF capacity in comparison to controls or Rapamycin group. These differences were statistically significant (Figure 3(c)).

Finally, we found that the number of blood and lymphatics vessels at the end of the experiment showed a significant linear correlation ($r^2 = 0.78$, $p < 0.001$), suggesting that both phenomena are in parallel (data not shown).

3.4. Rapamycin Decreased VEGF and TNF-α Levels in PD Effluent of PD. Treatment with Rapamycin decreased VEGF in the mice PD effluent (Figure 4(a)). This is consistent with our previous results showing that Rapamycin decreased angiogenesis and lymphangiogenesis. We also measured the effect of Rapamycin on inflammatory markers in the peritoneal cavity. To assess the peritoneal inflammatory state, we measured proinflammatory cytokines levels and the number of total cells in the PD effluent. Our results indicated that Rapamycin showed statistically significant lower amounts of TNF-α than that of the PDF group. Although we did not find

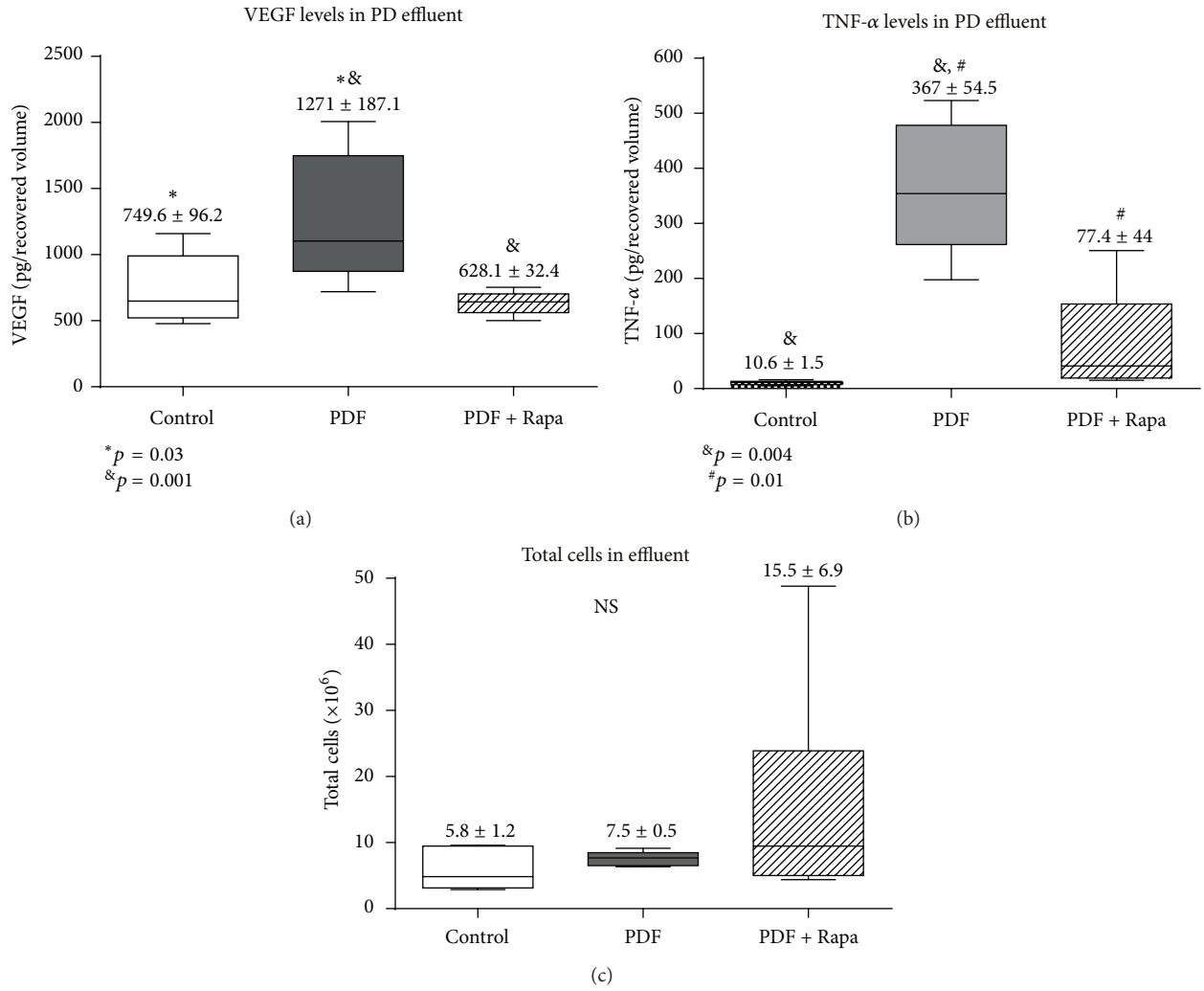

Figure 4: Rapamycin decreases VEGF and TNF-α levels in the peritoneal cavity. (a) Analysis of VEGF and (b) TNF-alpha in the drained volumes shows a strong increase of these factors in PD fluid-instilled animals, and administration of Rapamycin significantly reduces their production. The one-way ANOVA test resulted in a significance of $p < 0.0038$ and $p < 0.0001$, respectively. (c) Total numbers of cells in the drained effluent do not show statistical differences between groups. Box plots graphics represent 25th and 75th percentiles and median, minimum, and maximum values. Numbers above boxes depict means ± SE. Symbols represent the statistic differences between groups.

significant differences in the total cells number between the groups (Figures 4(b) and 4(c)), an anti-inflammatory effect may be defended.

3.5. Rapamycin Decreased VEGF Production by Human Peritoneal MCs, Mainly Those with Prolymphogenic Effects. In PD, angiogenesis and lymphangiogenesis are two crucial factors involved in peritoneal transport, which are generally parallel to peritoneal fibrosis [24, 25]. Rapamycin is considered an anti-VEGF agent; therefore we explored its effect on VEGF-A, VEGF-C, and VEGF-D production by human peritoneal MCs. We isolated and cultivated MCs from omentum and PD effluent which were stimulated with Rapamycin 2 nM during 48 h. Both groups showed and important decrease in VEGF-A, VEGF-C, and VEGF-D supernatant levels especially the last two which are considered as prolymphogenic forms (Figures 5(a) and 5(b)). Figure 5(c) shows the same data expressed in rate of decrease (%) of VEGF-A, VEGF-C, and VEGF-D decrease.

3.6. Rapamycin Attenuated MMT in PD Effluent and Omentum Derived MCs. Recent studies suggest that Rapamycin can have total or partial effect on MMT [26, 27]. For this reason we design the present experiment. We isolated and cultivated MCs from omentum and PD effluent, which were stimulated during 48 h with Rapamycin and/or rTGF-β to induce MMT. MCs were lysed and proteins extracted for analysis by WB.

Omentum-derived MCs were cotreated with Rapamycin and TGF-β. These did not show E-cadherin repression and had the Fibronectin and Collagen-I upregulation avoided, features of the MMT process (Figure 6(a)). Bar graphics show the measurement of the different gene expressions (Figures 6(b)-6(c)).

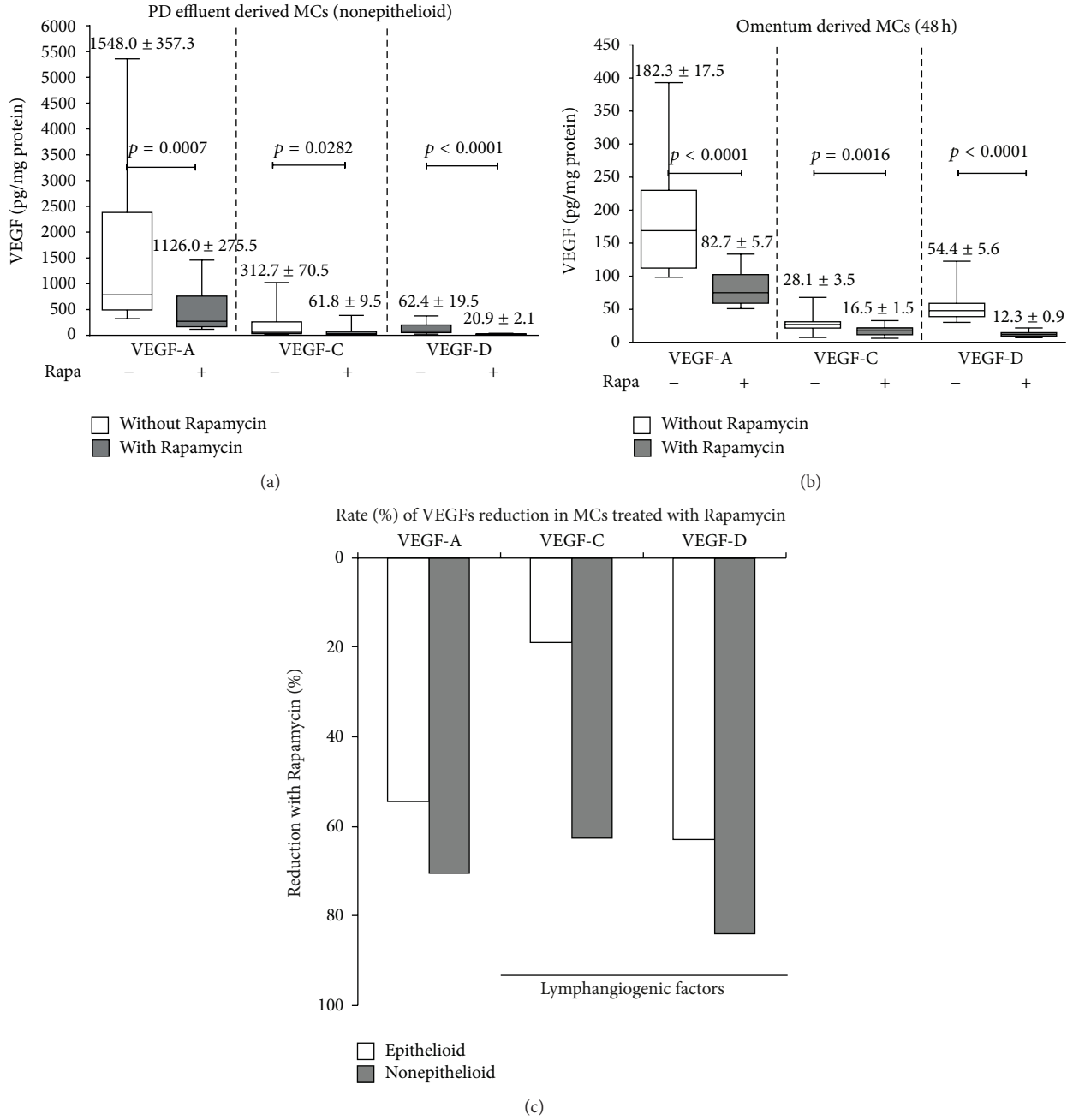

Figure 5: Rapamycin decreases the VEGF production by MCs. Omentum and PD effluent derived MCs were cultured and stimulated with Rapamycin 2 nM during 48 h. We performed two parallel cultures with equal numbers of MCs. A group received Rapamycin while the other was untreated. Supernatants were collected and VEGF-A, VEGF-C, and VEGF-D were measured. Rapamycin significantly decreased VEGFs, mainly the prolymphopenic VEGF-C and VEGF-D forms (a and b). We also calculated the reduction rate (%). Importantly in nonepithelioid MCs derived from PD effluent, VEGF-D was reduced by 82% and VEGF-C (gray bar graphic) by 63%. In omentum-derived MCs (white bar) the VEGF-D and VEGF-C were reduced by 63% and 20%, respectively (c). Box plots graphics represent 25th and 75th percentiles and median, minimum, and maximum values. Statistical differences between groups are shown (mean ± SD).

Figures 6(e)–6(h) show effluent derived MCs exposed to Rapamycin during 48 h. Rapamycin decreased α-SMA, collagen-I, fibronectin, and tubulin expression, suggesting that this drug not only reduces ECM but also decreases cellular protein synthesis in a dose-dependent manner (Figure 6(e)).

3.7. Rapamycin Blocked Cellular Proliferation and Protein Synthesis and Delayed Wound Heading. Given that Rapamycin downregulates tubulin expression, we wondered if this is due to a decrease in cell proliferation, decrease in protein synthesis, or cell death by toxicity or apoptosis. First, we confirmed that the decrease in tubulin expression was time- and

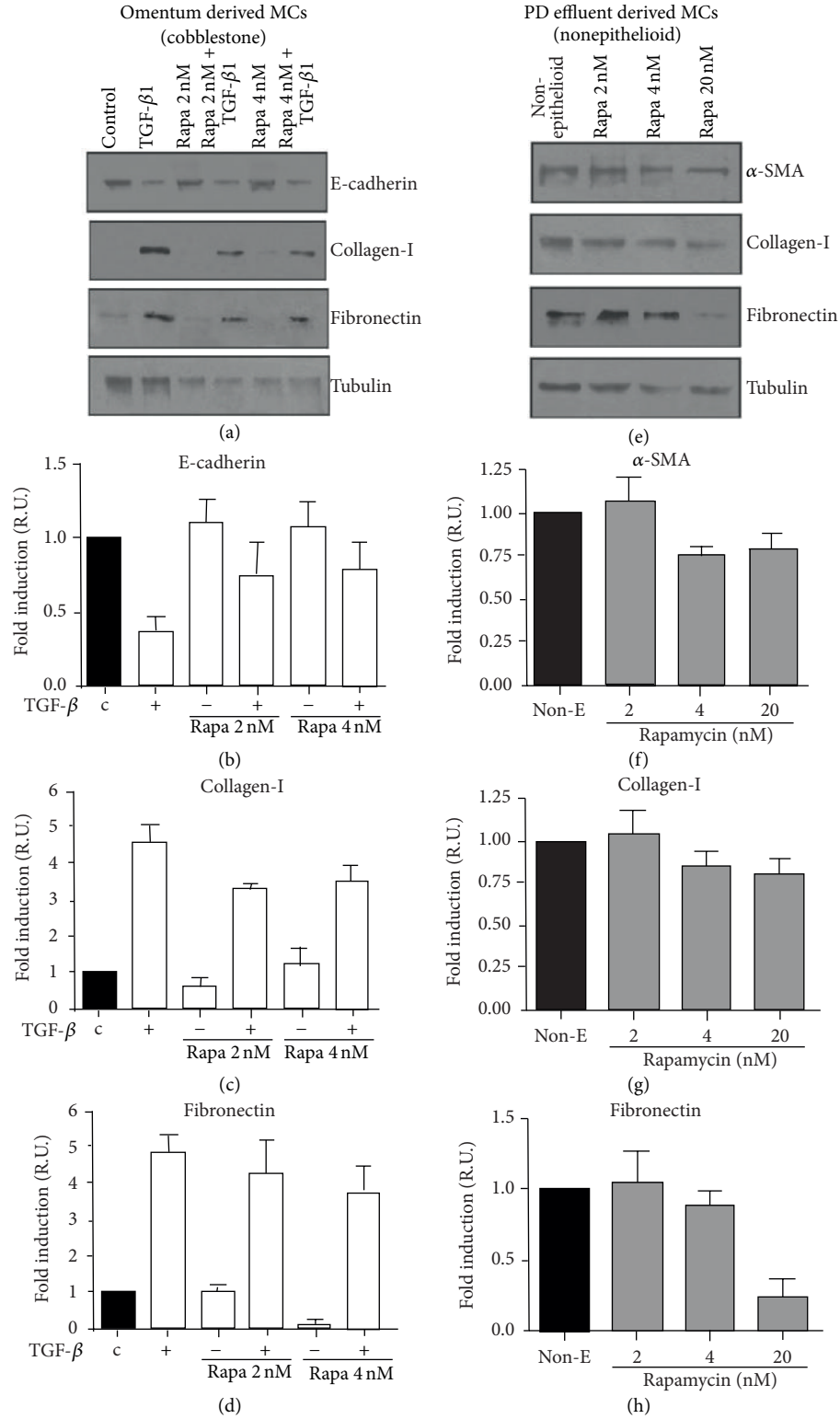

Figure 6: Rapamycin partially inhibits the MMT of MCs. (a–d) Omentum-derived MCs were treated or not with 1 ng/mL of TGF-β1 for 24 or 48 hours, in the presence of different doses of Rapamycin (2 and 4 nM). (a) Western blot analyses show that Rapamycin treatment prevents TGF-β1-induced E-cadherin downregulation as well as collagen I and fibronectin. (b) The E-cadherin expression was analyzed at 24 hours, whereas the expressions of (c) collagen-I and (d) fibronectin were analyzed at 48 hours of treatments. (e–h) Effect of Rapamycin on nonepithelioid phenotype MCs isolated from PD effluent (e) WB analysis in the presence of different Rapamycin's doses. Rapamycin inhibited the expression of (f) α-SMA, (g) Collagen-I, and (h) fibronectin expression in a dose-dependent manner (2, 4, and 20 nM). Results are presented relative to untreated MCs (black bars) which were arbitrarily assigned as value 1 (b to d and f to h). The experiments were repeated at least three times and results are depicted as means ± SE (bar graphics).

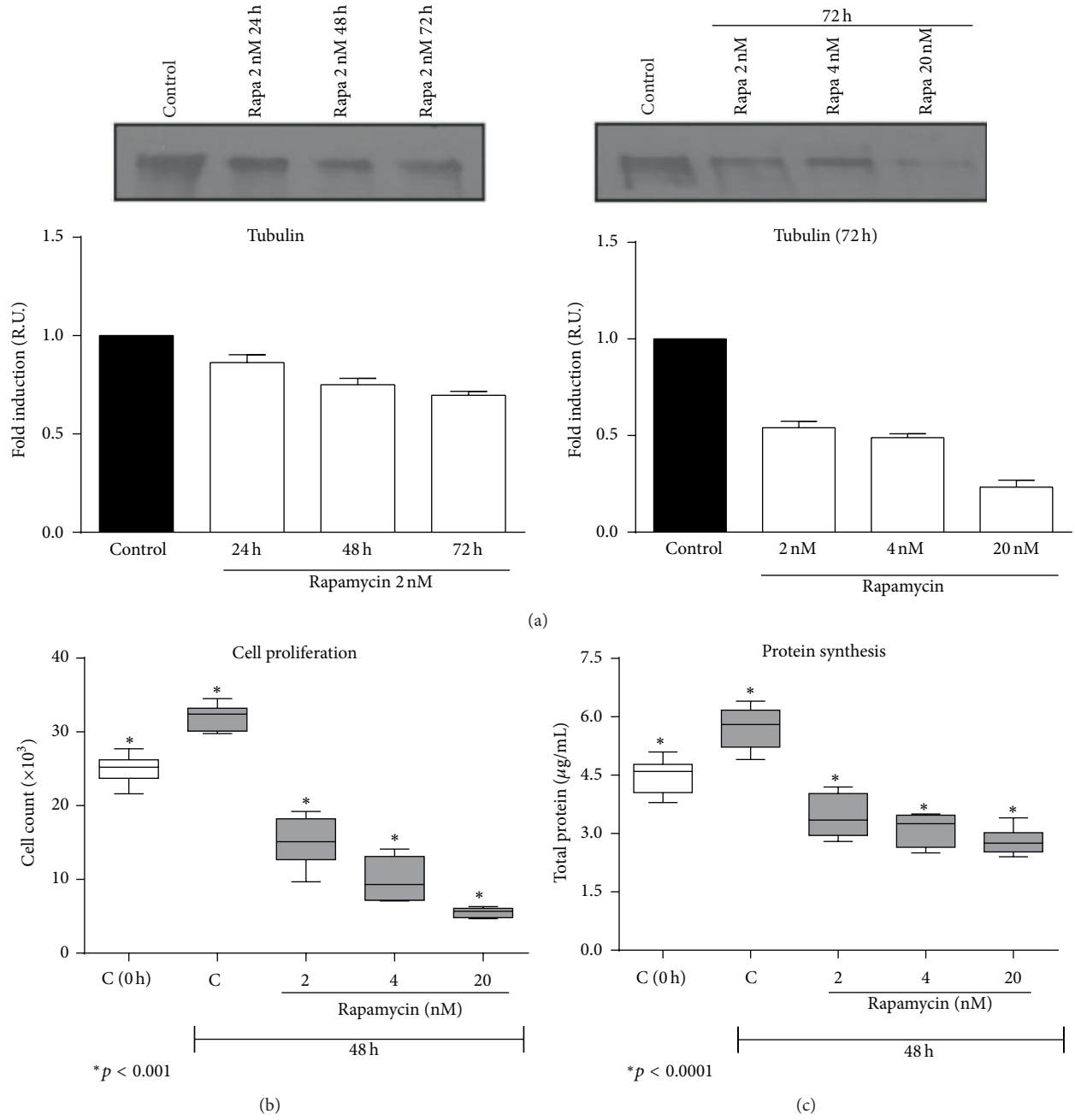

Figure 7: Rapamycin partially inhibited the MCs protein synthesis and MCs proliferation. (a) Rapamycin inhibits the tubulin expression in a time- and dose-dependent manner as shown in the Western blots analyses and their quantification graphics. Results are presented relative to untreated MCs (black bars) which were arbitrarily assigned as value 1. (b) MCs proliferation and (c) protein synthesis omentum cells cultured in semiconfluence. The first box represents baseline MCs (zero time). Second box shows the natural increases in MCs proliferation and protein synthesis at 48 h. The rest of the boxes show the decrease in both variables after the Rapamycin administration in a dose-dependent manner. In (b) and (c), one-way ANOVA analyses show a p value of $p < 0.001$ and $p < 0.0001$, respectively. Box plots represent the median, minimum, and maximum values, as well as the 25th and 75th percentiles.

dose-dependent (Figure 7(a)). Figure 7(b) shows the normal proliferation rate of MCs in subconfluence after 48 h in culture. This normal cell proliferation rate was blocked by Rapamycin, to levels even lower than those obtained in controls. A similar situation occurred with cell protein synthesis. When we analyzed the cell cycle (Table 1), Rapamycin increased the rate of MCs in resting (M1) and apoptosis (M4) and decreased MCs dividing DNA (M2). This effect also showed a dose-dependent pattern.

Supplementary Figure 2 in Supplementary Material available online at http://dx.doi.org/10.1155/2015/989560 shows the effect of time in culture and Rapamycin doses over cell

viability. Both factors decreased MCs life rate, but, in the worst case, dead MCs rate never exceeded 10%.

Given these results, we decided to explore the effect of Rapamycin over wound healing (WH). To close a wound it is necessary to maintain an adequate rate of cell proliferation, cell migration, and reproduction. As expected, Rapamycin delays WH to 72 hours showing again dose-dependent pattern (Supplementary Figure 3).

Table 1: Effect of Rapamycin on cell cycle on MC (%gated).

Cell cycle	Control	TGF-β	Rapa 2 nM	Rapa 4 nM	Rapa 20 nM
(M1)	75.77	76.34	78.97	79.74	79.98
(M2)	5.81	3.96	3.41	2.95	2.68
(M3)	15.01	16.19	13.93	13.36	13.22
(M4)	3.41	3.42	3.69	3.75	4.12

4. Discussion

In PD, type-I PM failure is characterized by progressive peritoneal thickening, inflammation, angiogenesis, and lymphangiogenesis, which ends in severe peritoneal fibrosis and peritoneal transport failure of water and solutes, shortening PM usefulness [24, 28].

To prevent PM damage, the main arrangement adopted so far has been to improve PDF biocompatibility (neutral pH or low GDPs). The administration of steroids, Tamoxifen, and some immunosuppressive drugs has become popular [29]. After promising results in animal and *in vitro* studies, the use of Rosiglitazone, COX_2 inhibitors (celecoxib), Statins, and anti-TGF-β molecules (among others) has been proposed [30, 31]. In many cases, the rationale for using these agents was MMT inhibition. MMT is responsible for a great number of submesothelial fibroblasts derived from transdifferentiated MCs, which perpetuate peritoneal fibrosis and also angiogenesis and lymphangiogenesis [3, 6], since these cells are active VEGF producers [10, 22]. As our results demonstrate, transdifferentiated MCs showed up to 10 times greater VEGF production than nontransdifferentiated MCs [6]. Clinically, it has been accepted that the composition of PDFs, with high content of glucose, GDPs, the osmolarity, low pH, and the formation of AGEs appear as the major inducers for VEGF release, directly or indirectly through the synthesis proinflammatory cytokines [2, 3, 24].

To our knowledge, few studies have considered VEGF as a therapeutic target for type-I PM failure preventing strategies. Rapamycin has traditionally been considered as an inhibitor of VEGF synthesis [12] and some successful clinical and animal experiences in treating EPS have been published [18, 32]. Herein, we present evidences for using Rapamycin as an antifibrotic and antiproliferative agent for blood and lymphatic vessels in PM failure.

Either after an acute (peritonitis) or chronic (long-term PDFs exposure) peritoneal aggression, a physiologic autocontrolled cellproliferation process occurs. However, in some cases this autocontrol is lost, leading to peritoneal fibrosis. The antifibrotic effect of mTOR inhibitors can be explained by a direct effect on cell cycle [33]. Rapamycin increases the rate of MCs in resting, apoptosis, and dead rate, and decreases MCs dividing DNA, as evidenced by our results (Table 1). Similarly, Xue et al. [23] demonstrated that Rapamycin binds the FK-binding protein 12, resulting in a complex that leads to phosphorylation and inactivation of p70S6 kinase, which normally has a stimulatory function in the production of ribosomal components necessary for protein synthesis and cell cycle, resulting in cell cycle arrest in G1 phase [33, 34].

Tulek et al. [35] demonstrated that, in pulmonary fibrosis, the antifibrotic effect of Rapamycin can be explained by an anti-inflammatory effect mediated by a decrease in IL-13 and platelet-derived growth factor- (PDGF-) A and TGF-β1 and an increase in interferon- (IFN-) γ levels in bronchoalveolar lavage fluid. Our results are in agreement with these findings, as Rapamycin decreased TNF-α and TGF-β in mice peritoneal effluent (Figure 4). We also found that Rapamycin treatment diminished the PM cellular infiltration.

Another anti-fibrotic pathway of Rapamycin is the partial or total inhibition of MMT. In normal conditions, TGF-β1 induces MMT through *Smads* dependent and independent pathways [36, 37]. Recently, Patel et al. [26] demonstrated that Rapamycin inhibited Smad-3 signalling, blocking MMT, and tissue peritoneal fibrosis in a PD mice model. During MMT, TGF-β activates mTORC1 (one of the two functionally distinct complexes in which mTOR is present). This results in an increase in protein synthesis, cell size, motility, and invasion. This translational regulation complements the Smad-dependent transcriptional regulation induced by TGF-β. The mTORC2 complex phosphorylates Akt, thus contributing to its activation, but its exact role in TGF-β-induced MMT remains to be discovered [38, 39].

Gao et al. [40] suggested that the protective mechanism of Rapamycin is Slug- and Akt/mTOR-dependent. Furthermore, the inhibition of cellular migration by metalloproteinase- (MMP-) 2 and MMP-9 blockade played a crucial role as antifibrotic and anti-MMT.

If we understand MMT as a physiological tissue repair process that needs an active MC cycle and active proliferation and migration, the effects of Rapamycin on both processes would delay tissue repair, but considering that in type-I PM failure peritoneal repair is uncontrolled and the process exerts an excessive proliferation, we could speculate that Rapamycin, used for short periods, could be a therapeutic alternative.

Another important anatomical change suffered by the PM in PD is submesothelial angiogenesis [6]. Although angiogenesis is supposed to participate in water peritoneal transport disorders, to our knowledge, it has never been considered as a therapeutic target itself. Our results indicate that Rapamycin inhibited the VEGF synthesis *in vitro* and *in vivo*. Consequently much less angiogenesis and lymphangiogenesis were found in the mice treated with PDF alone (Figure 2). In this group, peritoneal transport was altered compared to controls or Rapamycin-treated animals (Figure 3(c)). Another mechanism this drug has been related to is an inhibition of angiogenesis and fibrosis by HIF1α blockade [41]. However, we did not analyze this pathway in the present study.

Recent studies have shown that, in several fibrosing diseases, endothelial cells can also suffer a mesenchymal transdifferentiation (Endo-MT), generally commanded by similar signaling as MMT [8]. The importance of this process is given by its contribution to tissue fibrosis [42]. Herein, we found important evidence of submesothelial Endo-MT in PDF group, while in PDF + Rapamycin group this process was practically nonexistent (Figure 2).

Recently, Zhang et al. [43], using bleomycin to induce *in vitro* Endo-MT in HUVECs cells, observed mTOR activation, and Rapamycin reduced the rate of Endo-MT via Slug inhibition. Effectively, we observed preservation of E-cadherin and inhibition of Snail upregulation by Rapamycin, in MC cultures treated or not with TGF-β. Although in this study we only quantified Snail, both transcription factors (Snail and Slug) are intimately involved in the induction of the transdifferentiation process [42].

On the other hand our results indicate that Rapamycin inhibited the prolymphangiogenic VEGFs forms in MCs cultures. Lymphangiogenesis is a scarcely studied process in PD and its involvement in PD functional disorders has recently been recognized [25]. Generally, the lymphatic proliferation operates in parallel with fibrosis and MMT and its principal inductor is possibly TGF-β. TGF-β is activated in the peritoneal cavity by PDFs, AGEs, glucose, and proinflammatory cytokines [4] and is able to induce MMT, Endo-MT, fibrosis, and VEGF production (which induces blood and lymph vessels proliferation) [24]. In early stages of type-I PM failure, proliferation of both types of vessels could be responsible for hyperfiltration. In fact, in end-stages, when water and solute peritoneal transport fails, VEGF-C and podoplanin kept their overexpression in peritoneal tissue [25, 44].

Excessive lymphatic fluid drainage from the abdominal cavity can also raise concerns because of its potential role over macromolecule and isosmotic solutions reuptake, as well as convective reabsorption of solutes that were already cleared from plasma by diffusion [1, 45]. Our results show that the PDF group presented higher counts of blood and lymph vessels, which is normally associated with hyperfiltration. However, this group showed a lower UF rate (Figure 3(c)). This apparent contradiction is explained by the moment UF capacity was measured, because of the changing water transport speed during the dwell. This change is due to the functional alterations presented in the PM in the PDF-treated group (Supplementary Figure 1). Recently, Morelle et al. used fluorescent albumin and fluorescence spectroscopy to monitor the UF capacity of the PM in mice lacking the Aquaporin 1 (AQP1) (a water channel) [46]. Using this model they conclude that lymphatic absorption occur later, after 30 minutes of fluorescent marker intraperitoneal injection. However, this study was performed in mice with virgin peritoneum. With our data we cannot conclude that the maximum UF, which occurs early in the PDF group, could be caused by peritoneal lymphatic absorption; nevertheless, we can confirm that the anatomical changes (angiogenesis and fibrosis) in our mice after 30 days in PD play a key role in the peritoneal water transport.

Regarding the antilymphangiogenic mechanism of Rapamycin, we focused on the VEGFs forms levels and found that VEGF-C and VEGF-D decreased with Rapamycin treatment. Recently, Zheng et al. [11] demonstrated that normally the lymphatic proliferation starts with P13/AKT activation, which activates the mTOR pathway. The mTOR blockade (Rapamycin) acts through a dual effect, inhibiting this complex and interfering with VEGF-Receptor-3 and VEGF-C intracellular signaling [28, 47].

5. Conclusion

Rapamycin protected the PM through an antifibrotic and antiproliferative effect on blood and lymphatic vessels. It also inhibited Endo-MT and at least partially the MMT. Although this drug has been shown to delay the MCs proliferation, migration, cell cycle, and wound healing, by slowing peritoneal tissue repair, our results suggest that Rapamycin, given for short periods, could be beneficial to treat early stages of type-I PM failure.

Conflict of Interests

The authors declare that there is no conflict of interests regarding the publication of this paper.

Authors' Contribution

Guadalupe Tirma González-Mateo and Anna Rita Aguirre contributed equally to this work. Abelardo Aguilera and Georgios Liappas contributed equally to this work.

Acknowledgments

This work was supported by grant. This work was also partially supported by Grants PI 12/01175 from "Fondo de Investigaciones Sanitarias" (FIS), Instituto Carlos-III to Abelardo Aguilera, SAF2013-47611R from the "Ministerio de Economia y Competitividad", and S2010/BMD-2321 (FIBROTEAM Consortium) from "Comunidad Autónoma de Madrid" to Manuel López-Cabrera. This work was supported by European Union, Seventh Framework Program "EuTRiPD" under Grant agreement Marie Curie ITN-GA-2011-287813. The authors thank Carlos Gamallo for providing the anti-podoplanin antibody, Marta Ramírez, Laura García Ramírez, and Patricia Albar for the assistance in MCs culture, and Vanessa Fernández and Luiz Stark for the assistance with mouse experiments.

References

[1] R. T. Krediet, B. Lindholm, and B. Rippe, "Pathophysiology of peritoneal membrane failure," *Peritoneal Dialysis International*, vol. 20, supplement 4, pp. S22–S42, 2000.

[2] P. J. Margetts and P. Bonniaud, "Basic mechanisms and clinical implications of peritoneal fibrosis," *Peritoneal Dialysis International*, vol. 23, no. 6, pp. 530–541, 2003.

[3] L. S. Aroeira, A. Aguilera, J. A. Sánchez-Tomero et al., "Epithelial to mesenchymal transition and peritoneal membrane failure in peritoneal dialysis patients: pathologic significance and

potential therapeutic interventions," *Journal of the American Society of Nephrology*, vol. 18, no. 7, pp. 2004–2013, 2007.

[4] M. Yanez-Mo, E. Lara-Pezzi, R. Selgas et al., "Peritoneal dialysis and epithelial-to-mesenchymal transition of mesothelial cells," *The New England Journal of Medicine*, vol. 348, no. 5, pp. 403–413, 2003.

[5] J. A. Jiménez-Heffernan, A. Aguilera, L. S. Aroeira et al., "Immunohistochemical characterization of fibroblast subpopulations in normal peritoneal tissue and in peritoneal dialysis-induced fibrosis," *Virchows Archiv*, vol. 444, no. 3, pp. 247–256, 2004.

[6] L. S. Aroeira, A. Aguilera, R. Selgas et al., "Mesenchymal conversion of mesothelial cells as a mechanism responsible for high solute transport rate in peritoneal dialysis: role of vascular endothelial growth factor," *American Journal of Kidney Diseases*, vol. 46, no. 5, pp. 938–948, 2005.

[7] J. Loureiro, A. Aguilera, R. Selgas et al., "Blocking TGF-β1 protects the peritoneal membrane from dialysate-induced damage," *Journal of the American Society of Nephrology*, vol. 22, no. 9, pp. 1682–1695, 2011.

[8] S. Gurzu, S. Turdean, A. Kovecsi et al., "Epithelial-mesenchymal, mesenchymal-epithelial, and endothelial-mesenchymal transitions in malignant tumors: an update," *World Journal of Clinical Cases*, vol. 3, no. 5, pp. 393–404, 2015.

[9] S. Aoki, T. Takezawa, A. Oshikata-Miyazaki et al., "Epithelial-to-mesenchymal transition and slit function of mesothelial cells are regulated by the cross talk between mesothelial cells and endothelial cells," *American Journal of Physiology—Renal Physiology*, vol. 306, no. 1, pp. F116–F122, 2014.

[10] A. S. De Vriese, R. G. Tilton, C. C. Stephan, and N. H. Lameire, "Vascular endothelial growth factor is essential for hyperglycemia-induced structural and functional alterations of the peritoneal membrane," *Journal of the American Society of Nephrology*, vol. 12, no. 8, pp. 1734–1741, 2001.

[11] W. Zheng, A. Aspelund, and K. Alitalo, "Lymphangiogenic factors, mechanisms, and applications," *The Journal of Clinical Investigation*, vol. 124, no. 3, pp. 878–887, 2014.

[12] J. Li, S. G. Kim, and J. Blenis, "Rapamycin: one drug, many effects," *Cell Metabolism*, vol. 19, no. 3, pp. 373–379, 2014.

[13] D. J. Boffa, F. Luan, D. Thomas et al., "Rapamycin inhibits the growth and metastatic progression of non-small cell lung cancer," *Clinical Cancer Research*, vol. 10, no. 1, part 1, pp. 293–300, 2004.

[14] N. S. Dejneka, A. M. Kuroki, J. Fosnot, W. Tang, M. J. Tolentino, and J. Bennett, "Systemic rapamycin inhibits retinal and choroidal neovascularization in mice," *Molecular Vision*, vol. 10, pp. 964–972, 2004.

[15] Y. S. Kwon, H. S. Hong, J. C. Kim, J. S. Shin, and Y. Son, "Inhibitory effect of rapamycin on corneal neovascularization in vitro and in vivo," *Investigative Ophthalmology and Visual Science*, vol. 46, no. 2, pp. 454–460, 2005.

[16] W. Lieberthal and J. S. Levine, "The role of the mammalian target of rapamycin (mTOR) in renal disease," *Journal of the American Society of Nephrology*, vol. 20, no. 12, pp. 2493–2502, 2009.

[17] T. Xu, J. Y. Xie, W. M. Wang, H. Ren, and N. Chen, "Impact of rapamycin on peritoneal fibrosis and transport function," *Blood Purification*, vol. 34, no. 1, pp. 48–57, 2012.

[18] M. Ceri, S. Unverdi, M. Dogan et al., "Effect of sirolimus on the regression of peritoneal sclerosis in an experimental rat model," *International Urology and Nephrology*, vol. 44, no. 3, pp. 977–982, 2012.

[19] G. T. González-Mateo, J. Loureiro, J. A. Jiménez-Hefferman et al., "Chronic exposure of mouse peritoneum to peritoneal dialysis fluid: structural and functional alterations of the peritoneal membrane," *Peritoneal Dialysis International*, vol. 29, no. 2, pp. 227–230, 2009.

[20] J. Loureiro, P. Sandoval, G. del Peso et al., "Tamoxifen ameliorates peritoneal membrane damage by blocking mesothelial to mesenchymal transition in peritoneal dialysis," *PLoS ONE*, vol. 8, no. 4, Article ID e61165, 2013.

[21] M. López-Cabrera, A. Aguilera, L. S. Aroeira et al., "Ex vivo analysis of dialysis effluent-derived mesothelial cells as an approach to unveiling the mechanism of peritoneal membrane failure," *Peritoneal Dialysis International*, vol. 26, no. 1, pp. 26–34, 2006.

[22] A. W. D. Stavenuiter, M. N. Schilte, P. M. Ter Wee, and R. H. J. Beelen, "Angiogenesis in peritoneal dialysis," *Kidney and Blood Pressure Research*, vol. 34, no. 4, pp. 245–252, 2011.

[23] Q. Xue, J. A. Nagy, E. J. Manseau, T. L. Phung, H. F. Dvorak, and L. E. Benjamin, "Rapamycin inhibition of the Akt/mTOR pathway blocks select stages of VEGF-A164-driven angiogenesis, in part by blocking S6Kinase," *Arteriosclerosis, Thrombosis, and Vascular Biology*, vol. 29, no. 8, pp. 1172–1178, 2009.

[24] H. Kinashi, Y. Ito, M. Mizuno et al., "TGF-β1 promotes lymphangiogenesis during peritoneal fibrosis," *Journal of the American Society of Nephrology*, vol. 24, no. 10, pp. 1627–1642, 2013.

[25] J. Morelle, A. Sow, N. Hautem et al., "Interstitial fibrosis restricts osmotic water transport in encapsulating peritoneal sclerosis," *Journal of the American Society of Nephrology*, vol. 26, no. 10, pp. 2521–2533, 2015.

[26] P. Patel, Y. Sekiguchi, K.-H. Oh, S. E. Patterson, M. R. J. Kolb, and P. J. Margetts, "Smad3-dependent and-independent pathways are involved in peritoneal membrane injury," *Kidney International*, vol. 77, no. 4, pp. 319–328, 2010.

[27] A. Aguilera, L. S. Aroeira, M. Ramírez-Huesca et al., "Effects of rapamycin on the epithelial-to-mesenchymal transition of human peritoneal mesothelial cells," *International Journal of Artificial Organs*, vol. 28, no. 2, pp. 164–169, 2005.

[28] S. Huber, C. J. Bruns, G. Schmid et al., "Inhibition of the mammalian target of rapamycin impedes lymphangiogenesis," *Kidney International*, vol. 71, no. 8, pp. 771–777, 2007.

[29] G. Garosi, N. Mancianti, R. Corciulo, V. La Milia, and G. Virga, "Encapsulating peritoneal sclerosis," *Journal of Nephrology*, vol. 21, pp. 177–187, 2013.

[30] A. Aguilera, M. Yáñez-Mo, R. Selgas, F. Sánchez-Madrid, and M. López-Cabrera, "Epithelial to mesenchymal transition as a triggering factor of peritoneal membrane fibrosis and angiogenesis in peritoneal dialysis patients," *Current Opinion in Investigational Drugs*, vol. 6, no. 3, pp. 262–268, 2005.

[31] M. R. Korte, M. W. Fieren, D. E. Sampimon, H. F. Lingsma, W. Weimar, and M. G. H. Betjes, "Tamoxifen is associated with lower mortality of encapsulating peritoneal sclerosis: results of the Dutch Multicentre EPS study," *Nephrology Dialysis Transplantation*, vol. 26, no. 2, pp. 691–697, 2011.

[32] G. M. Frascà, M. D'Arezzo, A. M. Ricciatti et al., "m-TOR inhibitors may be useful in the treatment of encapsulating peritoneal sclerosis (EPS)," *Journal of Nephrology*, vol. 27, no. 5, pp. 587–590, 2014.

[33] A. Chatterjee, S. Mukhopadhyay, K. Tung, D. Patel, and D. A. Foster, "Rapamycin-induced G1 cell cycle arrest employs both TGF-β and Rb pathways," *Cancer Letters*, vol. 360, no. 2, pp. 134–140, 2015.

[34] D. C. Fingar and J. Blenis, "Target of rapamycin (TOR): an integrator of nutrient and growth factor signals and coordinator of cell growth and cell cycle progression," *Oncogene*, vol. 23, no. 18, pp. 3151–3171, 2004.

[35] B. Tulek, E. Kiyan, H. Toy, A. Kiyici, C. Narin, and M. Suerdem, "Anti-inflammatory and anti-fibrotic effects of sirolimus on bleomycininduced pulmonary fibrosis in rats," *Clinical and Investigative Medicine*, vol. 34, no. 6, pp. E341–E348, 2011.

[36] P. Bonniaud, P. J. Margetts, K. Ask, K. Flanders, J. Gauldie, and M. Kolb, "TGF-β and Smad3 signaling link inflammation to chronic fibrogenesis," *The Journal of Immunology*, vol. 175, no. 8, pp. 5390–5395, 2005.

[37] A. N. Kothari, Z. Mi, M. Zapf, and P. C. Kuo, "Novel clinical therapeutics targeting the epithelial to mesenchymal transition," *Clinical and Translational Medicine*, vol. 3, article 35, 2014.

[38] S. Lamouille and R. Derynck, "Emergence of the phosphoinositide 3-kinase-Akt-mammalian target of rapamycin axis in transforming growth factor-beta-induced epithelial-mesenchymal transition," *Cells Tissues Organs*, vol. 193, no. 1-2, pp. 8–22, 2011.

[39] S. Lamouille and R. Derynck, "Cell size and invasion in TGF-β-induced epithelial to mesenchymal transition is regulated by activation of the mTOR pathway," *Journal of Cell Biology*, vol. 178, no. 3, pp. 437–451, 2007.

[40] H. Gao, J. Zhang, T. Liu, and W. Shi, "Rapamycin prevents endothelial cell migration by inhibiting the endothelial-to-mesenchymal transition and matrix metalloproteinase-2 and -9: an in vitro study," *Molecular Vision*, vol. 17, pp. 3406–3414, 2011.

[41] Y. Sekiguchi, J. Zhang, S. Patterson et al., "Rapamycin inhibits transforming growth factor beta-induced peritoneal angiogenesis by blocking the secondary hypoxic response," *Journal of Cellular and Molecular Medicine*, vol. 16, no. 8, pp. 1934–1945, 2012.

[42] W. Yu, Z. Liu, S. An et al., "The endothelial-mesenchymal transition (EndMT) and tissue regeneration," *Current Stem Cell Research & Therapy*, vol. 9, no. 3, pp. 196–204, 2014.

[43] W. Zhang, G. Chen, J.-G. Ren, and Y.-F. Zhao, "Bleomycin induces endothelial mesenchymal transition through activation of mTOR pathway: a possible mechanism contributing to the sclerotherapy of venous malformations," *British Journal of Pharmacology*, vol. 170, no. 6, pp. 1210–1220, 2013.

[44] N. Braun, M. D. Alscher, P. Fritz et al., "The spectrum of podoplanin expression in encapsulating peritoneal sclerosis," *PLoS ONE*, vol. 7, no. 12, Article ID e53382, p. 31, 2012.

[45] J. Stachowska-Pietka, J. Waniewski, M. F. Flessner, and B. Lindholm, "Distributed model of peritoneal fluid absorption," *American Journal of Physiology—Heart and Circulatory Physiology*, vol. 291, no. 4, pp. H1862–H1874, 2006.

[46] J. Morelle, A. Sow, D. Vertommen, F. Jamar, B. Rippe, and O. Devuyst, "Quantification of osmotic water transport in vivo using fluorescent albumin," *The American Journal of Physiology—Renal Physiology*, vol. 307, no. 8, pp. F981–F989, 2014.

[47] Y. Luo, L. Liu, D. Rogers et al., "Rapamycin inhibits lymphatic endothelial cell tube formation by downregulating vascular endothelial growth factor receptor 3 protein expression," *Neoplasia*, vol. 14, no. 3, pp. 228–237, 2012.

Hindawi Publishing Corporation
BioMed Research International
Volume 2015, Article ID 431092, 7 pages
http://dx.doi.org/10.1155/2015/431092

Review Article

Overcoming the Underutilisation of Peritoneal Dialysis

Jernej Pajek

Department of Nephrology, University Medical Centre Ljubljana, Zaloška 2, SI-1525 Ljubljana, Slovenia

Correspondence should be addressed to Jernej Pajek; jernej.pajek@mf.uni-lj.si

Received 21 May 2015; Accepted 20 October 2015

Academic Editor: Peter Rutherford

Peritoneal dialysis is troubled with declining utilisation as a form of renal replacement therapy in developed countries. We review key aspects of therapy evidenced to have a potential to increase its utilisation. The best evidence to repopulate PD programmes is provided for the positive impact of timely referral and systematic and motivational predialysis education: average odds ratio for instituting peritoneal dialysis versus haemodialysis was 2.6 across several retrospective studies on the impact of predialysis education. Utilisation of PD for unplanned acute dialysis starts facilitated by implantation of peritoneal catheters by interventional nephrologists may diminish the vast predominance of haemodialysis done by central venous catheters for unplanned dialysis start. Assisted peritoneal dialysis can improve accessibility of home based dialysis to elderly, frail, and dependant patients, whose quality of life on replacement therapy may benefit most from dialysis performed at home. Peritoneal dialysis providers should perform close monitoring, preventing measures, and timely prophylactic therapy in patients judged to be prone to EPS development. Each peritoneal dialysis programme should regularly monitor, report, and act on key quality indicators to manifest its ability of constant quality improvement and elevate the confidence of interested patients and financing bodies in the programme.

1. Introduction

Over the last 15 years the proportion of all dialysis patients treated with peritoneal dialysis (PD) declined significantly in developed countries [1]. Slovenia is a good example of such a negative trend with the numbers of PD patients dropping significantly in the period from 2004 to 2014 (Figure 1).

A general shift towards a higher age at start of dialysis treatment and increasing comorbidity cannot in whole explain the causality of this problem [2]. Other possible factors affecting declining PD utilisation are proliferation of haemodialysis (HD) units and private dialysis provider penetration in some healthcare systems, both factors being associated with lower use of PD [3, 4]. Further impact on PD penetration may have come from insufficient patient education and physician bias [5]. A special concern with reducing numbers of patients is a possible (and probable) decrement in experience, expertise, and quality of PD programmes including the loss in quantity and quality of training for medical staff (physicians and nurses). Data from the USA raised concerns that there are an insufficient number of PD patients and allocation of time available for trainees in PD [6]. This may cause a further decline in PD utilisation thus starting a negative spiral for this dialysis modality.

The fall in PD utilisation is a concern since PD is a precious renal replacement modality that offers patients the convenience of home treatment, flexible schedule and increased freedom perception, less haemodynamic instability issues, and higher quality of life [7]. PD abolishes the inconvenience and costs of patient transport associated with in-centre haemodialysis. Further benefits of PD are associated with residual renal function preservation [8], lower hospitalisation and access intervention rates [9, 10], and perhaps better short-term outcome after transplantation [11, 12]. PD is able to provide equal outcomes as haemodialysis [13] and it may save lives when vascular access is exhausted. It is clear that the fall in utilisation of PD should be prevented; however there is no clear consensus on the actions that have to be taken and the responsibility of the governing bodies for implementation of these actions. Here we present several key opportunities and strategies for revitalisation of PD programmes with a special emphasis on their feasibility and published evidence.

Table 1: Summary of studies on the impact of predialysis education in modality choice.

Reference	Study type (number of patients)	Number of patients with structured/timely educational intervention versus controls	Modality choice (PD versus HD)
Ahlmén et al., 1993 [67]	Retrospective single-centre cohort ($N = 101$)	N/A (all patients invited to education)	38% chose PD versus 24% choosing HD
Prichard, 1996 [68]	Retrospective single-centre cohort ($N = 150$)	N/A (all patients exposed to an extensive education programme)	Of 74 patients with a free modality choice 50% chose PD
Little et al., 2001 [69]	Retrospective single-centre cohort ($N = 254$)	65% with timely counselling versus 35% counselled at or after dialysis start	50.9% chose PD versus 34.8% of controls
Marrón et al., 2005 [70]	Retrospective multicentre observational ($N = 626$)	37% versus 63%	31% chose PD versus 8.3% of controls
Ribitsch et al., 2013 [71]	Retrospective single-centre cohort ($N = 227$)	30.8% versus 69.2%	54.3% chose PD versus 28% of controls

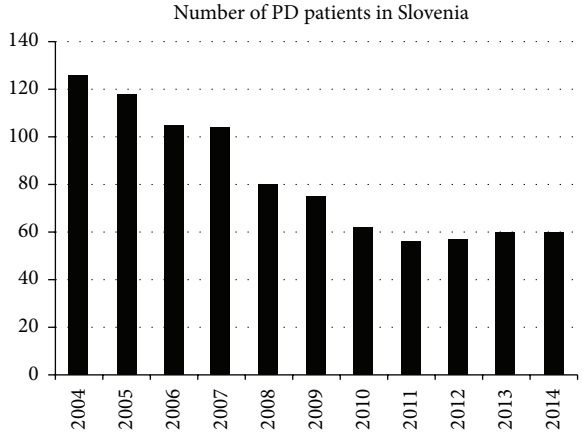

Figure 1: Dropping number of PD patients in the example of Slovenia's national PD cohort for the time period from 2004 to 2014.

2. Timely Referral and Predialysis Education

In Europe there is a domination of haemodialysis (HD) as a starting modality in late-referred chronic kidney disease (CKD) patients [14]. Late referral is associated with several well-known detrimental factors in advanced CKD: lost opportunity to slow CKD progression and to properly relieve CKD complications [15–17], lower rate of transplantation [18], deprivation of a proper choice of dialysis modality, and higher mortality [14, 19]. Prevention of late referral should include actions on a patient social level (improvement in education and income level, proper health insurance) and health-system levels (improvement of communication between referring physicians and nephrologists, education of referring physicians about the appropriate timing of referral), since these two categories of factors are both associated with late referral [20]. Since predialysis education may be associated with improved survival [21, 22], one of the most important additional benefits of timely referral is the opportunity for execution of a proper predialysis education.

A significant impact of predialysis education or timely referral on the choice of peritoneal dialysis is shown in the summary in Table 1. Motivating patients to start with peritoneal dialysis takes time and persuasive talent from the dialysis team and confidence and comprehension from the patient, which are all often absent in the late-referred patients [23]. As shown in Table 1 the impact of intensive or at least timely education and information on modality choice has so far only been demonstrated in retrospective studies. However with all the information about the benefits of timely predialysis referral, counselling, and education, undertaking the prospective randomised trial would seem unnecessary and unethical. The observational studies have been consistently showing that with predialysis education the proportion of patients choosing peritoneal dialysis increased and reached relatively high levels. An overview of data in Table 1 shows that the average odds ratio of choosing PD versus HD with timely predialysis education is 2.6 across the cited studies.

3. Unplanned Acute Start of Peritoneal Dialysis

Unplanned and suboptimal initiation is the term proposed to include dialysis initiation in hospital and/or with a central venous catheter (CVC) and/or with a patient not starting on their chronic modality of choice [24]. Rates of unplanned starts of dialysis are reported to be in the range of 24–49% in the survey of eight European studies [24]. Except for the units with established teams with skills for acute unplanned start of PD, the vast majority of unplanned cases are managed by placing a CVC and the first dialysis setting that these patients experience is a HD unit. It is a commonly held perception that once started on HD, the patients have a tendency to continue with this modality and there are a significantly lower number

of patients treated with PD than HD even after clinical stabilisation in unplanned dialysis starters [25]. Although at least part of excess mortality risk for HD patients dialysed through CVCs may be attributable to inferior catheter based vascular access [26], substantial number of patients may rely on this vascular access even after several months as the median time to fistula use from dialysis start may be more than 4 months [27]. On the other hand, units with established acute-start PD programmes can offer patients an alternative way to start dialysis treatment; however such a programme needs careful planning, dedication, and skills to be successful.

Acute unplanned start of peritoneal dialysis is generally offered to patients in two clinical scenarios: the patient had previously been given some information on dialysis modality and he opted for PD before the unexpected fast deterioration in kidney function happened or after a brief discussion in the hospital about the renal replacement modalities the patient finds peritoneal dialysis acceptable. Provided there is no uremic encephalopathy, pericarditis or colitis, severe hyperkalemia or pulmonary congestion, or another factor demanding dialysis sooner than within 48 hours, acute unplanned start of peritoneal dialysis is a feasible, effective, and safe option.

The PD catheter should be placed as soon as possible and an early start of PD with low fill volumes (750–1000 mL), automated PD tidal regime with a cycler in supine position can be started. The treatment time is variable, from 6 to 12 hours [28]. With such a start the proportion of early leaks along the catheter was reported to be 7.7% (4 out of 52 patients) and the total incidence of catheter dysfunction was 15.4% as compared to 5.8% in the control group with PD start at least 12 days after PD catheter placement [29]. The current practice of delaying the PD start for at least 2 weeks after catheter implantation (but for most patients clinicians may try to wait for 4–6 weeks) is based on a low level of evidence and currently there is a randomised research study in flow comparing the early start of PD 7 days after catheter insertion to later time points of PD start [30]. Early start of peritoneal dialysis enables increased utilisation of peritoneal dialysis in suboptimal initiation conditions and offers an escape from the complications associated with interim HD and presence of CVCs [27].

4. Peritoneal Catheter Insertion by Nephrologists

Dedicated catheter insertion team available 24/7 is the necessary condition for acute unplanned start of peritoneal dialysis. If there is an experienced and dedicated nephrologist performing catheter insertions available at the dialysis unit many logistic and operative schedule barriers for PD catheter insertion (such as competition for limited procedural rooms) may be more easily tackled. The set-up of interventional nephrology catheter insertion service was reported to enable growth of PD programmes [31]. The inclusion of interventional nephrologist catheter placement in the integrated care approach to dialysis start has resulted in a relatively large PD penetration of 44.8% in one of the reports [32]. Another study reported an increase in the prevalence of PD from the relative share of 16–18% to 22–32% [33]. Catheter implantation by nephrologists compared to surgical or radiological services was associated with higher rates of successfully finalised peritoneal dialysis utilisation in patients undergoing elective PD catheter insertion [34]. The Brazilian experience has shown similar outcomes and success of catheter implantation by interventional nephrologists and surgeons [35]. On the other hand the opinion has been expressed that the placement of PD catheters should optimally be done by surgeons using advanced laparoscopic techniques [36] due to ability to perform rectus sheath tunnelling, omentopexy, and adhesiolysis [37] making this issue a controversial one.

At some dialysis centres (including the author's) there are a long-term experience and positive results with divided care for establishment of vascular access for HD between interventional nephrologists and vascular surgeons (the bulk of operations being performed by interventional nephrologists [38]). It may be that such a model could prove to be optimal also for peritoneal access, the interventional nephrologists taking care of first implantation in cases without expected complications or adhesions and abdominal surgeons performing the access in demanding cases necessitating laparoscopy, adhesiolysis, hernia repair, cholecystectomy, and other cases necessitating general anaesthesia. In any case, PD programme leaders should gain good support for establishment of interventional nephrology service in PD catheter placement from hospital managers, lead clinicians, surgical teams, and the practicing nephrology team. With this it will be possible to train devoted nephrologists and maintain the number of procedures necessary for maintenance of skill and service quality.

5. Assisted Peritoneal Dialysis for Frail and Dependant Patients

The patient population reaching end-stage CKD is growing in age, frailty, comorbidity, and dependance. This is one of the major obstacles for institution of PD as it is a form of self-delivered home based therapy. The overwhelming association of having a strong social support network and being functionally able with choosing PD emphasizes the need for assisted PD [39]. The French experience published in 2006 has shown that patients on assisted PD were on average 74 years old, 22 years older than others, and had higher comorbidity and hospitalisation rate [40]. A Canadian survey has shown that the most prevalent conditions that act as barriers to self-care PD in elderly patients are exactly the ones that can be overcome by home assistance: decreased strength to lift PD bags, decreased dexterity or vision, anxiety, decreased cognition, and immobility [41]. In this study the probability of being considered eligible for PD significantly increased in the regions with home care assistance programme available. The indications for assisted PD use may be broadened from patients with physical and cognitive disabilities to patients with exhausted vascular access and haemodynamic instability during HD, thus likely extending the lives of those patients [42]. The possibility of assisted

PD and family support was shown to increase PD utilisation from 23 to 39% among patients with barriers to self-care in a Canadian centre [43]. Technique failure and peritonitis rates were in general within acceptable limits and independent of the method of assistance (done by either nurses or family members) [44, 45]. The possibility of having periods without assistance (e.g., the family provides assistance on weekends or helps with disconnections) enables assisted PD to become more cost-effective although elevated costs of reimbursed nursing assistance are a serious concern [46]. Training of staff at nursing homes for PD delivery is an additional area of a possible increment in utilisation of PD.

6. Encapsulating Peritoneal Sclerosis Prevention

"There is no evidence to withhold PD as a treatment option because of fear of development of EPS" was the final conclusion of an ISPD statement on length of time on PD and encapsulating peritoneal sclerosis (EPS) [47]. Although the major opinion has diverged from the proposal that simple peritoneal sclerosis is just a stage towards the development of EPS and if left enough time, all patients would sooner or later develop EPS [48], there is still doubt and anecdotal communication between nephrologists still reflects the fear of EPS as one of the major unavoidable detrimental factors when considering starting or maintaining patients on PD. The concept of "expiry date" for PD after 5 or so years still seems viable among nephrologists. So the crucial question to overcome this fear is this: what can we offer our patients on PD to prevent EPS?

The usage of new biocompatible solutions is associated with stabilisation of peritoneal transport rate [49], lower peritonitis rates [50], and improved histology with less fibrosis and vascular sclerosis [51, 52]. These are all risk factors associated with emergence of EPS, so the usage of biocompatible solutions might be one way towards reducing the risk of this complication. Lowering the peritoneal glucose exposure is a prudent task to ensure stability of peritoneal membrane [53] and protecting residual renal function may help in accomplishing this goal. The inhibition of renin-angiotensin system is additional therapy that should probably be offered to all PD patients that tolerate this treatment, due to its protective effects on the actions of transforming growth factor-beta [54], aldosterone, and deposition of collagen [55] and plasminogen activator inhibitor-1 level [56]. Beta-blockers should perhaps be excluded from the antihypertensive therapy [57].

After 4-5 years of treatment, the patients who are identified as EPS prone (increasing speed of peritoneal transport, severe infectious peritonitis with haematoperitoneum, overexposure to glucose, or ultrafiltration failure) may be treated with prophylactic tamoxifen [48, 58] and glucocorticoids in cases of sterile inflammatory peritoneal syndrome manifestations (unspecific abdominal pain, modestly elevated inflammatory markers (i.e., CRP) without another apparent cause, and worsening of nutritional status). An additional measure in long-term PD patients at EPS risk is the possibility of combining PD and HD therapy, to lower the glucose exposure, and avoiding abrupt termination of PD, which is a known possible second hit in the two-hit hypothesis of EPS development [59]. In EPS prone patients after renal transplantation, early minimisation or discontinuation of calcineurin inhibitors, institution of mTOR inhibitors, and maintaining glucocorticoids for at least 6–12 months are suggested as the best immunosuppressive strategy [60].

To properly monitor the patients on PD regular measurement of peritoneal membrane transport status is recommended. In patients with consistent rise in the speed of small solute transport, effluent carcinomic antigen-125 (CA-125) and interleukin-6 (IL-6) can be monitored as well [61]. The combination of longer time on PD (above 4-5 years), with sustained rise in speed of transport (D/P for creatinine), effluent IL-6, and a fall in effluent CA-125 should prompt the clinician to perform imaging study (CT scan is the current imaging technique of choice) and to consider prophylactic therapy and a possible conversion to HD. Before converting to HD great emphasis must be put on establishing vascular access since in general patients converted to HD via CVCs tend to do worse than patients staying on PD [62]. In patients not in fibrotic EPS phase, the Japanese authors propose maintaining the PD catheter and performing peritoneal lavage to offer an escape from additional "hit" of catheter removal and opportunity to monitor effluent levels of fibrin, IL-6, and CA-125. This is used to judge the success of prophylactic therapy and to more easily decide on the proper timing of catheter removal, when the levels of inflammatory markers in the effluent decrease [63, 64].

7. Constant Quality Monitoring and Improvement

There are several key parameters which are universally accepted as quality of service indicators in the field of peritoneal dialysis. Peritonitis rates below 1 episode in 18 patient-months [65] and *Staphylococcus aureus* catheter infection rates below 1 in 240 patient-months [66] are well established minimal quality indicators. PD programmes may wish to regularly monitor and act on some additional indicators such as technique failure and its causes, peritoneal infection causative agents and their susceptibility to antibiotics, mean haemoglobin levels and epoetin usage, mean phosphate serum levels, and perhaps EPS incidence. PD programmes able to manifest their updated results and quality indicators may be more easily benchmarked and be able to express a larger self-confidence in predialysis information given to patients. This would also help to balance physician and nurse bias towards HD. A PD programme with satisfactory and constantly improving quality indicators can be more readily and boldly advertised as a viable and good option for renal replacement therapy.

8. Conclusion

PD should be regarded as a safe and efficient form of renal replacement modality; however the declining numbers of

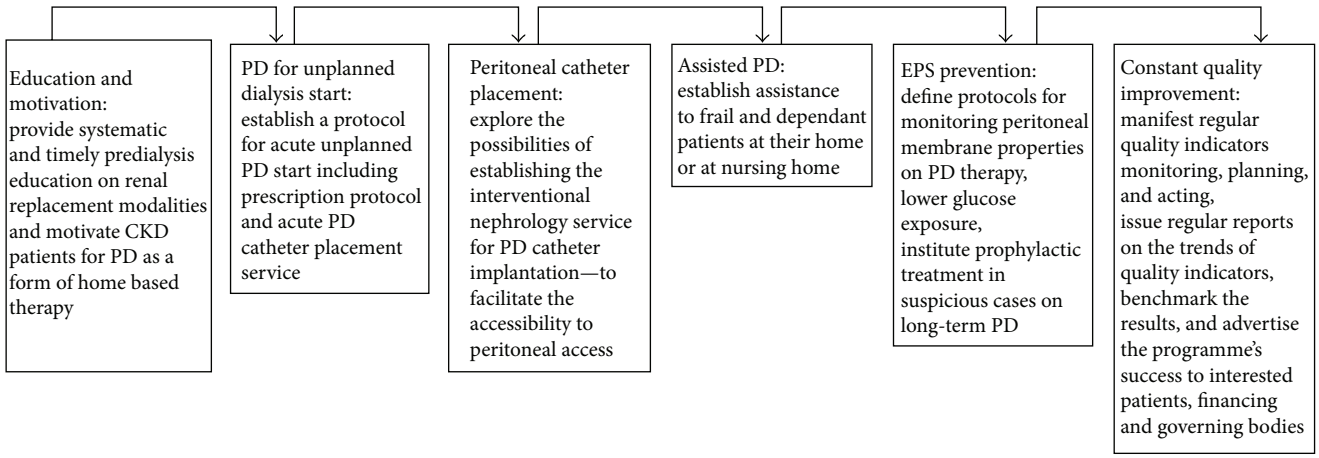

Figure 2: Summary of key steps in overcoming the underutilisation of peritoneal dialysis programmes.

patients in PD programmes in developed countries are a cause for concern. Several strategies summarized in Figure 2 can be pursued to reverse this unfavourable course. Timely referral and proper predialysis education are two crucial factors with the largest potential to repopulate PD programmes. Clinicians should consider using PD not only in planned but also for unplanned-suboptimal dialysis starts. This would be possible and easier in units having interventional nephrologists providing catheter implantation service. The possibility of offering assisted peritoneal dialysis to elderly frail patients should be a part of a modern PD programme, since these are the patients whose quality of life on replacement therapy may benefit most from assisted modality performed at patient's home. The concept of "expiry date for PD" should be abandoned and replaced by the close monitoring, preventing measures, and timely prophylactic therapy in patients judged to be prone to EPS development. The PD programmes should regularly monitor, report, and act on key quality indicators which would give them a higher level of confidence towards not only interested patients seeking optimal renal replacement care, but funding and governing authorities as well.

Conflict of Interests

The author declares no conflict of interests in association with this work.

References

[1] A. K. Jain, P. Blake, P. Cordy, and A. X. Garg, "Global trends in rates of peritoneal dialysis," *Journal of the American Society of Nephrology*, vol. 23, no. 3, pp. 533–544, 2012.

[2] C. van Walraven, D. G. Manuel, and G. Knoll, "Survival trends in ESRD patients compared with the general population in the United States," *American Journal of Kidney Diseases*, vol. 63, no. 3, pp. 491–499, 2014.

[3] P. Blake, "Proliferation of hemodialysis units and declining peritoneal dialysis use: an international trend," *American Journal of Kidney Diseases*, vol. 54, no. 2, pp. 194–196, 2009.

[4] W. H. Hörl, F. de Alvaro, and P. F. Williams, "Healthcare systems and end-stage renal disease (ESRD) therapies—an international review: access to ESRD treatments," *Nephrology Dialysis Transplantation*, vol. 14, supplement 6, pp. 10–15, 1999.

[5] A. R. Nissenson, S. S. Prichard, I. K. P. Cheng et al., "Non-medical factors that impact on ESRD modality selection," *Kidney International*, vol. 40, pp. S120–S127, 1993.

[6] R. Mehrotra, P. Blake, N. Berman, and K. D. Nolph, "An analysis of dialysis training in the United States and Canada," *American Journal of Kidney Diseases*, vol. 40, no. 1, pp. 152–160, 2002.

[7] K. Chaudhary, H. Sangha, and R. Khanna, "Peritoneal dialysis first: rationale," *Clinical Journal of the American Society of Nephrology*, vol. 6, no. 2, pp. 447–456, 2011.

[8] A. Y.-M. Wang and K.-N. Lai, "The importance of residual renal function in dialysis patients," *Kidney International*, vol. 69, no. 10, pp. 1726–1732, 2006.

[9] M. J. Oliver, M. Verrelli, J. M. Zacharias et al., "Choosing peritoneal dialysis reduces the risk of invasive access interventions," *Nephrology Dialysis Transplantation*, vol. 27, no. 2, pp. 810–816, 2012.

[10] R. R. Quinn, P. Ravani, X. Zhang et al., "Impact of modality choice on rates of hospitalization in patients eligible for both peritoneal dialysis and hemodialysis," *Peritoneal Dialysis International*, vol. 34, no. 1, pp. 41–48, 2014.

[11] R. Vanholder, P. Heering, A. Van Loo et al., "Reduced incidence of acute renal graft failure in patients treated with peritoneal dialysis compared with hemodialysis," *American Journal of Kidney Diseases*, vol. 33, no. 5, pp. 934–940, 1999.

[12] M. Z. Molnar, R. Mehrotra, U. Duong et al., "Dialysis modality and outcomes in kidney transplant recipients," *Clinical Journal of the American Society of Nephrology*, vol. 7, no. 2, pp. 332–341, 2012.

[13] R. Mehrotra, Y.-W. Chiu, K. Kalantar-Zadeh, J. Bargman, and E. Vonesh, "Similar outcomes with hemodialysis and peritoneal dialysis in patients with end-stage renal disease," *Archives of Internal Medicine*, vol. 171, no. 2, pp. 110–118, 2011.

[14] N. Lameire and W. Van Biesen, "The pattern of referral of patients with end-stage renal disease to the nephrologist—a European survey," *Nephrology Dialysis Transplantation*, vol. 14, supplement 6, pp. 16–23, 1999.

[15] P. Arora, G. T. Obrador, R. Ruthazer et al., "Prevalence, predictors, and consequences of late nephrology referral at a tertiary

care center," *Journal of the American Society of Nephrology*, vol. 10, no. 6, pp. 1281–1286, 1999.

[16] O. Ifudu, M. Dawood, P. Homel, and E. A. Friedman, "Excess morbidity in patients starting uremia therapy without prior care by a nephrologist," *American Journal of Kidney Diseases*, vol. 28, no. 6, pp. 841–845, 1996.

[17] R. Pérez-García, A. Martín-Malo, J. Fort et al., "Baseline characteristics of an incident haemodialysis population in Spain: results from ANSWER—a multicentre, prospective, observational cohort study," *Nephrology Dialysis Transplantation*, vol. 24, no. 2, pp. 578–588, 2009.

[18] A. Cass, J. Cunningham, P. Snelling, and J. Z. Ayanian, "Late referral to a nephrologist reduces access to renal transplantation," *American Journal of Kidney Diseases*, vol. 42, no. 5, pp. 1043–1049, 2003.

[19] S. M. Chandna, J. Schulz, C. Lawrence, R. N. Greenwood, and K. Farrington, "Is there a rationale for rationing chronic dialysis? A hospital based cohort study of factors affecting survival and morbidity," *British Medical Journal*, vol. 318, no. 7178, pp. 217–223, 1999.

[20] S. D. Navaneethan, S. Aloudat, and S. Singh, "A systematic review of patient and health system characteristics associated with late referral in chronic kidney disease," *BMC Nephrology*, vol. 9, article 3, 2008.

[21] G. M. Devins, D. C. Mendelssohn, P. E. Barré, K. Taub, and Y. M. Binik, "Predialysis psychoeducational intervention extends survival in CKD: a 20-year follow-up," *American Journal of Kidney Diseases*, vol. 46, no. 6, pp. 1088–1098, 2005.

[22] D. H. Kim, M. Kim, H. Kim et al., "Early referral to a nephrologist improved patient survival: prospective cohort study for end-stage renal disease in Korea," *PLoS ONE*, vol. 8, no. 1, Article ID e55323, 10 pages, 2013.

[23] N. Lameire, J.-P. Wauters, J. L. Górriz Teruel, W. Van Biesen, and R. Vanholder, "An update on the referral pattern of patients with end-stage renal disease," *Kidney International, Supplement*, vol. 61, no. 80, pp. 27–34, 2002.

[24] D. C. Mendelssohn, C. Malmberg, and B. Hamandi, "An integrated review of 'unplanned' dialysis initiation: reframing the terminology to 'suboptimal' initiation," *BMC Nephrology*, vol. 10, article 22, 2009.

[25] G. Baer, N. Lameire, and W. Van Biesen, "Late referral of patients with end-stage renal disease: an in-depth review and suggestions for further actions," *NDT Plus*, vol. 3, no. 1, pp. 17–27, 2010.

[26] R. L. Pisoni, C. J. Arrington, J. M. Albert et al., "Facility hemodialysis vascular access use and mortality in countries participating in DOPPS: an instrumental variable analysis," *American Journal of Kidney Diseases*, vol. 53, no. 3, pp. 475–491, 2009.

[27] T. Lobbedez, A. Lecouf, M. Ficheux, P. Henri, B. H. De Ligny, and J.-P. Ryckelynck, "Is rapid initiation of peritoneal dialysis feasible in unplanned dialysis patients? A single-centre experience," *Nephrology Dialysis Transplantation*, vol. 23, no. 10, pp. 3290–3294, 2008.

[28] R. Arramreddy, S. Zheng, A. B. Saxena, S. E. Liebman, and L. Wong, "Urgent-start peritoneal dialysis: a chance for a new beginning," *American Journal of Kidney Diseases*, vol. 63, no. 3, pp. 390–395, 2014.

[29] J. V. Povlsen and P. Ivarsen, "How to start the late referred ESRD patient urgently on chronic APD," *Nephrology Dialysis Transplantation*, vol. 21, supplement 2, pp. ii56–ii59, 2006.

[30] D. Ranganathan, R. Baer, R. G. Fassett et al., "Randomised controlled trial to determine the appropriate time to initiate peritoneal dialysis after insertion of catheter to minimise complications (Timely PD study)," *BMC Nephrology*, vol. 11, article 11, 2010.

[31] E. K. Ng, B. L. Goh, S. E. Chew et al., "Multicenter analysis on the impact of nephrologist-initiated catheter insertion program on peritoneal dialysis penetration," *Seminars in Dialysis*, vol. 25, no. 5, pp. 569–573, 2012.

[32] B. L. Goh, Y. M. Ganeshadeva, S. E. Chew, and M. S. Dalimi, "Does peritoneal dialysis catheter insertion by interventional nephrologists enhance peritoneal dialysis penetration?" *Seminars in Dialysis*, vol. 21, no. 6, pp. 561–566, 2008.

[33] A. Asif, T. A. Pflederer, C. F. Vieira, J. Diego, D. Roth, and A. Agarwal, "Does catheter insertion by nephrologists improve peritoneal dialysis utilization? A multicenter analysis," *Seminars in Dialysis*, vol. 18, no. 2, pp. 157–160, 2005.

[34] J. Perl, A. Pierratos, G. Kandasamy et al., "Peritoneal dialysis catheter implantation by nephrologists is associated with higher rates of peritoneal dialysis utilization: a population-based study," *Nephrology Dialysis Transplantation*, vol. 30, no. 2, pp. 301–309, 2015.

[35] T. P. de Moraes, R. P. Campos, M. T. de Alcântara et al., "Similar outcomes of catheters implanted by nephrologists and surgeons: analysis of the Brazilian peritoneal dialysis multicentric study," *Seminars in Dialysis*, vol. 25, no. 5, pp. 565–568, 2012.

[36] J. H. Crabtree, "Peritoneal dialysis catheter implantation: avoiding problems and optimizing outcomes," *Seminars in Dialysis*, vol. 28, no. 1, pp. 12–15, 2015.

[37] S. Haggerty, S. Roth, D. Walsh et al., "Guidelines for laparoscopic peritoneal dialysis access surgery," *Surgical Endoscopy*, vol. 28, no. 11, pp. 3016–3045, 2014.

[38] M. Malovrh, "Vascular access creation and care should be provided by nephrologists," *The Journal of Vascular Access*, vol. 16, supplement 9, pp. S20–S23, 2015.

[39] D. Chanouzas, K. P. Ng, B. Fallouh, and J. Baharani, "What influences patient choice of treatment modality at the pre-dialysis stage?" *Nephrology Dialysis Transplantation*, vol. 27, no. 4, pp. 1542–1547, 2012.

[40] T. Lobbedez, R. Moldovan, M. Lecame, B. Hurault de Ligny, W. El Haggan, and J.-P. Ryckelynck, "Assisted peritoneal dialysis. Experience in a French renal department," *Peritoneal Dialysis International*, vol. 26, no. 6, pp. 671–676, 2006.

[41] M. J. Oliver, R. R. Quinn, E. P. Richardson, A. J. Kiss, D. L. Lamping, and B. J. Manns, "Home care assistance and the utilization of peritoneal dialysis," *Kidney International*, vol. 71, no. 7, pp. 673–678, 2007.

[42] M. R. G. Franco, N. Fernandes, C. A. Ribeiro, A. R. Qureshi, J. C. divino-Filho, and M. da Glória Lima, "A Brazilian experience in assisted automated peritoneal dialysis: a reliable and effective home care approach," *Peritoneal Dialysis International*, vol. 33, no. 3, pp. 252–258, 2013.

[43] M. J. Oliver, A. X. Garg, P. G. Blake et al., "Impact of contraindications, barriers to self-care and support on incident peritoneal dialysis utilization," *Nephrology Dialysis Transplantation*, vol. 25, no. 8, pp. 2737–2744, 2010.

[44] C. Castrale, D. Evans, C. Verger et al., "Peritoneal dialysis in elderly patients: report from the French Peritoneal Dialysis Registry (RDPLF)," *Nephrology Dialysis Transplantation*, vol. 25, no. 1, pp. 255–262, 2010.

[45] A. Smyth, E. McCann, L. Redahan, B. Lambert, G. J. Mellotte, and C. A. Wall, "Peritoneal dialysis in an ageing population: a

10-year experience," *International Urology and Nephrology*, vol. 44, no. 1, pp. 283–293, 2012.

[46] M. Dratwa, "Costs of home assistance for peritoneal dialysis: results of a European survey," *Kidney International*, vol. 73, no. 108, pp. S72–S75, 2008.

[47] E. A. Brown, W. Van Biesen, F. O. Finkelstein et al., "Length of time on peritoneal dialysis and encapsulating peritoneal sclerosis: position paper for ISPD," *Peritoneal Dialysis International*, vol. 29, no. 6, pp. 595–600, 2009.

[48] G. Garosi and D. G. Oreopoulos, "No need for an 'expiry date' in chronic peritoneal dialysis to prevent encapsulating peritoneal sclerosis," *International Urology and Nephrology*, vol. 41, no. 4, pp. 903–907, 2009.

[49] D. W. Johnson, F. G. Brown, M. Clarke et al., "The effect of low glucose degradation product, neutral pH versus standard peritoneal dialysis solutions on peritoneal membrane function: The balANZ trial," *Nephrology Dialysis Transplantation*, vol. 27, no. 12, pp. 4445–4453, 2012.

[50] D. W. Johnson, F. G. Brown, M. Clarke et al., "The effects of biocompatible compared with standard peritoneal dialysis solutions on peritonitis microbiology, treatment, and outcomes: the *bal*ANZ trial," *Peritoneal Dialysis International*, vol. 32, no. 5, pp. 497–506, 2012.

[51] S. Mortier, D. Faict, C. G. Schalkwijk, N. H. Lameire, and A. S. De Vriese, "Long-term exposure to new peritoneal dialysis solutions: effects on the peritoneal membrane," *Kidney International*, vol. 66, no. 3, pp. 1257–1265, 2004.

[52] K. Kawanishi, K. Honda, M. Tsukada, H. Oda, and K. Nitta, "Neutral solution low in glucose degradation products is associated with less peritoneal fibrosis and vascular sclerosis in patients receiving peritoneal dialysis," *Peritoneal Dialysis International*, vol. 33, no. 3, pp. 242–251, 2013.

[53] S. J. Davies, L. Phillips, P. F. Naish, and G. I. Russell, "Peritoneal glucose exposure and changes in membrane solute transport with time on peritoneal dialysis," *Journal of the American Society of Nephrology*, vol. 12, no. 5, pp. 1046–1051, 2001.

[54] Y.-M. Subeq, C.-Y. Ke, N.-T. Lin, C.-J. Lee, Y.-H. Chiu, and B.-G. Hsu, "Valsartan decreases TGF-β1 production and protects against chlorhexidine digluconate-induced liver peritoneal fibrosis in rats," *Cytokine*, vol. 53, no. 2, pp. 223–230, 2011.

[55] A. Vazquez-Rangel, V. Soto, M. Escalona et al., "Spironolactone to prevent peritoneal fibrosis in peritoneal dialysis patients: a randomized controlled trial," *American Journal of Kidney Diseases*, vol. 63, no. 6, pp. 1072–1074, 2014.

[56] A. Trošt Rupnik, J. Pajek, A. Guček et al., "Influence of renin-angiotensin-aldosterone system-blocking drugs on peritoneal membrane in peritoneal dialysis patients," *Therapeutic Apheresis and Dialysis*, vol. 17, no. 4, pp. 425–430, 2013.

[57] G. Garosi, N. Mancianti, R. Corciulo, V. La Milia, and G. Virga, "Encapsulating peritoneal sclerosis," *Journal of Nephrology*, vol. 26, supplement 2, pp. 177–187, 2013.

[58] G. del Peso, M. A. Bajo, F. Gil et al., "Clinical experience with tamoxifen in peritoneal fibrosing syndromes," *Advances in Peritoneal Dialysis*, vol. 19, pp. 32–35, 2003.

[59] A. Tranaeus, "No need for an 'expiry date' in chronic peritoneal dialysis to prevent encapsulating peritoneal sclerosis: comments from around the world," *International Urology and Nephrology*, vol. 42, pp. 240–241, 2010.

[60] T. Cornelis and D. G. Oreopoulos, "Update on potential medical treatments for encapsulating peritoneal sclerosis; Human and experimental data," *International Urology and Nephrology*, vol. 43, no. 1, pp. 147–156, 2011.

[61] D. E. Sampimon, M. R. Korte, D. L. Barreto et al., "Early diagnostic markers for encapsulating peritoneal sclerosis: a case-control study," *Peritoneal Dialysis International*, vol. 30, no. 2, pp. 163–169, 2010.

[62] J. Pajek, A. J. Hutchison, S. Bhutani et al., "Outcomes of peritoneal dialysis patients and switching to hemodialysis: a competing risks analysis," *Peritoneal Dialysis International*, vol. 34, no. 3, pp. 289–298, 2014.

[63] H. Kawanishi, "No need for an 'expiry date' in chronic peritoneal dialysis to prevent encapsulating peritoneal sclerosis: comments from around the world," *International Urology and Nephrology*, vol. 42, no. 1, pp. 239–249, 2010.

[64] T. Yamamoto, K. Nagasue, S. Okuno, and T. Yamakawa, "The role of peritoneal lavage and the prognostic significance of mesothelial cell area in preventing encapsulating peritoneal sclerosis," *Peritoneal Dialysis International*, vol. 30, no. 3, pp. 343–352, 2010.

[65] P. K.-T. Li, C. C. Szeto, B. Piraino et al., "Peritoneal dialysis-related infections recommendations: 2010 update," *Peritoneal Dialysis International*, vol. 30, no. 4, pp. 393–423, 2010.

[66] B. Piraino, J. Bernardini, E. Brown et al., "ISPD position statement on reducing the risks of peritoneal dialysis-related infections," *Peritoneal Dialysis International*, vol. 31, no. 6, pp. 614–630, 2011.

[67] J. Ahlmén, L. Carlsson, and C. Schönborg, "Well-informed patients with end-stage renal disease prefer peritoneal dialysis to hemodialysis," *Peritoneal Dialysis International*, vol. 13, supplement 2, pp. S196–S198, 1993.

[68] S. S. Prichard, "Treatment modality selection in 150 consecutive patients starting ESRD therapy," *Peritoneal Dialysis International*, vol. 16, no. 1, pp. 69–72, 1996.

[69] J. Little, A. Irwin, T. Marshall, H. Rayner, and S. Smith, "Predicting a patient's choice of dialysis modality: experience in a United Kingdom renal department," *American Journal of Kidney Diseases*, vol. 37, no. 5, pp. 981–986, 2001.

[70] B. Marrón, J. C. Martínez Ocaña, M. Salgueira et al., "Analysis of patient flow into dialysis: role of education in choice of dialysis modality," *Peritoneal Dialysis International*, vol. 25, supplement 3, pp. S56–S59, 2005.

[71] W. Ribitsch, B. Haditsch, R. Otto et al., "Effects of a pre-dialysis patient education program on the relative frequencies of dialysis modalities," *Peritoneal Dialysis International*, vol. 33, no. 4, pp. 367–371, 2013.

Hindawi Publishing Corporation
BioMed Research International
Volume 2015, Article ID 382652, 9 pages
http://dx.doi.org/10.1155/2015/382652

Research Article

Senescence-Associated Changes in Proteome and *O*-GlcNAcylation Pattern in Human Peritoneal Mesothelial Cells

Rebecca Herzog,[1,2] Silvia Tarantino,[1] András Rudolf,[3] Christoph Aufricht,[1] Klaus Kratochwill,[1,2] and Janusz Witowski[3]

[1]*Department of Pediatrics and Adolescent Medicine, Medical University of Vienna, 1090 Vienna, Austria*
[2]*Zytoprotec GmbH, 1090 Vienna, Austria*
[3]*Department of Pathophysiology, University of Medical Sciences, 60-806 Poznan, Poland*

Correspondence should be addressed to Klaus Kratochwill; klaus.kratochwill@meduniwien.ac.at

Received 22 May 2015; Revised 24 October 2015; Accepted 25 October 2015

Academic Editor: Yudong Cai

Introduction. Senescence of peritoneal mesothelial cells represents a biological program defined by arrested cell growth and altered cell secretory phenotype with potential impact in peritoneal dialysis. This study aims to characterize cellular senescence at the level of global protein expression profiles and modification of proteins with O-linked N-acetylglucosamine (*O*-GlcNAcylation). *Methods*. A comparative proteomics analysis between young and senescent human peritoneal mesothelial cells (HPMC) was performed using two-dimensional gel electrophoresis. *O*-GlcNAc status was assessed by Western blot under normal conditions and after modulation with 6-diazo-5-oxo-L-norleucine (DON) to decrease *O*-GlcNAcylation or *O*-(2-acetamido-2-deoxy-D-glucopyranosylidene) amino *N*-phenyl carbamate (PUGNAc) to increase *O*-GlcNAcylation. *Results*. Comparison of protein pattern of senescent and young HPMC revealed 29 differentially abundant protein spots, 11 of which were identified to be actin (cytoplasmic 1 and 2), cytokeratin-7, cofilin-2, transgelin-2, Hsp60, Hsc70, proteasome β-subunits (type-2 and type-3), nucleoside diphosphate kinase A, and cytosolic 5′(3′)-deoxyribonucleotidase. Although the global level of *O*-GlcNAcylation was comparable, senescent cells were not sensitive to modulation by PUGNAc. *Discussion*. This study identified changes of the proteome and altered dynamics of *O*-GlcNAc regulation in senescent mesothelial cells. Whereas changes in cytoskeleton-associated proteins likely reflect altered cell morphology, changes in chaperoning and housekeeping proteins may have functional impact on cellular stress response in peritoneal dialysis.

1. Introduction

Cellular senescence has emerged as a powerful biological program initiated by various forms of stress that can jeopardize the integrity of the genome. The known triggers of senescence include telomere dysfunction, oncogene activation, reactive oxygen species, and epigenomic damage [1]. By irreversibly arresting cell growth and altering cell secretory phenotype, cellular senescence plays a significant role in tumor suppression, tissue repair, and embryogenesis [2]. Senescence of peritoneal mesothelial cells has been shown to rapidly occur *in vitro*, most likely in response to culture-associated oxidative stress [3]. However, the role of mesothelial cell senescence *in vivo* is less clear.

Senescent cells show flattened and enlarged morphology and they are typically characterized by the presence of senescence-associated β-galactosidase (SA-β). Senescent cells have been detected sporadically in the peritoneal dialysis (PD) effluent and in animals infused with PD fluids [4, 5]. Moreover, senescent cells have been visualized in fresh explants of omentum from patients undergoing abdominal surgery [6]. *In vitro* experiments showed that mesothelial cell senescence was accelerated by exposure to high glucose [7]. We recently found that exposure to high glucose also induced significant abundance changes of *O*-linked N-acetylglucosamine (*O*-GlcNAc) modification of mesothelial cell proteins, a posttranslational protein modification relevant in cellular survival [8]. These effects may therefore

be important in the context of PD, given the extensive use of glucose as osmotic agent in PD fluids. The effect of glucose on senescence is largely related to increased oxidative stress and upregulation of transforming growth factor beta (TGF-β) [6, 9]. Antioxidants and anti-TGF-β treatments can partly reduce this effect but fail to prevent mesothelial cell senescence, still influenced by multifactorial processes not yet fully elucidated in the literature. Identification of other mechanisms could be supported by detailed characterization of the senescent mesothelial cell phenotype through technologies that determine global expression profiles of genes and proteins. Proteomics has become a standard tool in molecular biology to explore cellular mechanisms at the level of effector proteins. Two-dimensional gel electrophoresis approaches still offer the highest available resolution on the intact protein level, with the added benefit of including protein isoforms and posttranslational modifications in the global picture. The proteomic approach has already been applied to study the occurrence of senescence in other cell types [10, 11]. Therefore, in our pilot study we have attempted to analyze for the first time the changes that may occur during cellular senescence of human peritoneal mesothelial cells at the level of protein expression profiles and modification of proteins with *O*-GlcNAc.

2. Methods

2.1. Materials. Standard chemicals were purchased from Sigma-Aldrich (St. Louis, MO, USA) if not specified otherwise. NUNC (Roskilde, Denmark) tissue culture plastics were used for all cell culture procedures.

2.2. Mesothelial Cells. Human peritoneal mesothelial cells (HPMC) were isolated from the specimens of omentum obtained from consenting nonuremic patients undergoing elective abdominal surgery. The cells were isolated, cultured, and characterized as previously described [12, 13]. Cells were grown into senescence as detailed elsewhere [14]. Cells were considered senescent when they failed to increase in number over 4 weeks, showed enlarged morphology, and stained in majority for senescence-associated β-galactosidase (SA-β-Gal). SA-β-Gal was detected according to Dimri et al. [15] using a senescence β-galactosidase staining kit (Cell Signaling Technology (Danvers, MA, USA)).

2.3. Protein Sample Preparation. Young (passage 2) and senescent (passages 6–8) HPMC from 3 different donors were lysed to prepare whole cell extracts as previously described [16]; in brief cells were washed two times (250 mM sucrose, 10 mM Tris, pH 7) and lysed by incubation with 800 μL lysis buffer (30 mM Tris, pH 8.5, 7 M urea, 2 M thiourea, 4% 3-[(3-cholamidopropyl) dimethylammonio]-1-propanesulfonate (CHAPS), 1 mM ethylenediaminetetraacetic acid (EDTA), one tablet of complete protease inhibitor (Roche, Basel, Switzerland), and one tablet of PhosStop phosphatase inhibitor (Roche) per 100 mL) per 75 cm^2 culture flask for 10 min at 25°C. The resulting lysates were stored at −80°C until further processing. Total protein concentration was determined by the 2D Quant kit (GE Healthcare, Uppsala, Sweden) according to the manufacturer's manual.

2.4. Two-Dimensional Gel Electrophoresis. 50 μg of total protein per sample, in triplicates, was brought to a final volume of 210 μL with rehydration buffer (5 M urea, 0.5% CHAPS, 0.5% Pharmalyte (Bio-Rad, Hercules, CA, USA), and 12 μL/mL of DeStreak reagent (GE Healthcare)) and subsequently applied on immobilized pH gradient (IPG) strips (ReadyStrip pH 3–10, nonlinear, 11 cm, Bio-Rad). The strip was covered with silicone oil, actively rehydrated (50 V, 12 h, 20°C), and then focused (Bio-Rad Protean I12) by increasing the voltage to 5000 V (total 50 kVh, current limit 30 μA/strip). Focused strips were stored at −80°C until further use. Before second dimension, each strip was incubated twice for 20 min in 2 mL equilibration buffer (6 M urea, 2% (w/v) sodium dodecyl sulfate (SDS), 25% glycerol, and 3.3% 50 mM Tris/HCl pH 8.8, stained with bromophenol blue) first supplemented with 10 mg/mL dithiothreitol (DTT) and then 48 mg/mL 2-iodoacetamide (IAA). The second dimension was carried out using precast Criterion TGX Stain-Free polyacrylamide gels (133 × 87 × 1 mm, Bio-Rad) on a Criterion cell (Bio-Rad) for 2 hours at 20 mA.

2.5. Visualization and Analysis of Proteins. Protein spots were visualized utilizing the ChemiDoc XRS system (Bio-Rad) by UV-induced reaction. Gel images were acquired and processed using Image Lab software (Bio-Rad). The images were analyzed using the Delta2D 4.5 software (Decodon GmbH, Greifswald, Germany) with group-wise image alignment and spot detection on the resulting fused image. Protein identifications of the mesothelial cell proteome from our recent work [17] accomplished by mass spectrometry were reassigned from the original images to the master image of the current study.

2.6. In Vitro Treatment with Modulators of O-GlcNAcylation. HPMC were seeded onto 12-well culture plates and incubated for 48 hours with chemical inhibitors of the hexosamine biosynthesis pathway (HBP) 6-diazo-5-oxo-L-norleucine (DON) to decrease *O*-GlcNAc abundance or O-(2-Acetamido-2-deoxy-D-glucopyranosylidene) amino *N*-phenyl carbamate (PUGNAc) to inhibit removal of *O*-GlcNAc and therefore increase *O*-GlcNAc abundance. After the treatment, cells were washed and lysed as described above.

2.7. Western Blot and ELISA. Cell extracts were prepared as described above, and equal amounts of total protein were separated by SDS-PAGE on a Bio-Rad Criterion cell using Criterion precast gels of 1 mm thickness (Bio-Rad). Proteins were electroblotted onto polyvinylidene fluoride (PVDF) membranes (Millipore, Billerica, MA, USA) immediately after the run by tank blotting using a Criterion blotting cell (Bio-Rad) and the respective transfer buffer (200 mM glycine, 25 mM Tris, 0.1% SDS, and 20% methanol). Membranes were blocked with 5% bovine serum albumin (BSA) and incubated with an antibody against *O*-GlcNAc (RL2, Abcam, Cambridge, UK) over night at 4°C. After incubation with the

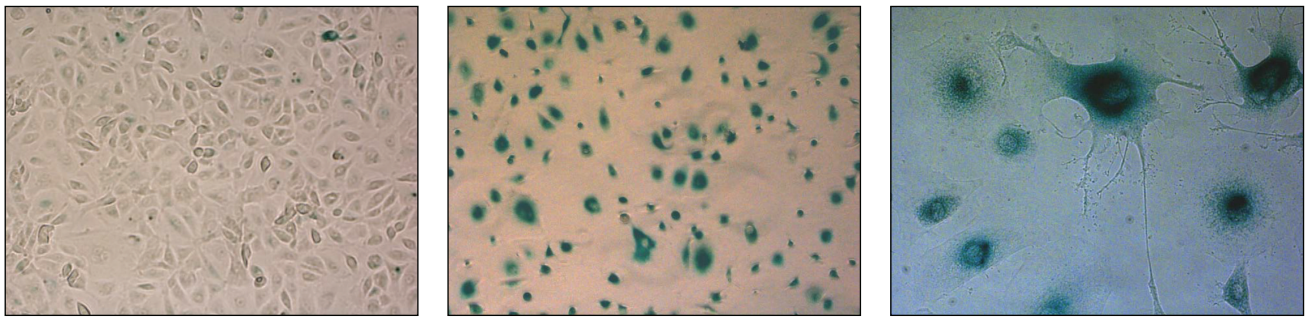

(a) (b) (c)

Figure 1: Morphology and senescent phenotype of HPMC. Expression of senescence-associated β-galactosidase (SA-β-Gal) was compared by light microscopy and SA-β-Gal staining in young (a) and senescent ((b) and (c)) HPMC. Magnification (a)-(b): 10x and (c) 40x.

secondary, peroxidase-coupled antibody (Polyclonal Rabbit Anti-Mouse Ig/HRP P0260; DakoCytomation, Carpinteria, CA) detection was accomplished by using enhanced chemiluminescence solution (Western Lightning reagent; Perkin Elmer, Boston, MA) and a ChemiDoc XRS chemiluminescence detection system (Bio-Rad). Densitometric quantification was accomplished using the Image Lab software (Bio-Rad).

2.8. Statistics. Statistical analyses were performed using SPSS 17 (SPSS Inc., Chicago, IL, USA) and Sigmaplot 11.0 (Systat Software GmbH, Erkrath, Germany). Values from different groups were compared using t-tests or ANOVA where appropriate. In case of ANOVA Tukey's HSD was used as post hoc test. p values lower than 0.05 were considered significant. The results are presented as means ± SEM.

3. Results

As previously described [14], serial passages of HPMC led to a gradual decline in cell proliferative capacity and to the development of senescent phenotype characterized by altered morphology and extensive staining for SA-β (Figure 1).

3.1. Proteomics Analysis of Total Protein Extracts of Young and Senescent HPMC. To assess the effects of cellular senescence with the aid of comparative proteomics techniques, three technical replicate gels per group (representative gel images in Figure 2(a)) were analyzed and compared using Delta2D 4.5 software (Decodon GmbH). Group-wise image alignment and spot detection on the resulting fused image revealed a common spot pattern of 305 protein spots (Figure 2(b)).

Quantitative spot analysis of the young and senescent cell proteome revealed 29 spots differing significantly in abundance ($p \leq 0.05$) (Figure 2(b)). Figure 3 shows the senescent/young spot ratio for each spot identified. Of those, the abundance of 10 (34%) and 19 (66%) proteins in senescent cells was found to be increased and decreased, respectively.

Based on protein identifications made in previous studies [17, 18] we were able to identify 11 unique proteins shown in Figure 2(b): actin (ACTG and ACTB), cytokeratin-7 (KRT7), cofilin-2 (CFL2), transgelin-2 (TAGLN2), Hsp60 (HSPD1), Hsc70 (HSPA8), proteasome subunits beta (PSMB2 and PSMB3), NDK A (NME1), and dNT-1 (NT5C).

Interestingly, the majority of these proteins are known to be involved in cellular processes that can be modulated by *O*-GlcNAcylation. Characteristics of individual proteins, their potential (number of serine and threonine residues), and predicted (based on the bioinformatic algorithm *O*-GlcNAcScan [19]) *O*-GlcNAc modification sites as well as references to experimentally validated *O*-GlcNAc modification sites of these proteins are listed in Table 1.

3.2. O-GlcNAc Dynamics under Chemical Modulators. Direct comparison of cellular proteins from young and senescent mesothelial cells shows similar levels of global *O*-GlcNAcylation (Figure 4). Nevertheless, modulation of *O*-GlcNAcylation by chemical inhibitors of the HBP revealed marked differences between the two cell statuses. The addition of DON, a glutamine fructose-6-phosphate amidotransferase (GFAT) inhibitor, resulted in a decrease of *O*-GlcNAc levels in both young and senescent cells (61.6% ± 3.7 versus 42.9% ± 3.7, resp.) (Figure 5). In contrast, addition of the *O*-GlcNAcase inhibitor PUGNAc resulted in increased *O*-GlcNAc levels in young but not in senescent cells (162.2% ± 10.6 versus 103.5% ± 5.0, resp.). Thus the *O*-GlcNAc status under control conditions showed a higher relative level in senescent than in young mesothelial cells.

4. Discussion

In this study we show that the senescent phenotype of mesothelial cells is associated with quantitative changes in the cellular proteome. These changes are seen predominantly in cytoskeleton-associated proteins but also in chaperoning and housekeeping proteins. Whereas changes in cytoskeletal proteins are likely to contribute to the altered senescent cell morphology, changes in the chaperone protein family may have functional impact on cellular stress responses. In this respect, previous studies have clearly demonstrated the importance of stress responses in mesothelial cells exposed to PD fluids [17, 18]. The global level of *O*-GlcNAcylation

Table 1: Identified proteins showing significant differential abundance between young and senescent HPMC cells ($p < 0.05$) with references of their predicted or reported *O*-GlcNAcylated sites.

Protein name	Gene name	SwissProt entry name	MW (kD)[a]	pI[b]	Length[c]	Spot[d]	Potential *O*-GlcNAc sites[e]	S[e]	T[e]	Predicted *O*-GlcNAc sites[f]	S[f]	T[f]	References[g]
Actin, cytoplasmic 2	ACTG1	ACTG_HUMAN	41.8	5.31	375	294	51	25	26	9	8	1	[43]
Actin, cytoplasmic 1	ACTB	ACTB_HUMAN	41.7	5.29	375	294	51	25	26	9	8	1	[38, 40, 44]
Keratin, type II cytoskeletal 7	KRT7	K2C7_HUMAN	51.4	5.39	469	52	63	46	17	4	4	0	—* [36–38, 44]
Cofilin-2	CFL2	COF2_HUMAN	18.7	7.88	166	198	20	12	8	4	4	0	[24]
Transgelin-2	TAGLN2	TAGL2_HUMAN	22.4	8.45	199	173	17	7	10	2	2	0	[41, 43]
60 kDa heat shock protein, mitochondrial	HSPD1	CH60_HUMAN	61.0	5.24	573	19	14	6	8	6	4	2	[37, 39, 41, 42, 44]
Heat shock cognate 71 kDa protein	HSPA8	HSP7C_HUMAN	70.9	5.37	646	16	82	35	47	4	2	2	[36–38, 41, 43–45]
Proteasome subunit beta type-2	PSMB2	PSB2_HUMAN	22.8	6.52	201	180	18	10	8	9	5	4	[41, 43]
Proteasome subunit beta type-3	PSMB3	PSB3_HUMAN	22.9	6.12	205	150	20	7	13	2	0	2	—* [41, 43]
Nucleoside diphosphate kinase A	NME1	NDKA_HUMAN	17.1	5.82	152	198	11	6	5	3	2	1	[41]
5′(3′)-deoxyribonucleotidase, cytosolic type	NT5C	NT5C_HUMAN	23.4	6.18	201	150	14	6	8	1	0	1	—

[a]Relative molecular mass of the protein as calculated from the amino acid sequence of the polypeptide without any co- or posttranslational modifications; [b]calculated pI of the protein as obtained from SwissProt database; [c]number of amino acids in the protein sequence; [d]spots numbered according to Figure 2; [e]potential *O*-GlcNAcylation sites expressed as the total number of serine (S) and threonine (T) residues in the protein sequence; [f]predicted *O*-GlcNAcylation sites expressed as the number of predicted serine (S) and threonine (T) residues in the protein, obtained from dbOGAP database using default settings in OGlcNAcScan tool; [g]references within protein candidates that have been reported to be *O*-GlcNAcylated. *proteins from the same protein family of the candidate have been reported to be *O*-GlcNAcylated. [dbOGAP: http://cbsb.lombardi.georgetown.edu/hulab/OGAP.html].

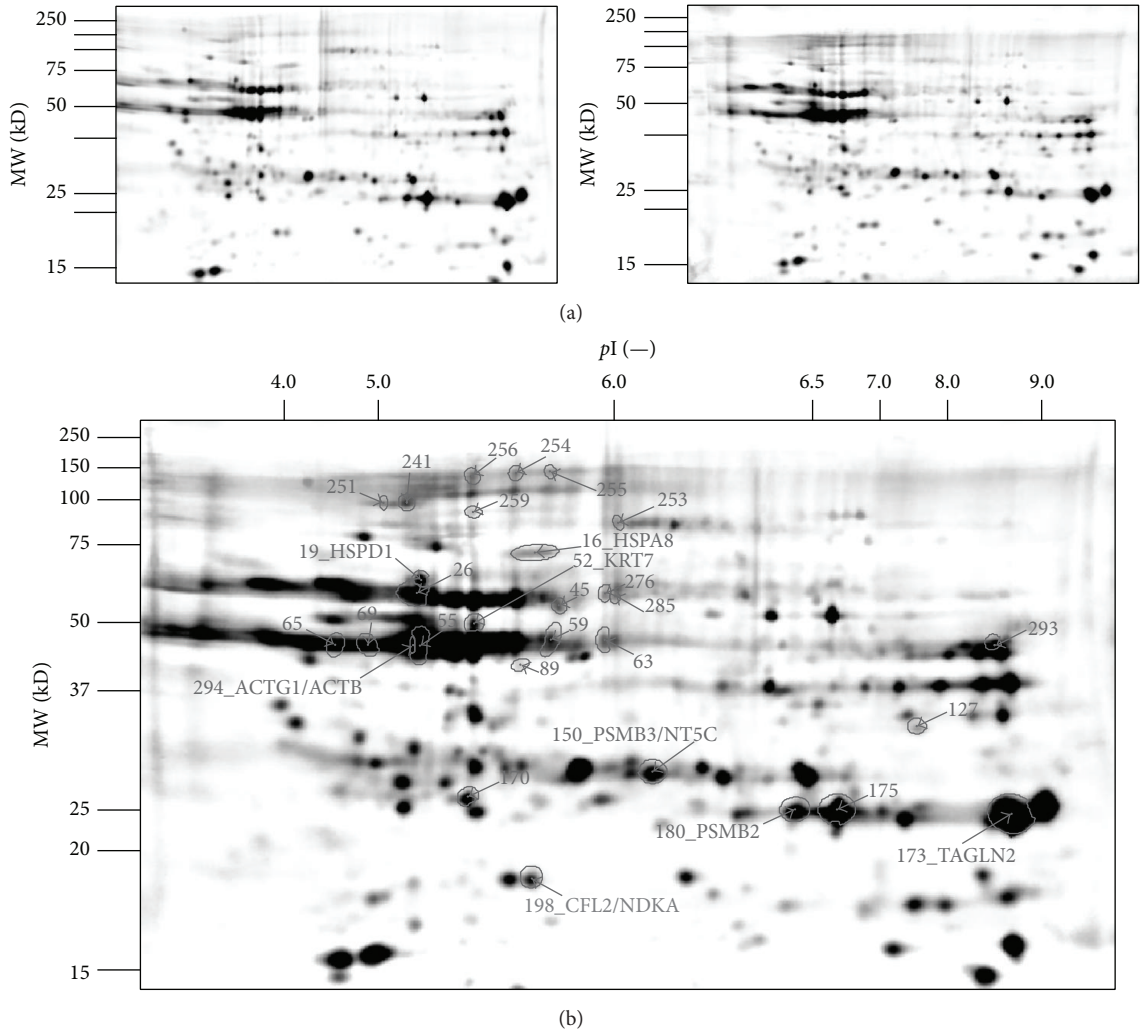

Figure 2: 2D Gel images of young and senescent HPMC. (a) Representative 2D Gel of senescent (left panel) and young (right panel) human peritoneal mesothelial cells (HPMC). (b) Fusion image of 2D protein pattern of senescent and young HPMC (total spot count: 305). Protein spots found statistically significant altered ($p < 0.05$) in the comparison between senescent and young ($n = 29$) are marked with spot boundaries, spot label, and name of identified proteins ($n = 11$).

showed comparable levels in young and senescent mesothelial cells; however, senescent cells were not able to increase their level of global protein *O*-GlcNAcylation, suggesting altered dynamics of *O*-GlcNAc regulation.

While many studies have clearly documented phenotypic changes in cell senescence, they have also revealed that the course and the rate of senescence very much depend on the cell type and on the specific pathophysiological setting. In this respect, senescence of HPMC in culture displays some interesting features [3], including a rather swift and sudden loss of proliferative capacity, extensive DNA damage in nontelomeric regions, and high susceptibility to oxidative stress. In the present study we have been able to further characterize this phenotype by identifying a set of proteins altered in their expression in senescent cells.

About half of the senescence-induced changes were identified in proteins involved in cytoskeletal organization. These included two isotypes of actin and cytokeratin, key structural proteins with major biological roles in early and late cellular development phases and status [20–22]. The actin-binding proteins cofilin and transgelin are described to be crucial regulators of actin dynamics [23]. Cofilin promotes actin filament elongation as an actin-severing protein [24]. Transgelin is a shape-change sensitive actin cross-linking/gelling protein found to be overexpressed as well in senescent fibroblasts [25–27]. The next functional group identified is composed of proteins that are key players in cellular stress response. They are exemplified by Hsp60 and Hsc70, which are molecular chaperons known to be involved in cellular repair, transport, and protein metabolism [28]. These processes are essential for cellular survival under both control and stress conditions and their role in senescence has recently been reviewed [29–31]. Similarly, changes in the abundance of the proteasome-associated proteins may be linked to altered proteolytic activities and proteasome content that have been reported to occur in senescent cells [32–34]. It has been shown that proteasome

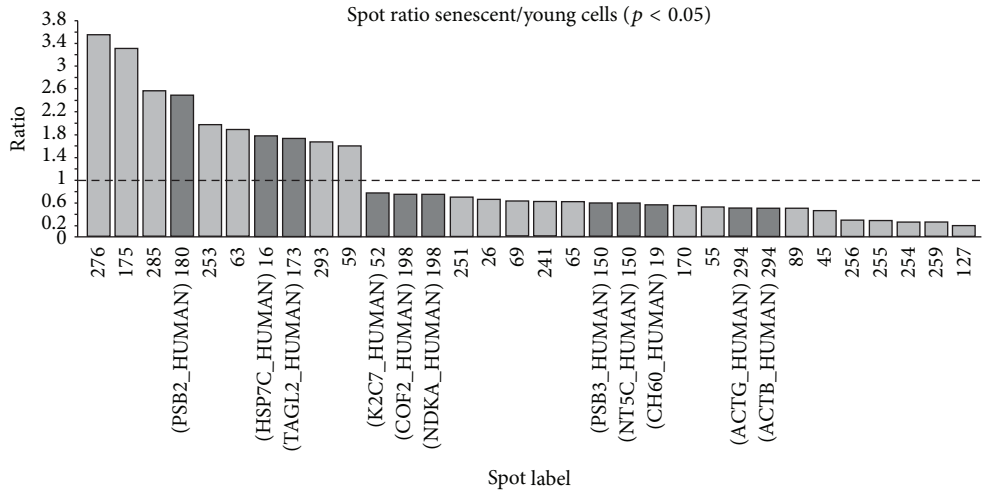

Figure 3: Spot abundance ratio of significantly altered spots ($p < 0.05$) between young and senescent HPMC. Changes in spot abundance are represented as spot volume ratio for the 29 significantly altered spots found in the comparison between young and senescent human peritoneal mesothelial cells (HPMC).

inhibition results in the appearance of a senescence-like phenotype in fibroblasts [35]. However, the number of proteins identified as differently expressed by senescent mesothelial cells may be viewed as relatively modest, which may point at other regulatory mechanisms modulating the protein activity in senescence. They may include posttranslational protein modifications, protein-protein interactions and networking, protein trafficking, and cellular localization.

In this respect it is interesting to note that all but one of these proteins have been previously reported to be potentially *O*-GlcNAcylated proteins and/or belong to protein families with *O*-GlcNAc modified members [24, 36–45]. This suggests that senescence-associated processes may be regulated partly by *O*-GlcNAc modifications. *O*-GlcNAcylation is a ubiquitous posttranslational mechanism regulated by nutrient availability and enzyme activity [46]. It has been estimated that at least 3,000 proteins can be modified by *O*-GlcNAc [47].

Although the assessment of global *O*-GlcNAcylation did not demonstrate significant differences between young and senescent cells under control conditions, pharmacological intervention led to significant changes in the dynamics of early versus late-passage mesothelial cells. These data supplement current knowledge of *O*-GlcNAc cycling during cell senescence and suggest that changes in *O*-GlcNAc dynamics in senescence may be more important than the global level of *O*-GlcNAcylation. *O*-GlcNAc modification of individual target proteins may thus contribute to senescence by modulating cytoskeletal organization, stress response, and proteasome activity.

In this respect, *O*-GlcNAcylation was reported to impact on structural and regulatory proteins of the cytoskeleton [46], modulating their solubility and preventing the aggregation of denatured proteins [48]. Dynamics in *O*-GlcNAc have been described in key players of the cellular architecture such as actin, cytokeratins, and actin-binding proteins [37]. For example, specific changes in the *O*-GlcNAcylation of cytokeratins have been reported to occur during cell cycle progression [37]. They probably modulate solubility of cytokeratins [36]. Recent studies also suggested a functional role for *O*-GlcNAcylation of cofilin in regulating actin dynamics, as silencing of cofilin by siRNA abolished *O*-GlcNAc transferase- (OGT-) enhanced cell mobility [24].

O-GlcNAcylation was also found to be involved in cellular stress response pathways [48]. For example, *O*-GlcNAcylation can regulate the key heat shock transcription factor HSF-1 and thus impact on subsequent expression of several heat shock protein (Hsp) families [49]. Enhanced *O*-GlcNAcylation of cytosolic Hsp60 was shown to be associated with decreased interactions between Hsp60 and Bax, resulting in translocation of Bax to mitochondria and leading to cell death [42]. This aspect might be relevant in the context of peritoneal dialysis (PD), as *O*-GlcNAcylation of Hsp60 was found to be upregulated by high glucose [39, 42]. On the other hand, increased *O*-GlcNAcylation of other proteins may promote cellular protection by increasing their binding to Hsp70 [48].

O-GlcNAcylation may also regulate proteasome function under control and stressful conditions [46]. Recent publications suggest that proteasome activity and cellular energy status might be coupled to *O*-GlcNAcylation, acting as a metabolic sensor: an increase in nutrient-dependent posttranslational modification of the proteasome was shown to correlate with decreased proteasome activity and protein degradation [50].

Taken together, our results add to recent literature describing association of *O*-GlcNAcylation with changes in proteins in aging [51–53]. In this respect, increased *O*-GlcNAc levels were found in vital tissues of aged rodents [51]. In *Caenorhabditis elegans*, genetic manipulation of enzymes regulating *O*-GlcNAcylation resulted in changes in life span and resistance to stress [53]. In that system, several hundred promoters, including those involved in aging, were found to display differential cycling of *O*-GlcNAc [52]. Thus, linking *O*-GlcNAc cycling to higher order protein structures may

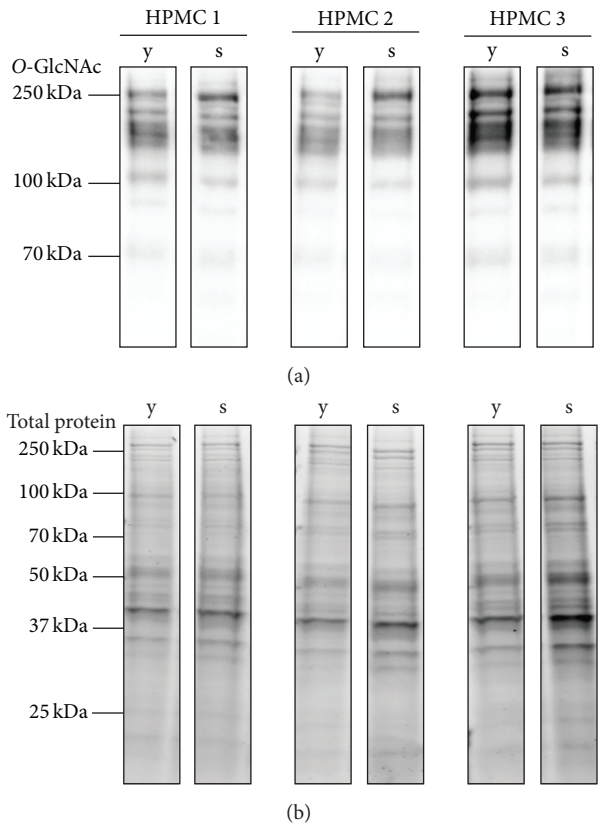

Figure 4: *O*-GlcNAc western blot of young and senescent HPMC. (a) *O*-GlcNAc specific western blot of young (y) and senescent (s) human peritoneal mesothelial cells (HPMC) from three different donors (HPMC 1–3). (b) Corresponding total protein loading (stain-free technology Bio-Rad).

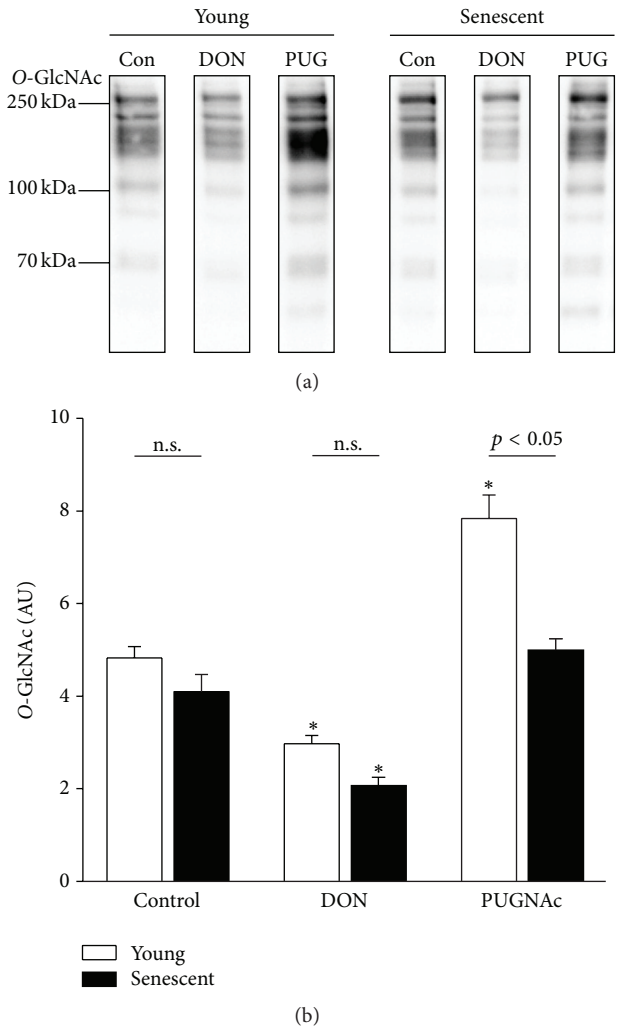

Figure 5: *O*-GlcNAc western blot of young and senescent HPMC treated with modulators of the hexosamine biosynthesis pathway (HBP). (a) Representative *O*-GlcNAc specific western blot of young (left) and senescent (right) human peritoneal mesothelial cells (HPMC) treated with *O*-GlcNAcylation inhibitor (DON) or an inhibitor of the *O*-GlcNAcase (PUG = PUGNAc). (b) Densitometric analysis of western blots for effects of DON and PUGNAc on *O*-GlcNAcylation ($n = 3$). n.s., not significant; $^{*}p < 0.05$ versus control.

provide insights into how cells respond to potential stressors and inducers of senescence. In mesothelial cells, senescence will likely influence stress response to glucose-based PD fluids [8].

In addition to antibody-based detection techniques of global *O*-GlcNAc-pattern identification, recently more and more studies emerged, investigating into sequence-specific localization of functional alterations caused by protein modification with *O*-GlcNAc. While these methods certainly will provide an important leap in understanding complex biological regulatory circuits, the analytical techniques, mainly relying on mass spectrometry combined with soft ionization methods, are still more suitable for focusing on an individual candidate protein than on global effects [44, 54]. Nevertheless, future studies will have to integrate these techniques for more detailed description of senescence-associated changes in specific *O*-GlcNAcylation.

We have previously demonstrated that, in primary peritoneal mesothelial cells, cultured from human omentum or from clinical effluent of PD patients, basal *O*-GlcNAc levels were in an intermediate range and sensitive to modulation (as confirmed in the present study for young cells). Exposure to commercially available PD fluids increased the global *O*-GlcNAc status close to maximum levels induced by PUGNAc. By testing single PD fluids components we showed that the increase of *O*-GlcNAcylation was mainly driven by glucose [8]. Chemical modulation of *O*-GlcNAc levels led to corresponding changes in HSP expression and cellular viability. These experiments suggested that the cytoprotective effect of the dipeptide alanyl-glutamine toward peritoneal mesothelial cells [8, 16] could be related to its ability to modulate *O*-GlcNAcylation. However, further studies are required to investigate in detail the consequences of senescence-associated changes in *O*-GlcNAcylation for mesothelial cell response to PD fluid. These studies will also need to assess the complex interplay of *O*-GlcNAc with specific target proteins involved in cellular senescence and to further define the

specific pattern of individual mesothelial proteins that are *O*-GlcNAcylated in young and senescent cells in response to PD fluid exposure.

Conflict of Interests

Rebecca Herzog and Klaus Kratochwill are employees of Zytoprotec GmbH. Christoph Aufricht is cofounder of Zytoprotec GmbH, a spin-off of the Medical University Vienna that holds the patent "Carbohydrate-Based Peritoneal Dialysis Fluid Comprising Glutamine Residue" (International Publication no.: WO 2008/106702 A1). All other authors declare that there is no conflict of interests regarding the publication of this paper.

Authors' Contribution

Rebecca Herzog, Silvia Tarantino, and András Rudolf contributed equally to this work. Christoph Aufricht, Klaus Kratochwill, and Janusz Witowski contributed equally to this work.

Acknowledgment

Silvia Tarantino, András Rudolf, Christoph Aufricht, Klaus Kratochwill, and Janusz Witowski were supported by the European Training and Research in Peritoneal Dialysis (EuTRiPD) program, a project funded by the European Union within the Marie Curie scheme (287813).

References

[1] D. G. A. Burton and V. Krizhanovsky, "Physiological and pathological consequences of cellular senescence," *Cellular and Molecular Life Sciences*, vol. 71, no. 22, pp. 4373–4386, 2014.

[2] J. Campisi, "Aging, cellular senescence, and cancer," *Annual Review of Physiology*, vol. 75, pp. 685–705, 2013.

[3] K. Ksiaz;ek, "Mesothelial cell: a multifaceted model of aging," *Ageing Research Reviews*, vol. 12, no. 2, pp. 595–604, 2013.

[4] L. Gotloib, L. G. Gotloib, and V. Khrizman, "The use of peritoneal mesothelium as a potential source of adult stem cells," *International Journal of Artificial Organs*, vol. 30, no. 6, pp. 501–512, 2007.

[5] L. Gotloib, V. Wajsbrot, and A. Shostak, "Icodextrin-induced lipid peroxidation disrupts the mesothelial cell cycle engine," *Free Radical Biology and Medicine*, vol. 34, no. 4, pp. 419–428, 2003.

[6] K. Ksiazek, J. Mikuła-Pietrasik, A. Jörres, and J. Witowski, "Oxidative stress-mediated early senescence contributes to the short replicative life span of human peritoneal mesothelial cells," *Free Radical Biology and Medicine*, vol. 45, no. 4, pp. 460–467, 2008.

[7] J. Witowski, K. Książek, and A. Jörres, "New insights into the biology of peritoneal mesothelial cells: the roles of epithelial-to-mesenchymal transition and cellular senescence," *Nephron—Experimental Nephrology*, vol. 108, no. 4, pp. e69–e73, 2008.

[8] R. Herzog, T. O. Bender, A. Vychytil, K. Bialas, C. Aufricht, and K. Kratochwill, "Dynamic *O*-linked *N*-acetylglucosamine modification of proteins affects stress responses and survival of mesothelial cells exposed to peritoneal dialysis fluids," *Journal of the American Society of Nephrology*, vol. 25, no. 12, pp. 2778–2788, 2014.

[9] K. Książek, K. Korybalska, A. Jörres, and J. Witowski, "Accelerated senescence of human peritoneal mesothelial cells exposed to high glucose: the role of TGF-β1," *Laboratory Investigation*, vol. 87, no. 4, pp. 345–356, 2007.

[10] D. Ortuño-Sahagún, M. Pallàs, and A. E. Rojas-Mayorquín, "Oxidative stress in aging: advances in proteomic approaches," *Oxidative Medicine and Cellular Longevity*, vol. 2014, Article ID 573208, 18 pages, 2014.

[11] A. D. Catherman, M. Li, J. C. Tran et al., "Top down proteomics of human membrane proteins from enriched mitochondrial fractions," *Analytical Chemistry*, vol. 85, no. 3, pp. 1880–1888, 2013.

[12] E. Stylianou, L. A. Jenner, M. Davies, G. A. Coles, and J. D. Williams, "Isolation, culture and characterization of human peritoneal mesothelial cells," *Kidney International*, vol. 37, no. 6, pp. 1563–1570, 1990.

[13] S. Yung, F. K. Li, and T. M. Chan, "Peritoneal mesothelial cell culture and biology," *Peritoneal Dialysis International*, vol. 26, no. 2, pp. 162–173, 2006.

[14] K. Książek, K. Piwocka, A. Brzezińska et al., "Early loss of proliferative potential of human peritoneal mesothelial cells in culture: the role of $P16^{INK4a}$-mediated premature senescence," *Journal of Applied Physiology*, vol. 100, no. 3, pp. 988–995, 2006.

[15] G. P. Dimri, X. Lee, G. Basile et al., "A biomarker that identifies senescent human cells in culture and in aging skin in vivo," *Proceedings of the National Academy of Sciences of the United States of America*, vol. 92, no. 20, pp. 9363–9367, 1995.

[16] K. Kratochwill, M. Boehm, R. Herzog et al., "Alanyl-glutamine dipeptide restores the cytoprotective stress proteome of mesothelial cells exposed to peritoneal dialysis fluids," *Nephrology Dialysis Transplantation*, vol. 27, no. 3, pp. 937–946, 2012.

[17] K. Kratochwill, M. Lechner, C. Siehs et al., "Stress responses and conditioning effects in mesothelial cells exposed to peritoneal dialysis fluid," *Journal of Proteome Research*, vol. 8, no. 4, pp. 1731–1747, 2009.

[18] K. Kratochwill, M. Lechner, A. M. Lichtenauer et al., "Interleukin-1 receptor-mediated inflammation impairs the heat shock response of human mesothelial cells," *The American Journal of Pathology*, vol. 178, no. 4, pp. 1544–1555, 2011.

[19] J. Wang, M. Torii, H. Liu, G. W. Hart, and Z.-Z. Hu, "dbOGAP—an integrated bioinformatics resource for protein O-GlcNAcylation," *BMC Bioinformatics*, vol. 12, article 91, 2011.

[20] K. Nishio and A. Inoue, "Senescence-associated alterations of cytoskeleton: extraordinary production of vimentin that anchors cytoplasmic p53 in senescent human fibroblasts," *Histochemistry and Cell Biology*, vol. 123, no. 3, pp. 263–273, 2005.

[21] I. P. Trougakos, A. Saridaki, G. Panayotou, and E. S. Gonos, "Identification of differentially expressed proteins in senescent human embryonic fibroblasts," *Mechanisms of Ageing and Development*, vol. 127, no. 1, pp. 88–92, 2006.

[22] G. Kasper, L. Mao, S. Geissler et al., "Insights into mesenchymal stem cell aging: involvement of antioxidant defense and actin cytoskeleton," *Stem Cells*, vol. 27, no. 6, pp. 1288–1297, 2009.

[23] S. J. Winder and K. R. Ayscough, "Actin-binding proteins," *Journal of Cell Science*, vol. 118, no. 4, pp. 651–654, 2005.

[24] X. Huang, Q. Pan, D. Sun et al., "O-GlcNAcylation of cofilin promotes breast cancer cell invasion," *The Journal of Biological Chemistry*, vol. 288, no. 51, pp. 36418–36425, 2013.

[25] S. J. Assinder, J.-A. L. Stanton, and P. D. Prasad, "Transgelin: an actin-binding protein and tumour suppressor," *International Journal of Biochemistry & Cell Biology*, vol. 41, no. 3, pp. 482–486, 2009.

[26] R. Thweatt, C. K. Lumpkin Jr., and S. Goldstein, "A novel gene encoding a smooth muscle protein is overexpressed in senescent human fibroblasts," *Biochemical and Biophysical Research Communications*, vol. 187, no. 1, pp. 1–7, 1992.

[27] P. Dumont, M. Burton, Q. M. Chen et al., "Induction of replicative senescence biomarkers by sublethal oxidative stresses in normal human fibroblast," *Free Radical Biology and Medicine*, vol. 28, no. 3, pp. 361–373, 2000.

[28] K. Richter, M. Haslbeck, and J. Buchner, "The heat shock response: life on the verge of death," *Molecular Cell*, vol. 40, no. 2, pp. 253–266, 2010.

[29] G. Kim, A. B. Meriin, V. L. Gabai et al., "The heat shock transcription factor Hsf1 is downregulated in DNA damage-associated senescence, contributing to the maintenance of senescence phenotype," *Aging Cell*, vol. 11, no. 4, pp. 617–627, 2012.

[30] J. E. Fleming, J. K. Walton, R. Dubitsky, and K. G. Bensch, "Aging results in an unusual expression of *Drosophila* heat shock proteins," *Proceedings of the National Academy of Sciences of the United States of America*, vol. 85, no. 11, pp. 4099–4103, 1988.

[31] T. Finkel and N. J. Holbrook, "Oxidants, oxidative stress and the biology of ageing," *Nature*, vol. 408, no. 6809, pp. 239–247, 2000.

[32] N. Chondrogianni, F. L. L. Stratford, I. P. Trougakos, B. Friguet, A. J. Rivett, and E. S. Gonos, "Central role of the proteasome in senescence and survival of human fibroblasts. Induction of a senescence-like phenotype upon its inhibition and resistance to stress upon its activation," *The Journal of Biological Chemistry*, vol. 278, no. 30, pp. 28026–28037, 2003.

[33] N. Chondrogianni and E. S. Gonos, "Proteasome dysfunction in mammalian aging: steps and factors involved," *Experimental Gerontology*, vol. 40, no. 12, pp. 931–938, 2005.

[34] N. Sitte, K. Merker, T. Von Zglinicki, K. J. A. Davies, and T. Grune, "Protein oxidation and degradation during cellular senescence of human BJ fibroblasts: Part II - Aging of nondividing cells," *FASEB Journal*, vol. 14, no. 15, pp. 2503–2510, 2000.

[35] N. Chondrogianni and E. S. Gonos, "Proteasome inhibition induces a senescence-like phenotype in primary human fibroblasts cultures," *Biogerontology*, vol. 5, no. 1, pp. 55–61, 2004.

[36] V. Champattanachai, P. Netsirisawan, P. Chaiyawat et al., "Proteomic analysis and abrogated expression of O-GlcNAcylated proteins associated with primary breast cancer," *Proteomics*, vol. 13, no. 14, pp. 2088–2099, 2013.

[37] L. Drougat, S. O.-V. Stichelen, M. Mortuaire et al., "Characterization of O-GlcNAc cycling and proteomic identification of differentially O-GlcNAcylated proteins during G1/S transition," *Biochimica et Biophysica Acta*, vol. 1820, no. 12, pp. 1839–1848, 2012.

[38] R. Fujiki, W. Hashiba, H. Sekine et al., "GlcNAcylation of histone H2B facilitates its monoubiquitination," *Nature*, vol. 480, no. 7378, pp. 557–560, 2011.

[39] Y. Gu, S. R. Ande, and S. Mishra, "Altered O-GlcNAc modification and phosphorylation of mitochondrial proteins in myoblast cells exposed to high glucose," *Archives of Biochemistry and Biophysics*, vol. 505, no. 1, pp. 98–104, 2011.

[40] C. Gurcel, A.-S. Vercoutter-Edouart, C. Fonbonne et al., "Identification of new O-GlcNAc modified proteins using a click-chemistry-based tagging," *Analytical and Bioanalytical Chemistry*, vol. 390, no. 8, pp. 2089–2097, 2008.

[41] H. Hahne, N. Sobotzki, T. Nyberg et al., "Proteome wide purification and identification of O-GlcNAc-modified proteins using click chemistry and mass spectrometry," *Journal of Proteome Research*, vol. 12, no. 2, pp. 927–936, 2013.

[42] H. S. Kim, E. M. Kim, J. Lee et al., "Heat shock protein 60 modified with *O*-linked *N*-acetylglucosamine is involved in pancreatic β-cell death under hyperglycemic conditions," *FEBS Letters*, vol. 580, no. 9, pp. 2311–2316, 2006.

[43] A. Nandi, R. Sprung, D. K. Barma et al., "Global identification of O-GlcNAc-modified proteins," *Analytical Chemistry*, vol. 78, no. 2, pp. 452–458, 2006.

[44] A.-S. Vercoutter-Edouart, I. E. Yazidi-Belkoura, C. Guinez et al., "Detection and identification of *O*-GlcNAcylated proteins by proteomic approaches," *Proteomics*, vol. 15, no. 5-6, pp. 1039–1050, 2015.

[45] N. E. Zachara, H. Molina, K. Y. Wong, A. Pandey, and G. W. Hart, "The dynamic stress-induced '*O*-GlcNAc-ome' highlights functions for *O*-GlcNAc in regulating DNA damage/repair and other cellular pathways," *Amino Acids*, vol. 40, no. 3, pp. 793–808, 2011.

[46] M. R. Bond and J. A. Hanover, "O-GlcNAc cycling: a link between metabolism and chronic disease," *Annual Review of Nutrition*, vol. 33, pp. 205–229, 2013.

[47] J. A. Groves, A. Lee, G. Yildirir, and N. E. Zachara, "Dynamic O-GlcNAcylation and its roles in the cellular stress response and homeostasis," *Cell Stress and Chaperones*, vol. 18, no. 5, pp. 535–558, 2013.

[48] N. E. Zachara, N. O'Donnell, W. D. Cheung, J. J. Mercer, J. D. Marth, and G. W. Hart, "Dynamic O-GlcNAc modification of nucleocytoplasmic proteins in response to stress. A survival response of mammalian cells," *The Journal of Biological Chemistry*, vol. 279, no. 29, pp. 30133–30142, 2004.

[49] Z. Kazemi, H. Chang, S. Haserodt, C. McKen, and N. E. Zachara, "O-linked β-N-acetylglucosamine (O-GlcNAc) regulates stress-induced heat shock protein expression in a GSK-3β-dependent manner," *The Journal of Biological Chemistry*, vol. 285, no. 50, pp. 39096–39107, 2010.

[50] F. Zhang, K. Su, X. Yang, D. B. Bowe, A. J. Paterson, and J. E. Kudlow, "O-GlcNAc modification is an endogenous inhibitor of the proteasome," *Cell*, vol. 115, no. 6, pp. 715–725, 2003.

[51] N. Fülöp, W. Feng, D. Xing et al., "Aging leads to increased levels of protein O-linked *N*-acetylglucosamine in heart, aorta, brain and skeletal muscle in Brown-Norway rats," *Biogerontology*, vol. 9, no. 3, pp. 139–151, 2008.

[52] D. C. Love, S. Ghosh, M. A. Mondoux et al., "Dynamic O-GlcNAc cycling at promoters of *Caenorhabditis elegans* genes regulating longevity, stress, and immunity," *Proceedings of the National Academy of Sciences of the United States of America*, vol. 107, no. 16, pp. 7413–7418, 2010.

[53] M. M. Rahman, O. Stuchlick, E. G. El-Karim, R. Stuart, E. T. Kipreos, and L. Wells, "Intracellular protein glycosylation modulates insulin mediated lifespan in *C.elegans*," *Aging*, vol. 2, no. 10, pp. 678–690, 2010.

[54] J. Ma and G. W. Hart, "Protein *O*-GlcNAcylation in diabetes and diabetic complications," *Expert Review of Proteomics*, vol. 10, no. 4, pp. 365–380, 2013.

Hindawi Publishing Corporation
BioMed Research International
Volume 2015, Article ID 468574, 12 pages
http://dx.doi.org/10.1155/2015/468574

Research Article

Protective Effects of Paricalcitol on Peritoneal Remodeling during Peritoneal Dialysis

Andrea W. D. Stavenuiter,[1] Karima Farhat,[2] Marc Vila Cuenca,[1] Margot N. Schilte,[1] Eelco D. Keuning,[1] Nanne J. Paauw,[1] Pieter M. ter Wee,[2] Robert H. J. Beelen,[1] and Marc G. Vervloet[1,2,3]

[1]*Department of Molecular Cell Biology & Immunology, VU University Medical Center, 1081 BT Amsterdam, Netherlands*
[2]*Department of Nephrology, VU University Medical Center, 1007 MB Amsterdam, Netherlands*
[3]*Institute for Cardiovascular Research VU (ICaR-VU), VU University Medical Center, 1007 MB Amsterdam, Netherlands*

Correspondence should be addressed to Marc G. Vervloet; m.vervloet@vumc.nl

Received 15 May 2015; Revised 10 September 2015; Accepted 1 October 2015

Academic Editor: Gernot Zissel

Peritoneal dialysis (PD) is associated with structural and functional alterations of the peritoneal membrane, consisting of fibrosis, angiogenesis, and loss of ultrafiltration capacity. Vitamin D receptor activation (VDRA) plays an important role in mineral metabolism and inflammation, but also antiangiogenic and antifibrotic properties have been reported. Therefore, the effects of active vitamin D treatment on peritoneal function and remodeling were investigated. Rats were either kept naïve to PDF exposure or daily exposed to 10 mL PDF and were treated for five or seven weeks with oral paricalcitol or vehicle control. Non-PDF-exposed rats showed no peritoneal changes upon paricalcitol treatment. Paricalcitol reduced endogenous calcitriol but did not affect mineral homeostasis. However, upon PDF exposure, loss of ultrafiltration capacity ensued which was fully rescued by paricalcitol treatment. Furthermore, PD-induced ECM thickening was significantly reduced and omental PD-induced angiogenesis was less pronounced upon paricalcitol treatment. No effect of paricalcitol treatment on total amount of peritoneal cells, peritoneal leukocyte composition, and epithelial to mesenchymal transition (EMT) was observed. Our data indicates that oral VDRA reduces tissue remodeling during chronic experimental PD and prevents loss of ultrafiltration capacity. Therefore, VDRA is potentially relevant in the prevention of treatment technique failure in PD patients.

1. Introduction

Peritoneal dialysis (PD) is a renal replacement therapy for patients with end-stage renal disease (ESRD). During long-term PD, morphological changes occur in the peritoneum including interstitial fibrosis leading to thickening of the membrane and neovascularization [1]. Together with the induction of inflammatory processes, this can lead to loss of peritoneal membrane function, technique failure, and premature discontinuation of PD therapy [2]. The mechanisms involved in these pathological changes are incompletely understood.

Vitamin D was originally identified as a key regulator for bone metabolism and calcium homeostasis. Novel insights revealed that its biological actions go beyond this and also include regulation of inflammation and angiogenesis, as well as cell growth and differentiation and apoptosis of many cell types [3, 4]. Chronic kidney disease (CKD) patients have low levels of active vitamin D as conversion of vitamin D_3, 25-hydroxyvitamin D_3 (25D), into the bioactive form, 1,25-dihydroxyvitamin D_3 (1,25D), occurs mainly in the kidney [5].

Based on these previous findings we hypothesized that active vitamin D can attenuate or prevent the changes observed after long-term PD. To address this question we applied an experimental model of peritoneal dialysis.

2. Methods

2.1. Animals and Experimental Design. Male Wistar rats (Harlan CPB, Horst, Netherlands) weighing 280–330 grams

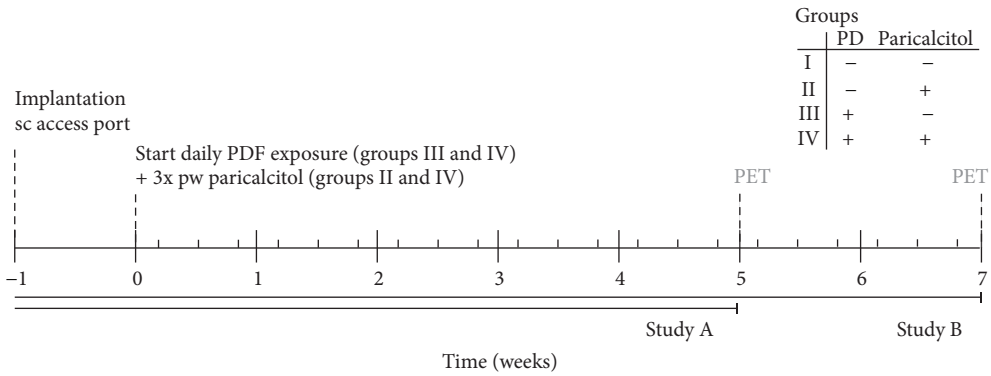

Figure 1: Time schedule animal experiments.

were used in all experiments. After arrival, the rats were allowed one week of acclimatization. Animals were maintained under conventional laboratory conditions and were given food and water *ad libitum*. The experimental design (Figure 1) was approved by the Animal Care Committee of the VU University Medical Center, Amsterdam.

Animals were randomly assigned to one of four groups and treated for five weeks: I: controls receiving 3 times weekly sugar water (orally) as vehicle control ($n = 9$), II: control rats receiving 3 times weekly orally paricalcitol, dissolved in sugar water (40 ng/kg rat, Zemplar, kindly provided by AbbVie, Chicago, USA; $n = 9$), III: animals receiving daily instillation of 10 mL conventional PDF and 3 times per week sugar water according to the same regime as group I (Dianeal, 3.86% glucose, pH5.2, Baxter R&D, Utrecht, Netherlands; $n = 13$), and IV: rats receiving daily instillation of 10 mL conventional PDF and paricalcitol treatment according to the same regime as group II ($n = 13$). PDF was instilled via a subcutaneously implanted access port as described previously [6]. Oral administration of paricalcitol was achieved in the following way: the rats were taught to drink sugar water via a syringe when offered. In this way we could limit the discomfort for the animals caused by oral gavage. Since multiple animals were housed per cage dissolving paricalcitol in drinking water would lead to unknown amounts of paricalcitol administered per animal.

To corroborate our results, additional animals were also treated for seven weeks as described above (I: $n = 8$; II: $n = 8$; III: $n = 15$; IV: $n = 15$, resp.) with a small dose adjustment of the oral treatment of paricalcitol to 30 ng/kg rat paricalcitol, three times weekly, in order to maintain a stable cumulative dose of paricalcitol among treated groups.

2.2. Readouts. Table 1 summarizes the analysis performed after five or seven weeks of treatment.

2.2.1. Analysis of Effluent. At the end of the experiment, a 90-minute peritoneal equilibrium test (PET) was performed under fentanyl citrate-fluanisone (0.05 mL/100-gram bodyweight; VetaPharma, Leeds, UK) and midazolam (0.08 mL/100-gram bodyweight; Actavis B.V., Baarn, Netherlands) anesthesia. 30 mL conventional PDF was instilled into the peritoneal cavity via a direct intraperitoneal catheter (Venflon Pro, BD Medical Systems, Franklin Lakes, NJ, USA). After drainage, the ultrafiltration capacity was calculated (effluent volume minus 30 mL) and the cell pellet was collected. Cell number and viability were determined in a hemocytometer by trypan blue exclusion. Cytocentrifuge preparations were stained with May-Grünwald-Giesma and cells were differentiated. Cell-free effluent was stored at −20°C or −80°C for determination of biomarkers for both five- and seven-week PETs.

In the animals treated for five weeks, glucose, creatinine, urea (GLUC3, CREA, and UREAL, resp., COBAS 8000, Roche Diagnostics, Basel, Switzerland), and sodium (ABL 800 FLEX, Radiometer, Zoetermeer, Netherlands) concentrations were analysed in serum samples, collected via a heart punction after sacrificing the animals by CO_2/O_2 induction, and in cell-free effluents and dialysis/serum (D/P) transport ratios were calculated. Based on a glucose determination of a pure Dianeal sample, and glucose detection in the cell-free effluent of the PETs, the percentage of glucose absorption was calculated. In the calculation a correction for the PET volume was included.

Hyaluronic acid (HA) was determined in the effluent using an ELISA-based assay according to Fosang et al. [7]. The concentrations TGF-β (TGF-β1, Promega GmbH, Manheim, Germany), VEGF (R&D systems, Abingdon, UK, or Milliplex MAP rat cytokine kits, Millipore, Billerica, MA, USA), and MCP-1 (Merck MILLIPORE, Darmstadt, Germany, or Milliplex MAP rat cytokine kits) were also analyzed in the PET effluents of both experiments. In addition, IL4, IL10, IL12p70, IL5, and GRO/KC (IL8 related protein in rodents) were analyzed only for the PET effluents collected after 7 weeks of PDF exposure using multiplex bead arrays (Milliplex MAP rat cytokine kit). Milliplex MAP is based on Luminex xMAP technology and used as recommended by the manufacturers.

2.2.2. Morphological Analysis. Parietal peritoneum samples were taken at the contralateral side of the tip of the catheter. Cryostat sections were cut and stained with Van Gieson (Merck, Darmstadt, Germany) to quantify fibrosis. To determine the submesothelial thickness, images were analyzed by measuring, on average, 10 independent points per animal

Table 1: Analyses performed after 5 and/or 7 weeks of treatment.

Analysis	Time period treatment	
	5 weeks	7 weeks
Effluent		
Ultrafiltration	+	+
Transport parameters	+	−
Cell count	+	+
Cell differentiation	+	+
Hyaluronic acid	+	+
TGF-beta	+	+
VEGF	+	+
MCP-1	+	+
IL4	−	+
IL10	−	+
IL12p70	−	+
IL5	−	+
GRO/KC	−	+
Morphological		
ECM thickness	+	+
Liver imprints	−	+
Omentum		
Vasculature	+	+
Macrophages	+	+
Mesentery		
Vasculature	+	−
Macrophages	+	−
Serum		
Transport parameters	+	−
25D	−	+
1,25D	+	+
Ca	+	+
P	+	+

+ indicates the analysis has been performed; − indicates the analysis has not been performed.

(Leica LAS AF version 2.6.0, Leica Microsystems, CMS GmbH, Mannheim, Germany). A part of the omentum, of both rats treated for five weeks and rats treated for seven weeks, and mesenteric tissue, only of rats treated for five weeks, was dissected and spread on a glass slide. To visualize vasculature and macrophages the tissues were stained with CD31 (PECAM; Serotec, Oxford, UK) and ED2 (Serotec, Oxford, UK). Images were analyzed by digital image analysis (AnalySIS Soft Imaging System, Olympus, Hamburg, Germany, or CellProfiler: image analysis software for identifying and quantifying cell phenotypes).

Liver imprints of the mesothelial monolayer were made, after seven weeks of treatment, by pressing 6% gelatine coated glass slides on the slightly dried liver after sacrificing, and stained for vimentin (Serotec, Oxford, UK), cytokeratin (DakoCytomation, Glostrup, Denmark), and DAPI (Invitrogen, Breda, Netherlands) to determine epithelial to mesenchymal transition [8]. On average seven images per rat were analyzed manually (Leica LAS AF version 2.6.0, Leica Microsystems, CMS GmbH, Mannheim, Germany), whereby increased vimentin expression and change in morphology from cobbled stone like cells towards spindle like cells were counted as cells that underwent EMT.

2.2.3. Serum Analysis. Serum samples were analyzed for 25-hydroxyvitamin D3 by competitive binding protein assay (DiaSorin, Stillwater, Minnesota, USA), 1,25-dihydroxyvitamin D3 by radioimmunoassay after immunoextraction (IDS, Tyne and Wear, UK), PTH by ELISA (Scantibodies Laboratory, Santee, CA, USA), and calcium (Ca) and phosphate (P) by colorimetric assays (Roche Diagnostics, Mannheim, Germany). With exception of 25D, only measured in serum samples of animals treated for seven weeks, the analysis was performed after both five and seven weeks of treatment.

2.2.4. In Vitro Macrophage Migration Assay. Macrophage migration was examined in Boyden transwell cell culture chambers using gelatine-treated polycarbonate membranes with 10 μm pore size (Neuro Probe, Inc., Gaithersburg, MD, USA). Briefly, rat bone marrow cells were isolated and macrophages were allowed to adhere for 7 days in the presence of DMEM (Gibco, BRL, Gaithersburg, MD, USA) enriched with 15% v/v L-cell conditioned medium (LCM) and supplemented with 2% v/v penicillin-streptomycin-glutamine (PSG; Invitrogen, Breda, Netherlands) and 10% fetal calf serum (Biowest, Nuaillé, France). Other cells were washed away and macrophages were harvested by lidocaine treatment. Cells were resuspended in serum-free DMEM to a concentration of $2 * 10^5$ cells/mL. Aliquots of 50 μL were added to the upper chamber, while the lower chamber was filled with 25 μL of DMEM containing MCP-1 (10 ng/mL), paricalcitol ($1 * 10^{-6}$ M), or a combination of both, with or without the addition of Dianeal (1 : 4 with DMEM). After 6 hours of incubation at 37°C, cells were removed from the upper chamber side of the membrane. The membrane was washed and stained with Coomassie. The cells on the bottom side of the filter were counted and expressed as percentage of migrated cells compared to control DMEM medium without chemoattractant. The experiment was performed in triplicate using different cell isolations.

2.3. Statistical Analysis. Data presented as median and interquartile range are analysed by using the Kruskal-Wallis test followed by Dunn's Multiple Comparison test to compare the following groups: I versus II, I versus III, I versus IV, and III versus IV. The detection limit was used for statistical analysis for VEGF, IL4, IL10, IL12p70, IL5, and GRO/KC levels in the effluent, when the concentrations were below detection limit.

3. Results

The well-being of all rats was monitored daily and no unexpected abnormalities were observed. Twelve of the total 56 animals exposed to PDF were taken out of the experiment

Table 2: Effect of paricalcitol on mineral homeostasis.

Treatment	Five weeks				Seven weeks			
Group	I	II	III	IV	I	II	III	IV
1.25 vitamin D3 (pmol/L)	436.0	342.0	564.0	310.5	255.5	33.5[a]	384	42[b]
IQR	[352.8–519.3]	[256.0–427.0]	[427.5–673.5]	[288.0–365.3]	[225–279]	[30.8–36]	[330.8–456.8]	[39–45]
25 vitamin D3	No data	No data	No data	No data	63	39[a]	75.5	52[b]
IQR					[59.5–70.8]	[37.8–40.5]	[69.3–79.8]	[51–54]
Phosphate (mmol/L)	3.4	4.6[a,b]	3.3[a]	3.2	3.0	3.4	3.6	4.1
IQR	[2.7–4.1]	[4.0–4.7]	[3.2–3.4]	[2.8–3.6]	[3.0–3.2]	[3.1–3.5]	[3.6–4.5]	[3.6–5.4]
Calcium (mmol/L)	3.6	3.6	3.5	3.4	3.2	3.1	3.4	3.4
IQR	[3.6–3.8]	[3.4–3.8]	[3.2–3.5]	[3.3–3.5]	[3.1–3.3]	[3.2–3.0]	[3.3–3.6]	[3.4–3.2]

All data presented as median and interquartiles.
[a] $p < 0.05$ compared to group I; [b] $p < 0.05$ compared to group III.

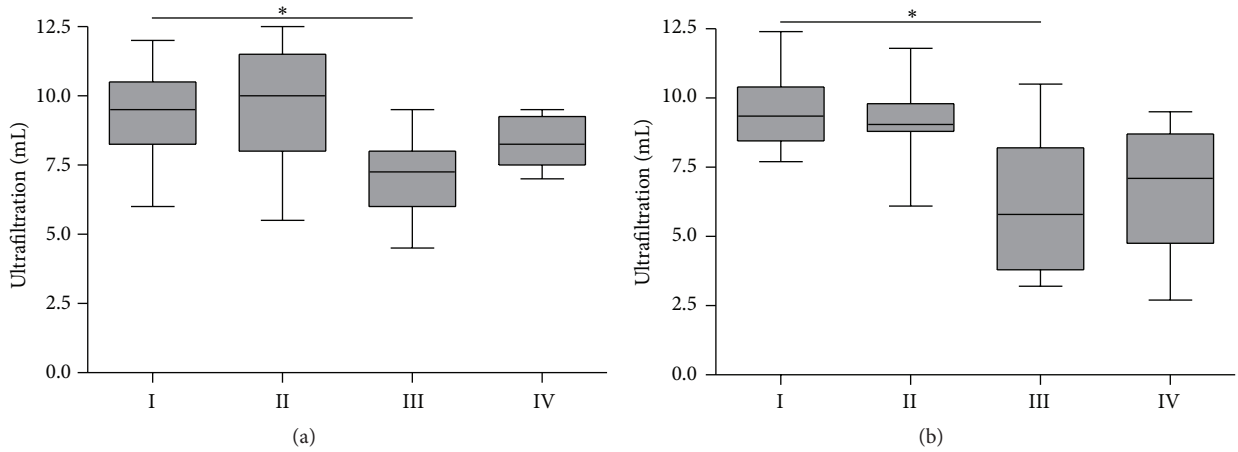

Figure 2: Net ultrafiltration after 90-minute PET. Net ultrafiltration after a 90-minute PET with 30 mL conventional PD fluid after five (a) and seven (b) weeks of treatment. All data presented as median and interquartiles. Whiskers indicate the extremes. * $p < 0.05$ compared to group I.

due to abdominal fat or omental tissue wrapping around the tip of the catheter, which was consistent with previous experience [8]. All control animals (groups I and II), 25 out of 30 in group III and 19 out of 30 in group IV, remained for analysis after five and seven weeks of PDF exposure.

3.1. Vitamin D Mineral Homeostasis. 1,25D levels showed a declining trend in paricalcitol treated animals after five weeks and a significant decrease after seven weeks of treatment compared to the control animals (Table 2). In addition, the same effect of paricalcitol on 25D levels was detected in the serum samples measured after seven weeks of treatment. Ca and P levels were not affected by paricalcitol treatment, except for animals in the control group receiving 40 ng/kg paricalcitol, which had significantly higher P level compared to the control animals.

3.2. Peritoneal Transport. The PET resulted in ~10 mL net ultrafiltration (UF) in control animals (groups I and II). Chronic PD treatment significantly reduced ultrafiltration capacity towards a median of 7.3 mL after five weeks and, even worse, 5.8 mL net UF after seven weeks ($p = 0.05$, group III versus group I; Figure 2). Paricalcitol treatment in the PDF-exposed group prevented these significant changes in UF ($p > 0.05$ versus group I) and resulted in a 10–15% increase in UF capacity compared to PDF exposure alone.

To further analyze the effect of PDF exposure and vitamin D receptor activation on peritoneal functional decline, transport parameters were measured in serum and PET effluents after five weeks of treatment (Table 3). Exposure to PDF changed D/P creatinine from 0.2 to 0.4 ($p < 0.01$ versus group I). Paricalcitol did not affect the D/P creatinine in both control and PD treated rats. Although compared to control levels (group I) D/P urea (0.5) and D/P sodium (0.8) were slightly higher in group III (0.6, $p > 0.05$, and 0.9, $p < 0.05$, resp.) and group IV (0.6, $p < 0.01$, and 0.8, $p > 0.05$, resp.), absolute changes in ratios were minimal. Glucose absorption increased, although not significantly, from 33.3% to 42.8% upon PDF exposure. Paricalcitol treatment lowered, but not significantly, glucose absorption in both non-PDF-exposed and PDF-exposed animals (33.3% in group I versus 22.3% in group II) and PDF-exposed animals (46.5% in group III versus 42.8% in group IV).

3.3. Cell Numbers and Macrophage Migration. Total cell numbers increased significantly upon PD treatment and were

Table 3: Peritoneal transport parameters determined by PET effluent D/serum P after 5 weeks of treatment.

Group	I	II	III	IV
Glucose absorption (%)	33.3 [28.5–38.5]	22.3 [21.5–28.2]	46.5 [35.6–53.7]	42.8 [36.9–48.8]
D/S creatinine	0.2 [0.1–0.2]	0.2 [0.2–0.3]	0.4[b] [0.3–0.5]	0.4[b] [0.3–0.5]
D/S urea	0.5 [0.4–0.5]	0.5 [0.4–0.5]	0.6 [0.5–0.7]	0.6[b] [0.6–0.7]
D/S sodium	0.8 [0.6–0.8]	0.8 [0.7–0.8]	0.9[a] [0.8–0.9]	0.8 [0.8–0.9]

All data presented as median and interquartiles.
[a] $p < 0.05$ compared to group I; [b] $p < 0.01$ compared to group I.

Table 4: Composition of peritoneal leukocytes.

Treatment	Five weeks				Seven weeks			
Group	I	II	III	IV	I	II	III	IV
Cell number $\times 10^6$	22.1	19.5	99.8[b]	153.9[b]	24.95	22.9	122.75	92.25
IQR	[12.5–24.8]	[16.2–24.2]	[89.0–130.1]	[108.1–186.1]	[20.3–26.7]	[17.3–26.3]	[109.4–144.9]	[46.9–153.4]
Macrophages (%)	77.0	80.0	84.7	78.9	89	88.5	88	86.5
IQR	[74.0–81.0]	[76.6–82.1]	[72.3–90.4]	[68.8–87.7]	[85.8–90.3]	[87.5–90.3]	[85.8–92.5]	[79.5–91.8]
Lymphocytes (%)	0.0[a]	0.0	0.5[c]	0.4	0	0	1	3
IQR	[0.0–0.0]	[0.0–0.0]	[0.3–1.3]	[0.0–0.9]	[0–1.25]	[0–0.3]	[0.5–1.8]	[0.8–4.5]
Neutrophils (%)	0.0	0.0	7.25[c]	14.1[c]	0.5	0	4	2
IQR	[0.0–0.0]	[0.0–0.0]	[2.5–25.8]	[10.6–20.2]	[0–1]	[0–0]	[0–8.8]	[0–9]
Eosinophils (%)	11.3	13.8	2.3[a]	1.75	10.5	11	3[b]	5.5[a]
IQR	[9.0–13.9]	[11.3–14.6]	[1.5–5.4]	[0.6–11.9]	[9.8–11.3]	[9.8–11.8]	[1.8–5.3]	[2–6.5]
Mast cells (%)	9.8	7.3	0.0[c]	0.0[c]	0	0	0	0
IQR	[8.8–13.6]	[4.5–10.4]	[0.0–0.3]	[0.0–0.2]	[0–0]	[0–0]	[0–0]	[0–0]

All data presented as median and interquartiles.
[a] $p < 0.05$ compared to C group; [b] $p < 0.01$ compared to C group; [c] $p < 0.001$ compared to C group.

approximately five times higher compared to control animals ($p < 0.01$ and $p < 0.001$ for groups III and IV versus group I, resp.; Figures 3(a) and 3(b)). However, there was no significant difference between the paricalcitol and vehicle control treated groups. Cell differentiation of peritoneal cells in the effluents revealed a reduction of eosinophil and mast cell count and an increase in neutrophils after PD treatment. In all groups macrophages remained the dominant cell type (±80%; Table 4). Paricalcitol treatment did not induce significant differences in leukocyte composition in control or PD treated rats after five or seven weeks of PDF exposure.

3.4. Analysis of Peritoneal Effluents and In Vitro Macrophage Migration. MCP-1 was measured in the PET effluents and showed to be unaffected by paricalcitol treatment in the control situation (group II, Figure 3(c)). After five weeks of PD treatment, MCP-1 levels were ~5-fold increased in PD rats compared to control rats ($p = 0.05$). Paricalcitol treatment in combination with PD tended to increase MCP-1 levels even further, although not significantly, to a median of 2 ng/mL compared to 1.2 ng/mL in group III and 0.3 ng/mL in both control groups. No difference was found in MCP-1 levels between the different groups in the animals treated for seven weeks.

To examine the effect of paricalcitol and peritoneal dialysis fluid on macrophage migration, *in vitro* migration assays with primary rat macrophages were performed. As expected, MCP-1 induced macrophage migration. Paricalcitol did not change migration under these (control) conditions (Figure 3(d), white bars). However, when Dianeal was added to the culture medium (1 : 4), which is known to result in macrophage activation [9], paricalcitol enhanced migration, similar to the levels of MCP-1 induced migration ($p < 0.05$) (Figure 3(d), grey bars). Simultaneous addition of paricalcitol and MCP-1 did not further increase macrophage migration when Dianeal was present.

VEGF levels in peritoneal effluents were below detection limits in most control animals but were statistically significantly higher in the PDF-exposed groups. Seven weeks of paricalcitol treatment reduced VEGF levels to 40 pg/mL (median) compared to 72 pg/mL in the PDF-exposed group ($p = 0.01$; Figure 4(a)). However, after five weeks, no effect of paricalcitol treatment on effluent VEGF concentration was found (data not shown).

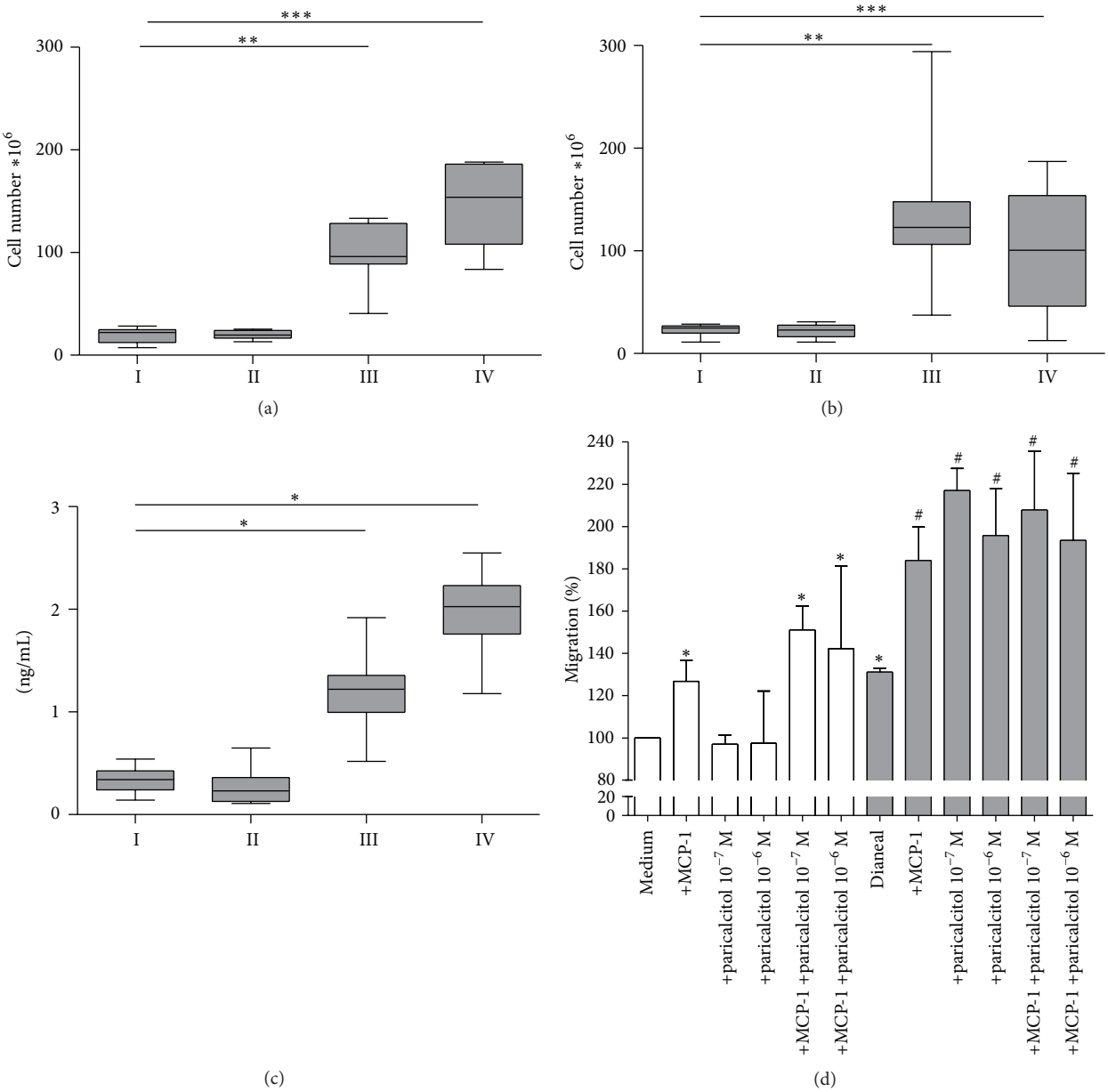

FIGURE 3: Cell numbers and macrophage migration. Total peritoneal cell number in effluent after 90-minute PET with 30 mL of conventional PD fluid after five (a) and seven (b) weeks of treatment; $^{**}p < 0.01$; $^{***}p < 0.001$. Effluent concentration of MCP-1 after five weeks of treatment (c); $^{*}p < 0.05$. Rat macrophage migration towards paricalcitol; MCP-1 in standard medium (white bars) or medium containing Dianeal (1 : 4) (grey bars; (d) $^{*}p < 0.05$ versus medium; $^{\#}p < 0.05$ versus Dianeal + medium).

As shown previously [8, 10], PD treatment induced a significant increase in HA production, indicating an inflammatory state in the peritoneum ($p = 0.001$) (Figure 4(b)). Paricalcitol treatment mitigated the increase in HA concentrations in the rats exposed to PDF after five and seven weeks of treatment.

In PD treated animals, TGF-β concentrations were on average 2.7 times higher compared to control animals ($p = 0.05$) after five (data not shown) or seven (Figure 4(c)) weeks of treatment. Paricalcitol treatment did not affect the TGF-β levels in the effluent.

IL4 levels were below detection limit in almost all animals in the control groups (18 pg/mL; groups I and II). IL4 levels were significantly increased in group III compared to group I ($p = 0.001$) with an average of 186 pg/mL. Although there was no significant difference between groups III and IV, IL4 levels were less pronounced upon paricalcitol treatment with an average concentration of 92 pg/mL (Figure 4(d)).

IL12p70 concentrations in the effluent significantly increased upon PD treatment in groups III and IV compared to group I, in which all levels were found to be below detection limit (24 pg/mL); $p = 0.001$ and $p = 0.05$, respectively.

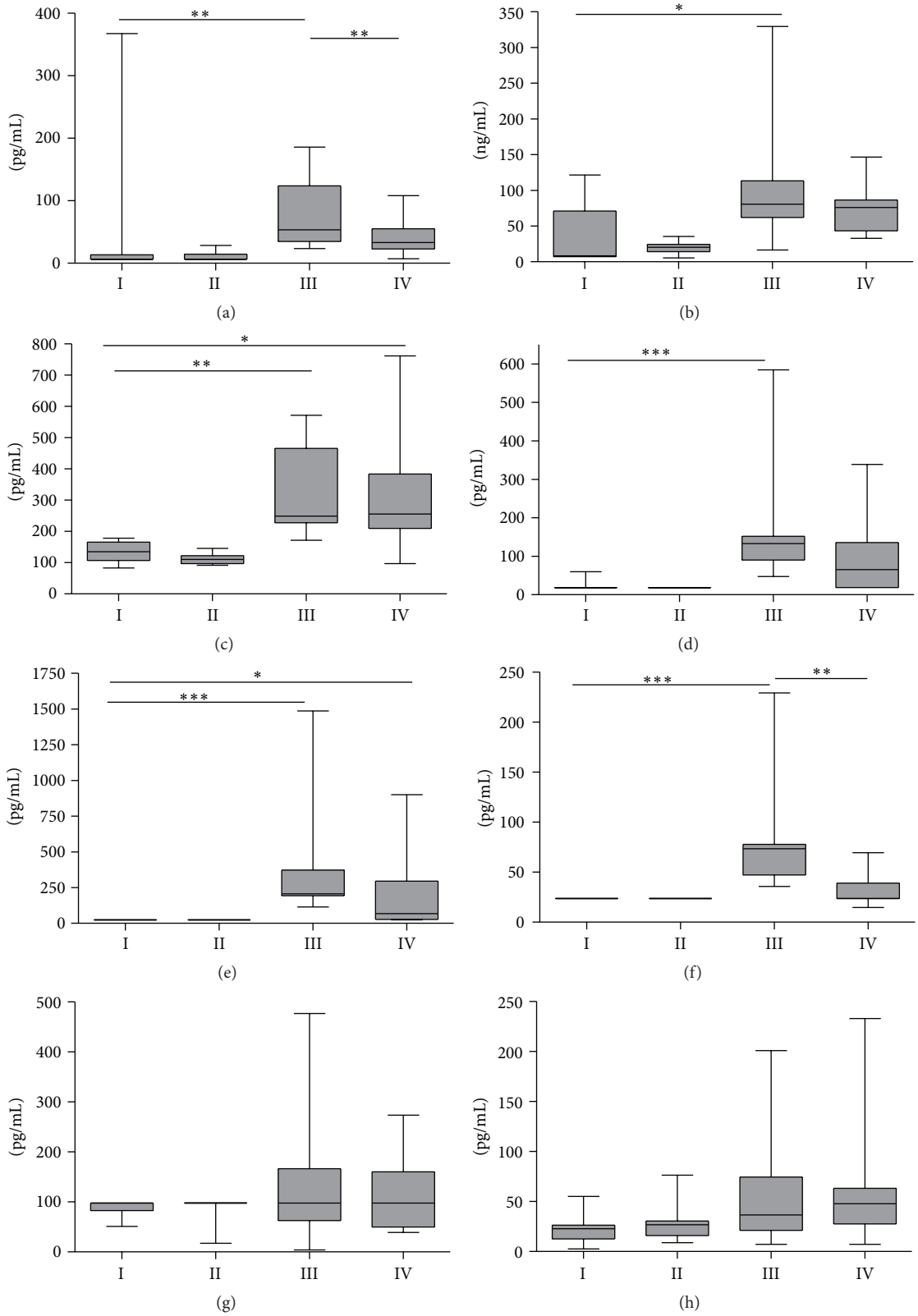

Figure 4: Peritoneal effluent concentrations. VEGF (a), HA (b), TGF-beta (c), IL4 (d), IL12p70 (e), IL5 (f), IL10 (g), and GRO/KC (h) levels in the peritoneal effluent after seven weeks of treatment. Data presented as median and interquartiles. Whiskers indicate the extremes. $^{*}p < 0.05$; $^{**}p < 0.01$; $^{***}p < 0.001$.

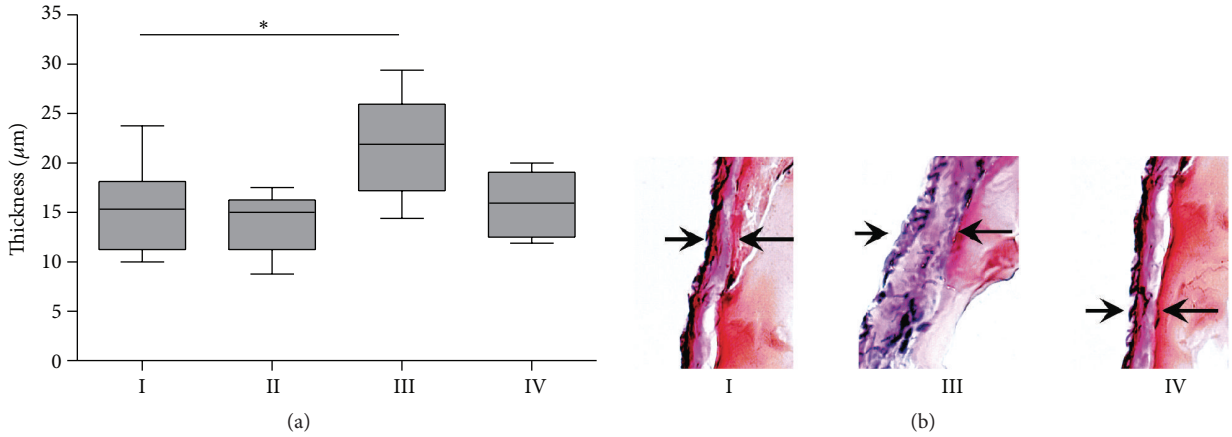

Figure 5: Extra cellular matrix thickness. ECM thickness of parietal peritoneum (a) and representative examples of peritoneal sections of groups I, III, and IV, respectively, after 5 weeks of treatment. All data presented as median and interquartiles. Whiskers indicate the extremes. $^{*}p < 0.05$.

A nonsignificant trend was observed whereby, upon PDF exposure, paricalcitol mitigated the rise of IL12p70 with a median concentration of 68 pg/mL compared to 207 pg/mL in group III (Figure 4(e)).

Also IL5 concentrations were below detection limit (24 pg/mL) in all control animals (groups I and II). PDF exposure alone led to an increase of IL5 concentrations in the effluent (74 pg/mL), whereas paricalcitol treatment completely prevented this significant elevation (24 pg/mL; $p = 0.01$ versus group III; Figure 4(f)).

Even though a few animals in the PDF-exposed groups had IL10 levels above the detection limit, the medians of all groups were 98 pg/mL IL10, so no difference was determined (Figure 4(g)). GRO/KC concentrations were not significantly increased upon PDF exposure and no effect of paricalcitol treatments was observed. Median GRO/KC levels were 23, 27, 37, and 48 pg/mL for groups I, II, III, and IV, respectively (Figure 4(h)).

3.5. Peritoneal Tissue Remodeling. Histological analysis showed that five-week PDF exposure resulted in increased submesothelial matrix thickness (median 22 μm) compared to control rats (median 15 μm; $p = 0.05$ versus group I; Figure 5). Additional paricalcitol treatment prevented thickening of the parietal mesothelial matrix layer (16 μm; $p > 0.05$ versus group I). After seven weeks of PDF exposure no difference in submesothelial matrix thickness was found between all groups, thus also not between PDF and non-PDF treated groups (data not shown).

Chronic PD treatment resulted in increased recruitment of activated M2 tissue macrophages and in new vessel formation in omentum and mesentery, determined by, respectively, ED2 and CD31 staining (Figure 6). In the mesentery, paricalcitol treatment could not prevent PD-induced macrophage accumulation or angiogenesis (Figures 6(b) and 6(d)). However, a declining trend in median omental ED2 positive macrophage accumulation was observed during paricalcitol treatment for both the control (group II 1% versus group I 3% positive area) and the PDF-exposed groups (group IV 5% versus group III 10% positive area; Figures 6(c) and 6(e)). Moreover, PD-induced angiogenesis in the omentum (14% positive area; $p = 0.01$ compared to group I) was less pronounced for paricalcitol treated animals (4% positive area; $p > 0.05$ compared to group I) after five weeks of treatment (Figures 6(d) and 6(e)). Although no significant differences in omental CD31 positive area were observed after seven weeks between groups I and III, a declining trend in the CD31 positive area upon paricalcitol treatment was observed (33% versus 14% and 32% versus 27% for groups I versus II and III versus IV, resp.; data not shown).

3.6. Liver Imprints. Liver imprints were taken after seven weeks of PDF exposure. Mesothelial cell density and the number of vimentin positive-cytokeratin negative cells increased in the PDF-exposed animals (Figure 7(a); groups III and IV compared to group I) indicating mesothelial cell regeneration and epithelial to mesenchymal transition. In addition, the cobblestone appearance of the mesothelial cells (Figure 7(b), group I) is partly lost in groups III and IV, in which the cells are more stretched. The ratio vimentin positive-cytokeratin negative cells/mesothelial cells approximately doubled in the PDF-exposed groups (III and IV) compared to the control (group I). Paricalcitol treatment did not influence this process (Figure 7(a)).

4. Discussion

In the present study, the role of VDR activation in peritoneal remodeling in a chronic rat PD model was investigated while validating our model by comparing the control and PDF exposure only groups as well (group I versus group III). In the animals exposed to PDF, compared to the control situation, we observed worsening of ultrafiltration capacity, elevation in inflammation markers, partly increased vascular surface area, and a higher number of cells undergoing epithelial to mesenchymal transition. This is in line with previous

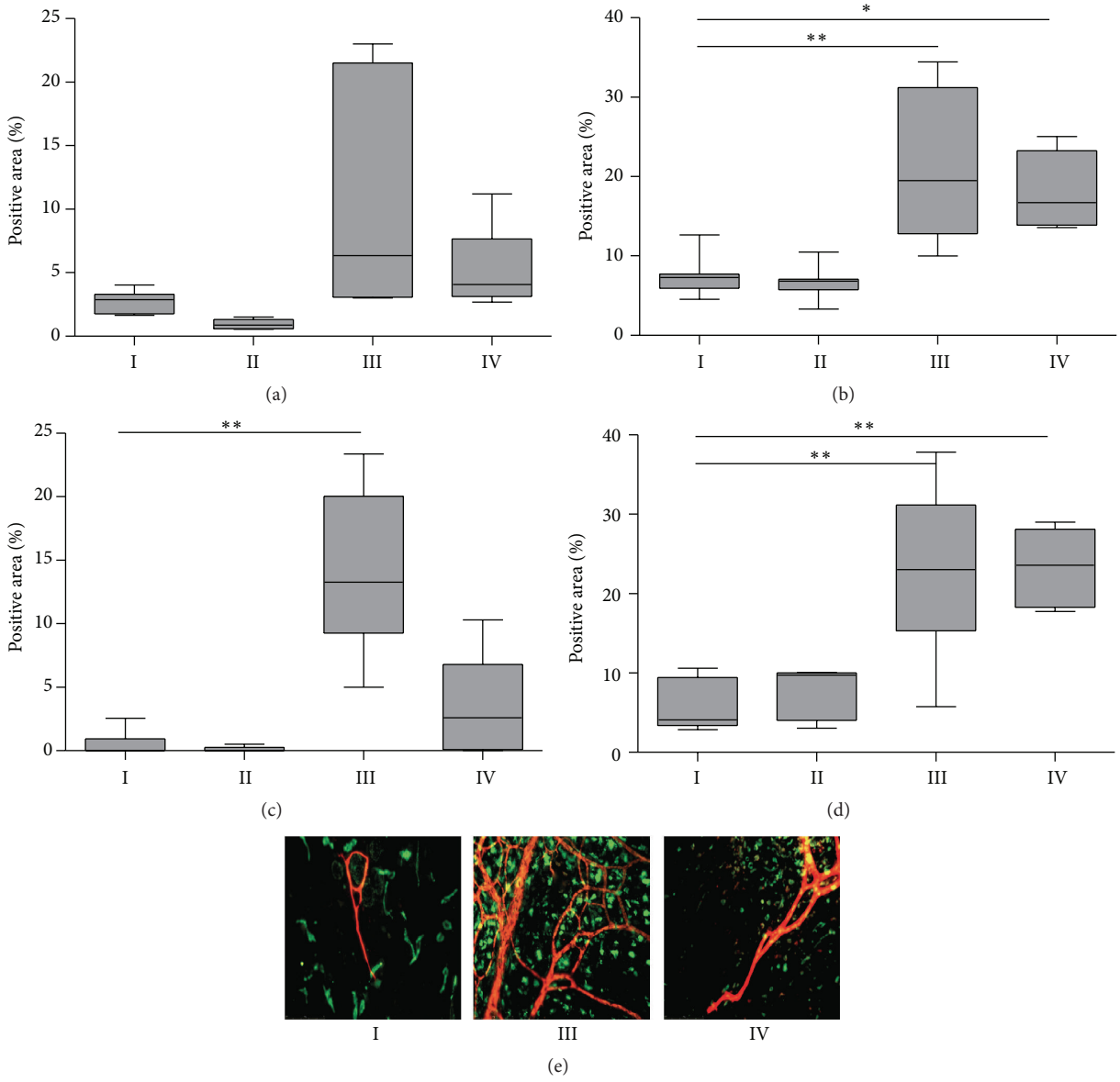

FIGURE 6: Angiogenesis and macrophage accumulation in visceral peritoneum. Macrophage accumulation (Ed2 positive staining) in omentum (a) and mesentery (b) and angiogenesis (CD31 positive staining) in omentum (c) and mesentery (d) after 5 weeks of PDF exposure and paricalcitol treatment. Representative examples of the omentum with ED2 in green and CD31 in red of control rat (group I), PDF-exposed rat (group III), and PDF-exposed rat treated with paricalcitol (group IV) (e). All data presented as median and interquartiles. Whiskers indicate the extremes. $^{*}p < 0.05$; $^{**}p < 0.01$.

observations [8, 10]. Paricalcitol treatment influenced several of the examined parameters. Loss of ultrafiltration capacity, increase in ECM thickness, angiogenesis, and IL5 levels due to PDF exposure were significantly attenuated by paricalcitol treatment. In addition, a trend towards decreased glucose absorption, less ED2 positive macrophage accumulation in the omentum and mesentery, and lower HA, VEGF, IL12p70, and IL4 levels was observed upon paricalcitol treatment in PDF-exposed animals. However, not all factors involved in peritoneal remodeling upon PD were affected by paricalcitol treatment, such as total cell number and epithelial to mesenchymal transition.

Importantly, paricalcitol treatment decreased endogenous 1,25D levels, which has also been found by others in both animal and human studies [11, 12] and is the consequence of upregulation of the catabolic enzyme 25(OH)D-24-hydroxylase. This indicates successfulness of applying oral paricalcitol treatment in our rat model.

The main finding of this paper is the demonstration that paricalcitol can attenuate the loss in ultrafiltration capacity upon PDF exposure. Driving forces for ultrafiltration in peritoneal dialysis are the maintenance of an osmotic gradient and the existence of low barrier resistance for water transport. Glucose absorption showed a slight, although not significant,

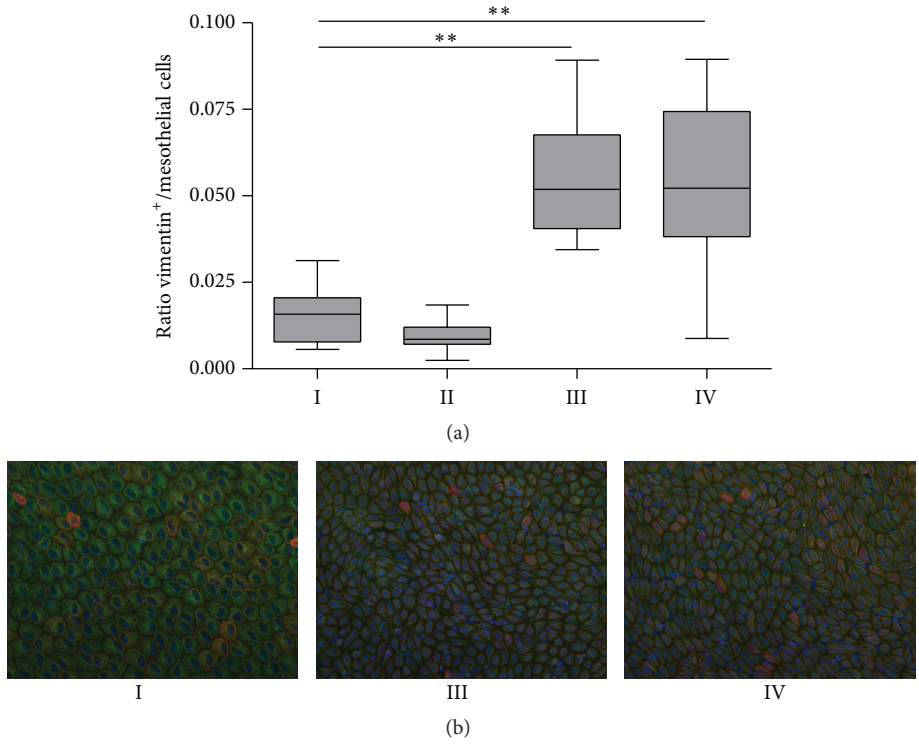

Figure 7: Epithelial to mesenchymal transition on liver imprints. Ratio vimentin positive/mesothelial cells on liver imprints (a). Representative examples of liver imprints with nuclei in blue, vimentin in green, and cytokeratin in red of control rat (group I), PDF-exposed rat (group III), and PDF-exposed rat treated with paricalcitol (group IV) (b). All data presented as median and interquartiles. Whiskers indicate the extremes. $^{**}p < 0.01$.

increase after five weeks of PDF exposure, indicating a small loss of osmotic gradient. In the control situation, and to lesser extent in the PDF-exposed group, addition of paricalcitol resulted in a trend towards positively affecting the osmotic gradient. Despite the fact that the trend was small and not significant, this could have contributed to the partial preservation of the ultrafiltration capacity in animals receiving oral paricalcitol in a PD environment. Consistent with this is the observed attenuated neovascularization by paricalcitol. Neovascularization results in increased perfusion of the peritoneal membrane, which is considered to be one mechanism leading to enhanced dissipation of the osmotic gradient, by early enhanced glucose uptake from the peritoneal dialysis fluid.

In line with the observed partial prevention of ultrafiltration failure by paricalcitol treatment, we showed prevention of increasing ECM thickness, which may indicate a lower barrier resistance for water transport, upon PDF exposure after five weeks of treatment with paricalcitol. This latter finding is in accordance with the compelling evidence that vitamin D treatment can reduce fibrosis [13, 14]. Possible explanations for reduced fibrosis after paricalcitol treatment may be found in proteins involved in the thickening of the ECM-layer such as collagen type-1 and the renin-angiotensin-aldosterone (RAAS) system, which are downregulated upon VDR activation [15, 16].

The immunomodulatory effects of paricalcitol could have beneficially contributed to the development of ECM thickness. In our experiments paricalcitol modulated the concentrations of IL5 and IL4 and possibly also affected HA and VEGF, factors derived from cells of the immune system and/or mesothelial cells. Although we cannot prove the direct effect of these cytokines on peritoneal membrane remodeling, our data are in line with a recent study showing the importance of cytokines by correlating reduction in IL-17 and activation of regulatory T-cells with reduced fibrosis [17].

In our experiments paricalcitol treatment led to a ~50% decreased population of ED2 positive "M2" macrophages in the omentum in both control and PDF-exposed rats, which might have led to lesser thickening of the submesothelial matrix we observed after five weeks of treatment. In other studies, it has also been shown that macrophages play an important role in fibrosis, whereby M2 macrophages correlate with fibrosis in sclerotic skin and pulmonary and kidney fibrosis [18–21]. Moreover, there is compelling evidence that M2 macrophages are involved in peritoneal fibrosis in PD [22, 23]. In addition, paricalcitol treatment mitigated IL12p70 concentrations, whose production is related to M1 macrophages [24], upon PDF exposure.

Vitamin D receptor activation has acknowledged antiangiogenic properties [25]. In this study it is also shown that paricalcitol tended to reduce angiogenesis, especially in the omentum. This observation is in line with previous *in vitro* studies. These studies demonstrate reduced proliferation of human umbilical vein endothelial cells upon paricalcitol treatment [26]. In addition, in a mouse model for PD, it

has been shown that paricalcitol can prevent angiogenesis [17]. Several humoral factors can be involved in this reduced angiogenesis following paricalcitol. IL12p70, however, which is described to have antiangiogenic properties, declined in the paricalcitol group. This suggests that the effects of paricalcitol are not mediated by this factor. VEGF is another prominent proangiogenic factor [27]. Here, we show indeed that the PDF exposure-induced increase in VEGF, after seven weeks of treatment, is attenuated by paricalcitol treatment. Finally, MCP-1, which has been shown also to have proangiogenic capacities [28], was not reduced by paricalcitol.

In line with previous studies, we found an increase in peritoneal cells observed after PD treatment. The higher cell numbers could be due to the enhanced levels of chemoattractants such as MCP-1 and IL5 [10, 29]. Although paricalcitol did not influence total cell numbers, as described above, it tended to influence the type of cells including the decrease of ED2 positive cells.

The ratio vimentin positive/mesothelial cells, as indicator of EMT, increased upon PDF exposure compared to the control situation, which makes our model suitable to study the effects of paricalcitol on EMT. However, contrary to other studies, we were not able to find a decrease in EMT which might be due to the different models or concentrations of paricalcitol used [30, 31].

To summarize, although we did not observe an effect of paricalcitol on EMT, parts of the effects of paricalcitol are found to be consistent. Paricalcitol partly preserved the ultrafiltration capacity upon PDF exposure. We observed partial prevention of angiogenesis, and thus a smaller vascular surface area, which could contribute to the observed trend in preservation of the glucose driven osmotic gradient. In addition, prevention of increase in ECM thickness was found, which indicates less resistance of the peritoneal membrane and thus a better ultrafiltration capacity.

Our study has several limitations. Firstly, differences between the control and PDF-exposed groups, such as ultrafiltration capacity and ECM thickness, were less pronounced after seven weeks of PDF exposure. This was likely caused by the apparent less mesothelial toxic effects in this particular control group of animals. We know from earlier experiments that differences in separate experiments may occur. Besides sampling error and inequal distribution of toxicity could be of importance too. Therefore, we could have missed potential protective effects of paricalcitol treatment in this group due to a lack of pathological changes in the PD control animals. However, we did use a wide range of additional parameters in which morphological, functional, and biochemical components were included and did observe all well-described changes in the PD treated groups for five weeks.

A second limitation is that we did not use uremic model and vitamin D deficient model. However, we hypothesize that under those conditions the effect of VDR activation is likely even more pronounced.

Taken together, we have shown that VDR activation can partly restore ultrafiltration failure due to limiting ECM thickening and angiogenesis even in a calcitriol sufficient environment. Future studies should be carried out to address the clinical benefit of improved PD efficacy on ultrafiltration in particular.

Conflict of Interests

The authors declare that there is no conflict of interests regarding the publication of this paper.

Authors' Contribution

Karima Farhat and Marc Vila Cuenca contributed equally to this work and Robert H. J. Beelen and Marc G. Vervloet also share equal contribution.

Acknowledgment

This work was supported by the Dutch Kidney Foundation (Grant nos. C05-2142 and C09-2331).

References

[1] J. D. Williams, K. J. Craig, N. Topley et al., "Morphologic changes in the peritoneal membrane of patients with renal disease," *Journal of the American Society of Nephrology*, vol. 13, no. 2, pp. 470–479, 2002.

[2] P. K.-T. Li, C. C. Szeto, B. Piraino et al., "Peritoneal dialysis-related infections recommendations: 2010 update," *Peritoneal Dialysis International*, vol. 30, no. 4, pp. 393–423, 2010.

[3] E. Baroni, M. Biffi, F. Benigni et al., "VDR-dependent regulation of mast cell maturation mediated by 1,25-dihydroxyvitamin D3," *Journal of Leukocyte Biology*, vol. 81, no. 1, pp. 250–262, 2007.

[4] A. S. Dusso, A. J. Brown, and E. Slatopolsky, "Vitamin D," *American Journal of Physiology: Renal Physiology*, vol. 289, no. 1, pp. F8–F28, 2005.

[5] A. S. Dusso, "Kidney disease and vitamin D levels: 25-hydroxyvitamin D, 1,25-dihydroxyvitamin D, and VDR activation," *Kidney International Supplements*, vol. 1, pp. 136–141, 2011.

[6] L. H. Hekking, M. C. Aalders, E. van Gelderop et al., "Effect of peritoneal dialysis fluid measured in vivo in a rat-model of continuous peritoneal dialysis," *Advances in Peritoneal Dialysis*, vol. 14, pp. 14–18, 1998.

[7] A. J. Fosang, N. J. Hey, S. L. Carney, and T. E. Hardingham, "An Elisa plate based assay for hyaluronan using biotinylated proteoglycan G1 domain (HA-binding region)," *Matrix*, vol. 10, no. 5, pp. 306–313, 1990.

[8] M. N. Schilte, J. Loureiro, E. D. Keuming et al., "Long-term intervention with heparins in a rat model of peritoneal dialysis," *Peritoneal Dialysis International*, vol. 29, no. 1, pp. 26–35, 2009.

[9] F. K. Li, "Effect of peritoneal dialysis on peritoneal macrophages," *Peritoneal Dialysis International*, vol. 19, supplement 2, pp. S343–S347, 1999.

[10] P. Fabbrini, M. N. Schilte, M. Zareie et al., "Celecoxib treatment reduces peritoneal fibrosis and angiogenesis and prevents ultrafiltration failure in experimental peritoneal dialysis," *Nephrology Dialysis Transplantation*, vol. 24, no. 12, pp. 3669–3676, 2009.

[11] F. Takahashi, J. L. Finch, M. Denda, A. S. Dusso, A. J. Brown, and E. Slatopolsky, "A new analog of 1,25-$(OH)_2D_3$, 19-NOR-1,25-$(OH)_2D_2$, suppresses serum PTH and parathyroid gland growth

in uremic rats without elevation of intestinal vitamin D receptor content," *American Journal of Kidney Diseases*, vol. 30, no. 1, pp. 105–112, 1997.

[12] I. H. de Boer, M. Sachs, A. N. Hoofnagle et al., "Paricalcitol does not improve glucose metabolism in patients with stage 3-4 chronic kidney disease," *Kidney International*, vol. 83, no. 2, pp. 323–330, 2013.

[13] X. Y. Tan, Y. J. Li, and Y. H. Liu, "Paricalcitol attenuates renal interstitial fibrosis in obstructive nephropathy," *Journal of the American Society of Nephrology*, vol. 17, no. 12, pp. 3382–3393, 2006.

[14] Y. Zhang, J. Kong, D. K. Deb, A. Chang, and Y. C. Li, "Vitamin D receptor attenuates renal fibrosis by suppressing the renin-angiotensin system," *Journal of the American Society of Nephrology*, vol. 21, no. 6, pp. 966–973, 2010.

[15] D. L. Andress, "Vitamin D in chronic kidney disease: a systemic role for selective vitamin D receptor activation," *Kidney International*, vol. 69, no. 1, pp. 33–43, 2006.

[16] M. Freundlich, Y. Quiroz, Z. Zhang et al., "Suppression of renin-angiotensin gene expression in the kidney by paricalcitol," *Kidney International*, vol. 74, no. 11, pp. 1394–1402, 2008.

[17] G. T. González-Mateo, V. Fernández-Míllara, T. Bellón et al., "Paricalcitol reduces peritoneal fibrosis in mice through the activation of regulatory T Cells and reduction in IL-17 production," *PLoS ONE*, vol. 9, no. 10, Article ID e108477, 2014.

[18] N. Higashi-Kuwata, T. Makino, Y. Inoue, M. Takeya, and H. Ihn, "Alternatively activated macrophages (M2 macrophages) in the skin of patient with localized scleroderma," *Experimental Dermatology*, vol. 18, no. 8, pp. 727–729, 2009.

[19] D. V. Pechkovsky, A. Prasse, F. Kollert et al., "Alternatively activated alveolar macrophages in pulmonary fibrosis-mediator production and intracellular signal transduction," *Clinical Immunology*, vol. 137, no. 1, pp. 89–101, 2010.

[20] H.-J. Anders and M. Ryu, "Renal microenvironments and macrophage phenotypes determine progression or resolution of renal inflammation and fibrosis," *Kidney International*, vol. 80, no. 9, pp. 915–925, 2011.

[21] T. T. Braga, M. Correa-Costa, Y. F. S. Guise et al., "MyD88 signaling pathway is involved in renal fibrosis by favoring a T_H2 immune response and activating alternative M2 macrophages," *Molecular Medicine*, vol. 18, no. 8, pp. 1231–1239, 2012.

[22] T. Bellón, V. Martínez, B. Lucendo et al., "Alternative activation of macrophages in human peritoneum: implications for peritoneal fibrosis," *Nephrology Dialysis Transplantation*, vol. 26, no. 9, pp. 2995–3005, 2011.

[23] J. Wang, Z.-P. Jiang, N. Su et al., "The role of peritoneal alternatively activated macrophages in the process of peritoneal fibrosis related to peritoneal dialysis," *International Journal of Molecular Sciences*, vol. 14, no. 5, pp. 10369–10382, 2013.

[24] D. Y. S. Vogel, J. E. Glim, A. W. D. Stavenuiter et al., "Human macrophage polarization in vitro: maturation and activation methods compared," *Immunobiology*, vol. 219, no. 9, pp. 695–703, 2014.

[25] T. Oikawa, K. Hirotani, H. Ogasawara et al., "Inhibition of angiogenesis by vitamin D3 analogues," *European Journal of Pharmacology*, vol. 178, no. 2, pp. 247–250, 1990.

[26] D. Zehnder, R. Bland, R. S. Chana et al., "Synthesis of 1,25-dihydroxyvitamin D_3 by human endothelial cells is regulated by inflammatory cytokines: a novel autocrine determinant of vascular cell adhesion," *Journal of the American Society of Nephrology*, vol. 13, no. 3, pp. 621–629, 2002.

[27] A. W. D. Stavenuiter, M. N. Schilte, P. M. ter Wee, and R. H. J. Beelen, "Angiogenesis in peritoneal dialysis," *Kidney and Blood Pressure Research*, vol. 34, no. 4, pp. 245–252, 2011.

[28] J. Niu, A. Azfer, O. Zhelyabovska, S. Fatma, and P. E. Kolattukudy, "Monocyte chemotactic protein (MCP)-1 promotes angiogenesis via a novel transcription factor, MCP-1-induced protein (MCPIP)," *The Journal of Biological Chemistry*, vol. 283, no. 21, pp. 14542–14551, 2008.

[29] M. Zareie, E. D. Keuning, P. M. ter Wee, C. G. Schalkwijk, R. H. J. Beelen, and J. van den Born, "Improved biocompatibility of bicarbonate/lactate-buffered PDF is not related to pH," *Nephrology Dialysis Transplantation*, vol. 21, no. 1, pp. 208–216, 2006.

[30] S. H. Kang, S. O. Kim, K. H. Cho, J. W. Park, K. W. Yoon, and J. Y. Do, "Paricalcitol ameliorates epithelial-to-mesenchymal transition in the peritoneal mesothelium," *Nephron: Experimental Nephrology*, vol. 126, no. 1, 2014.

[31] X. Tan, Y. Li, and Y. Liu, "Paricalcitol attenuates renal interstitial fibrosis in obstructive nephropathy," *Journal of the American Society of Nephrology*, vol. 17, no. 12, pp. 3382–3393, 2006.

Hindawi Publishing Corporation
BioMed Research International
Volume 2015, Article ID 106902, 7 pages
http://dx.doi.org/10.1155/2015/106902

Research Article

A Novel Mouse Model of Peritoneal Dialysis: Combination of Uraemia and Long-Term Exposure to PD Fluid

E. Ferrantelli,[1] G. Liappas,[2] E. D. Keuning,[1] M. Vila Cuenca,[1] G. González-Mateo,[2] M. Verkaik,[3] M. López-Cabrera,[2] and R. H. J. Beelen[1]

[1]*Department of Molecular Cell Biology and Immunology, VU University Medical Center, Van der Boechorststraat 7, 1081 BT Amsterdam, Netherlands*
[2]*Centro de Biología Molecular Severo Ochoa, CSIC-UAM, Cantoblanco, 28049 Madrid, Spain*
[3]*Department of Nephrology, VU University Medical Center, 1007 MB Amsterdam, Netherlands*

Correspondence should be addressed to E. Ferrantelli; e.ferrantelli@vumc.nl

Received 22 June 2015; Revised 28 September 2015; Accepted 30 September 2015

Academic Editor: Yu-Chang Tyan

Different animal models for peritoneal dialysis (PD) have been used in the past decades to develop PD fluids compatible with patient life and to identify markers of peritoneal fibrosis and inflammation. Only few of those studies have taken into account the importance of uraemia-induced alterations at both systemic and peritoneal levels. Moreover, some animal studies which have reported about PD in a uremic setting did not always entirely succeed in terms of uraemia establishment and animal survival. In the present study we induced uraemia in the recently established mouse PD exposure model in order to obtain a more clinically relevant mouse model for kidney patients. This new designed model reflected both the slight thickening of peritoneal membrane induced by uraemia and the significant extracellular matrix deposition due to daily PD fluid instillation. In addition the model offers the opportunity to perform long-term exposure to PD fluids, as it is observed in the clinical setting, and gives the advantage to knock out candidate markers for driving peritoneal inflammatory mechanisms.

1. Introduction

End Stage Renal Disease (ESRD) affects more than 200,000 people in Europe per year and 20,000 of those are peritoneal dialysis (PD) patients. This number is higher in the rest of the world and although in Europe patients undergoing PD are still less than the inmates on hospital-based haemodialysis (HD), this number is expected to increase over the time since PD succeeds over HD in terms of quality of life [1] and cost effectiveness [2, 3]. Moreover, much research on PD has been carried out to improve patient survival and thus qualifies a good alternative for HD treated patients.

Uraemia is represented by accumulation in the body of urea and other organic waste products of metabolism normally filtered out by the kidneys. It can only be treated by replacing kidney function that nowadays, due to the insufficient number of kidneys available worldwide for transplantation, occurs mainly by dialysis.

In the last decade different animal models for PD fluid exposure have been designed and have been mainly performed in rat [4, 5]. The combining effort of our present groups to study the effect of additions in the rat PD exposure model [6, 7] resulted also in the development of the first established mouse PD exposure model published by González-Mateo et al. [8]. PD rodent models have been used to introduce in the market PD fluids more compatible with the patient life and have offered opportunities to study PD fluid additions. Moreover those models allowed identifying important biomarkers driving peritoneal inflammatory mechanisms that occur during long-term exposure to PD fluids and, as a matter of fact, the failure of the technique itself.

Only few animal studies reported PD in a uremic setting, which is most likely caused by the difficult and delicate procedure needed to induce uraemia, resulting in a low success rate of this technique.

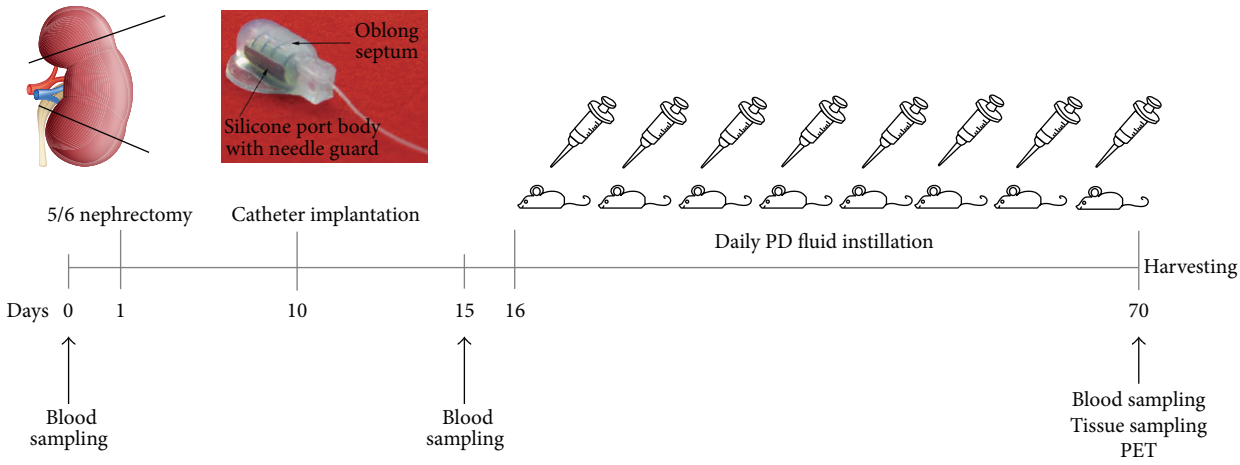

Figure 1: Experimental design. 5/6 nephrectomy was executed at day 1. After a resting period of 10 days a customer made catheter was implanted under the skin at the back side with the tip positioned within the peritoneal membrane. Daily PD fluid instillation was performed from day 16 to day 70 when the mice were sacrificed; PET test and tissue sampling were carried out. Blood withdrawal was performed at days 0, 15, and 70 in order to verify uraemia establishment.

In the present study we wanted to get close to the PD patient clinical condition by combining a long-term exposure model of PD in mouse with uraemia, *sine qua non* condition for a patient to start PD treatment or a renal replacement therapy in general.

2. Methods

2.1. Animals and Experimental Design. The study was performed on 30 female C57BL/6 mice (Harlan CPB, Horst, Netherlands) aged 12–14 weeks, weighing approximately 20 g at the start of the study. Animals were randomly assigned to the following groups: 10 uremic mice undergoing 5/6 nephrectomy (5/6 NX), 10 uremic PD mice undergoing 5/6 nephrectomy and catheter implantation and exposed to PD fluid (5/6 NX + PD), and 10 healthy controls (control). Mice were housed under standard conditions and were given food and water *ad libitum*. Health conditions were checked daily. Mice were weighed daily after surgery during a period of 10 days and weekly for the remainder of the experiment. Animals that lost more than 20% of their body weight or showed abnormal activity were excluded from the experiment. The experimental protocol was approved by the Animal Welfare Committee at the VU University Medical Center, Amsterdam. Experimental design is shown in Figure 1.

2.2. 5/6 Nephrectomy. In order to make mice uremic, 5/6 nephrectomy was performed under isoflurane anaesthesia (4% for induction, 2-3% for maintenance). 0.05–0.1 mg/kg of buprenorphine (Temgesic) was injected intramuscularly 15–30 minutes preoperatively. The animal was shaved around the abdominal region and was placed on a heating pad. A ventral midline incision was made through the skin followed by an incision along the linea alba. Through the laparotomy the left kidney was released from its capsule by using surgical forceps and wet cotton swabs. At this point the kidney could be easily positioned on top of the peritoneum and was placed on a wound pad. The anterior and posterior 1/3 part of the kidney were impaired by using a monopolar electric blade. The remaining functional 1/3 of the left kidney was placed back into its original position in the abdominal cavity. Following the same procedure, also the right kidney was removed from the abdominal cavity and released from the capsule. A total ligation with insoluble suture was applied, which included the kidney vein, artery, and urethra. After ligation, the right kidney was completely removed. This procedure resulted in a reduced kidney function by 5/6th of its original function. The main steps of the procedure are shown in Figure 2.

2.3. Catheter Implantation. Customized mouse catheter (MMP-4S-061108A, Access Technologies, Ridgeway, USA) was implanted at day 10 under isoflurane anaesthesia (4% for induction, 2-3% for maintenance). An incision in the skin was made, skin was separated from muscle layer, and a small hole was made in the lateral side of the abdomen by means of a needle. The catheter was implanted under the skin with the mouse-o-port positioned subcutaneously at the back-right side and the tip within the peritoneal cavity through the hole previously made. The whole procedure is described by González-Mateo et al. [8].

2.4. Peritoneal Exposure Model. Instillation of 2 mL of peritoneal dialysis fluid (PDF) (Dianeal 3, 86%, Baxter, USA) was performed daily during a period of 8 weeks via the previously implanted mouse-o-port connected to the peritoneal cavity via the catheter. First injection was conducted after a resting period of 7 days from surgery to allow the operational wound's healing process around the catheter and avoid leakage of fluid outside the peritoneal cavity.

2.5. Serum Analysis. 200 μL of blood was drawn via facial vein puncture at days 0 and 15 (resp., before the nephrectomy and the first injection of PD fluid) and at day 70 (end point).

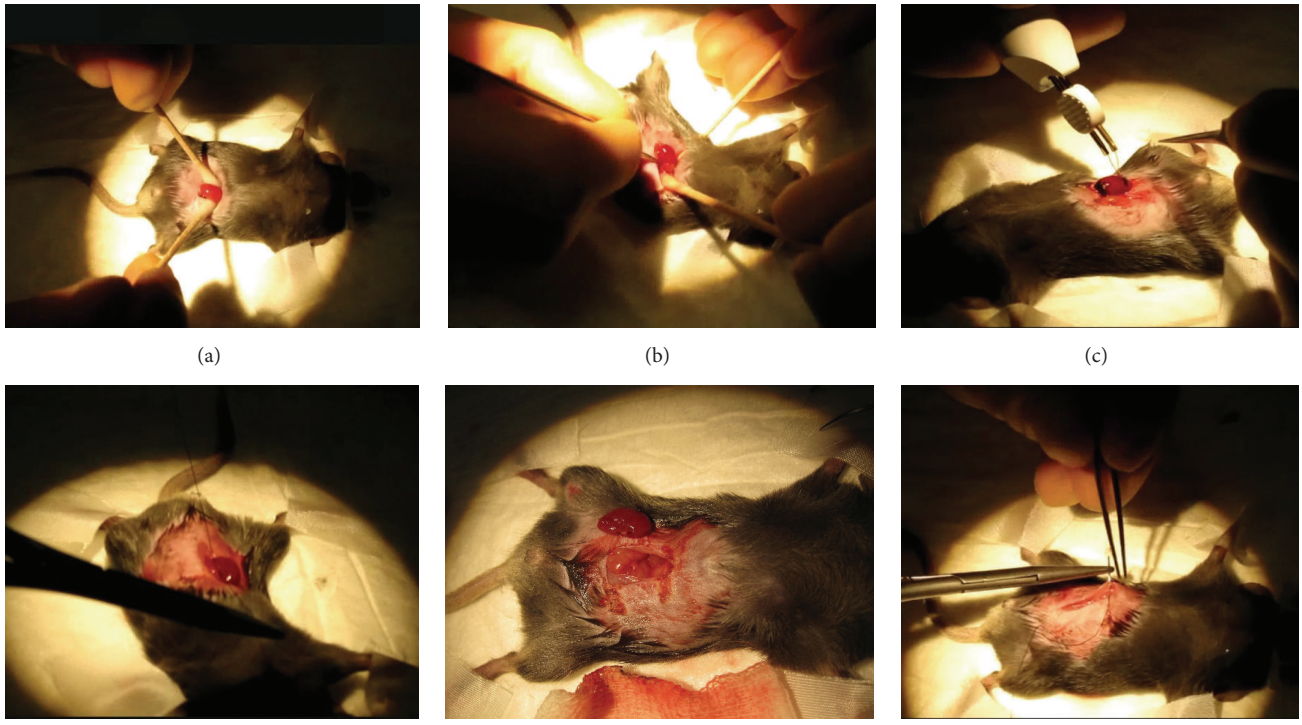

Figure 2: 5/6 nephrectomy: surgical procedure. (a) Through the laparotomy the left kidney was released from its capsule by using surgical forceps and wet cotton swabs. (b) Left kidney was released from the capsule. (c) A monopolar electric blade was used to impair the anterior and posterior 1/3 part of the kidney. (d) A total ligation with insoluble suture was applied, which included the kidney vein, artery, and urethra. (e) Right kidney was totally removed from the body. (f) Both muscle layer and skin were closed by continuous sutures.

At all the time points, serum samples were analysed for urea and creatinine levels. For determination of urea levels a kinetic test with urease and glutamate dehydrogenase was used. Creatinine levels were detected by indirect immunofluorescence assay. Measurements were performed by using spectrophotometer Cobas8000 (c702), Roche Diagnostics.

2.6. Immunostaining for Peritoneal Thickness. Parietal peritoneal biopsies were collected from the opposite side from the catheter installation. Biopsies were fixed in Bouin's solution, embedded in paraffin, cut into 5 μm sections, and stained with Masson's trichrome. Peritoneal membrane thickness was determined using light microscopy (Leica CTR6000, with Leica Microsystems LAS-AF6000). Photographs were made using Olympus BX41 clinical microscope and Olympus DP20 digital camera using cell acquisition software. Peritoneal thickness of each animal was calculated by the median of measurement taken every 50 μm from one side to the other of the tissue sample.

2.7. Statistical Analysis. Data were analysed using GraphPad Prism software (La Jolla, CA). Statistical analysis was performed using one-way ANOVA test to compare the groups. A P value < 0.05 was considered statistically significant. Urea and creatinine data were shown as means ± SD. Thickness is represented in boxplots.

3. Results

In order to mimic in mice the clinical situations of peritoneal dialysis patients, uraemia was induced by performing 5/6 nephrectomy. This 5/6 nephrectomy surgery resulted in a functional kidney capacity 1/6th of the original kidney volume. 15 days after surgery a significant increase of serum urea levels was already seen (data not shown), which was maintained throughout the study period. At the end of the study the nephrectomized mice showed an almost twofold increase in both urea (15 ± 2.71 versus 8.32 ± 2.38; $P < 0.01$) and creatinine serum levels (70.80 ± 40.00 versus 33.50 ± 6.95) when compared to the healthy control group (Figures 3(a) and 3(b)), indicative for a uremic status. Throughout the experiment nephrectomized mice were in good health as indicated by increasing body weight during the study period, which was comparable between all three groups. As expected, all nephrectomized mice showed a drop in body weight within the first week after surgery but recovered the following week (Figure 3(c)).

The PDF-treated group showed a significant increase in peritoneal thickness compared to both the 5/6 NX and the control groups (Figure 4; 41.14 ± 5.04 versus 26.71 ± 3.59 versus 13.00 ± 3.16; $P < 0.001$). This demonstrates that chronic instillation of PDF in our mouse model caused peritoneal thickening and inflammation of the submesothelial compact zone comparable with the clinic situation of a patient

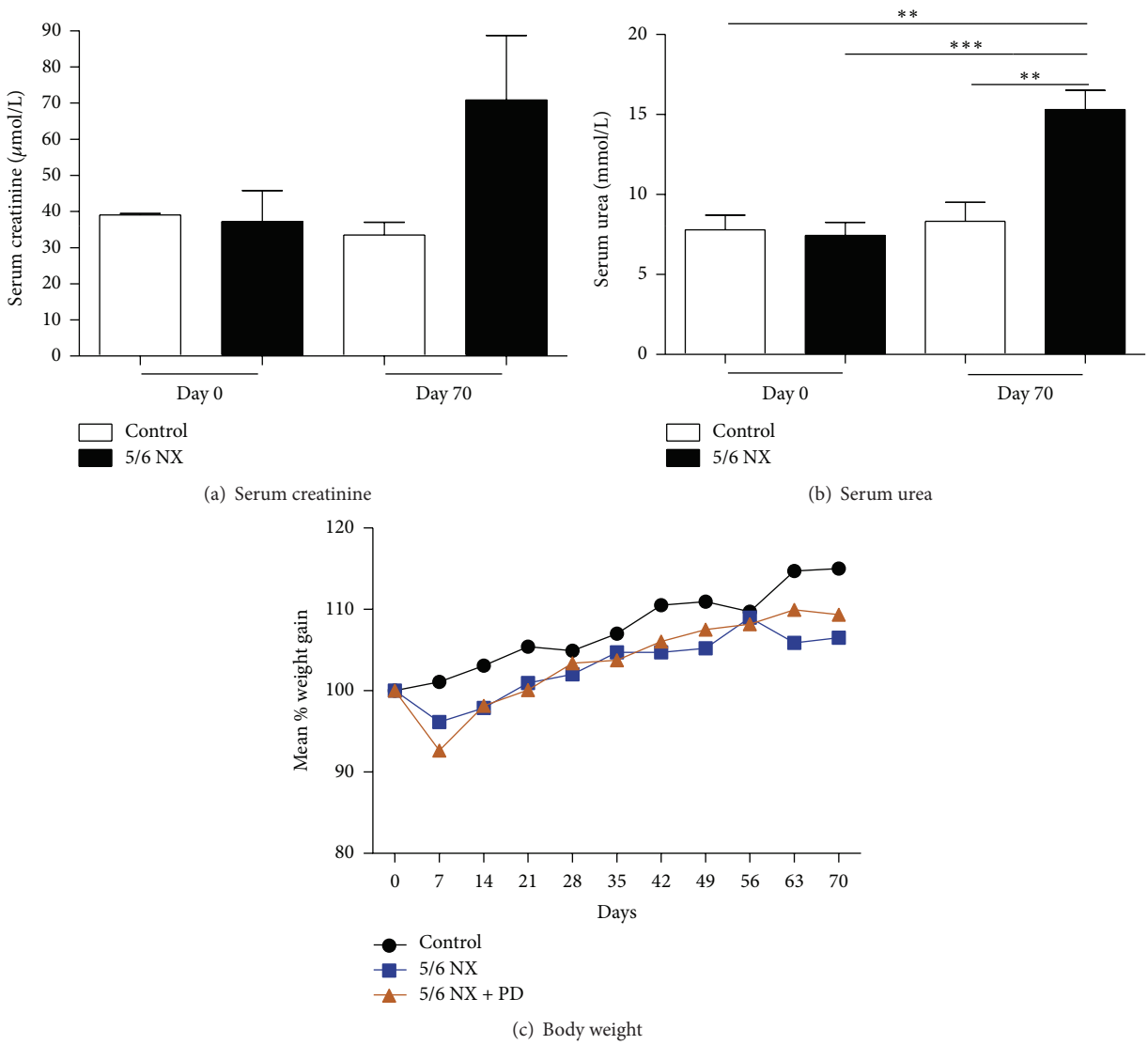

FIGURE 3: (a and b) Blood chemistries at days 0 and 70, respectively, before and after induction of uraemia with 5/6 nephrectomy. (a) Serum levels of creatinine. Time 0: 37.20 ± 19.16 5/6 NX versus 39.00 ± 0.82 control; time 70: 70.80 ± 40.00 5/6 NX versus 33.50 ± 6.95 control. (b) Serum levels of urea: white bars indicate healthy controls; black bars indicate mice undergoing 5/6 nephrectomy. P values ** < 0.01, *** < 0.001. (c) Mean increases in body weight during uraemia induction. Values are expressed as percent of starting body weight. Black line indicates healthy controls, blue line indicates uremic group, and red line indicates uremic group undergoing PD.

undergoing PD. Moreover, the peritoneal thickening already found in the nephrectomized group showed that uraemia cannot be omitted in a model of PD.

4. Discussion

Uraemia is the terminal clinical manifestation of kidney failure and it represents the main reason for a patient to be introduced to a dialysis treatment. Systemic changes that occur in uremic patients such as the significant increase in advanced glycation end products (AGEs), nitric oxide synthase (NOS), Tumor Necrosis Factor Alpha (TNFα), and Vascular Endothelial Growth Factor (VEGF) levels, but also hyperosmolarity and blood pressure itself, may influence peritoneal permeability and cause thickening of the extracellular matrix and mild vasculopathy [9, 10]. These alterations induce peritoneal damage and may therefore complicate the PD procedure in patients.

Peritoneal damage in PD patients mainly depends on the balance between chronic damage caused by bioincompatibility of the PD fluids currently available in the market and repair mechanisms. Over the years different animal models of PD have been used to research into the use of different peritoneal dialysis fluids [11–14] and addition of substances to the dialysis fluid and treatment [6, 15].

Animal studies have shown an independent contribution of uraemia to modulating inflammatory events that alter the function of the peritoneal membrane although these events

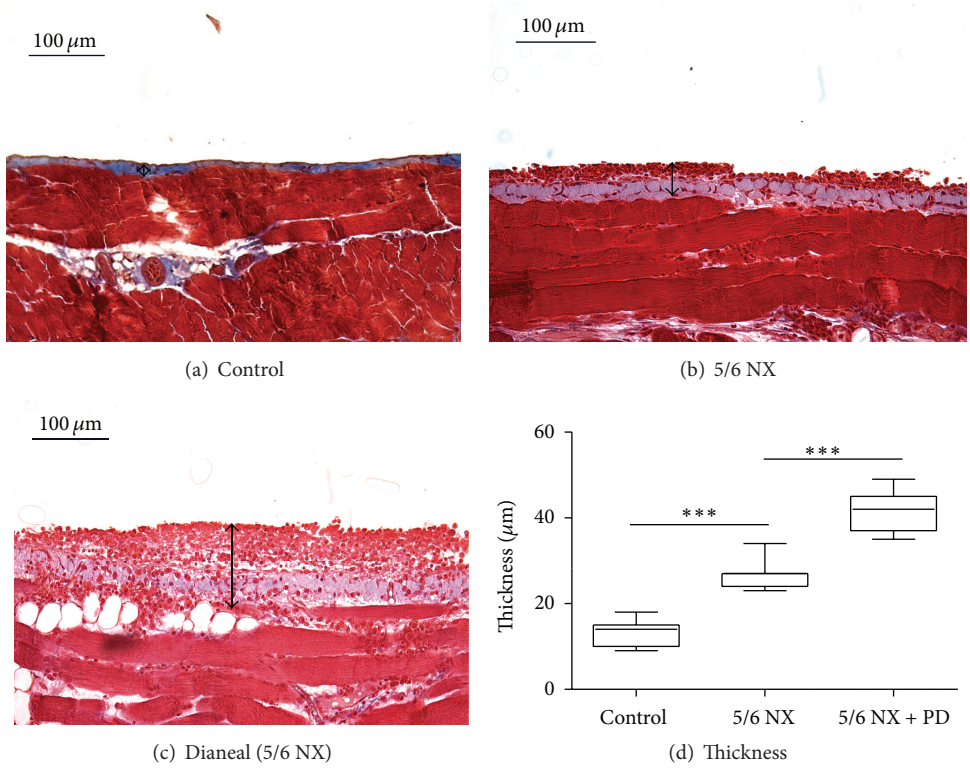

(a) Control (b) 5/6 NX

(c) Dianeal (5/6 NX) (d) Thickness

Figure 4: Effect of uraemia and PD fluid exposure on the parietal peritoneal thickness. (a–d) Masson's trichrome staining of parietal peritoneum showed a slight and a high increase of extracellular matrix deposition in mice undergoing 5/6 nephrectomy, respectively, exposed (c) or not (b) to standard PD fluid. Magnification ×20. (Control: 13.00 ± 3.16; 5/6 NX: 26.71 ± 3.59; 5/6 NX + PD: 41.14 ± 5.04.) P values $***< 0.001$.

are often obscured by the effects of PD fluid induced injury [11]. Nevertheless, in anephric rats undergoing continuous ambulatory peritoneal dialysis (CAPD) uraemia modifies the permeability of peritoneum to both water and solutes [16]. In rat models exposed to PD fluid uraemia contributed to ultrafiltration failure, leading to angiogenesis and causing an increment in omental mast cells number [13].

Uraemia-induced alterations at both systemic and peritoneal level should not be underestimated and experimental animal models of renal disease should take into account the important effect of uraemia. Although the study of the peritoneal membrane alterations promoted by the PD fluids alone, avoiding the effect of other variables, is a very helpful model, it could be very interesting for several approaches to analyse the combined effect of PD exposure and uraemia.

Despite that, only few studies report on PD in uremic animals. The procedure to obtain uraemia in animals indeed is not so easy and many models still show high percentage of drop-out and low rate of success especially when combined with long-term exposure to PD fluids. In rabbit models partial nephrectomy (total removal of one kidney and 5/6 nephrectomy of the other one) has been performed but only moderate uraemia has been reached [17]. More studies have been performed on rats: bilateral nephrectomy caused acute uraemia and, on the other hand, the removal of only one kidney did not induce significant changes in urea and creatinine blood levels. Moreover, animals were experiencing diarrhea and loss of appetite and body weight [16].

Our group also had previously developed a uremic rat PD model consisting of total removal of the left kidney and double artery ligation of the right one (5/6 nephrectomy). In this model both urea and creatinine serum levels were shown to be threefold increased after only three weeks from the nephrectomy and kept stable during five weeks of exposure to PD fluid (Ferrantelli et al., pending revision). Although this model allowed us to obtain important striking results regarding the protective effect of some additive to the PD fluid, the percentage of drop-out was still too high. Unfortunately, 5/6 nephrectomy itself in rats caused 20% of drop-out, with even higher drop-out when technical failure due to omentum wrapping of the catheter during the PD treatment was taken into account.

In this study we present a novel animal model where both uraemia and daily PD treatment were combined in mouse. As a consequence of the 5/6 nephrectomy only 1/6th of the total kidney volume is preserved and remains functional during the whole period of daily peritoneal fluid administration.

This model fulfils the need to reduce the percentage of drop-out due to both nephrectomy and PD treatment. Drop-out caused by 5/6 nephrectomy was decreased from 20% in the rat model to less than 5% in the mouse model. Moreover, this model circumvents PD treatment-related loss of animals

such as omentum overgrowth and wrapping of the catheter (drop-out due to catheter obstruction is about 50% in the rat model) [5].

Taken together, this new technique reduces the number of animals needed for research and enables extending time of exposure to PDFs. Indeed, daily treatment of this mouse model with PDF for 8 weeks was well tolerated and might be extended for a longer period. Our consideration is based on the evidences that the animals were healthy during and till the end of the experiment (no evidences of discomfort and no loss of body weight or decrease of appetite) and the serum levels of both creatinine and urea were twofold increased compared to the controls but still within acceptable levels.

The PD mouse model represents a gold standard procedure [8] and many experiments based on it have been performed in the last years in order to study Epithelial-to-Mesenchymal Transition (EMT) and the involvement of Th17 cells in fibrotic mechanisms occurring during long-term exposure to PDF [18, 19].

In our study we wanted to propose the PD mouse model within a uremic setting in order to mimic as closely as possible the situation in a patient with chronic kidney failure undergoing PD. In addition our mouse model will give the advantage to knock out genes playing a crucial role in the peritoneal inflammatory mechanism that occurs during PD and will open opportunities to study pathways involved in fibrosis, since much more reagents are available in mice.

5. Conclusions

Besides the PD-related effects on fibrosis in mice, we showed that uraemia also affects this phenomenon, which is in accordance with patient studies.

To mimic this clinical setting, we developed a mouse model with important features observed in renal failure patients. Indeed this new mouse model gives the opportunity to study PD in concomitance with peritoneal and systemic changes caused by uraemia, often not taken into account in animal studies. Importantly, long-term in vivo experiments can be performed in this model, eventually resulting in less harmful effects of biocompatible PDFs as well as PDFs supplemented with protective additives, both favorable for patients.

Conflict of Interests

The authors declare that there is no conflict of interests regarding the publication of this paper.

Acknowledgment

EuTRiPD, Marie Curie actions, supported this work, Grant no. ITN 287813.

References

[1] A. Berger, J. Edelsberg, G. W. Inglese, S. K. Bhattacharyya, and G. Oster, "Cost comparison of peritoneal dialysis versus hemodialysis in end-stage renal disease," *American Journal of Managed Care*, vol. 15, no. 8, pp. 509–518, 2009.

[2] A. J. Collins, R. N. Foley, C. Herzog et al., "Excerpts from the US renal data system 2009 annual data report," *American Journal of Kidney Diseases*, vol. 55, no. 1, supplement 1, pp. S1–S420, A6–A7, 2010.

[3] D. C. Mendelssohn, S. K. Mujais, S. D. Soroka et al., "A prospective evaluation of renal replacement therapy modality eligibility," *Nephrology Dialysis Transplantation*, vol. 24, no. 2, pp. 555–561, 2009.

[4] N. Lameire, W. Van Biesen, M. Van Landschoot et al., "Experimental models in peritoneal dialysis: a European experience," *Kidney International*, vol. 54, no. 6, pp. 2194–2206, 1998.

[5] R. H. J. Beelen, L. H. P. Hekking, M. Zareie, and J. van den Born, "Rat models in peritoneal dialysis," *Nephrology Dialysis Transplantation*, vol. 16, no. 3, pp. 672–674, 2001.

[6] J. Loureiro, M. Schilte, A. Aguilera et al., "BMP-7 blocks mesenchymal conversion of mesothelial cells and prevents peritoneal damage induced by dialysis fluid exposure," *Nephrology Dialysis Transplantation*, vol. 25, no. 4, pp. 1098–1108, 2010.

[7] M. N. Schilte, J. W. A. M. Celie, P. M. Ter Wee, R. H. J. Beelen, and J. van den Born, "Factors contributing to peritoneal tissue remodeling in peritoneal dialysis," *Peritoneal Dialysis International*, vol. 29, no. 6, pp. 605–617, 2009.

[8] G. T. González-Mateo, J. Loureiro, J. A. Jiménez-Hefferman et al., "Chronic exposure of mouse peritoneum to peritoneal dialysis fluid: structural and functional alterations of the peritoneal membrane," *Peritoneal Dialysis International*, vol. 29, no. 2, pp. 227–230, 2009.

[9] J. D. Williams, K. J. Craig, N. Topley et al., "Morphologic changes in the peritoneal membrane of patients with renal disease," *Journal of the American Society of Nephrology*, vol. 13, no. 2, pp. 470–479, 2002.

[10] S. Combet, M.-L. Ferrier, M. Van Landschoot et al., "Chronic uremia induces permeability changes, increased nitric oxide synthase expression, and structural modifications in the peritoneum," *Journal of the American Society of Nephrology*, vol. 12, no. 10, pp. 2146–2157, 2001.

[11] M. Zareie, A. A. van Lambalgen, P. M. ter Wee et al., "Better preservation of the peritoneum in rats exposed to amino acid-based peritoneal dialysis fluid," *Peritoneal Dialysis International*, vol. 25, no. 1, pp. 58–67, 2005.

[12] M. Zareie, L. H. P. Hekking, A. G. A. Welten et al., "Contribution of lactate buffer, glucose and glucose degradation products to peritoneal injury in vivo," *Nephrology Dialysis Transplantation*, vol. 18, no. 12, pp. 2629–2637, 2003.

[13] M. N. Schilte, P. Fabbrini, P. M. Ter Wee et al., "Peritoneal dialysis fluid bioincompatibility and new vessel formation promote leukocyte-endothelium interactions in a chronic rat model for peritoneal dialysis," *Microcirculation*, vol. 17, no. 4, pp. 271–280, 2010.

[14] L. H. Hekking, M. C. Aalders, E. Van Gelderop et al., "Effect of peritoneal dialysis fluid measured in vivo in a rat-model of continuous peritoneal dialysis," *Advances in Peritoneal Dialysis*, vol. 14, pp. 14–18, 1998.

[15] P. Fabbrini, M. N. Schilte, M. Zareie et al., "Celecoxib treatment reduces peritoneal fibrosis and angiogenesis and prevents ultrafiltration failure in experimental peritoneal dialysis," *Nephrology Dialysis Transplantation*, vol. 24, no. 12, pp. 3669–3676, 2009.

[16] K. Pawlaczyk, M. Kuzlan-Pawlaczyk, K. Wieczorowska-Tobis, A. Polubinska, A. Breborowicz, and D. Oreopoulos, "Evaluation

of the effect of uremia on peritoneal permeability in an experimental model of continuous ambulatory peritoneal dialysis in anephric rats," *Advances in Peritoneal Dialysis—Conference on Peritoneal Dialysis*, vol. 15, pp. 32–35, 1999.

[17] L. Gotloib, P. Crassweller, H. Rodella et al., "Experimental model for studies of continuous peritoneal'dialysis in uremic rabbits," *Nephron*, vol. 31, no. 3, pp. 254–259, 1982.

[18] G. T. González-Mateo, V. Fernández-Míllara, T. Bellón et al., "paricalcitol reduces peritoneal fibrosis in mice through the activation of regulatory T cells and reduction in IL-17 production," *PLoS ONE*, vol. 9, no. 10, Article ID e108477, 2014.

[19] R. Rodrigues-Díez, L. S. Aroeira, M. Orejudo et al., "IL-17A is a novel player in dialysis-induced peritoneal damage," *Kidney International*, vol. 86, no. 2, pp. 303–315, 2014.

Hindawi Publishing Corporation
BioMed Research International
Volume 2015, Article ID 427038, 12 pages
http://dx.doi.org/10.1155/2015/427038

Review Article

Regulation of Synthesis and Roles of Hyaluronan in Peritoneal Dialysis

Timothy Bowen,[1] Soma Meran,[1] Aled P. Williams,[1] Lucy J. Newbury,[1] Matthias Sauter,[2,3] and Thomas Sitter[2]

[1] *Wales Kidney Research Unit, School of Medicine, College of Biomedical and Life Sciences, Cardiff University, Heath Park, Cardiff CF14 4XN, UK*
[2] *Medizinische Klinik und Poliklinik IV, Klinikum der Universität München, Ziemssenstrasse 1, 80336 München, Germany*
[3] *Klinikum Kempten, Robert-Weixler-Strasse 50, 87439 Kempten, Germany*

Correspondence should be addressed to Timothy Bowen; bowent@cf.ac.uk

Received 22 June 2015; Accepted 16 August 2015

Academic Editor: Robert Beelen

Hyaluronan (HA) is a ubiquitous extracellular matrix glycosaminoglycan composed of repeated disaccharide units of alternating D-glucuronic acid and D-N-acetylglucosamine residues linked via alternating β-1,4 and β-1,3 glycosidic bonds. HA is synthesized in humans by HA synthase (HAS) enzymes 1, 2, and 3, which are encoded by the corresponding *HAS* genes. Previous in vitro studies have shown characteristic changes in HAS expression and increased HA synthesis in response to wounding and proinflammatory cytokines in human peritoneal mesothelial cells. In addition, in vivo models and human peritoneal biopsy samples have provided evidence of changes in HA metabolism in the fibrosis that at present accompanies peritoneal dialysis treatment. This review discusses these published observations and how they might contribute to improvement in peritoneal dialysis.

1. Hyaluronan: Multiple Functions and Clinical Significance

Hyaluronan (HA) is a linear glycosaminoglycan associated most commonly with the extracellular matrix (ECM). HA was first isolated from the optic vitreous [1] and is composed of tandem repeats of a D-glucuronic acid and D-N-acetylglucosamine disaccharide motif linked via alternating β-1,4 and β-1,3 glycosidic bonds [2]. Unique amongst glycosaminoglycans, HA is unsulfated and contains no epimerised uronic acid residues. To export HA to the ECM, the HA synthase (HAS) proteins traverse the plasma membrane and act as glycosyltransferases, combining precursor UDP-glucuronic acid and UDP-N-acetylglucosamine to form HA. HA polymers are thus synthesised at the HAS active site on the intracellular side of the membrane and exported instantaneously as linear, unaltered polymers [3].

HA was thought initially to be an inert, space-filling molecule [4]. More recent analyses, however, have shown that HA is a multifunctional molecule for which a number of key roles have already been identified during and following development. These inter- and intracellular functions include roles in cell migration, tumour invasion, and cellular response to injury (e.g., [5–10]).

The importance of HA in the ECM is underlined by the expanding range of pathological contexts in which modified or aberrant HA metabolism appears to play a role. These include autoimmune renal injury, fibrosis of the kidney and other large organs, diabetic nephropathy, malignancy, osteoarthritis, and pulmonary and vascular disorders, along with other immune and inflammatory diseases (e.g., [6, 9–30]). HA deposition is characteristic of peritoneal fibrosis subsequent to dialysis treatment [31, 32]. HA has also been implicated in regenerative processes such as wound healing in the peritoneum and elsewhere [33–39] and as a key immune mediator [20, 21]. Upregulation of HA synthesis has also been reported in inflammation that occurs commonly as a consequence of treatment of renal failure by peritoneal dialysis (PD) [32, 33]. The focus of this review will be on the regulation and function of HA in PD.

2. Regulation of HA Synthase (HAS) Expression

HA is synthesised by the enzymes HAS1-3. These proteins are encoded by the corresponding *HAS* genes *HAS1*, *HAS2*, and *HAS3*, with each human gene located at a discrete autosomal locus [40].

The human peritoneal mesothelial cells (HPMCs) that line the peritoneal membrane synthesise HA as a normal constituent of peritoneal effluent, and this synthesis is upregulated during periods of peritonitis [41]. In an in vitro model of peritoneal wound healing [42], mechanical disruption of HPMC monolayers led to upregulated HAS2 transcription together with an increase in HA synthesis [33].

However, despite the above array of pathological and physiological functions already ascribed to HA, comparatively little is known about the regulation of human HAS expression in peritoneal inflammation and fibrosis.

We began our studies on the regulation of HAS expression by defining genomic structures for each human *HAS* gene [43]. As part of this study, we prepared luciferase reporter constructs spanning approximately 0.5 kb of genomic DNA upstream of each putative HAS transcription start site (TSS) [43, 44]. Each sequence showed significant promoter ability to drive transcription of the luciferase gene [43].

To locate the HAS2 promoter, we carried out HAS2-specific 5′-rapid amplification of cDNA ends (5′RACE) on polyadenylated RNA extracted from renal proximal tubular epithelial cells and located the TSS 0.130 kb upstream of the 5′ end of HAS2 reference mRNA sequence NM_005328 [45]. We then generated luciferase reporter vectors bearing nested fragments spanning the first 0.8 kb upstream of this new TSS [45, 46]. Luciferase analysis showed consistent promoter activity mediated by a minimum-sized fragment of 0.121 kb, within which we identified promoter sequences conserved in selected mammals [45, 46]. Similar methods have recently been used to identify the human HAS3 promoter [47].

Using electrophoretic mobility shift and supershift data, we then demonstrated binding of transcription factors Sp1 and Sp3 to three sites immediately upstream of the HAS2 TSS [48]. Luciferase analysis of mutated reporter constructs was abrogated, while RT-qPCR analysis following siRNA knockdown of either transcription factor significantly reduced the level of HAS2 transcription [48]. Chromatin immunoprecipitation analysis of this locus has since been used to analyse HAS2 transcriptional induction by retinoic acid and tumour necrosis factor-α [49].

The tetraexonic, long noncoding RNA transcript HAS2-AS1 is transcribed from the opposite genomic DNA strand to HAS2 mRNA at 8q24.13 [50]. The second exon of HAS2-AS1 shares partial sequence complimentary with HAS2 exon 1, and HAS2-AS1 can therefore be described as a "natural antisense" to HAS2 [50]. In osteosarcoma cells, transcription of HAS2 mRNA synthesis and subsequent HA production are downregulated by HAS2-AS1 [50]. By contrast, in renal proximal tubular epithelial cells, we showed that HAS2-AS1 expression augments and/or stabilises HAS2 mRNA and detected cytoplasmic HAS2:HAS2-AS1 RNA duplexes [51]. In aortic smooth muscle cells, HAS2-AS1 also upregulates HAS2 expression and mediates posttranscriptional modification of HAS2 by O-GlcNAcylation [52].

We have also identified the HAS1 TSS, adding a further 26 nucleotides to reference sequence NM_001523, and analysed the upstream HAS1 promoter region in renal proximal tubular epithelial cells [46, 53], but a full characterisation of factors regulating HAS expression in HPMCs has not been carried out. In addition, little is known about HPMC expression of long noncoding RNAs (including HAS2-AS1) and of microRNAs, both of which are highly likely to regulate HAS expression. Indeed, understanding the transcriptional and posttranscriptional mechanisms regulating HPMC HAS expression will provide useful information on the control of HA synthesis during PD and has the potential to inform future approaches to antifibrotic PD therapy.

3. Synthesis of HA by Peritoneal Mesothelial Cells

HA is an important component of the HPMC ECM and is also produced by fibroblasts and macrophages in the peritoneal cavity [54–56]. According to in vivo findings, HA levels are increased in peritoneal dialysate during peritonitis [54]. It has also been shown in vitro that the synthesis of HA in mesothelial cells is enhanced by various inflammatory mediators including prostaglandin E2, PDGF, transforming growth factor-beta1, tumour necrosis factor-alpha (TNF-α), and interleukin-6 (IL-6), with IL-1β producing the strongest effect [41, 55, 57].

HA is found predominantly in connective tissue where the polymer chain is bound to interacting molecules such as cell surface receptor CD44, the receptor for HA-mediated motility, and proteoglycans including aggrecan and versican [58, 59].

Under homeostasis, HA polymers are typically between 2,000 and 25,000 disaccharide units in length, and these chains have been sized at 2–25 μm [11]. Yung and Chan [32] have ably summarised much previous work on the properties and effects of low and high molecular weight HA. Despite this sizeable body of accumulated data, attribution of functions dependent on the number of disaccharide repeat units in the HA polymer remains controversial. Understanding the potential functional differences is complicated by the fact that HA can be digested by the hyaluronidase (HYAL) enzymes encoded by the *HYAL* multigene family [60] and by HA degradation at different sites. An early in vivo study in which radiolabelled HA was injected into rabbit knee joints showed degradation locally and in the liver [61].

The biological effects of adding exogenous HA preparations to cultured HPMCs have been studied in vitro in numerous cell culture systems. Yung and colleagues [33] showed that addition of HA accelerated in vitro healing of wounded HPMC monolayers in a dose-dependent manner between 50 and 3300 ng/mL. Mediation of these proliferative HA effects by interaction with CD44 remains unproven [62]. The key role played by HA in the process of remesothelialisation was confirmed in a further in vitro model of HPMC cell migration [63].

When HPMCs were exposed to spent dialysates supplemented with 0.1 or 0.5 mg/mL high molecular weight HA, synthesis of chemokine monocyte chemoattractant protein (MCP-1), adhesion molecule soluble intercellular adhesion molecule (s-ICAM), vascular endothelial cell growth factor (VEGF), and fibronectin was significantly reduced [64]. However, these differences were not observed in vivo when the same inflammatory mediators were measured in drained dialysate patient samples [64]. In accordance with the above in vitro findings, high molecular weight HA also inhibits the nuclear factor-kappa B- (NF-κB-) dependent synthesis of cytokines IL-1α, IL-6, and TNF-α in mouse macrophage line J774 [65].

Since HA alters the fibrinolytic properties of numerous cell types [66], we investigated the effect of HA on the synthesis of tissue plasminogen activator (tPA) and plasminogen activator-1 (PAI-1) in HPMCs. Only very high concentrations of HA (>50 mg/dL) downregulated fibrinolytic HPMC activity by decreasing t-PA synthesis, but changes in t-PA and PAI-1 expression were not observed at concentrations up to 30 mg/dL [66]. A subsequent study has shown that monocyte/macrophage system cells interfered with HA-associated changes in the fibrinolytic capacity of HPMCs treated with lipopolysaccharide [67].

HA fragments activate nitric-oxide synthase in murine macrophages through an NF-κB-dependent mechanism, increasing expression of chemokines macrophage inflammatory protein-alpha (MIP-1α), MIP-1β, and MCP-1 [68, 69]. In renal cortical tubular cells the synthesis of adhesion molecules ICAM-1 and vascular cell adhesion protein-1 (VCAM-1), and MCP-1, were upregulated following stimulation with low molecular weight HA [70]. Similarly, we found that HA fragments of approximate molecular mass 1–7 $\times$ 10^5 Da induced the synthesis of the chemokines MCP-1 and IL-8 in HPMCs [71]. The upregulation of these chemokines was preceded by an increase in NF-κB and activating protein-1 DNA binding activity in HPMCs [71].

Breborowicz and coworkers found changes in HPMC synthetic activity following exposure to dialysis fluids, including downregulated HA synthesis [72]. Glutathione precursor L-2-oxothiazolidine-4-carboxylic acid prevented this effect, suggesting that it may be driven by glucose-induced free radicals during PD [72]. Chronic exposure of HPMCs to glucose or N-acetylglucosamine showed the latter to be more biocompatible, despite the fact that it upregulated HA synthesis [73]. Treatment with peroxisome-proliferator activator receptor-gamma agonist ciglitazone decreased endometrial cell attachment to HPMC line LP9 and decreased LP9 attachment to HA-treated tissue culture plate wells [74]. HPMC senescence in vitro was accelerated by glucose but not N-acetylglucosamine [75].

In summary, the effects of in vitro HA application to HPMCs are complex and dependent on HA molecular weight. High molecular weight HA appears to have anti-inflammatory and preservative effects, while low molecular weight HA stimulates proinflammatory processes. However, as several studies have failed to discriminate clearly between the effects of HA of different sizes, an unambiguous interpretation of these data is challenging, and new data will be required to resolve this issue.

4. HA in Peritoneal and Endothelial Glycocalyces

Emerging evidence suggests that HA at the mesothelial cell surface contributes significantly to the peritoneal glycocalyx [32, 76–78]. This structure performs a number of roles including protection and lubrication, and denudation during PD and/or injury is likely to accelerate HPMC and peritoneal damage and thereby treatment failure [32, 77]. HA is also a key component of the endothelial glycocalyx, contributing significantly to its permeability [79, 80], and a recent study has investigated the potential importance of the systemic microvascular endothelial glycocalyx as a transport barrier during PD [81].

5. Intraperitoneal In Vivo Administration of HA to Prevent Surgery-Induced Adhesions

Postoperative adhesions are a frequent outcome of abdominal surgery and may lead to bowel obstruction, chronic pelvic pain, infertility, and technical difficulties in further surgical procedures [82]. Both in humans and in animal models, intraperitoneal (IP) administration of HA has been tested in an attempt to prevent the formation of postsurgical adhesion. Numerous HA preparations for IP application are commercially available or in development. Interpretation of the diverse outcomes following their use is not straightforward, as is clear from the studies described below.

A number of prospective randomized trials have been carried out to determine the efficacy of HA-based adhesion-preventing agents. One such study analysed the antiadhesion efficacy of a 0.5% ferric hyaluronate gel in severe peritoneal trauma caused by bipolar coagulation in a laparoscopic rat model. Adhesion scores were decreased significantly, but none of the animals was free of adhesions, and the authors did not show a significant difference between the HA gel treatment and the use of the adhesion-preventing agents Ringer's lactate solution and 4% icodextrin solution [83]. In a prospective randomized study of peritoneal laparoscopic resection in rabbits using 0.5% ferric hyaluronate gel, saline, or control, no differences in adhesion scores and number of animals with adhesions were reported [84]. By contrast, a prospective randomized multicentre study in humans showed that a glycerol-HA/carboxymethylcellulose membrane effectively reduced intra-abdominal adhesions in patients who underwent proctocolectomy and ileal-pouch-anal anastomosis [85]. However, the increase in infectious complications caused the manufacturer not to market this product [85].

Considerable research efforts have been devoted to analysis of membranes composed of HA and carboxymethylcellulose (HA/CMC; commercially available as Seprafilm) both alone and in conjunction with additional agents, while other treatments have also been tested. For instance, Nilsson and colleagues [86] investigated the use of HAPXL01, a novel

polypeptide derived from human lactoferrin, in the sidewall-defect cecal abrasion model in the rat [86]. An HA-based formulation of HAPXL01 inhibited scar formation, prohibiting inflammation and promoting fibrinolysis and significantly reducing adhesion formation without affecting wound healing [86].

In the first of two studies by Lim and coworkers, HA/CMC Seprafilm mediated effective reduction in adhesion formation by peritoneal ischemic buttons created either side of a midline incision that was limited to the site of application [87]. Irrespective of the bioresorbable material at predicted adhesion sites, peritoneal adhesions formed readily at unprotected sites [87]. In a later study, coadministration of neurokinin 1 receptor antagonist significantly augmented the effect of the HA/CMC membrane on adhesion prevention from experimentally induced peritoneal ischaemic buttons, and combined use of these treatments reduced adhesion formation both at the site of application and at distal sites [88].

In a rat laparotomy/cecal injury model, IP-administered atorvastatin proved to be equally as effective as Seprafilm in the prevention of postoperative adhesion, but there was no additive effect when both treatments were combined [89].

Data on HA-based membranes has not always been positive, however. The study of Economidou and coworkers [90] set out to evaluate the effects of administration of two (unidentified) commercial membranes: a thicker membrane composed of macromolecular polysaccharides and a thinner HA-hydroacid methylcellulose-based membrane. The use of the former resulted in elevated serum creatinine and urea levels, tubular epithelial cell vacuolization, and mild interstitial infiltration [90]. These lesions were milder when the HA-based membrane was used, and serum creatinine did not change [90].

Use of HA/CMC powder and film applied either directly or contralaterally was compared in a rat peritoneal sidewall defect model and a rabbit cecal abrasion/sidewall defect model [91]. Both additives reduced adhesions to the same degree on direct application, while powder alone was effective on remote application but did not inhibit wound healing [91]. In a severe adhesion model in which 1 cm^2 of intra-abdominal wall was excised and *n*-butyl-2-cyanoacrylate was applied, Hwang and colleagues [92] compared HA/sodium CMC gel (Guardix-sol), 4% icodextrin, and Seprafilm. Scoring for both fibrosis and adhesion showed a significant reduction in both when Seprafilm alone was used [92].

A comparison of IP-administered linezolid with Seprafilm [93] found both to be significant in reducing formation of rat peritoneal adhesions following sterile antimesenteric (side) surface cecal abrasion, when compared to controls. Similarly, both IP lovastatin and Seprafilm were equally effective in preventing postoperative intra-abdominal adhesions of cecal, ileal, and uteral abrasions [94]. Observations from a rabbit model showed that the combined use of 3% trehalose solution and Seprafilm had additive effects in the prevention of adhesion formation [95]. A recent study using a biodegradable HA-based hydrogel formed in situ showed a promising and significant reduction in adhesion formation [96].

In summary, the use of a variety of HA and HA-derived preparations used in past studies complicates the process of data interpretation. However, a significant body of evidence now supports the use of HA/CMC agents, and the utility of intraperitoneally administered HA has potential for future development.

6. Animal Studies on PD Examining In Vivo HA Application

Where appropriate, selected data from the studies discussed below are summarized in Table 1. The therapeutic application of the addition of HA to PD fluid is based on the assumption that HA is lost from the peritoneal cavity during PD [97]. In PD patients, IP production of HA increases during episodes of peritonitis [41, 98], and with the duration of PD therapy the HA concentration rises in the effluent of PD patients [99]. Consequently, the first animal studies were performed to determine the role of HA in peritoneal function during PD [97]. A number of studies using IP-soluble HA administration have been described, the majority being in animal models.

6.1. Effects of HA-Containing Fluid on PD Transportation Characteristics. Significantly lower transperitoneal protein equilibration for albumin and for total protein in rats receiving a Dianeal solution containing 10 mg/dL HA twice daily for 4 weeks has been reported [97], and these data have been supported by the results of other studies [100, 101]. Furthermore, the total drained volume after a 4-hour dwell was significantly higher in the HA group, yielding a positive net ultrafiltration (UF) in the HA group versus a negative net UF in the control group [97].

The above effect was based mainly on a decreased peritoneal fluid absorption rate, which was demonstrated independently following 4-hour HA solution dwell, together with increased urea clearance [102]. The same authors showed that there was no difference in the transcapillary UF rate (Qu) between different concentrations and various molecular weights of HA in control groups or even a reduced Qu in one HA group receiving 4 MD molecular weight HA [103]. They also reported that the effect of HA on peritoneal fluid absorption and net UF appeared to be both size- and concentration-dependent [104] and noted that this HA-mediated effect was potentially useful to prevent a decrease in net UF caused by increased peritoneal dialysate fill volume [105]. With respect to small solute clearance, it was shown that HA administration resulted in a significantly increased urea clearance [100, 105].

Rosengren et al. [106] provided evidence that both small solute transfer and glucose-induced osmotic water transfer (using a 3.86% glucose-based solution) was not influenced by HA supplementation of dialysis fluid. HA did, however, reduce backfiltration of fluid from peritoneum to plasma by forming a "filter-cake" [106]. These researchers also found that hyaluronidase incubation resulted in a 78% reduction of HA in the superficial layer of the peritoneal membrane which did not produce any significant changes in solute and fluid transport across the peritoneal membrane [107].

Table 1: Summary of studies discussed in the text.

(a)

Study	Organism	HA concentration and application	HA Effects on UF	Other HA Effects
Wang et al., 1997 [102]	Rat	Single 4 h dwell with HA 0.005% and 0.01%	Increased UF, mainly through decreased peritoneal fluid absorption	Increased peritoneal clearance of urea
Wang et al., 1999 [103]	Rat	Single 4 h dwell with HA 0.01%	Increased net UF, mainly by decreased peritoneal fluid absorption	Increased peritoneal clearance of urea. HA may prevent decreased net UF caused by an increased dialysate fill volume
Wang et al., 1999 [104]	Rat	Single 4 h dwell with HA in various concentrations (0.01–0.5%) and molecular weights (MW; 85 kDa–4 MDa)	Increased size and concentration of HA resulted in decreased peritoneal fluid absorption. Low concentrations of high MW HA might decrease transcapillary UF rate	
Połubinska et al., 2000 [97]	Rat	High MW HA 10 mg/dL twice daily for 4 weeks	Total drained volume in HA group was significantly higher (positive net UF in HA group versus negative net UF in control group)	Clearance of total protein and albumin tended to be lower; clearance of urea and creatinine tended to be higher. Significantly decreased percentage of IP neutrophils and levels of MCP-1 and TNF-α
Guo et al., 2001 [101]	Rat	0.025% HA in a 4 h dwell for 1 week	Decreased peritoneal fluid absorption (similar to native animals)	Significant decrease in protein transportation rate
Breborowicz et al., 2001 [100]	Rat	One infusion of 10 mg/dL HA for a 1–8 h dwell	Net UF was significantly greater at 4, 6, and 8 h compared to controls	During 8 h exchange, creatinine clearance was significantly higher and total protein clearance significantly lower. After 8 h, 25.7% HA absorbed from peritoneal cavity and peritoneal tissue HA increased to 117%; plasma HA levels increased to 435%. Plasma HA normalized within 24 h in uremic and nonuremic animals
Breborowicz et al., 2001 [108]	Rat	Acute peritonitis induced with lipopolysaccharide; HA at 10 mg/dL; 4 and 8 h dwell	Significant reduction in loss of UF	Significantly increased creatinine clearance. Greater dialysate interferon-γ-levels and less pronounced elastase levels
Moberly et al., 2003 [109]	Human	Prospective randomized crossover study with 6 h application of Dianeal and Dianeal containing HA (0.1 and 0.5 g/L). 2-week washout analysed after exchange	No significant differences in net UF or peritoneal volume profiles	No adverse effects of HA
Breborowicz et al., 2004 [64]	Human	One 6 h dwell with 13.6 g/L glucose-based solution ±0.1 and 0.5 g/L of exogenous high MW HA. 2-week application intervals		Significant increased concentration of nitrites in HA 0.5 g/L supplemented dialysate. No difference in concentrations of MCP-1, s-ICAM1, EGF, and fibronectin

(b)

Study	Organism	PD regime (not HA)	Other HA effects
Wieczorowska-Tobis et al., 2004 [111]	Rat	2 daily injections of 4.25% glucose-containing PDF for 6 weeks. PDFs tested: CAPD3 (single-chamber bag, low pH, and high GDP), CAPD3 pH 7.4 (single-chamber bag, neutral pH, and high GDP), CAPD3 balance (double-chamber bag, neutral pH, and low GDP)	Reduced concentrations of protein and HA in dialysate. Introduced PD fluids with physiologic pH and low GDP level producing less irritation to the peritoneal membrane, better preserving its structural integrity
Zareie et al., 2005 [112]	Rat	Uraemic and control rats received daily 10 mL conventional glucose containing PD fluid, via peritoneal catheters during a 6-week period	Increased MCP-1 and HA levels in peritoneal lavage fluid
Flessner et al., 2006 [113]	Rat	Filtered solutions with 4% N-acetylglucosamine (NAG) or 4% glucose (G) IP injected daily in 2–300 g rats compared with controls (C). At 2 months, transport studies using chamber affixed to parietal peritoneum determined small-solute and protein mass transfer, osmotic filtration, and hydraulic flow	Tissue analysis showed treatment effects on tissue HA (microg/g: C, 962 ± 73; G, 1,169 ± 69; NAG, 1,428 ± 69; and $p < 0.05$) and collagen (microg/g: C, 56.9 ± 12.0; G, 107 ± 12; NAG, 97.6 ± 11.4; and $p < 0.05$) but not sulfated glycosaminoglycan
Schilte et al., 2009 [114]	Rat	Used 10 mL PD fluid daily, ±unfractionated heparin, or low MW heparin in PD fluid (1 mg/10 mL) IP via mini access port, untreated control rats. At 5 weeks, peritoneal transport was tested; tissues and peritoneal leukocytes were sampled	Increased peritoneal cell influx and HA production ($p < 0.02$) as well as an exchange of mast cells and eosinophils for neutrophils after PD treatment observed in PD rats
Loureiro et al., 2010 [115]	Rat	Over 5 weeks, rats instilled daily using PD fluid ± BMP-7	rhBMP-7-treatment did not significantly affect any of these processes induced by PD fluid exposure, except for a tendency to reduce HA production ($p = 0.054$), suggesting decreased peritoneal fibrosis
Rosengren et al., 2013 [119]	Human	After 8 weeks PD, interstitial fluid (IF) from peritoneum was isolated via centrifugation; IF and plasma were analyzed for cytokine content and colloid osmotic pressure	IF colloid osmotic pressure decreased significantly in PD group, while collagen and HA content was increased
Kinashi et al., 2013 [120]	Human	Role of the lymphangiogenesis mediator VEGF-C analysed in human dialysate effluents, peritoneal tissues, and HPMCs	Peritoneal tissue from patients with UF failure expressed higher levels of VEGF-C, LYVE-1, and podoplanin mRNA and contained more lymphatic vessels than tissue from patients without UF failure

6.2. Effect of HA-Containing Fluids on Peritoneal Inflammation. The effect of HA on peritoneal inflammation has also been analysed in animal studies. IP administration of HA in rats reduced the percentage of neutrophils in PD effluent, but the total cell number in the effluent did not change [97]. This study also reported lower levels of TNF-α and MCP-1 in rats treated with HA-containing PD solution in comparison to rats treated with Dianeal [97]. In a model of lipopolysaccharide-induced peritonitis in rats, 10 mg/dL HA administration reduced loss of UF and provided a greater creatinine clearance [108]. Furthermore, the presence of HA led to increased dialysate interferon-γ levels, whereas elastase levels decreased [108].

6.3. HA Absorption and Metabolism after IP Application. Breborowicz and coworkers have investigated the absorption and metabolism of 10 mg/dL HA in Dianeal after IP administration [100]. After 8 hours, one quarter of the HA had been absorbed from the peritoneal cavity and peritoneal tissue, and plasma HA concentrations were significantly increased to 116% in peritoneal tissue and 435% in plasma [100]. HA levels returned to normal within 24 hours after IP administration in both healthy and uremic rats [100].

6.4. Histological Evaluation of the Peritoneal Membrane after HA Application. Only one study has provided histological evaluation of the peritoneal membrane following HA administration, showing a similar increase in the thickness of the peritoneal interstitium in rats exposed to HA and in control animals [97].

7. HA Supplementation in Human PD

Moberly et al. [109] examined 13 patients in a prospective randomized crossover study. The PD solutions investigated were Dianeal alone or supplemented with either 0.1 g/L HA or 0.5 g/L HA. Each 6-hour dialysis exchange was separated from the other exchanges by a 2-week washout period. The authors did not report any adverse events related to HA administration. HA application did not result in significant changes in net UF or peritoneal volume profiles, but mean net UF tended to be slightly higher during treatment with HA-containing fluid. Peritoneal fluid reabsorption also tended to be lower during the HA treatment, but the differences were not significant. Solute clearances, dialysate/plasma ratios, and mass transfer area coefficients for sodium, urea, creatinine, albumin, and glucose were similar for the three treatment solutions [109]. While these data failed to reach significance, only 10 patients completed the study. In addition, HA concentrations exceeding 0.5 g/L were not used due to increased viscosity resulting in significantly increased filling and drainage times [109]. It remains possible that a longer application period than one test solution every 2 weeks might have been more effective.

A recent review by Cho and colleagues of randomized control trials and quasirandomised control trials in adults and children compared the effects of biocompatible PD solutions [110]. These authors concluded, on the basis of what they referred to as "generally suboptimal quality evidence," that the use of neutral pH, low glucose degradation product (GDP) solutions led to greater UF and renal preservation without statistically significant effects of peritonitis, technique failure, or patient survival [110].

7.1. HA as a Biomarker of Inflammation in PD. In more recent work on rat models and in PD patients, HA has been used as a biomarker to monitor PD progress.

Wieczorowska-Tobis and colleagues showed reduced HA concentration in dialysate from neutral pH and low GDP PD solutions when compared with conventional solutions in rats [111], while a study on uremic rats reported increased HA and MCP-1 in peritoneal lavage fluid [112]. A rise in the parietal peritoneal concentrations of HA and collagen followed the use of PD solutions containing N-acetylglucosamine or glucose [113]. Increased peritoneal cell influx and HA synthesis, together with increased neutrophil counts and decreased mast cell/eosinophil numbers, were observed in rats following PD, and these affects were not changed by the presence of unfractionated or low molecular weight heparin [114]. Reduced HA production was reported in a rat model using bone morphogenetic protein-7 (BMP-7) over a 5-week period, suggesting decreased fibrosis [115]. Use of icodextrin in PD solutions resulted in increased patient dialysate HA compared to glucose/lactate solution, suggesting increased subclinical inflammation [116].

Breborowicz et al. [64] examined the effect of Dianeal alone or Dianeal with HA supplementation of 0.1 or 0.5 g/L. Exchanges at 6 hours were performed with each of the fluids randomly at 2-week intervals. Patient dialysate nitrite concentration (as an index of NO production) was significantly higher after dialysis exchange performed with HA 0.5 g/L, but concentrations of MCP-1, s-ICAM 1, VEGF, and fibronectin were similar after exchanges with the HA-supplemented dialysate fluids and did not differ from Dianeal alone. When cultured HPMCs were exposed for 24 hours to these dialysates, the HA-containing fluids inhibited the synthesis of MCP-1, s-ICAM, VEGF, and fibronectin, accelerating the growth rate of proliferating cells [64].

Use of icodextrin or amino acid-based PD solutions did not result in significant changes in HA production in human dialysates [117], whereas upregulated HA synthesis was reported in whole peritoneal samples from long-term PD patients [118]. Recent reports have shown increased HA after 8 weeks of PD [119] and upregulated expression of endothelial HA receptor-1 (LYVE-1) in human dialysate effluents, peritoneal tissues, and HPMCs [120]. Most recently, Yung and colleagues analysed data from a comprehensive panel of fibrotic and inflammatory biomarkers, including HA, in a randomised prospective study of 80 PD patients [121]. This study compared a low-glucose treatment protocol of Physioneal, Extraneal, and Nutrineal with a control group treated with Dianeal; the biomarker data suggested better preservation of membrane integrity in the multitreatment group [121].

8. Summary

The roles of HA in peritoneal biology, fibrosis, and dialysis require further investigation. A more complete understanding of the regulation of peritoneal HAS expression and HA

synthesis, and of peritoneal and mesothelial responses to exogenous HA, has the potential to provide new tools with which PD treatment and prevention of surgical adhesions are improved. The manipulation of HAS expression and HA metabolism via long noncoding RNAs such as HAS2-AS1 and/or microRNAs, together with recent advances in molecular analysis techniques, hold much promise in these contexts [50–52, 122–128].

Disclaimer

The views expressed in this paper are those of the authors and not necessarily those of the NHS, the NIHR, or the Department of Health, UK.

Conflict of Interests

The authors declare that there is no conflict of interests regarding the publication of this paper.

Acknowledgments

Timothy Bowen thanks Soma Meran, Aled P. Williams, and Lucy J. Newbury for their help in preparing this review, as well as Thomas Sitter (HPMC in vitro section) and Matthias Sauter (in vivo analysis section) for their contributions. The Wales Kidney Research Unit is funded by Health and Care Research Wales. The authors also acknowledge support from Kidney Research UK Project Grant Award RP44/2014 to Timothy Bowen and a Medical Research Council Clinician Scientist Award to Soma Meran. This is a publication of independent research funded by the National Institute for Health Research (NIHR) Invention for Innovation (i4i) Programme (Grant Reference no. II-LA-0712-20003). Principal Investigator for the grant is Timothy Bowen.

References

[1] K. Meyer and J. W. Palmer, "The polysaccharide of the vitreous humor," *The Journal of Biological Chemistry*, vol. 107, no. 3, pp. 629–634, 1934.

[2] B. Weissmann and K. Meyer, "The structure of hyalobiuronic acid and of hyaluronic acid from umbilical cord," *Journal of the American Chemical Society*, vol. 76, no. 7, pp. 1753–1757, 1954.

[3] P. H. Weigel, V. C. Hascall, and M. Tammi, "Hyaluronan synthases," *The Journal of Biological Chemistry*, vol. 272, no. 22, pp. 13997–14000, 1997.

[4] B. P. Toole, "Hyaluronan is not just a goo!," *Journal of Clinical Investigation*, vol. 106, no. 3, pp. 335–336, 2000.

[5] J. Y. Lee and A. P. Spicer, "Hyaluronan: A multifunctional, megaDalton, stealth molecule," *Current Opinion in Cell Biology*, vol. 12, no. 5, pp. 581–586, 2000.

[6] V. C. Hascall, A. K. Majors, C. A. De La Motte et al., "Intracellular hyaluronan: a new frontier for inflammation?" *Biochimica et Biophysica Acta*, vol. 1673, no. 1-2, pp. 3–12, 2004.

[7] A. P. Spicer and J. Y. L. Tien, "Hyaluronan and Morphogenesis," *Birth Defects Research Part C—Embryo Today*, vol. 72, no. 1, pp. 89–108, 2004.

[8] J. Y. L. Tien and A. P. Spicer, "Three vertebrate hyaluronan synthases are expressed during mouse development in distinct spatial and temporal patterns," *Developmental Dynamics*, vol. 233, no. 1, pp. 130–141, 2005.

[9] A. Moustakas and P. Heldin, "TGFbeta and matrix-regulated epithelial to mesenchymal transition," *Biochimica et Biophysica Acta—General Subjects*, vol. 1840, no. 8, pp. 2621–2634, 2014.

[10] P. Moffatt, E. R. Lee, B. St-Jacques, K. Matsumoto, Y. Yamaguchi, and P. J. Roughley, "Hyaluronan production by means of Has2 gene expression in chondrocytes is essential for long bone development," *Developmental Dynamics*, vol. 240, no. 2, pp. 404–412, 2011.

[11] B. P. Toole, "Hyaluronan: from extracellular glue to pericellular cue," *Nature Reviews Cancer*, vol. 4, no. 7, pp. 528–539, 2004.

[12] R. P. Wüthrich, "The proinflammatory role of hyaluronan-CD44 interactions in renal injury," *Nephrology Dialysis Transplantation*, vol. 14, no. 11, pp. 2554–2556, 1999.

[13] S. Jones, S. Jones, and A. O. Phillips, "Regulation of renal proximal tubular epithelial cell hyaluronan generation: implications for diabetic nephropathy," *Kidney International*, vol. 59, no. 5, pp. 1739–1749, 2001.

[14] C. M. Milner and A. J. Day, "TSG-6: a multifunctional protein associated with inflammation," *Journal of Cell Science*, vol. 116, part 10, pp. 1863–1873, 2003.

[15] Y. Nishida, C. B. Knudson, and W. Knudson, "Osteogenic protein-1 inhibits matrix depletion in a hyaluronan hexasaccharide-induced model of osteoarthritis," *Osteoarthritis and Cartilage*, vol. 12, no. 5, pp. 374–382, 2004.

[16] T. S. Wilkinson, S. Potter-Perigo, C. Tsoi, L. C. Altman, and T. N. Wight, "Pro- and anti-inflammatory factors cooperate to control hyaluronan synthesis in lung fibroblasts," *American Journal of Respiratory Cell and Molecular Biology*, vol. 31, no. 1, pp. 92–99, 2004.

[17] T. S. Wilkinson, S. L. Bressler, S. P. Evanko, K. R. Braun, and T. N. Wight, "Overexpression of hyaluronan synthases alters vascular smooth muscle cell phenotype and promotes monocyte adhesion," *Journal of Cellular Physiology*, vol. 206, no. 2, pp. 378–385, 2006.

[18] L. Zhuo, V. C. Hascall, and K. Kimata, "Inter-α-trypsin inhibitor, a covalent protein-glycosaminoglycan-protein complex," *The Journal of Biological Chemistry*, vol. 279, no. 37, pp. 38079–38082, 2004.

[19] A. Zoltan-Jones, L. Huang, S. Ghatak, and B. P. Toole, "Elevated hyaluronan production induces mesenchymal and transformed properties in epithelial cells," *The Journal of Biological Chemistry*, vol. 278, no. 46, pp. 45801–45810, 2003.

[20] M. E. Mummert, "Immunologic roles of hyaluronan," *Immunologic Research*, vol. 31, no. 3, pp. 189–205, 2005.

[21] S. Misra, V. C. Hascall, R. R. Markwald, and S. Ghatak, "Interactions between hyaluronan and its receptors (CD44, RHAMM) regulate the activities of inflammation and cancer," *Frontiers in Immunology*, vol. 6, article 201, 2015.

[22] M. Rienks, A.-P. Papageorgiou, N. G. Frangogiannis, and S. Heymans, "Myocardial extracellular matrix: an ever-changing and diverse entity," *Circulation Research*, vol. 114, no. 5, pp. 872–888, 2014.

[23] S. Yung, K. F. Cheung, Q. Zhang, and T. M. Chan, "Mediators of inflammation and their effect on resident renal cells: implications in lupus nephritis," *Clinical and Developmental Immunology*, vol. 2013, Article ID 317682, 10 pages, 2013.

[24] A. Migliore and S. Procopio, "Effectiveness and utility of hyaluronic acid in osteoarthritis," *Clinical Cases in Mineral and Bone Metabolism*, vol. 12, no. 1, pp. 31–33, 2015.

[25] D. F. Remst, E. N. Blaney Davidson, and P. M. van der Kraan, "Unravelling osteoarthritis-related synovial fibrosis: a step closer to solving joint stiffness," *Rheumatology*, 2015.

[26] A. C. Midgley, L. Duggal, R. Jenkins et al., "Hyaluronan regulates bone morphogenetic protein-7-dependent prevention and reversal of myofibroblast phenotype," *The Journal of Biological Chemistry*, vol. 290, no. 18, pp. 11218–11234, 2015.

[27] S. Meran and R. Steadman, "Fibroblasts and myofibroblasts in renal fibrosis," *International Journal of Experimental Pathology*, vol. 92, no. 3, pp. 158–167, 2011.

[28] A. Wang, J. Ren, C. P. Wang, and V. C. Hascall, "Heparin prevents intracellular hyaluronan synthesis and autophagy responses in hyperglycemic dividing mesangial cells and activates synthesis of an extensive extracellular monocyte-adhesive hyaluronan matrix after completing cell division," *Journal of Biological Chemistry*, vol. 289, no. 13, pp. 9418–9429, 2014.

[29] L. Zhang, T. Bowen, F. Grennan-Jones et al., "Thyrotropin receptor activation increases hyaluronan production in preadipocyte fibroblasts," *Journal of Biological Chemistry*, vol. 284, no. 39, pp. 26447–26455, 2009.

[30] T. Bowen, R. H. Jenkins, and D. J. Fraser, "MicroRNAs, transforming growth factor beta-1, and tissue fibrosis," *Journal of Pathology*, vol. 229, no. 2, pp. 274–285, 2013.

[31] J. D. Williams, N. Topley, K. J. Craig et al., "The Euro-Balance Trial: the effect of a new biocompatible peritoneal dialysis fluid (balance) on the peritoneal membrane," *Kidney International*, vol. 66, no. 1, pp. 408–418, 2004.

[32] S. Yung and T. M. Chan, "Pathophysiology of the peritoneal membrane during peritoneal dialysis: the role of hyaluronan," *Journal of Biomedicine and Biotechnology*, vol. 2011, Article ID 180594, 11 pages, 2011.

[33] S. Yung, G. J. Thomas, and M. Davies, "Induction of hyaluronan metabolism after mechanical injury of human peritoneal mesothelial cells in vitro," *Kidney International*, vol. 58, no. 5, pp. 1953–1962, 2000.

[34] J. A. Mack, S. R. Abramson, Y. Ben et al., "Hoxb13 knockout adult skin exhibits high levels of hyaluronan and enhanced wound healing," *The FASEB Journal*, vol. 17, no. 10, pp. 1352–1354, 2003.

[35] Y. Yamada, N. Itano, K.-I. Hata, M. Ueda, and K. Kimata, "Differential regulation by IL-1beta; and EGF of expression of three different hyaluronan synthases in oral mucosal epithelial cells and fibroblasts and dermal fibroblasts: quantitative analysis using real-time RT-PCR," *Journal of Investigative Dermatology*, vol. 122, no. 3, pp. 631–639, 2004.

[36] R. Tammi, S. Pasonen-Seppänen, E. Kolehmainen, and M. Tammi, "Hyaluronan synthase induction and hyaluronan accumulation in mouse epidermis following skin injury," *Journal of Investigative Dermatology*, vol. 124, no. 5, pp. 898–905, 2005.

[37] A. C. Midgley, M. Rogers, M. B. Hallett et al., "Transforming growth factor-β1 (TGF-β1)-stimulated fibroblast to myofibroblast differentiation is mediated by hyaluronan (HA)-facilitated epidermal growth factor receptor (EGFR) and CD44 co-localization in lipid rafts," *Journal of Biological Chemistry*, vol. 288, no. 21, pp. 14824–14838, 2013.

[38] K. L. Aya and R. Stern, "Hyaluronan in wound healing: rediscovering a major player," *Wound Repair and Regeneration*, vol. 22, no. 5, pp. 579–593, 2014.

[39] R. M. L. Simpson, S. Meran, D. Thomas et al., "Age-related changes in pericellular hyaluronan organization leads to impaired dermal fibroblast to myofibroblast differentiation," *The American Journal of Pathology*, vol. 175, no. 5, pp. 1915–1928, 2009.

[40] A. P. Spicer, M. F. Seldin, A. S. Olsen et al., "Chromosomal localization of the human and mouse hyaluronan synthase genes," *Genomics*, vol. 41, no. 3, pp. 493–497, 1997.

[41] S. Yung, G. A. Coles, and M. Davies, "IL-1 beta, a major stimulator of hyaluronan synthesis in vitro of human peritoneal mesothelial cells: relevance to peritonitis in CAPD," *Kidney International*, vol. 50, no. 4, pp. 1337–1343, 1996.

[42] S. Yung and M. Davies, "Response of the human peritoneal mesothelial cell to injury: an in vitro model of peritoneal wound healing," *Kidney International*, vol. 54, no. 6, pp. 2160–2169, 1998.

[43] J. Monslow, J. D. Williams, N. Norton et al., "The human hyaluronan synthase genes: genomic structures, proximal promoters and polymorphic microsatellite markers," *International Journal of Biochemistry and Cell Biology*, vol. 35, no. 8, pp. 1272–1283, 2003.

[44] B. Hoogendoorn, S. L. Coleman, C. A. Guy et al., "Functional analysis of human promoter polymorphisms," *Human Molecular Genetics*, vol. 12, no. 18, pp. 2249–2254, 2003.

[45] J. Monslow, J. D. Williams, C. A. Guy et al., "Identification and analysis of the promoter region of the human hyaluronan synthase 2 gene," *The Journal of Biological Chemistry*, vol. 279, no. 20, pp. 20576–20581, 2004.

[46] A. C. Midgley and T. Bowen, "Analysis of human hyaluronan synthase gene transcriptional regulation and downstream hyaluronan cell surface receptor mobility in myofibroblast differentiation," *Methods in Molecular Biology*, vol. 1229, pp. 605–618, 2015.

[47] S. Wang, L. Zhen, Z. Liu et al., "Identification and analysis of the promoter region of the human HAS3 gene," *Biochemical and Biophysical Research Communications*, vol. 460, no. 4, pp. 1008–1014, 2015.

[48] J. Monslow, J. D. Williams, D. J. Fraser et al., "Sp1 and Sp3 mediate constitutive transcription of the human hyaluronan synthase 2 gene," *Journal of Biological Chemistry*, vol. 281, no. 26, pp. 18043–18050, 2006.

[49] K. Saavalainen, M. I. Tammi, T. Bowen, M. L. Schmitz, and C. Carlberg, "Integration of the activation of the human hyaluronan synthase 2 gene promoter by common cofactors of the transcription factors retinoic acid receptor and nuclear factor κB," *The Journal of Biological Chemistry*, vol. 282, no. 15, pp. 11530–11539, 2007.

[50] H. Chao and A. P. Spicer, "Natural antisense mRNAs to hyaluronan synthase 2 inhibit hyaluronan biosynthesis and cell proliferation," *Journal of Biological Chemistry*, vol. 280, no. 30, pp. 27513–27522, 2005.

[51] D. R. Michael, A. O. Phillips, A. Krupa et al., "The human hyaluronan synthase 2 (HAS2) gene and its natural antisense RNA exhibit coordinated expression in the renal proximal tubular epithelial cell," *Journal of Biological Chemistry*, vol. 286, no. 22, pp. 19523–19532, 2011.

[52] D. Vigetti, S. Deleonibus, P. Moretto et al., "Natural antisense transcript for hyaluronan synthase 2 (HAS2-AS1) induces transcription of HAS2 via protein O-GlcNAcylation," *The Journal of Biological Chemistry*, vol. 289, no. 42, pp. 28816–28826, 2014.

[53] L. Chen, R. D. Neville, D. R. Michael et al., "Identification and analysis of the human hyaluronan synthase 1 gene promoter

reveals Smad3- and Sp3-mediated transcriptional induction," *Matrix Biology*, vol. 31, no. 7-8, pp. 373–379, 2012.

[54] S. Yung, G. A. Coles, J. D. Williams, and M. Davies, "The source and possible significance of hyaluronan in the peritoneal cavity," *Kidney International*, vol. 46, no. 2, pp. 527–533, 1994.

[55] A. Breborowicz, J. Wisniewska, A. Polubinska, K. Wieczorowska-Tobis, L. Martis, and D. G. Oreopoulos, "Role of Peritoneal Mesothelial cells and fibroblasts in the synthesis of hyaluronan during peritoneal dialysis," *Peritoneal Dialysis International*, vol. 18, no. 4, pp. 382–386, 1998.

[56] K. N. Lai, C. C. Szeto, K. B. Lai, C. W. K. Lam, D. T. M. Chan, and J. C. K. Leung, "Increased production of hyaluronan by peritoneal cells and its significance in patients on CAPD," *American Journal of Kidney Diseases*, vol. 33, no. 2, pp. 318–324, 1999.

[57] A. Honda, Y. Sekiguchi, and Y. Mori, "Prostaglandin E2 stimulates cyclic AMP-mediated hyaluronan synthesis in rabbit pericardial mesothelial cells," *Biochemical Journal*, vol. 292, no. 2, pp. 497–502, 1993.

[58] B. P. Toole, "Hyaluronan and its binding proteins, the hyaladherins," *Current Opinion in Cell Biology*, vol. 2, no. 5, pp. 839–844, 1990.

[59] L. Sherman, J. Sleeman, P. Herrlich, and H. Ponta, "Hyaluronate receptors: key players in growth, differentiation, migration and tumor progression," *Current Opinion in Cell Biology*, vol. 6, no. 5, pp. 726–733, 1994.

[60] R. Stern and M. J. Jedrzejas, "Hyaluronidases: their genomics, structures, and mechanisms of action," *Chemical Reviews*, vol. 106, no. 3, pp. 818–839, 2006.

[61] U. B. G. Laurent, J. R. E. Fraser, A. Engstrom-Laurent, R. K. Reed, L. B. Dahl, and T. C. Laurent, "Catabolism of hyaluronan in the knee joint of the rabbit," *Matrix*, vol. 12, no. 2, pp. 130–136, 1992.

[62] M. M. P. J. Reijnen, P. Falk, H. van Goor, and L. Holmdahl, "The antiadhesive agent sodium hyaluronate increases the proliferation rate of human peritoneal mesothelial cells," *Fertility and Sterility*, vol. 74, no. 1, pp. 146–151, 2000.

[63] T. Horiuchi, K. Miyamoto, S. Miyamoto et al., "Image analysis of remesothelialization following chemical wounding of cultured human peritoneal mesothelial cells: the role of hyaluronan synthesis," *Kidney International*, vol. 64, no. 6, pp. 2280–2290, 2003.

[64] A. Breborowicz, M. Pyda, J. Moberly, L. Martis, and D. Oreopoulos, "Effect of haluronan-supplemented dialysate on in vitro function of human peritoneal mesothelial cells," *American Journal of Nephrology*, vol. 24, no. 3, pp. 316–321, 2004.

[65] A. Neumann, R. Schinzel, D. Palm, P. Riederer, and G. Münch, "High molecular weight hyaluronic acid inhibits advanced glycation endproduct-induced NF-kappaB activation and cytokine expression," *FEBS Letters*, vol. 453, no. 3, pp. 283–287, 1999.

[66] T. Sitter, M. Sauter, and B. Haslinger, "Modulation of fibrinolytic system components in mesothelial cells by hyaluronan," *Peritoneal Dialysis International*, vol. 23, no. 3, pp. 222–227, 2003.

[67] C. J. J. M. Sikkink, M. M. P. J. Reijnen, P. Falk, H. van Goor, and L. Holmdahl, "Influence of monocyte-like cells on the fibrinolytic activity of peritoneal mesothelial cells and the effect of sodium hyaluronate," *Fertility and Sterility*, vol. 84, no. 2, pp. 1072–1077, 2005.

[68] C. M. McKee, M. B. Penno, M. Cowman et al., "Hyaluronan (HA) fragments induce chemokine gene expression in alveolar macrophages. The role of HA size and CD44," *The Journal of Clinical Investigation*, vol. 98, no. 10, pp. 2403–2413, 1996.

[69] C. M. McKee, C. J. Lowenstein, M. R. Horton et al., "Hyaluronan fragments induce nitric-oxide synthase in murine macrophages through a nuclear factor kappaB-dependent mechanism," *The Journal of Biological Chemistry*, vol. 272, no. 12, pp. 8013–8018, 1997.

[70] B. Beck-Schimmer, B. Oertli, T. Pasch, and R. P. Wüthrich, "Hyaluronan induces monocyte chemoattractant protein-1 expression in renal tubular epithelial cells," *Journal of the American Society of Nephrology*, vol. 9, no. 12, pp. 2283–2290, 1998.

[71] B. Haslinger, S. Mandl-Weber, A. Sellmayer, and T. Sitter, "Hyaluronan fragments induce the synthesis of MCP-1 and IL-8 in cultured human peritoneal mesothelial cells," *Cell and Tissue Research*, vol. 305, no. 1, pp. 79–86, 2001.

[72] A. Breborowicz, M. Breborowicz, and D. G. Oreopoulos, "Glucose-induced changes in the phenotype of human peritoneal mesothelial cells: effect of L-2-oxothiazolidine carboxylic acid," *American Journal of Nephrology*, vol. 23, no. 6, pp. 471–476, 2003.

[73] M. Ciszewicz, G. Wu, P. Tam, A. Polubinska, and A. Bręborowicz, "Changes in peritoneal mesothelial cells phenotype after chronic exposure to glucose or *N*-acetylglucosamine," *Translational Research*, vol. 150, no. 6, pp. 337–342, 2007.

[74] S. K. Kavoussi, C. A. Witz, P. A. Binkley, A. S. Nair, and D. I. Lebovic, "Peroxisome-proliferator activator receptor-gamma activation decreases attachment of endometrial cells to peritoneal mesothelial cells in an in vitro model of the early endometriotic lesion," *Molecular Human Reproduction*, vol. 15, no. 10, pp. 687–692, 2009.

[75] M. Ciszewicz, G. Wu, P. Tam, A. Polubinska, and A. B. Borowicz, "Glucose but not N-acetylglucosamine accelerates in vitro senescence of human peritoneal mesothelial cells," *International Journal of Artificial Organs*, vol. 34, no. 6, pp. 489–494, 2011.

[76] S. P. Evanko, M. I. Tammi, R. H. Tammi, and T. N. Wight, "Hyaluronan-dependent pericellular matrix," *Advanced Drug Delivery Reviews*, vol. 59, no. 13, pp. 1351–1365, 2007.

[77] S. Yung and T. M. Chan, "Glycosaminoglycans and proteoglycans: overlooked entities?" *Peritoneal Dialysis International*, vol. 27, supplement 2, pp. S104–S109, 2007.

[78] V. Koistinen, R. Kärnä, A. Koistinen, A. Arjonen, M. Tammi, and K. Rilla, "Cell protrusions induced by hyaluronan synthase 3 (HAS3) resemble mesothelial microvilli and share cytoskeletal features of filopodia," *Experimental Cell Research*, vol. 337, no. 2, pp. 179–191, 2015.

[79] C. B. S. Henry and B. R. Duling, "Permeation of the luminal capillary glycocalyx is determined by hyaluronan," *The American Journal of Physiology—Heart and Circulatory Physiology*, vol. 277, no. 2, part 2, pp. H508–H514, 1999.

[80] L. Gao and H. H. Lipowsky, "Composition of the endothelial glycocalyx and its relation to its thickness and diffusion of small solutes," *Microvascular Research*, vol. 80, no. 3, pp. 394–401, 2010.

[81] C. A. Vlahu, D. Lopes Barreto, D. G. Struijk, H. Vink, and R. T. Krediet, "Is the systemic microvascular endothelial glycocalyx in peritoneal dialysis patients related to peritoneal transport?" *Nephron Clinical Practice*, vol. 128, no. 1-2, pp. 159–165, 2014.

[82] S. Tsuji, K. Takahashi, H. Yomo et al., "Effectiveness of antiadhesion barriers in preventing adhesion after myomectomy in patients with uterine leiomyoma," *European Journal of Obstetrics Gynecology and Reproductive Biology*, vol. 123, no. 2, pp. 244–248, 2005.

[83] H. Roman, M. Canis, M. Kamble, R. Botchorishvili, J.-L. Pouly, and G. Mage, "Efficacy of three adhesion-preventing

agents in reducing severe peritoneal trauma induced by bipolar coagulation in a laparoscopic rat model," *Fertility and Sterility*, vol. 83, no. 4, supplement, pp. 1113–1118, 2005.

[84] R. Detchev, M. Bazot, D. Soriano, and E. Darai, "Prevention of de novo adhesion by ferric hyaluronate gel after laparoscopic surgery in an animal model," *Journal of the Society of Laparoendoscopic Surgeons*, vol. 8, no. 3, pp. 263–268, 2004.

[85] Z. Cohen, A. J. Senagore, M. T. Dayton et al., "Prevention of postoperative abdominal adhesions by a novel, glycerol/sodium hyaluronate/carboxymethylcellulose-based bioresorbable membrane: a prospective, randomized, evaluator-blinded multicenter study," *Diseases of the Colon and Rectum*, vol. 48, no. 6, pp. 1130–1139, 2005.

[86] E. Nilsson, C. Björn, V. Sjöstrand et al., "A novel polypeptide derived from human lactoferrin in sodium hyaluronate prevents postsurgical adhesion formation in the rat," *Annals of Surgery*, vol. 250, no. 6, pp. 1021–1028, 2009.

[87] R. Lim, J. M. Morrill, R. C. Lynch et al., "Practical limitations of bioresorbable membranes in the prevention of intra-abdominal adhesions," *Journal of Gastrointestinal Surgery*, vol. 13, no. 1, pp. 35–42, 2009.

[88] R. Lim, A. F. Stucchi, J. M. Morrill, K. L. Reed, R. Lynch, and J. M. Becker, "The efficacy of a hyaluronate-carboxymethylcellulose bioresorbable membrane that reduces postoperative adhesions is increased by the intra-operative co-administration of a neurokinin 1 receptor antagonist in a rat model," *Surgery*, vol. 148, no. 5, pp. 991–999, 2010.

[89] M. A. Lalountas, K. D. Ballas, C. Skouras et al., "Preventing intraperitoneal adhesions with atorvastatin and sodium hyaluronate/carboxymethylcellulose: a comparative study in rats," *American Journal of Surgery*, vol. 200, no. 1, pp. 118–123, 2010.

[90] D. Economidou, D. Kapoukranidou, C. Dimitriadis et al., "Osmotic nephrosis due to the use of anti-adhesive membrane intraperitoneally," *Nephrology Dialysis Transplantation*, vol. 26, no. 2, pp. 697–701, 2011.

[91] K. E. Greenawalt, M. J. Colt, R. L. Corazzini, O. L. Syrkina, and T. H. Jozefiak, "Remote efficacy for two different forms of hyaluronate-based adhesion barriers," *Journal of Investigative Surgery*, vol. 25, no. 3, pp. 174–180, 2012.

[92] H. J. Hwang, M. S. An, T. K. Ha et al., "All the commercially available adhesion barriers have the same effect on adhesion prophylaxis?; a comparison of barrier agents using a newly developed, severe intra-abdominal adhesion model," *International Journal of Colorectal Disease*, vol. 28, no. 8, pp. 1117–1125, 2013.

[93] K. Caglayan, B. Gungor, H. Cinar, N. Y. Erdogan, and B. Koca, "Preventing intraperitoneal adhesions with linezolid and hyaluronic acid/carboxymethylcellulose: a comparative study in cecal abrasion model," *American Journal of Surgery*, vol. 208, no. 1, pp. 106–111, 2014.

[94] E. Arslan, T. Talih, B. Oz, B. Halaclar, K. Caglayan, and M. Sipahi, "Comparison of lovastatin and hyaluronic acid/carboxymethyl cellulose on experimental created peritoneal adhesion model in rats," *International Journal of Surgery*, vol. 12, no. 2, pp. 120–124, 2014.

[95] A. Ohata, N. Tamura, K. Iwata et al., "Trehalose solution protects mesothelium and reduces bowel adhesions," *Journal of Surgical Research*, vol. 191, no. 1, pp. 224–230, 2014.

[96] S. Sakai, K. Ueda, and M. Taya, "Peritoneal adhesion prevention by a biodegradable hyaluronic acid-based hydrogel formed in situ through a cascade enzyme reaction initiated by contact with body fluid on tissue surfaces," *Acta Biomaterialia*, vol. 24, pp. 152–158, 2015.

[97] A. Połubinska, K. Pawlaczyk, M. Kuzlan-Pawlaczyk et al., "Dialysis solution containing hyaluronan: effect on peritoneal permeability and inflammation in rats," *Kidney International*, vol. 57, no. 3, pp. 1182–1189, 2000.

[98] G. W. Lipkin, M. A. Forbes, E. H. Cooper, and J. H. Turney, "Hyaluronic acid metabolism and its clinical significance in patients treated by continuous ambulatory peritoneal dialysis," *Nephrology Dialysis Transplantation*, vol. 8, no. 4, pp. 357–360, 1993.

[99] K. Yamagata, C. Tomida, and A. Koyama, "Intraperitoneal hyaluronan production in stable continuous ambulatory peritoneal dialysis patients," *Peritoneal Dialysis International*, vol. 19, no. 2, pp. 131–137, 1999.

[100] A. Breborowicz, A. Polubinska, K. Pawlaczyk et al., "Intraperitoneal hyaluronan administration in conscious rats: absorption, metabolism, and effects on peritoneal fluid dynamics," *Peritoneal Dialysis International*, vol. 21, no. 2, pp. 130–135, 2001.

[101] Q.-Y. Guo, W.-X. Peng, H.-H. Cheng, R.-G. Ye, B. Lindholm, and T. Wang, "Hyaluronan preserves peritoneal membrane transport properties," *Peritoneal Dialysis International*, vol. 21, no. 2, pp. 136–142, 2001.

[102] T. Wang, C. Chen, O. Heimbürger, J. Waniewski, J. Bergström, and B. Lindholm, "Hyaluronan decreases peritoneal fluid absorption in peritoneal dialysis," *Journal of the American Society of Nephrology*, vol. 8, no. 12, pp. 1915–1920, 1997.

[103] T. Wang, H.-H. Cheng, O. Heimbürger et al., "Intraperitoneal addition of hyaluronan improves peritoneal dialysis efficiency," *Peritoneal Dialysis International*, vol. 19, supplement 2, pp. S106–S111, 1999.

[104] T. Wang, H.-H. Cheng, O. Heimbürger et al., "Hyaluronan decreases peritoneal fluid absorption: effect of molecular weight and concentration of hyaluronan," *Kidney International*, vol. 55, no. 2, pp. 667–673, 1999.

[105] T. Wang, H.-H. Cheng, O. Heimbürger, J. Waniewski, J. Bergström, and B. Lindholm, "Hyaluronan prevents the decreased net ultrafiltration caused by increased peritoneal dialysate fill volume," *Kidney International*, vol. 53, no. 2, pp. 496–502, 1998.

[106] B.-I. Rosengren, O. Carlsson, and B. Rippe, "Hyaluronan and peritoneal ultrafiltration: a test of the "filter-cake" hypothesis," *American Journal of Kidney Diseases*, vol. 37, no. 6, pp. 1277–1285, 2001.

[107] O. Carlsson, B.-I. Rosengren, and B. Rippe, "Effects of peritoneal hyaluronidase treatment on transperitoneal solute and fluid transport in the rat," *Acta Physiologica Scandinavica*, vol. 168, no. 3, pp. 371–376, 2000.

[108] A. Breborowicz, A. Polubinska, J. Moberly, K. Ogle, L. Martis, and D. Oreopoulos, "Hyaluronan modifies inflammatory response and peritoneal permeability during peritonitis in rats," *American Journal of Kidney Diseases*, vol. 37, no. 3, pp. 594–600, 2001.

[109] J. B. Moberly, M. Sorkin, A. Kucharski et al., "Effects of intraperitoneal hyaluronan on peritoneal fluid and solute transport in peritoneal dialysis patients," *Peritoneal Dialysis International*, vol. 23, no. 1, pp. 63–73, 2003.

[110] Y. Cho, D. W. Johnson, J. C. Craig, G. F. M. Strippoli, S. V. Badve, and K. J. Wiggins, "Biocompatible dialysis fluids for peritoneal dialysis," *Cochrane Database of Systematic Reviews*, vol. 3, Article ID CD007554, 2014.

[111] K. Wieczorowska-Tobis, R. Brelinska, J. Witowski et al., "Evidence for less irritation to the peritoneal membrane in rats

dialyzed with solutions low in glucose degradation products," *Peritoneal Dialysis International*, vol. 24, no. 1, pp. 48–57, 2004.

[112] M. Zareie, A. S. De Vriese, L. H. P. Hekking et al., "Immunopathological changes in a uraemic rat model for peritoneal dialysis," *Nephrology Dialysis Transplantation*, vol. 20, no. 7, pp. 1350–1361, 2005.

[113] M. F. Flessner, J. Choi, H. Vanpelt et al., "Correlating structure with solute and water transport in a chronic model of peritoneal inflammation," *American Journal of Physiology—Renal Physiology*, vol. 290, no. 1, pp. F232–F240, 2006.

[114] M. N. Schilte, J. Loureiro, E. D. Keuming et al., "Long-term intervention with heparins in a rat model of peritoneal dialysis," *Peritoneal Dialysis International*, vol. 29, no. 1, pp. 26–35, 2009.

[115] J. Loureiro, M. Schilte, A. Aguilera et al., "BMP-7 blocks mesenchymal conversion of mesothelial cells and prevents peritoneal damage induced by dialysis fluid exposure," *Nephrology Dialysis Transplantation*, vol. 25, no. 4, pp. 1098–1108, 2010.

[116] A. Parikova, M. M. Zweers, D. G. Struijk, and R. T. Krediet, "Peritoneal effluent markers of inflammation in patients treated with icodextrin-based and glucose-based dialysis solutions," *Advances in Peritoneal Dialysis*, vol. 19, pp. 186–190, 2003.

[117] T. A. Martikainen, A.-M. Teppo, C. Grönhagen-Riska, and A. V. Ekstrand, "Glucose-free dialysis solutions: inductors of inflammation or preservers of peritoneal membrane?" *Peritoneal Dialysis International*, vol. 25, no. 5, pp. 453–460, 2005.

[118] S. Osada, C. Hamada, T. Shimaoka, K. Kaneko, S. Horikoshi, and Y. Tomino, "Alterations in proteoglycan components and histopathology of the peritoneum in uraemic and peritoneal dialysis (PD) patients," *Nephrology Dialysis Transplantation*, vol. 24, no. 11, pp. 3504–3512, 2009.

[119] B.-I. Rosengren, S. J. Sagstad, T. V. Karlsen, and H. Wiig, "Isolation of interstitial fluid and demonstration of local proinflammatory cytokine production and increased absorptive gradient in chronic peritoneal dialysis," *American Journal of Physiology—Renal Physiology*, vol. 304, no. 2, pp. F198–F206, 2013.

[120] H. Kinashi, Y. Ito, M. Mizuno et al., "TGF-β1 promotes lymphangiogenesis during peritoneal fibrosis," *Journal of the American Society of Nephrology*, vol. 24, no. 10, pp. 1627–1642, 2013.

[121] S. Yung, S. L. Lui, C. K. Ng et al., "Impact of a low-glucose peritoneal dialysis regimen on fibrosis and inflammation biomarkers," *Peritoneal Dialysis International*, vol. 35, no. 2, pp. 147–158, 2015.

[122] A. C. Midgley, T. Bowen, A. O. Phillips, and R. Steadman, "MicroRNA-7 inhibition rescues age-associated loss of epidermal growth factor receptor and hyaluronan-dependent differentiation in fibroblasts," *Aging Cell*, vol. 13, no. 2, pp. 235–244, 2014.

[123] K. Röck, J. Tigges, S. Sass et al., "miR-23a-3p causes cellular senescence by targeting hyaluronan synthase 2: possible implication for skin aging," *Journal of Investigative Dermatology*, vol. 135, no. 2, pp. 369–377, 2015.

[124] T. Bowen, "A role for fibrocytes in peritoneal fibrosis?" *Peritoneal Dialysis International*, vol. 32, no. 1, pp. 4–6, 2012.

[125] C. Beltrami, A. Clayton, A. O. Phillips, D. J. Fraser, and T. Bowen, "Analysis of urinary microRNAs in chronic kidney disease," *Biochemical Society Transactions*, vol. 40, no. 4, pp. 875–879, 2012.

[126] J. Martin, R. H. Jenkins, R. Bennagi et al., "Post-transcriptional regulation of transforming growth factor β-1 by microRNA-744," *PLoS ONE*, vol. 6, no. 10, Article ID e25044, 2011.

[127] R. H. Jenkins, J. Martin, A. O. Phillips, T. Bowen, and D. J. Fraser, "Transforming growth factor β1 represses proximal tubular cell microRNA-192 expression through decreased hepatocyte nuclear factor DNA binding," *Biochemical Journal*, vol. 443, no. 2, pp. 407–416, 2012.

[128] R. H. Jenkins, L. C. Davies, P. R. Taylor et al., "MiR-192 induces G2/M growth arrest in aristolochic acid nephropathy," *The American Journal of Pathology*, vol. 184, no. 4, pp. 996–1009, 2014.

Hindawi Publishing Corporation
BioMed Research International
Volume 2015, Article ID 578453, 6 pages
http://dx.doi.org/10.1155/2015/578453

Review Article

The Potential Role of NFAT5 and Osmolarity in Peritoneal Injury

Harald Seeger,[1,2] Daniel Kitterer,[3] Joerg Latus,[3] Mark Dominik Alscher,[3] Niko Braun,[3] and Stephan Segerer[1,2]

[1]*Division of Nephrology, University Hospital Zurich, 8091 Zurich, Switzerland*
[2]*Institute of Physiology and Zurich Center for Integrative Human Physiology (ZIHP), University of Zurich, 8057 Zurich, Switzerland*
[3]*Division of Nephrology, Department of Internal Medicine, Robert-Bosch-Hospital, 70376 Stuttgart, Germany*

Correspondence should be addressed to Stephan Segerer; stephan.segerer@usz.ch

Received 9 June 2015; Accepted 12 July 2015

Academic Editor: Donald Fraser

A rise in osmotic concentration (osmolarity) activates the transcription factor Nuclear Factor of Activated T Cells 5 (NFAT5, also known as Tonicity-responsive Enhancer Binding Protein, TonEBP). This is part of a regulatory mechanism of cells adjusting to environments of high osmolarity. Under physiological conditions these are particularly important in the kidney. Activation of NFAT5 results in the modulation of various genes including some which promote inflammation. The osmolarity increases in patients with renal failure. Additionally, in peritoneal dialysis the cells of the peritoneal cavity are repeatedly exposed to a rise and fall in osmotic concentrations. Here we review the current information about NFAT5 activation in uremic patients and patients on peritoneal dialysis. We suggest that high osmolarity promotes injury in the "uremic" milieu, which results in inflammation locally in the peritoneal membrane, but most likely also in the systemic circulation.

1. Introduction

During the last decades, we have witnessed a rapid growth of the patient population in need for renal replacement therapy [1]. Peritoneal dialysis is the most common form of home dialysis and favoring peritoneal dialysis (PD) as first strategy termed "PD first" is widely recommended [2]. Yet, due to various factors such as misconceptions concerning contraindications to PD, physician training, and apparent simplicity of HD initiation, but also superior reimbursement for hemodialysis in some places, this policy has hitherto not been consequently implemented [3]. "Uremia" has been described as an inflammatory state, caused by a myriad of factors accumulating in our patients with progressive loss of renal function [4]. In addition to this proinflammatory milieu, in patients on peritoneal dialysis we implant a catheter and expose them to dialysate. This is a lifesaving therapy but exposes the patients to additional "stressors." These include a foreign body reaction (catheter), glucose toxicity with induction of advanced glycation endproducts and formation of glucose degradation products, mechanical stress, changes in pH, and repeated exposure to a high osmotic concentration. Over time these "stressors" cause the peritoneal membrane to deteriorate, which is a major contributor to treatment failure in patients on PD [5–7]. We became interested in studying the response of peritoneal cells and biopsies from patients on PD concerning the response to osmolarity as one "puzzle stone" which could contribute to the decreased longevity of the peritoneal membrane.

2. Current View of the Mechanisms Leading to Peritoneal Fibrosis

The biological membrane used in peritoneal dialysis is a complex network of various cell types (e.g., mesothelial cells, peritoneal fibroblasts, inflammatory cells, vascular endothelial cells, and pericytes) and matrix components. The peritoneal membrane thickens with a progressive accumulation of submesothelial matrix, which already reaches a significant level prior to the start of PD [8]. In this "uremic" phase, factors not

related to the PD procedure already pave the way to the so-called simple peritoneal fibrosis. Later the clinical decrease in ultrafiltration capacity is associated with an expansion of the extracellular matrix (peritoneal fibrosis), formation of small vessels (neoangiogenesis), vasculopathy, increased number of lymphatic vessels, and loss of mesothelial cells (denudation) [9–13].

3. Cellular Responses to Osmotic "Stress"

The osmosensitive transcription factor NFAT5 plays a key role in the protection of cells against an increase in osmotic concentration [14]. It regulates the expression of genes which in part counteract the high osmolarity. Therefore it induces genes involved in the production and uptake of organic osmolytes. The role of NFAT5 in hyperosmolar conditions has been most intensively studied in kidney cells, as in the renal medulla cells typically face high concentrations of urea and sodium chloride [14]. The cellular response to high extracellular solute concentrations is highly conserved in evolution and not confined to the kidney. Consequently, expression of NFAT5 has been demonstrated to be ubiquitous throughout the entire organism. The prototypical reaction of mammalian cells exposed to high extracellular osmolarity is immediate shrinkage due to water efflux via aquaporins. Subsequently, the cell actively increases the concentration of intracellular organic osmolytes such as taurine, betaine, inositol, sorbitol, and glycerophosphocholine (GPC) via expression of certain enzymes such as aldose reductase (AR) or transporter molecules such as the betaine/GABA transporter (BGT1), the sodium/myoinositol cotransporter (*SLC5A3*), or the taurine transporter (TauT), thus equilibrating intra- and extracellular osmolar pressure. The above enzymes and transporters have been shown to be transcriptionally coregulated by NFAT5 (reviewed in [14]).

Certain chronic inflammatory conditions are associated with local or systemic hyperosmolality. For example, in patients with diabetes mellitus intermittent hyperglycemia is associated with increased plasma concentrations of the proinflammatory cytokines tumor necrosis factor- (TNF-) α, Interleukin- (IL-) 6, and IL-18 [15]. In peripheral blood mononuclear cells from diabetic patients with chronic microvascular lesions increased NFAT5 DNA binding activity was demonstrated [16]. IL-1β, IL-6, and IL-18 display NFAT5 target sequences in their promoter [15], TNF-α and LTβ are known target genes of NFAT5 in inflammatory cells [17], and exposure of human peripheral blood mononuclear cells to osmotic stress resulted in increased expression of IL-1 and IL-8 [18]. Consequently, in diabetic patients systemic hyperosmolality might lead to NFAT5 mediated release of proinflammatory cytokines.

Osmotic stress also increases nuclear factor-κB (NF-κB) activity, a key regulator in the induction of inflammatory responses via the regulation of chemokines, cytokines, and growth factors. Induction of NF-κB by hyperosmolarity involves p38 kinase and is independent of NFAT5; however, NF-κB induced transcription of target genes is significantly enhanced by binding to NFAT5 [19]. On the other hand, it is plausible that cytokines such as TNFα or LTβ, which are released via hyperosmolarity induced NFAT5 activation [17], lead to secondary activation of the NF-κB pathway. One of the most extensively studied chemokines is chemokine (C-C motif) ligand 2 (CCL2), also known as Monocyte Chemoattractant Protein-1 (MCP-1). It regulates the migration and infiltration of monocytes/macrophages. It can be produced by a variety of cell types after induction by oxidative stress, cytokines, growth factors, and hyperosmolarity [20–23]. In summary there are close interactions between the response to increased osmotic concentrations and the inflammatory cascade.

4. Osmotic Concentration in Patients with Renal Failure and on Dialysis

We became interested in studying NFAT5 in PD patients, as with the PD solution the peritoneal cavity is continuously exposed to cycles of a rapid rise and slow fall of osmolarity. An unexpected finding in our studies was a prominent induction of NFAT5 in uremic patients [24].

Other authors demonstrated that osmolarity increases in patients while progressing through the stages of chronic renal failure [25]. The serum osmolarity averaged 294 mosmol/kg H_2O in patients with normal kidney function and increased to a mean of 323 mosmol/kg H_2O in predialytic patients (CKD stage 5). Similar predialysis osmolalities were measured in dialysis dependent patients [25]. These results were confirmed in pediatric patients [26]. The underlying mechanisms are not completely understood, as blood urea does not fully account for the increase in osmolality. A hypothesis is that the retention of unmeasured solutes accounts for the increased osmolality as demonstrated by a rise in the osmolal gap. After a hemodialysis session, the serum osmolality was found to be reduced, but standard hemodialysis is not sufficient to return serum osmolality and osmolal gap back to normal [26, 27]. The chronic hyperosmolar state might be looked at as an "uremic toxin." Exposure of cells to hyperosmolar stress might result in cell cycle arrest, apoptosis, DNA damage, inhibition of transcription, and translation and might therefore have various detrimental effects [14].

5. Osmotic Response of the Peritoneal Membrane

Osmotic pressure has a significant impact on peritoneal cells, which was demonstrated by Breborowicz and others, who showed that exposure of mesothelial cells to hyperosmolar solutions in vitro leads to acute cell shrinkage [28]. Early studies on immortalized and primary human peritoneal mesothelial cells demonstrated that upon incubation with hyperosmolar solutions (osmolytes: glucose, mannitol, or NaCl) the matrix metalloproteinase 9 (MMP9) was down-regulated favoring accumulation of collagen type IV, thereby potentially promoting the development of peritoneal fibrosis [29]. The exposure of the peritoneum to hyperosmolar solutions led to vasodilation in another study [30]. This effect was hypothesized to be caused by water efflux through

aquaporin-1 channels of the microvascular endothelium, which consecutively leads to NO release by the endothelial cells [31, 32]. Furthermore, induction of apoptosis has been demonstrated by high osmolarity in mesothelial cells [33].

Lee and others were the first to demonstrate that glucose induced the expression of the proinflammatory cytokine CCL2 in human peritoneal mesothelial cells, thereby potentially favoring the influx of proinflammatory cells [21]. The effects were mediated by glucose itself, since mannitol did not stimulate CCL2 release. In contrast Matsuo and coworkers used rat peritoneal mesothelial cells (RPMCs) which responded to hyperosmolar concentrations of glucose (2.5% (140 mM) glucose) with increased transcription and release of CCL2. The effect was not glucose specific since it was also observed in cells exposed to the same concentration of mannitol. This implies that the response was elicited by hyperosmolarity and not glucose per se. The release of CCL2 was time and concentration dependent. The effects of hyperosmolarity (glucose or mannitol) on CCL2 mRNA expression were mediated by protein kinase C (PKC), in part via NF-κB activation. It could be blocked by micromolar concentrations of the glucocorticoid prednisolone via inhibition of NF-κB activation mediated by increased expression of I-κB-α [22]. The finding that NF-κB activation was only partially responsible for mediating the downstream effects of PKC was consistent with earlier findings that also the tyrosine kinase AP-1 pathway is involved in CCL2 induction elicited by high glucose concentrations in mesothelial cells [21]. The finding that the upregulation of CCL2 is mediated by hyperosmolarity rather than glucose was supported by Wong and others who demonstrated that mannitol had similar effects on human peritoneal mesothelial cells compared to glucose with respect to CCL2 induction [23]. These findings were recently recapitulated in immortalized human mesothelial cells stimulated by hyperosmolar concentrations of glucose, mannitol, or NaCl [34].

Little or no information is currently available on the role of peritoneal fibroblasts or the potential cross-talk between mesothelial cells and mesothelial cells in this complex system. In summary hyperosmolarity can produce a proinflammatory milieu in mesothelial cells.

6. Potential Role of the Transcription Factor NFAT5 in Response to Osmotic Stress in Peritoneal Cells

As described above, peritoneal cells are chronically exposed to high osmolality during peritoneal dialysis due to the supraphysiologic osmolality of the dialysis fluids ranging from 380 to 510 mosmol/kg H_2O, but also to increased serum osmolality in the predialytic phase in chronic kidney disease.

It has been demonstrated that NFAT5 activation in a hyperosmotic environment leads to the release of proinflammatory mediators [15, 35]. CCL2, especially, was upregulated in renal tubular epithelial cells upon osmotic stress in an NFAT5 dependent manner [19, 36]. This has led several groups to investigate the role of NFAT5 in the response of peritoneal cells to hyperosmolarity. Küper and colleagues demonstrated that NFAT5 activity was increased in human immortalized mesothelial (Met5A) cells upon exposure to hyperosmolar concentrations of NaCl, mannitol, or glucose in an osmolality dependent manner [34]. Peak activation of NFAT5 was reached at 400 mosmol/kg H_2O for glucose and mannitol and 450 mosmol/kg H_2O for NaCl and decreased at an osmolality >450 mosmol/kg H_2O. Interestingly, in renal cells, maximal NFAT5 activation was observed at osmolalities of >500 mosmol/kg H_2O. Knockdown of NFAT5 by siRNA abrogated CCL2 mRNA and protein upregulation of these cells stimulated by hyperosmolarity [34]. These results point to a crucial role of NFAT5 in CCL2 upregulation by mesothelial cells exposed to osmotic stress. In a further set of experiments the authors uncovered that the transcription factor NF-κB was activated under hyperosmotic conditions and that pharmacologic blockade of NF-κB abolished CCL2 expression. This confirms that NFAT5 and NF-κB cooperate also in cells of mesothelial origin in the stimulation of cytokine release upon osmotic stress as has previously been shown for renal cells ([34], Figure 1). One caveat of this study is that an immortalized cell line (Met5A) was used and results were not confirmed in primary human mesothelial cells.

Human peritoneal fibroblasts (HPFBs) have a crucial role in the pathogenesis of peritoneal fibrosis via release of proinflammatory cytokines and synthesis of extracellular matrix [37]. Our group has thus investigated the response of HPFBs to hyperosmolar glucose solutions in vitro. Upon exposure to increasing glucose concentrations in vitro, NFAT5 mRNA was significantly upregulated in an osmolality dependent fashion in these cells after six hours. Yet, after 24 and 96 hours no further increase of NFAT5 mRNA could be observed compared to controls. CCL2 mRNA was only induced after six hours in the cells exposed to the highest glucose concentration (125 mosmol/kg H_2O). However, after 96 hours a robust, concentration dependent upregulation of CCL2 mRNA could be witnessed. Interestingly, CCL2 upregulation occurred at a time point where NFAT5 mRNA levels were not upregulated any longer compared to controls. Therefore, there was a significant delay between NFAT5 mRNA induction and upregulation of CCL2, which could be explained by two scenarios. First, the delay between NFAT5 mRNA induction and upregulation of CCL2 might be explained by the time necessary for the translation of NFAT5 mRNA, synthesis of the protein, and nuclear translocation of the transcription factor before downstream targets can be induced. Secondly the more likely scenario is that CCL2 could have been induced in an NFAT5 independent fashion [24].

In further experiments, peritoneal biopsies were evaluated from uremic patients before the start of peritoneal dialysis and patients already on peritoneal dialysis and compared to controls. It was observed that in patients not on PD there was already a thickening of the peritoneal membrane. This has previously been described by other groups [8, 9]. Unexpectedly, NFAT5 expression was increased not only in patients on PD, but also in uremic patients not yet on PD. In healthy controls NFAT5 expression was significantly lower than in the other two groups. There was no significant difference in the expression level between uremic patients and patients on PD. This was true, even when the PD group was split up into patients with <8 h since the last exposure

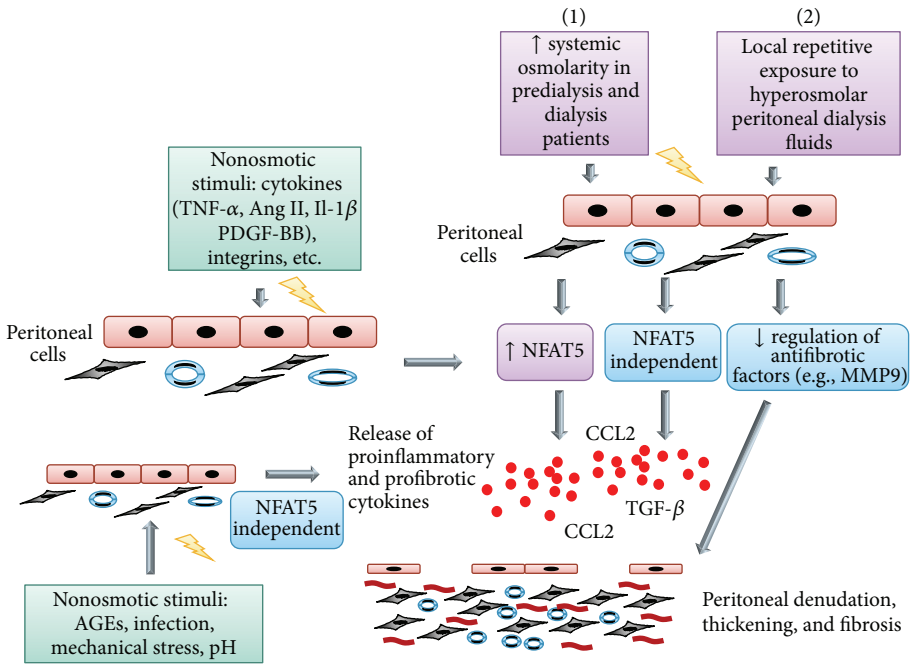

Figure 1: Involvement of osmotic and nonosmotic mechanism in peritoneal fibrosis. (1) Rise in osmolarity stimulates NFAT5 in patients with "uremia." Activation of NFAT5 results in a counterregulatory response protecting cells from hyperosmolarity but also induces inflammatory mediators (e.g., the chemokine CCL2) and growth factors. Additionally antifibrotic factors are downregulated. (2) Exposure to hyperosmolar dialysate might perpetuate NFAT5 induction. The balance between pro- and antifibrotic factors is shifted towards matrix deposition. Note that there are osmotic and nonosmotic factors inducing NFAT5 and also direct inducers of CCL2, which increases the complexity of the system and might lead to several vicious cycles promoting injury. Abbreviations: TNF-α = tumor necrosis factor α, Ang II = angiotensin II, PDGF-BB = platelet derived growth factor BB, TGF-β = transforming growth factor b, CCL2 = chemokine (C-C motif) ligand 2, MMP9 = matrix metalloproteinase 9, AGE = advanced glycation end products, NFAT5 = nuclear factor of activated T cells 5, and Il-1β = interleukin-1β.

to dialysate and those with >8 h. The stimulus for NFAT5 upregulation in peritoneum of patients prior to the start of PD is unclear. One possibility is that the increase in plasma osmolality in patients with preterminal CKD already suffices to induce NFAT5. Alternatively induction of NFAT5 might have been induced in a non-osmolality-dependent fashion. In fact, various circumstances have been described in which NFAT5 appears to be activated non-osmolality-dependent, for example, during embryonic development and cancer metastasis [38, 39]. Also cross-linking of the T cell receptor in T cells within an isotonic environment resulted in NFAT5 upregulation via calcineurin signaling [40]. In rheumatoid arthritis NFAT5 expression was shown to be increased in the synovium and in synovial fibroblast-like cells the cytokines Il-1β and TNF-α strongly induced NFAT5 expression [41]. Finally, Haltermann and others recently demonstrated in vascular smooth muscle cells (SMCs) that angiotensin II leads to nuclear translocation of NFAT5 and downstream gene transcription. PDGF-BB resulted in increased NFAT5 protein expression and SMC proliferation and migration [42].

However, many of the above findings face a similar problem, that, particularly in the in vivo studies, it cannot be excluded that a hyperosmolar microenvironment contributed to NFAT5 activation.

Contrary to NFAT5, CCL2 demonstrated a strong induction in the peritoneum of patients on PD, whereas the CCL2 message was only slightly upregulated in patients prior to PD. This was confirmed by immunohistochemistry. In the group prior to PD only occasional staining in MCs was observed; yet the MCs and fibroblasts (FBCs) of patients on PD displayed strong CCL2 immunoreactivity. Finally, while in patients on PD the peritoneal immunostaining for the NF-κB subunits p50 and p65 was markedly positive mainly in FBCs, there was barely immunopositivity in peritoneal FBCs in predialysis patients and no staining in controls [37].

Taken together, the above data strongly suggests that osmotic stress during peritoneal dialysis significantly affects the peritoneum and may contribute to peritoneal inflammation and fibrosis via stimulation of cytokine release from peritoneal cells. Our data suggests that osmotic stress to the peritoneal membrane exists even prior to the commencement of peritoneal dialysis and exposure to hyperosmolar dialysis fluids in uremic patients as evidenced by upregulation of NFAT5 mRNA and protein in peritoneal membranes of predialyis patients. This pathomechanism is fairly conceivable since uremic individuals display significantly increased serum osmolality as described above. Though speculative, it is imaginable that serum hyperosmolality in uremic patients leads to NFAT5 activation within cells of the peritoneal membrane and the release of proinflammatory and profibrotic factors finally leading to thickening of the peritoneal membrane which has been repeatedly observed in predialytic patients.

7. Conclusion

Increased osmolarity is the basis of water elimination in PD. There is now evidence in uremic patients and PD patients of an intraperitoneal induction of NFAT5. Osmotic and nonosmotic trigger might be present in PD, which could promote an inflammatory response. Also in mesothelial cells and peritoneal fibroblasts a response to hyperosmolar dialysate has been illustrated; until now the role of NFAT5 induced by dialysate needs to be shown in vivo. The blockade of NFAT5 might inhibit the inflammatory response and needs to be studied in models of peritoneal injury.

Conflict of Interests

Stephan Segerer received grant and travel support from Baxter. Harald Seeger received travel support from Baxter.

Acknowledgments

This study was supported by a grant by Fundação Pesquisa e Desenvolvimento Humanitario and a grant from the Else Kröner-Fresenius Stiftung to Stephan Segerer. Daniel Kitterer, Joerg Latus, and Niko Braun were supported by the Robert-Bosch Foundation.

References

[1] A. M. El Nahas and A. K. Bello, "Chronic kidney disease: the global challenge," *The Lancet*, vol. 365, no. 9456, pp. 331–340, 2005.

[2] K. Chaudhary, H. Sangha, and R. Khanna, "Peritoneal dialysis first: rationale," *Clinical Journal of the American Society of Nephrology*, vol. 6, no. 2, pp. 447–456, 2011.

[3] F. X. Liu, X. Gao, G. Inglese, P. Chuengsaman, R. Pecoits-Filho, and A. Yu, "A global overview of the impact of peritoneal dialysis first or favored policies: an opinion," *Peritoneal Dialysis International*, 2014.

[4] T. W. Meyer and T. H. Hostetter, "Uremia," *The New England Journal of Medicine*, vol. 357, no. 13, pp. 1316–1325, 2007.

[5] S. J. Davies, L. Phillips, A. M. Griffiths, L. H. Russell, P. F. Naish, and G. I. Russell, "What really happens to people on long-term peritoneal dialysis?" *Kidney International*, vol. 54, no. 6, pp. 2207–2217, 1998.

[6] S. J. Davies, J. Bryan, L. Phillips, and G. I. Russell, "Longitudinal changes in peritoneal kinetics: the effects of peritoneal dialysis and peritonitis," *Nephrology Dialysis Transplantation*, vol. 11, no. 3, pp. 498–506, 1996.

[7] D. N. Churchill, K. E. Thorpe, K. D. Nolph, P. R. Keshaviah, D. G. Oreopoulos, and D. Pagé, "Increased peritoneal membrane transport is associated with decreased patient and technique survival for continuous peritoneal dialysis patients," *Journal of the American Society of Nephrology*, vol. 9, no. 7, pp. 1285–1292, 1998.

[8] K. Honda, C. Hamada, M. Nakayama et al., "Impact of uremia, diabetes, and peritoneal dialysis itself on the pathogenesis of peritoneal sclerosis: a quantitative study of peritoneal membrane morphology," *Clinical Journal of the American Society of Nephrology*, vol. 3, no. 3, pp. 720–728, 2008.

[9] J. D. Williams, K. J. Craig, N. Topley et al., "Morphologic changes in the peritoneal membrane of patients with renal disease," *Journal of the American Society of Nephrology*, vol. 13, no. 2, pp. 470–479, 2002.

[10] Y. Cho, D. W. Johnson, S. V. Badve, J. C. Craig, G. F. M. Strippoli, and K. J. Wiggins, "The impact of neutral-pH peritoneal dialysates with reduced glucose degradation products on clinical outcomes in peritoneal dialysis patients," *Kidney International*, vol. 84, no. 5, pp. 969–979, 2013.

[11] Y. Cho, D. W. Johnson, S. Badve, J. C. Craig, G. F. K. Strippoli, and K. J. Wiggins, "Impact of icodextrin on clinical outcomes in peritoneal dialysis: a systematic review of randomized controlled trials," *Nephrology Dialysis Transplantation*, vol. 28, no. 7, pp. 1899–1907, 2013.

[12] J. Witowski, T. O. Bender, J. Wisniewska-Elnur et al., "Mesothelial toxicity of peritoneal dialysis fluids is related primarily to glucose degradation products, not to glucose per se," *Peritoneal Dialysis International*, vol. 23, no. 4, pp. 381–390, 2003.

[13] J. Witowski, T. O. Bender, G. M. Gahl, U. Frei, and A. Jörres, "Glucose degradation products and peritoneal membrane function," *Peritoneal Dialysis International*, vol. 21, no. 2, pp. 201–205, 2001.

[14] M. B. Burg, J. D. Ferraris, and N. I. Dmitrieva, "Cellular response to hyperosmotic stresses," *Physiological Reviews*, vol. 87, no. 4, pp. 1441–1474, 2007.

[15] W. Neuhofer, "Role of NFAT5 in inflammatory disorders associated with osmotic stress," *Current Genomics*, vol. 11, no. 8, pp. 584–590, 2010.

[16] B. Yang, A. D. Hodgkinson, P. J. Oates, H. M. Kwon, B. A. Millward, and A. G. Demaine, "Elevated activity of transcription factor nuclear factor of activated T-cells 5 (NFAT5) and diabetic nephropathy," *Diabetes*, vol. 55, no. 5, pp. 1450–1455, 2006.

[17] C. López-Rodríguez, J. Aramburu, L. Jin, A. S. Rakeman, M. Michino, and A. Rao, "Bridging the NFAT and NF-kappaB families: NFAT5 dimerization regulates cytokine gene transcription in response to osmotic stress," *Immunity*, vol. 15, no. 1, pp. 47–58, 2001.

[18] L. Shapiro and C. A. Dinarello, "Hyperosmotic stress as a stimulant for proinflammatory cytokine production," *Experimental Cell Research*, vol. 231, no. 2, pp. 354–362, 1997.

[19] I. Roth, V. Leroy, H. M. Kwon, P.-Y. Martin, E. Féraille, and U. Hasler, "Osmoprotective transcription factor NFAT5/TonEBP modulates nuclear factor-κB activity," *Molecular Biology of the Cell*, vol. 21, no. 19, pp. 3459–3474, 2010.

[20] H. Ha and H. B. Lee, "Effect of high glucose on peritoneal mesothelial cell biology," *Peritoneal Dialysis International*, vol. 20, supplement 2, pp. S15–S18, 2000.

[21] S. K. Lee, B. S. Kim, W. S. Yang, S. B. Kim, S. K. Park, and J. S. Park, "High glucose induces MCP-1 expression partly via tyrosine kinase-AP-1 pathway in peritoneal mesothelial cells," *Kidney International*, vol. 60, no. 1, pp. 55–64, 2001.

[22] H. Matsuo, M. Tamura, N. Kabashima et al., "Prednisolone inhibits hyperosmolarity-induced expression of MCP-1 via NF-κB in peritoneal mesothelial cells," *Kidney International*, vol. 69, no. 4, pp. 736–746, 2006.

[23] T. Y. H. Wong, A. O. Phillips, J. Witowski, and N. Topley, "Glucose-mediated induction of TGF-beta 1 and MCP-1 in mesothelial cells in vitro is osmolality and polyol pathway dependent," *Kidney International*, vol. 63, no. 4, pp. 1404–1416, 2003.

[24] D. Kitterer, J. Latus, C. Ulmer et al., "Activation of nuclear factor of activated T cells 5 in the peritoneal membrane of uremic patients," *The American Journal of Physiology—Renal Physiology*, vol. 308, no. 11, pp. F1247–F1258, 2015.

[25] G. Shaikh, R. Sehgal, S. Sandhu, S. Vaddineni, J. Fogel, and S. Rubinstein, "Changes in osmol gap in chronic kidney disease: an exploratory study," *Renal Failure*, vol. 36, no. 2, pp. 198–201, 2014.

[26] H. Dursun, A. Noyan, N. Cengiz et al., "Changes in osmolal gap and osmolality in children with chronic and end-stage renal failure," *Nephron: Physiology*, vol. 105, no. 2, pp. p19–p21, 2007.

[27] I. Griveas, A. Gompou, I. Kyritsis et al., "Osmolal gap in hemodialyzed uremic patients," *Artificial Organs*, vol. 36, no. 1, pp. 16–20, 2012.

[28] A. Breborowicz, A. Polubinska, and D. G. Oreopoulos, "Changes in volume of peritoneal mesothelial cells exposed to osmotic stress," *Peritoneal Dialysis International*, vol. 19, no. 2, pp. 119–123, 1999.

[29] J.-P. Rougier, P. Moullier, R. Piedagnel, and P. M. Ronco, "Hyperosmolality suppresses but TGFβ1 increases MMP9 in human peritoneal mesothelial cells," *Kidney International*, vol. 51, no. 1, pp. 337–347, 1997.

[30] F. N. Miller, K. D. Nolph, I. G. Joshua, D. L. Wiegman, P. D. Harris, and D. B. Andersen, "Hyperosmolality, acetate, and lactate: dilatory factors during peritoneal dialysis," *Kidney International*, vol. 20, no. 3, pp. 397–402, 1981.

[31] R. Zakaria, A. Althani, A. A. Fawzi, and O. M. Fituri, "Hyperosmolality-mediated peritoneal microvascular vasodilation is linked to aquaporin function," *Advances in Peritoneal Dialysis*, vol. 30, pp. 63–74, 2014.

[32] E. R. A. Zakaria, A. Althani, A. A. Fawzi, and O. M. Fituri, "Molecular mechanisms of peritoneal dialysis-induced microvascular vasodilation," *Advances in Peritoneal Dialysis*, vol. 30, pp. 98–109, 2014.

[33] D. M. Alscher, D. Biegger, T. Mettang, H. van der Kuip, U. Kuhlmann, and P. Fritz, "Apoptosis of mesothelial cells caused by unphysiological characteristics of peritoneal dialysis fluids," *Artificial Organs*, vol. 27, no. 11, pp. 1035–1040, 2003.

[34] C. Küper, F.-X. Beck, and W. Neuhofer, "NFAT5 contributes to osmolality-induced MCP-1 expression in mesothelial cells," *Mediators of Inflammation*, vol. 2012, Article ID 513015, 12 pages, 2012.

[35] W. Y. Go, X. Liu, M. A. Roti, F. Liu, and S. N. Ho, "NFATS/TonEBP mutant mice define osmotic stress as a critical feature of the lymphoid microenvironment," *Proceedings of the National Academy of Sciences of the United States of America*, vol. 101, no. 29, pp. 10673–10678, 2004.

[36] R. Kojima, H. Taniguchi, A. Tsuzuki, K. Nakamura, Y. Sakakura, and M. Ito, "Hypertonicity-induced expression of monocyte chemoattractant protein-1 through a novel cis-acting element and MAPK signaling pathways," *Journal of Immunology*, vol. 184, no. 9, pp. 5253–5262, 2010.

[37] J. Witowski and A. Jörres, "Peritoneal cell culture: fibroblasts," *Peritoneal Dialysis International*, vol. 26, no. 3, pp. 292–299, 2006.

[38] D. Maouyo, J. Y. Kim, S. D. Lee, Y. Wu, S. K. Woo, and H. M. Kwon, "Mouse TonEBP-NFAT5: expression in early development and alternative splicing," *The American Journal of Physiology—Renal Physiology*, vol. 282, no. 5, pp. F802–F809, 2002.

[39] S. Jauliac, C. López-Rodriguez, L. M. Shaw, L. F. Brown, A. Rao, and A. Toker, "The role of NFAT transcription factors in integrin-mediated carcinoma invasion," *Nature Cell Biology*, vol. 4, no. 7, pp. 540–544, 2002.

[40] J. Trama, Q. Lu, R. G. Hawley, and S. N. Ho, "The NFAT-related protein NFATL1 (TonEBP/NFAT5) is induced upon T cell activation in a calcineurin-dependent manner," *Journal of Immunology*, vol. 165, no. 9, pp. 4884–4894, 2000.

[41] H.-J. Yoon, S. You, S.-A. Yoo et al., "NF-AT5 is a critical regulator of inflammatory arthritis," *Arthritis & Rheumatism*, vol. 63, no. 7, pp. 1843–1852, 2011.

[42] J. A. Halterman, H. M. Kwon, R. Zargham, P. D. S. Bortz, and B. R. Wamhoff, "Nuclear factor of activated T cells 5 regulates vascular smooth muscle cell phenotypic modulation," *Arteriosclerosis, Thrombosis, and Vascular Biology*, vol. 31, no. 10, pp. 2287–2296, 2011.

Hindawi Publishing Corporation
BioMed Research International
Volume 2015, Article ID 628158, 12 pages
http://dx.doi.org/10.1155/2015/628158

Research Article

Cross-Omics Comparison of Stress Responses in Mesothelial Cells Exposed to Heat- versus Filter-Sterilized Peritoneal Dialysis Fluids

Klaus Kratochwill,[1,2] Thorsten O. Bender,[1,3] Anton M. Lichtenauer,[1,2] Rebecca Herzog,[1,2] Silvia Tarantino,[1] Katarzyna Bialas,[2] Achim Jörres,[3] and Christoph Aufricht[1]

[1]*Department of Pediatrics and Adolescent Medicine, Medical University of Vienna, 1090 Vienna, Austria*
[2]*Zytoprotec GmbH, 1090 Vienna, Austria*
[3]*Department of Nephrology and Medical Intensive Care, Campus Virchow-Klinikum, Charité Universitätsmedizin Berlin, 13353 Berlin, Germany*

Correspondence should be addressed to Christoph Aufricht; christoph.aufricht@meduniwien.ac.at

Received 13 May 2015; Accepted 31 August 2015

Academic Editor: Robert Beelen

Recent research suggests that cytoprotective responses, such as expression of heat-shock proteins, might be inadequately induced in mesothelial cells by heat-sterilized peritoneal dialysis (PD) fluids. This study compares transcriptome data and multiple protein expression profiles for providing new insight into regulatory mechanisms. Two-dimensional difference gel electrophoresis (2D-DIGE) based proteomics and topic defined gene expression microarray-based transcriptomics techniques were used to evaluate stress responses in human omental peritoneal mesothelial cells in response to heat- or filter-sterilized PD fluids. Data from selected heat-shock proteins were validated by 2D western-blot analysis. Comparison of proteomics and transcriptomics data discriminated differentially regulated protein abundance into groups depending on correlating or noncorrelating transcripts. Inadequate abundance of several heat-shock proteins following exposure to heat-sterilized PD fluids is not reflected on the mRNA level indicating interference beyond transcriptional regulation. For the first time, this study describes evidence for posttranscriptional inadequacy of heat-shock protein expression by heat-sterilized PD fluids as a novel cytotoxic property. Cross-omics technologies introduce a novel way of understanding PDF bioincompatibility and searching for new interventions to reestablish adequate cytoprotective responses.

1. Introduction

Peritoneal dialysis (PD) is a cost effective and safe form of renal replacement therapy in end stage renal disease. However, PD-fluids (PDF) are bioincompatible solutions and may induce severe peritoneal damage, to a large part mediated by cytotoxic injury to the mesothelial cell layer, mostly due to low pH, lactate, high glucose, and its degradation products [1, 2].

In experimental PD we and others have shown that acute exposure to cytotoxic contents of PDF results in rapid induction of heat shock proteins (HSP) in mesothelial cells during the recovery phase, counteracting toxic injury [3–6]. HSP are the most prominent protein members of the cellular stress response and transient overexpression of these important molecules of the cellular repair machinery has been shown to mediate strong cytoprotective effects during experimental PD [5, 6].

Recently, we have described unexpectedly low HSP expression upon more extended exposure to diluted heat-sterilized PDF [7]. Albeit this setting still represents a highly artificial system, the exposure to diluted cytotoxic properties of PDF likely reflects intraperitoneal conditions during a PD dwell more closely than acute exposure to pure PDF [8–10]. Heat-sterilization and storage of glucose-based PDF result in formation of highly reactive glucose degradation

products (GDPs) that are known to mediate their cytotoxicity via oxidative stress [11–13]. These findings suggest that exposure to PDF containing high levels of GDP may even dampen cellular stress responses, increasing the vulnerability of mesothelial cells against PDF cytotoxicity. Recent research suggests that oxidative stress might indeed suppress the cellular stress responses [14, 15].

In this study we have used two-dimensional difference gel electrophoresis (2D-DIGE) based proteomics and topic defined gene expression microarray-based transcriptomics techniques to evaluate mesothelial stress responses in response to exposure to heat- versus filter-sterilized PDF, thus comparing effects of GDPs on a global level. For the first time transcriptome data and multiple protein expression profiles were compared in experimental PD in order to provide new insight into regulatory mechanisms.

2. Materials and Methods

2.1. Materials. All chemicals, unless otherwise stated, were purchased from Sigma-Aldrich (St. Louis, MI, USA). All tissue culture plastics were Falcon (Becton Dickinson, San José, CA, USA). The PD solutions heat-sterilized PDF (H-PDF), containing GDPs, and filter-sterilized PDF (F-PDF), containing no GDPs, were prepared in the laboratory according to the following formulation: NaCl 5.786 g/L, $CaCl_2 \cdot 2H_2O$ 0.257 g/L, $MgCl_2 \cdot 6H_2O$ 0.102 g/L, sodium D/L-lactate 3.925 g/L, and anhydrous D-glucose 15.0 or 42.5 g/L, with a final composition in mmol/L: Na^+ 132, Ca^{2+} 1.25, Mg^{2+} 0.25, Cl^- 95, lactate 40, and 3.86% glucose and a pH of 5.5. The solutions from the same stock were then sterilized either by heat (121°C, 0.2 MPa, 20 min) or by filtration through a 0.2-μm pore size filter (Nalgene, Nalge Nunc International, Rochester, NY, USA).

2.2. Exposure of Human Peritoneal Mesothelial Cells to PD Solutions. Human peritoneal mesothelial cells (HPMC) were isolated from fully anonymized specimens of omentum obtained from three consenting nonuremic patients undergoing elective abdominal surgery. The study was accomplished in accordance with the institutional review board, consistent with the principles of the Declaration of Helsinki. Cells were isolated and characterized as previously described [16]. HPMC were propagated in M199 culture medium supplemented with 2 mM L-glutamine, 100 U/mL penicillin, 100 μg/mL streptomycin, 0.4 μg/mL hydrocortisone, and 10%$_{v/v}$ fetal calf serum (FCS; Invitrogen, Carlsbad, CA, USA). All experiments were performed using cells from the second passage since later subcultures may contain an increasing number of senescent cells [16, 17]. HPMC were plated into multiwell clusters and grown until confluence. The standard medium containing 10% FCS was replaced by medium supplemented with 0.3% FCS for 48 hours prior to experiments to render the cells in a quiescent state.

PDF Exposure. In three independent experiments HPMC cultures obtained from the three above mentioned donors were exposed to a 1 : 1 mixture of regular culture medium containing 0.6% FCS (final concentration 0.3%) and the mentioned PD solution (either filter- or heat-sterilized) for 24 h. At the end of the exposure period the cells were harvested according to the procedure given below for 2D-DIGE and the supernatants were saved at −80°C until use in the viability assay (LDH release).

2.3. Protein Expression Profiling 2D-DIGE

2.3.1. Protein Sample Preparation. The cells were lysed by incubation with 1 mL lysis buffer (30 mM Tris, pH 8.5, 7 M urea, 2 M thiourea, 4% 3-[(3-cholamidopropyl) dimethylammonio]-1-propanesulfonate (CHAPS), 1 mM EDTA, 1 tablet of Complete Protease Inhibitor (Roche, Basel; Switzerland) per 100 mL, and 10 μL/mL of each of the phosphatase inhibitor cocktails 1 and 2 (Sigma-Aldrich)) per 3×10^7 cells for 10 min at 25°C. The resulting lysates were centrifuged for 30 minutes (14,000 ×g, 4°C) and stored at −80°C until further processing. Total protein concentration was determined by the 2D-Quant Kit (GE Healthcare, Uppsala, Sweden) according to the manufacturer's manual.

2.3.2. Cell Harvesting and Protein Labeling. An internal pooled standard (IPS) containing all sample pools was prepared and used in all gels. IPS therefore represents a mixture of all proteins expressed in any cell under all tested conditions and should thus contain every protein spot that can be detected. Aliquots of the samples (H-PDF, F-PDF) were each labeled with Cy5 as well as protein lysates from immortalized HPMC, which were used as reference material. Labeling of the IPS was performed with Cy3 dye using the DIGE minimal labeling kit (GE Healthcare) following the recommendations of the manufacturer with minor modifications. In brief, 40 μg of total protein per sample was mixed with 200 pmol of the reconstituted Cy5 dye solution (400 μM stock solution in anhydrous DMF) and per gel 40 μg of total protein of the internal pooled standard (IPS) of all samples was mixed with 200 pmol of the reconstituted Cy3 CyDye solution. Labeling of the IPS was performed in one batch to achieve a uniform standard. The labeling reactions were incubated on ice in the dark for 30 min and then stopped with 1 μL of 10 mM L-lysine solution. For every gel one Cy5 labeled sample and an aliquot of the Cy3 labeled IPS were mixed.

2.4. Isoelectric Focusing. The rehydration mix was brought to a final volume of 450 μL with rehydration buffer consisting of 5 M urea, 0.5% CHAPS, 0.5% Pharmalyte, and 12 μL/mL of DeStreak reagent (GE Healthcare). Each mixture was applied by rehydration loading to one IPG strip (ReadyStrip pH 3–10, nonlinear, 24 cm, Bio-Rad, Hercules, CA, USA) in the focusing tray of a Bio-Rad Protean IEF unit, sealed with silicone oil (Bio-Rad). The strips were rehydrated with the samples by "active rehydration" at 50 V and 20°C for 15 h and then focused for 3 h at 100 V, before the voltage was constantly increased to 8000 V within 17.5 hours, applying altogether 65 kVh with a maximum of 30 μA per strip.

2.5. Vertical Electrophoresis. Gels for second-dimension vertical SDS-PAGE were cast using a Bio-Rad multicasting

chamber, low-fluorescent glass plates, and 1 mm spacers (Bio-Rad). For a final concentration of the separation gels of 12%, 240 mL acrylamide stock solution (40%, T : C = 29 : 1, Bio-Rad) was mixed with 200 mL 1.5 M Tris-HCl pH 8.8, 40 mL glycerol, and 320 mL H_2O_{UHQ}. TEMED (80 μL) and ammonium persulfate (1 mL, APS, 10% in H_2O_{UHQ}) were added after degassing of the mixture and right before filling of the casting chamber. The gels were left to polymerize overnight, overlaid with water-saturated n-butanol. Vertical second-dimension SDS-PAGE was carried out on a Bio-Rad Dodeca system with the current set to 60 mA for 100 Vh and then to 200 mA for 1200 Vh.

2.6. Fluorescence Image Acquisition and Data Analysis. DIGE labeled gels were scanned sandwiched between the low-fluorescent glass plates of the cassettes immediately after the run. Gel images were acquired using a Typhoon Trio laser scanner (GE Healthcare) using excitation and emission wavelengths recommended for the used dyes (Cy3: Ex 532 nm, Em 580 nm, and BP 30; Cy5: Ex 633 nm, Em 670 nm, and BP 30). The photomultiplier voltage was chosen so that the most abundant protein spots were close to saturation. Sensitivity level was set to "normal."

Gel images were analyzed using the Delta2D 3.6 software (Decodon GmbH, Greifswald, Germany) using the algorithm designated for DIGE experiments. The images, containing the IPS, were aligned by pairwise warping and spot detection was carried out on a fused image of all gels (see Supplemental Figure 1 in Supplementary Material available online at http://dx.doi.org/10.1155/2015/628158). Protein identifications, accomplished in our laboratory [18], were processed with the aid of the ID mapping feature offered by the UniProt database (http://www.uniprot.org; [19]) to a short list of proteins overlapping with the genes investigated by RNA array used in this study (see Supplemental Table 1 for a summary of all used mass spectrometric identification data). The protein annotations of this short list were assigned to the respective spots on the 2D gels. Relative spot volumes normalized to the IPS of 28 unique proteins (see Table 1) were quantified among exposure of HPMC to H-PDF or F-PDF. Significance values were derived from group comparisons utilizing Student's t-test with the obtained p values given in Table 1. Details on individual proteins and corresponding spots are provided as bar graphs for each spot (Supplemental Figure 2) and spot album (Supplemental Figure 3).

2.7. RNA Expression Array Analysis. For analysis on the transcriptional level topic defined microarray experiments were employed. In brief, HPMC exposed to H-PDF or F-PDF were homogenized in 350 μL RLT buffer (Qiagen, Hilden, Germany) and then extracted using the RNeasy Mini Kit (Qiagen) according to the manufacturer's protocol. Total RNA was checked for integrity with the Agilent Bioanalyzer 2100 (Agilent Technologies, Inc., Palo Alto, CA). 0.8 μg of total RNA was then used for amplification and analysis with topic defined PIQOR Toxicology Human Microarray (Miltenyi Biotec, Bergisch Gladbach, Germany) containing 1264 human genes comprising the subject areas apoptosis, DNA damage and repair, inflammation, cell proliferation and response to oxidative stress, and xenobiotic metabolism. Each PIQOR microarray contains six housekeeping genes (ACTA2, CYPA, GAPDH, HPRT, TUBA, and TUBB) and six controls (herring sperm DNA, salt, and four artificial control RNAs) for the correct quantification of the differential expression patterns. Genes are spotted in quadruplicate. All steps between RNA isolation and data interpretation, including sample labelling, microarray hybridization, and scanning, were carried out by Miltenyi Biotec Microarray Services.

Data analysis included exclusion of low-quality spots, background subtraction to obtain the net signal intensity, data normalization, and calculation of the Cy5/Cy3 ratios. Additionally only spots that had at least in one channel a signal intensity that was 2-fold higher than the mean background were taken into account for the ratio calculation. Normalized mean Cy5/Cy3 ratios of the four replicates per gene and the respective coefficient of variation (% CV) were calculated. This CV refers to the average of the Cy5/Cy3 ratios for the gene replicates.

Finally, for the genes overlapping with identified proteins in the proteomics experiment mean ratios were calculated by averaging the values obtained from the three individual chips, one per biological experiment. The standard deviation (SD) and CV (Chip CV) are also given in the results (see Table 1).

2.8. Two-Dimensional Western Blotting (Adapted from [20]). For 2D western analysis, gels were prepared as described above. Proteins were electroblotted onto PVDF membranes (Millipore; Billerica, MA, USA) immediately after the run by semidry transfer using the Novablot unit of the MultiPhor II electrophoresis system and an according transfer buffer (200 mM glycine, 25 mM Tris base, 0.1% SDS, and 20% methanol). The membranes were washed in TBST buffer (150 mM NaCl, 0.05% Tween 20, and 10 mM Tris-HCl at pH 7.4) and stained using ruthenium II tris-bathophenanthroline disulfonate (RuBPS) following a fluorescent staining protocol, modified for staining membranes. In brief, RuBPS was prepared as published by Rabilloud et al. [21] and used as stock solution without further processing. The proteins were fixed by incubation for 15 min with fixing solution (10% acetic acid, 20% methanol). Membranes were washed 4 times for 5 min with H_2O_{UHQ} and then incubated for 30 min with staining solution (10 μL RuBPS stock solution made up to 1000 mL with H_2O_{UHQ}). After again washing 4 times for 5 min with H_2O_{UHQ} the membranes were dried and scanned with the aid of the Typhoon Trio laser scanner mentioned above using excitation and emission wavelengths optimized for the used protocol (Ex 488 nm, Em 670 nm, and BP 30). The photomultiplier voltage was chosen so that the stained protein spots were clearly distinguishable from the background. Sensitivity level was set to "normal." The obtained total protein pattern was used for later alignment to the specific immunodetected signals. The membranes were rehumidified with methanol and washed again in TBST buffer before proceeding to the blocking step. The membranes were blocked with 5% dry milk in TBST and then incubated

Table 1: Proteins and transcripts analyzed by 2D-DIGE and mRNA expression microarrays.

Gene name	Gene ID	Protein name	RefSeq	Transcriptomics data				SwissProt entry name	Proteomics data					
				Heat/filter					Heat		Filter		Heat/filter	
				Mean ratio[1]	SD[2]	CV[3]	Chip CV[4]		Mean spot volume[5]	SD[6]	Mean spot volume[5]	SD[6]	Ratio[7]	p value[8]
Increased protein abundance (proteomics ratio > 1)														
Increased gene expression (transcriptomics ratio > 1)														
HSPA8	3312	Heat shock cognate 71 kDa protein	NM_006597 NM_153201	1.60	0.02	3%	4%	HSP7C_HUMAN	132.893	9.736	112.899	11.838	1.177	0.203
HSPB1	3315	Heat shock protein beta-1*	NM_001540	1.32	0.13	17%	4%	HSPB1_HUMAN	207.830	35.162	71.975	17.335	2.888	0.061
GSTP1	2950	Glutathione S-transferase P	NM_000852	1.16	0.04	5%	4%	GSTP1_HUMAN	88.029	66.625	61.654	10.343	1.428	0.562
GSR	2936	Glutathione reductase, mitochondrial	NM_000637	1.19	0.07	9%	0%	GSHR_HUMAN	140.743	12.299	129.512	4.931	1.087	0.438
PDIA3	2923	Protein disulfide-isomerase A3**	NM_005313	1.07	0.14	14%	14%	PDIA3_HUMAN	185.997	3.950	125.444	20.051	1.483	0.031
PDIA3	2923	Protein disulfide-isomerase A3*	NM_005313	1.07	0.14	14%	14%	PDIA3_HUMAN	147.417	4.727	115.852	16.524	1.272	0.094
Decreased gene expression (transcriptomics ratio < 1)														
CCT5	22948	T-complex protein 1 subunit epsilon**	NM_012073	0.82	0.09	7%	9%	TCPE_HUMAN	177.988	10.033	122.697	8.415	1.451	0.019
PSMB2	5690	Proteasome subunit beta type-2	NM_002794	0.87	0.09	7%	18%	PSB2_HUMAN	100.167	7.492	83.670	13.559	1.197	0.161
HSPA5	3309	78 kDa glucose-regulated protein***	NM_005347	0.81	0.14	11%	4%	GRP78_HUMAN	254.121	5.404	106.676	15.450	2.382	0.001
P4HB	5034	Protein disulfide-isomerase**	NM_000918	0.56	0.35	20%	7%	PDIA1_HUMAN	192.710	6.746	112.938	26.334	1.706	0.025
PDIA6	10130	Protein disulfide-isomerase A6*	NM_005742	0.65	0.04	2%	4%	PDIA6_HUMAN	125.940	2.434	106.148	11.478	1.186	0.090
COPS4	51138	COP9 signalosome complex subunit 4	NM_016129	0.77	0.11	8%	7%	CSN4_HUMAN	151.484	17.903	108.440	17.368	1.397	0.139
HSPD1	3329	60 kDa heat shock protein, mitochondrial***	NM_002156 NM_199440	0.82	0.06	5%	3%	CH60_HUMAN	275.662	1.224	155.233	8.962	1.776	0.001
RPSA	3921	40S ribosomal protein SA	NM_002295	0.75	0.24	18%	0.05	RSSA_HUMAN	111.019	23.693	110.845	9.474	1.002	0.993

Table 1: Continued.

Gene name	Gene ID	Protein name	RefSeq	Transcriptomics data				SwissProt entry name	Proteomics data					
				Heat/filter					Heat		Filter		Heat/filter	
				Mean ratio[1]	SD[2]	CV[3]	Chip CV[4]		Mean spot volume[5]	SD[6]	Mean spot volume[5]	SD[6]	Ratio[7]	p value[8]
Decreased protein abundance (proteomics ratio < 1)														
Increased gene expression (transcriptomics ratio > 1)														
HSPA9	3313	Stress-70 protein, mitochondrial	NM_004134	1.32	0.07	9%	4%	GRP75_HUMAN	108.049	9.256	123.253	5.843	0.877	0.156
HSPA1A	3303	*Heat shock 70 kDa protein 1*	NM_005345 NM_005346	2.59	0.07	17%	6%	HSP71_HUMAN	108.049	9.256	123.253	5.843	0.877	0.156
HSPA8	3312	Heat shock cognate 71 kDa protein	NM_006597 NM_153201	1.60	0.02	3%	4%	HSP7C_HUMAN	108.049	9.256	123.253	5.843	0.877	0.156
HSPA1A	3303	Heat shock 70 kDa protein 1*	NM_005345 NM_005346	2.59	0.07	17%	6%	HSP71_HUMAN	104.254	14.587	130.041	4.812	0.802	0.091
HSPA8	3312	Heat shock cognate 71 kDa protein	NM_006597 NM_153201	1.60	0.02	3%	4%	HSP7C_HUMAN	106.853	10.219	123.120	6.412	0.868	0.163
HSPA1A	3303	Heat shock 70 kDa protein 1**	NM_005345 NM_005346	2.59	0.07	17%	6%	HSP71_HUMAN	87.591	12.214	113.858	5.948	0.769	0.043
G6PD	2539	Glucose-6-phosphate 1-dehydrogenase**	NM_000402	1.02	0.08	8%	6%	G6PD_HUMAN	80.836	16.641	121.330	10.229	0.666	0.035
GSTP1	2950	Glutathione S-transferase P	NM_000852	1.16	0.04	5%	4%	GSTP1_HUMAN	65.268	7.174	85.964	20.885	0.759	0.190
CCT2	10576	T-complex protein 1 subunit beta	NM_006431	1.19	0.03	3%	2%	TCPB_HUMAN	104.714	6.378	119.187	12.088	0.879	0.267
TXNRD1	7296	Thioredoxin reductase 1, cytoplasmic	NM_001093771 NM_003330 NM_182729 NM_182742 NM_182743	1.47	0.12	17%	6%	TRXR1_HUMAN	104.714	6.378	119.187	12.088	0.879	0.267
G6PD	2539	Glucose-6-phosphate 1-dehydrogenase***	NM_000402	1.02	0.08	8%	6%	G6PD_HUMAN	85.848	8.356	124.140	5.506	0.692	0.005
HSPB1	3315	Heat shock protein beta-1	NM_001540	1.32	0.13	17%	4%	HSPB1_HUMAN	69.930	23.921	86.813	8.060	0.806	0.258
NME1	4830	Nucleoside diphosphate kinase A	NM_000269 NM_198175	1.14	0.08	9%	8%	NDKA_HUMAN	59.789	20.657	144.627	66.411	0.413	0.283
Decreased gene expression (transcriptomics ratio < 1)														
CCT7	10574	T-complex protein 1 subunit eta	NM_006429	0.81	0.04	3%	2%	TCPH_HUMAN	95.381	7.459	95.731	10.280	0.996	0.969
PSMA2	5683	Proteasome subunit alpha type-2	NM_002787	0.69	0.15	10%	4%	PSA2_HUMAN	116.477	11.780	148.569	14.466	0.784	0.150
FKBP1A	2280	Peptidyl-prolyl cis-trans-isomerase FKBP1A	NM_054014	0.65	0.26	17%	15%	FKB1A_HUMAN	473.565	141.421	65245.936	99.946	0.007	0.275
PPIA	5478	Peptidyl-prolyl cis-trans-isomerase A***	NM_021130	0.86	0.04	4%	6%	PPIA_HUMAN	60.340	16.561	121.603	9.785	0.496	0.005
PCNA	5111	Proliferating cell nuclear antigen***	NM_002592 NM_182649	0.46	0.26	12%	7%	PCNA_HUMAN	87.296	8.040	123.909	6.426	0.705	0.008
HADHA	3030	Trifunctional enzyme subunit alpha, mitochondrial	NM_000182	0.85	0.05	4%	5%	ECHA_HUMAN	85.564	23.723	90.073	12.598	0.950	0.798

Table 1: Continued.

Gene name	Gene ID	Protein name	RefSeq	Transcriptomics data Heat/filter				SwissProt entry name	Proteomics data Heat		Filter		Heat/filter	
				Mean ratio[(1)]	SD[(2)]	CV[(3)]	Chip CV[(4)]		Mean spot volume[(5)]	SD[(6)]	Mean spot volume[(5)]	SD[(6)]	Ratio[(7)]	p value[(8)]
PPIA	5478	Peptidyl-prolyl cis-trans-isomerase A***	NM_021130	0.86	0.04	4%	6%	PPIA_HUMAN	62.919	11.686	115.738	10.498	0.544	0.006
PSMD4	5710	26S proteasome non-ATPase regulatory subunit 4***	NM_002810 NR_002319	0.74	0.09	7%	8%	PSMD4_HUMAN	85.455	14.214	148.812	10.063	0.574	0.010
HSPD1	3329	60 kDa heat shock protein, mitochondrial***	NM_002156 NM_199440	0.82	0.06	5%	3%	CH60_HUMAN	101.423	11.218	170.552	7.472	0.595	0.005
HSP90B1	7184	Endoplasmin	NM_003299	0.59	0.19	11%	5%	ENPL_HUMAN	92.818	33.376	93.651	22.914	0.991	0.977
HSPA4	3308	Heat shock 70 kDa protein 4	NM_002154	0.68			4%	HSP74_HUMAN	123.829	30.682	141.986	16.324	0.872	0.595

Proteins and transcripts, which could be mapped and analyzed by both proteomics by 2D-DIGE combined with MS protein identification and topic defined mRNA expression microarray analysis (Miltenyi PIQOR toxicology array). [(1)]Ratio: fold-change of mRNA expression of cells treated with H-PDF versus cells treated with F-PDF as obtained from the PIQOR microarray service. [(2)]Standard deviation of mRNA expression ratios of cells treated with H-PDF versus cells treated with F-PDF. [(3)]Coefficient variation: relative standard deviation in percent of mRNA expression ratios of cells treated with H-PDF versus cells treated with F-PDF. [(4)]Chip CV: the column contains the relative standard deviation in percent for the respective rRNA by the number of multiple features on the microarray ($n = 4$) as obtained from the PIQOR microarray service. [(5)]Mean spot volume: mean of the spot quantification data over the biological replicates within the given groups. [(6)]Standard deviation of the spot quantification data within the given groups. [(7)]Ratio: fold-change of protein spot abundance in cells treated with H-PDF versus cells treated with F-PDF as obtained from 2D-DIGE analysis. [(8)]The column contains the p value of the t-test comparing relative spot abundance of cells treated with H-PDF versus cells treated with F-PDF. Protein quantifications, reaching the according levels of statistical significance, are marked with asterisks ($^{*}p < 0.1$, $^{**}p < 0.05$, and $^{***}p < 0.01$) after the protein name.

with the primary murine antibody against Hsp72 (SPA-810, Stressgen/Assay Designs, Ann Arbor, MI, USA), Hsp27 (SPA-801, Stressgen/Assay Designs), or Hsp60 (SPA-806 Stressgen/Assay designs) dissolved in TBST containing 1% dry milk for 6 hours. After washing 3 times for 20 min in TBST and incubation with a secondary, peroxidase-coupled antibody (polyclonal rabbit anti-mouse Ig/HRP P0260, Dako Cytomation, Carpinteria, CA, USA) detection was accomplished by using enhanced chemiluminescence solution (Western Lightning Reagent, Perkin Elmer, Boston, MA, USA) and a ChemiDoc XRS chemiluminescence detection system (Bio-Rad).

3. Results

Exposure to H-PDF and F-PDF resulted in sublethal injury, evaluated by indiscernible cell density, assessed by light microscopy and cell counting, and comparable total protein concentrations of the cell lysates (H-PDF/F-PDF 76.6 ± 36.7% mean ± SD, $p = 0.338$). LDH release as a marker of loss of cellular membrane integrity was significantly higher following exposure to H-PDF than to F-PDF (H-PDF/F-PDF 887 ± 277% mean ± SD, $p = 0.011$).

For investigating potentially involved regulatory mechanisms both protein and RNA levels of HPMC undergoing treatment with H-PDF or F-PDF for 24 h were analyzed by 2D-DIGE and topic defined gene expression microarrays. In order to cover the largest possible number of transcripts and proteins we used all available mass spectrometric protein identifications in MC performed by our group until today [18, 22] and built a comprehensive 2D proteome map (see Supplemental Figure 1 and Supplemental Table 1). These identifications were screened for overlaps with the transcripts successfully quantified in the mRNA microarray. Of the 1264 genes contained on the microarray and the overall 185 protein identifications in mesothelial cells by mass spectrometry we could identify an overlap of 28 unique genes with the according proteins contained in 38 distinct spots (see Table 1, Supplemental Figure 2, and Supplemental Figure 3). The high reproducibility of the proteomics data obtained by 2D-DIGE was reflected by a low variability of the quantified spots (median CV was 9.7% for all protein spots contained in Table 1). The observation of more than one spot per protein is explained by the capability of this technique to detect individual isoforms or posttranslationally modified variants of the same protein. Exploration of the combined RNA and protein profiles allowed functional grouping of the analyzed candidates according to observed regulation patterns.

When grouping these protein spots according to their expression on the protein and RNA level by calculation of a H-PDF/F-PDF ratio, four discrete groups could be built (see Figure 1). Thirteen spots had a protein ratio below 1.0, meaning less protein abundance when exposed to H-PDF, whereas their RNA ratio was above 1.0. Seven of these spots (54%) contained HSP (protein symbols: HSPA9, HSPA1A, HSPA8, HSPA1A, HSPA8, HSPA1A, G6PD, GSTP1, CCT2, TXNRD1, G6PD, HSPB1, and NME1). Six protein spots showed a protein ratio above 1.0 with simultaneously elevated RNA expression (>1.0). Two of these spots contained

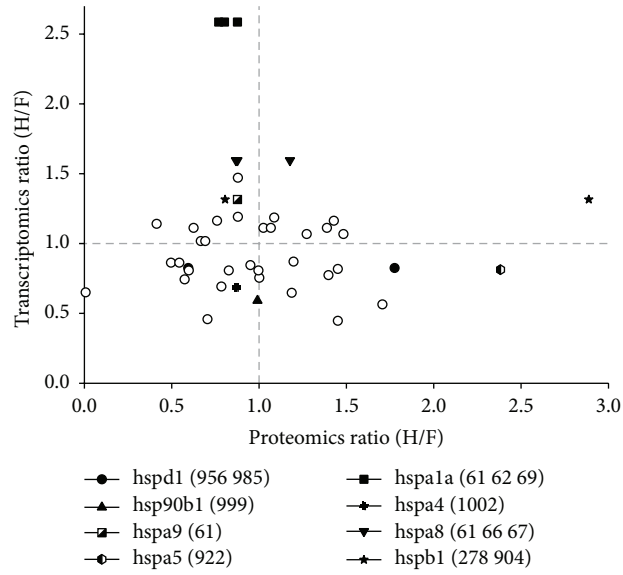

Figure 1: Cross-omics comparison of stress responses in mesothelial cells exposed to heat-versus filter-sterilized peritoneal dialysis fluid. HPMC cultures ($n = 3$) were continuously exposed to a 1 : 1 mix of heat- or filter-sterilized PDF ("H" or "F") and cell culture medium for 24 hours. Data are expressed as ratio of the respective proteomics and transcriptomics results from heat- over those of filter-sterilized PDF exposed mesothelial cells (H/F). The comparison of proteomics and transcriptomics data allowed the discrimination of differentially regulated protein expression into groups depending on correlating or noncorrelating transcripts. The inadequate expression of several HSP (full symbols) on the protein level is not reflected on the transcriptional level indicating potential interference of GDPs in translational activity and regulation.

HSP (HSPA8, HSPB1, GSTP1, GSR, PDIA3, and PDIA3). However, other protein isoforms of these two HSP (HSPA8, HSPB1) were also contained in the previously mentioned group. Eight protein spots showed higher abundance on the protein level although their RNA expression ratio was below 1.0. Two of these spots contained HSP (CCT5, PSMB2, HSPA5, P4HB, PDIA6, COPS4, HSPD1, and RPSA). Eleven protein spots had a H-PDF/F-PDF ratio of less than 1.0 with concomitantly downregulated RNA expression. Three of these spots contained HSP (CCT7, PSMA2, FKBP1A, PPIA, PCNA, HADHA, PPIA, PSMD4, HSPD1, HSP90B1, and HSPA4). In addition to the graphical presentation in Figure 1, numerical values of RNA expression ratios as well as spot abundance data under the experimental conditions of extended heat- versus filter-sterilized PDF treatment are given in Table 1 together with their statistical parameters and p values indicating significant changes. Additional bioinformatics analysis of the transcriptomics data only found enrichment of biological processes attributable to immune response, angiogenesis, injury/repair mechanism, and apoptosis (see Supplemental Table 2).

In Figure 2, results of 2D western blotting are shown for the protein spots of prototypical members of the major HSP families, that is, Hsp72 (HSPA1A), Hsp27 (HSPB1), and Hsp60 (HSPD1), demonstrating that the mass spectrometric

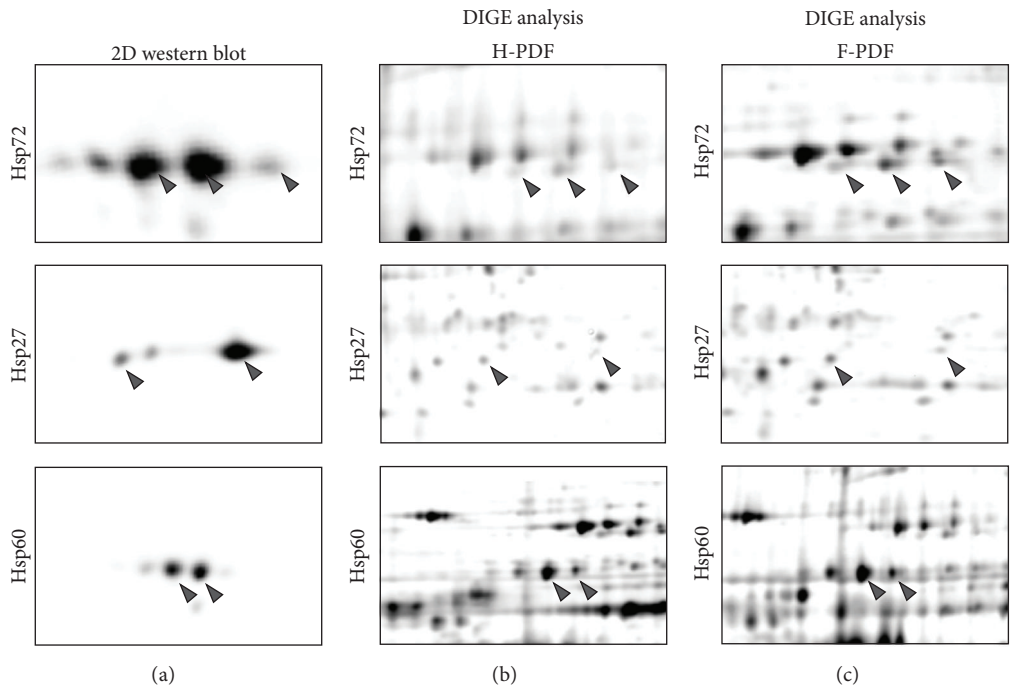

Figure 2: Two-dimensional western analysis of the chaperones Hsp70, Hsp27, and Hsp60. (a) shows the result of the immunoblots with positive signals for the respective specific antibodies given in each line and the MS identified protein spots indicated by grey arrow heads. For immunodetection of all relevant spots, pooled samples were used in order to represent all relevant isoforms and modifications. (b, c) show the identical regions in the DIGE gels, where the middle panel shows the protein separation of total cell extracts from mesothelial cells following exposure to H-PDF, and (c) shows the protein separation of total cell extracts from mesothelial cells following exposure to F-PDF. Again the MS identified protein spots are indicated by grey arrow heads.

data on protein identities might not cover all isoforms that are recognized by specific antibodies. Whereas the antibody-based detection might yield unspecific signals, the spot identities that were confirmed by both western blotting and mass spectrometric data represent very robust information.

4. Discussion

Comparing the effects of two PDF that only differ in their modality of sterilization, either by heat or by filtration, can be regarded as surrogate method to evaluate the effects of GDPs formed through heat-sterilization [23]. Specific effects of heat-sterilized PDF on the cellular stress response might thus be largely attributed to these toxic compounds. GDPs are known to mediate their cytotoxicity via oxidative stress, and recent research suggests that oxidative stress might dampen the cellular stress responses [14, 15].

The advent of omics technologies, such as gel- or mass spectrometry-based proteomics of the protein level and microarray techniques on the transcriptional level, allowed unbiased global analyses, searching for yet unknown differentially regulated proteins or transcripts under given experimental conditions.

Whereas the use of a single analytical level allows candidate search and functional interpretation based on common features, for example, characterized in gene ontology databases, the cross-omics approach allows generating hypotheses by comparing gene expression profiling to (functional active) protein abundances. In this study we used a topic defined mRNA microarray for toxicology relevant genes, provided by Miltenyi as the PIQOR platform. In contrast to quantification of mRNA levels by rt-PCR, which relies on the consistency of single housekeeping genes, the array technique allows more elaborate approaches of normalization.

Together with our proteomics platform based on 2D-DIGE we compared effects of heat- versus filter-sterilized PDF in mesothelial cells in the extended exposure model, for proteins identified by mass spectrometry in earlier *in vitro* PD studies.

The high relevance of the chosen candidate proteins and transcripts becomes evident by the considerable overlap of MS identified proteins and genes represented on the PIQOR array in experimental PD. We could therefore use this set, mainly consisting of chaperones and stress-relevant proteins involved in detoxification and protein homeostasis, to search for global systematic effects of heat- versus filter-sterilized PDF on the cellular stress response. In recent work, we have shown at the protein level that expression levels of such a stress proteome can be related to mesothelial cell susceptibility to PDF induced injury [24]. This stress proteome was found to be downregulated following exposure to heat-sterilized PDF and could be restored by addition of cytoprotective additives, such as alanyl-glutamine dipeptide [24]. The cross-omics approach used in the current study gives additional information beyond the observed inadequate induction of the heat shock response at the protein level [7, 24].

In our dataset a rather large group of candidates showed a protein abundance ratio below 1.0 (downregulated by H-PDF compared to F-PDF) and at the same time an mRNA expression ratio above 1.0 (upregulated by H-PDF compared to F-PDF), when the two fluid types were compared. This phenomenon is of growing interest in the omics-field, as the observed perturbations might allow deducing regulatory mechanisms [25]. Future studies are needed to investigate whether the reverse relationship of protein and mRNA indicates a higher degree of protein turnover (i.e., shortened half-life of the protein by increased degradation) or translational inhibition or posttranslational modifications [26, 27]. This group contains many HSP but the effect only reached the level of significance for the proteins Hsp72 (HSPA1A) and glucose-6-phosphate dehydrogenase (G6PD), which might be due to inherent limited power of these hypotheses-generating omics studies. HSP are molecular chaperones and known to incorporate transport and folding of other proteins by binding to hydrophobic normal hidden domains of immature or denatured proteins. Thereby, these proteins have been shown to promote cytoskeletal repair and preserve the mesothelial monolayer [5, 6]. Whereas G6PD was already found upregulated in the acute exposure model in an earlier study [28] this key-enzyme of the pentose phosphate pathway, which is substantial for the production of NADPH and the cell's resistance to oxidative stress [29, 30], is significantly downregulated by heat-sterilized PDF compared to filter-sterilized PDF after extended exposure. The initial observation that the cells are not able to adequately respond to stress mediated by toxic factors of PDF, such as glucose and GDPs, is further reflected by the fact that all candidates in the dataset belonging to the glutathione system (GSTP1, TXNRD1, and GSR), which is dedicated to detoxification and neutralization of reactive oxygen species, are found to be upregulated on the transcriptional level. However, none of these candidates show significant upregulation of protein abundance. The deleterious effect of the cooccurrence of hyperglycemia, toxic aldehydes, such as GDPs, and a lack of reductive power (e.g., by NADPH and glutathione) has been demonstrated extensively in the diabetes model and beyond [31–33].

Two further subgroups of our dataset were characterized by either simultaneously increased or decreased abundance of both protein and mRNA. Concurrent regulation of protein and mRNA likely indicates undisturbed translation of transcriptional regulation of gene expression into proteins.

One clearly upregulated player identified in our study is PDIA3, a protein disulfide-isomerase predominantly found in the endoplasmic reticulum lumen, which is involved in the unfolded protein response [34]. Interestingly, knockdown of PDIA3, also known as endoplasmic reticulum resident protein 57 or 58 kDa glucose-regulated protein, protected against tunicamycin-induced apoptosis, with associated induction of the 78 kDa glucose-regulated protein (GRP-78, BiP, and HSPA5) [35], which was identified as downregulated on the transcriptional level but upregulated on the protein level in our study. GRP-78 is an ER stress protein (glucose-regulated protein) and, as suggested by its name, expected to be upregulated by the physicochemical properties of PDF.

Another protein found with significantly higher abundance, when H-PDF was compared to F-PDF, was Hsp27 (HSPB1) which is well known to be involved in the stress response to PDF [3, 4]. Hsp27 is a highly abundant effector of the heat shock response directly interacting with the actin cytoskeleton and thereby protecting mesothelial cell integrity by increased abundance [36]. However, it is well known that Hsp27 is extensively modified by phosphorylation leading to reciprocal abundance changes of multiple spots on 2D gels [36, 37]. Indeed we also identified Hsp27 in a spot with lowered abundance, as can be better made evident by direct comparison between 2D proteomic gels and 2D western analysis. As the phosphorylation status is functionally highly relevant for its chaperoning effect, Hsp27 is a particularly informative candidate to demonstrate the role of posttranslational modification on the level of functionally active protein isoforms versus total protein abundance and gene expression.

One clearly downregulated player, on the protein level as well as on the transcriptional level, identified in our study is PPIA which is a peptidyl-prolyl cis-trans-isomerase and is thereby active in protein folding [38]. PPIA is also a member of the immunophilin family (cyclophilin A) [39] and the receptor for the immunosuppressive drugs tacrolimus and cyclosporine [40, 41]. Other examples for proteins with significantly downregulated transcripts were the important ER chaperone Hsp60 (HSPD1), which was as Hsp27 also found in a significantly upregulated spot, and the proliferating cell nuclear antigen (PCNA), which is also known as cyclin, reflecting an increase in MC proliferation as previously described in the *in vivo* setting [42].

A small group of candidates showed a protein abundance ratio above 1.0 (upregulated by H-PDF compared to F-PDF) and at the same time an mRNA expression ratio below 1.0 (downregulated by H-PDF compared to F-PDF), when the two fluid types were compared. In this case the increased levels of protein expression with concomitantly depressed transcription of the same genes allow generating interesting hypotheses, such as prolonged half-life of the proteins by decreased degradation, possibly mediated by lack of protein degrading mechanisms such as the ubiquitin-proteasome pathway [26].

Interestingly all identified members associated with the ubiquitin-proteasome pathway (PSMB2, COPS4, PSMA2, and PSMD4) showed downregulated levels of mRNA and one of them was also significantly lower abundant on the protein level. This effect is concordant with the literature, where hyperglycemia and methylglyoxal led to an impaired ubiquitin-proteasome pathway in bovine and murine endothelial cells [32]. Indeed methylglyoxal is one of the GDPs detected in considerable concentrations in conventional PDF [43]. In this study nonuremic patients were used to obtain primary mesothelial cells from omentum. It has been demonstrated before that the uremic milieu per se can change the behavior of the mesothelial cells. Thus, future studies are needed to investigate whether specific GDPs in PDF might impair or deplete this essential part of the cellular stress response and what the role of the uremic milieu with even more toxic small molecules might be [44, 45].

Our data show that under stressful conditions the correlation between mRNA and protein cannot be regarded as linear for a wide range of tightly involved players of the stress response. The transcription of mRNA is the initial level of gene regulation, where transcription factors lead to situation-dependent usage of genetic sequence. However a plethora of intermitting mechanisms, such as RNA interference, regulatory proteins, or translational efficiency, can promote or hinder cellular protein production. Finally the amounts of functional proteins are influenced by protein folding, posttranslational modification, and turnover [26, 27]. Albeit the observed changes on the protein level are quite low, they are in a reasonable biological range, given that the proteins that can be detected by 2D gel electrophoresis represent the most abundant portion of soluble proteins. These findings highlight the limitations of gene expression profiling concerning the prediction of abundance of functionally active proteins and/or their isoforms. Future studies need to carefully assess these regulatory mechanisms to monitor the abundance of effector proteins that ultimately reflect biological reality.

Bioinformatics analysis yields similar information on activated stress responses using data derived from this transcriptomics dataset as we have previously reported in a proteomics approach [22]. Direct comparison between these "omics" technologies at the level of individual gene products, however, as we performed in our cross-omics approach, might allow additional interesting insights into specific pathogenic processes caused by PDF exposure. Moreover, the results of the current study underline that information of potential diagnostic (such as biomarker candidates) and/or therapeutic (such as novel drug targets) implications derived from proteomics and/or transcriptomics findings cannot be utilized interchangeably but rather request specific separate analysis and interpretation.

Taken together, the comparison of proteomics and transcriptomics data allowed the discrimination of differentially regulated protein expression according to correlating or noncorrelating transcripts. The results of this study are particularly interesting in terms of limitations of gene expression profiling with regard to prediction of abundance of functionally active proteins, indicating the need for future studies to investigate potential interference in translational activity and regulation.

Conflict of Interests

Klaus Kratochwill, Anton M. Lichtenauer, Rebecca Herzog, and Katarzyna Bialas are employees of Zytoprotec GmbH. Christoph Aufricht is cofounder of Zytoprotec GmbH, a spin-off of the Medical University of Vienna that holds the patent "Carbohydrate-Based Peritoneal Dialysis Fluid Comprising Glutamine Residue" (International Publication no. WO 2008/106702 A1). Thorsten O. Bender is a recipient of an EMBO (ERA-EDTA) stipend. Achim Jörres is consultant to Fresenius Medical Care.

Authors' Contribution

Klaus Kratochwill and Thorsten O. Bender contributed equally to this work.

Acknowledgments

This study was funded by the ZIT, the Technology Agency of the City of Vienna (ID 648625). Klaus Kratochwill, Silvia Tarantino, Katarzyna Bialas, Achim Jörres, and Christoph Aufricht were supported by the European Training and Research in Peritoneal Dialysis (EuTRiPD) program, a project funded by the European Union within the Marie Curie scheme (287813). The authors are grateful for the technical support by Astrid Scherr and Axana Hellmann in preparing the paper and figures.

References

[1] O. Devuyst, N. Topley, and J. D. Williams, "Morphological and functional changes in the dialysed peritoneal cavity: impact of more biocompatible solutions," *Nephrology Dialysis Transplantation*, vol. 17, supplement 3, pp. 12–15, 2002.

[2] A. Jorres and J. Witowski, "Lessons from basic research for PD treatment," *Peritoneal Dialysis International*, vol. 25, supplement 3, pp. S35–S38, 2005.

[3] K. Arbeiter, B. Bidmon, M. Endemann et al., "Peritoneal dialysate fluid composition determines heat shock protein expression patterns in human mesothelial cells," *Kidney International*, vol. 60, no. 5, pp. 1930–1937, 2001.

[4] C. Aufricht, M. Endemann, B. Bidmon et al., "Peritoneal dialysis fluids induce the stress response in human mesothelial cells," *Peritoneal Dialysis International*, vol. 21, no. 1, pp. 85–88, 2001.

[5] B. Bidmon, M. Endemann, K. Arbeiter et al., "Overexpression of HSP-72 confers cytoprotection in experimental peritoneal dialysis," *Kidney International*, vol. 66, no. 6, pp. 2300–2307, 2004.

[6] M. Endemann, H. Bergmeister, B. Bidmon et al., "Evidence for HSP-mediated cytoskeletal stabilization in mesothelial cells during acute experimental peritoneal dialysis," *American Journal of Physiology—Renal Physiology*, vol. 292, no. 1, pp. F47–F56, 2007.

[7] T. O. Bender, M. Böhm, K. Kratochwill et al., "Peritoneal dialysis fluids can alter HSP expression in human peritoneal mesothelial cells," *Nephrology Dialysis Transplantation*, vol. 26, no. 3, pp. 1046–1052, 2011.

[8] N. Topley, "What is the ideal technique for testing the biocompatibility of peritoneal dialysis solutions?" *Peritoneal Dialysis International*, vol. 15, no. 6, pp. 205–209, 1995.

[9] X. L. Zhang, N. Topley, T. Ito, and A. Phillips, "Interleukin-6 regulation of transforming growth factor (TGF)-β receptor compartmentalization and turnover enhances TGF-β1 signaling," *Journal of Biological Chemistry*, vol. 280, no. 13, pp. 12239–12245, 2005.

[10] C. J. Holmes, "Pre-clinical biocompatibility testing of peritoneal dialysis solutions," *Peritoneal Dialysis International*, vol. 20, supplement 5, pp. S5–S9, 2001.

[11] M. Erixon, T. Lindén, P. Kjellstrand et al., "PD fluids contain high concentrations of cytotoxic GDPs directly after sterilization," *Peritoneal Dialysis International*, vol. 24, no. 4, pp. 392–398, 2004.

[12] M. Erixon, A. Wieslander, T. Lindén et al., "How to avoid glucose degradation products in peritoneal dialysis fluids," *Peritoneal Dialysis International*, vol. 26, no. 4, pp. 490–497, 2006.

[13] A. Jörres, T. O. Bender, and J. Witowski, "Glucose degradation products and the peritoneal mesothelium," *Peritoneal Dialysis International*, vol. 20, supplement 5, pp. S19–S22, 2001.

[14] P. L. Hooper and J. J. Hooper, "Loss of defense against stress: diabetes and heat shock proteins," *Diabetes Technology and Therapeutics*, vol. 7, no. 1, pp. 204–208, 2005.

[15] M. Adachi, Y. Liu, K. Fujii et al., "Oxidative stress impairs the heat stress response and delays unfolded protein recovery," *PLoS ONE*, vol. 4, no. 11, Article ID e7719, 2009.

[16] E. Stylianou, L. A. Jenner, M. Davies, G. A. Coles, and J. D. Williams, "Isolation, culture and characterization of human peritoneal mesothelial cells," *Kidney International*, vol. 37, no. 6, pp. 1563–1570, 1990.

[17] K. Książek, K. Piwocka, A. Brzezińska et al., "Early loss of proliferative potential of human peritoneal mesothelial cells in culture: the role of p16INK4a-mediated premature senescence," *Journal of Applied Physiology*, vol. 100, no. 3, pp. 988–995, 2006.

[18] K. Kratochwill, M. Lechner, A. M. Lichtenauer et al., "Interleukin-1 receptor-mediated inflammation impairs the heat shock response of human mesothelial cells," *The American Journal of Pathology*, vol. 178, no. 4, pp. 1544–1555, 2011.

[19] The-UniProt-Consortium, "The universal protein resource (UniProt)," *Nucleic Acids Research*, vol. 36, pp. D190–D195, 2008.

[20] A. M. Lichtenauer, R. Herzog, S. Tarantino, C. Aufricht, and K. Kratochwill, "Equalizer technology followed by DIGE-based proteomics for detection of cellular proteins in artificial peritoneal dialysis effluents," *Electrophoresis*, vol. 35, no. 10, pp. 1387–1394, 2014.

[21] T. Rabilloud, J.-M. Strub, S. Luche, A. van Dorsselaer, and J. Lunardi, "A comparison between Sypro Ruby and ruthenium II tris (bathophenanthroline disulfonate) as fluorescent stains for protein detection in gels," *Proteomics*, vol. 1, no. 5, pp. 699–704, 2001.

[22] K. Kratochwill, M. Lechner, C. Siehs et al., "Stress responses and conditioning effects in mesothelial cells exposed to peritoneal dialysis fluid," *Journal of Proteome Research*, vol. 8, no. 4, pp. 1731–1747, 2009.

[23] A. Wieslander, T. Linden, and P. Kjellstrand, "Glucose degradation products in peritoneal dialysis fluids: how they can be avoided," *Peritoneal Dialysis International*, vol. 21, 3, pp. S119–S124, 2001.

[24] K. Kratochwill, M. Boehm, R. Herzog et al., "Alanyl-glutamine dipeptide restores the cytoprotective stress proteome of mesothelial cells exposed to peritoneal dialysis fluids," *Nephrology Dialysis Transplantation*, vol. 27, no. 3, pp. 937–946, 2012.

[25] S. P. Gygi, Y. Rochon, B. R. Franza, and R. Aebersold, "Correlation between protein and mRNA abundance in yeast," *Molecular and Cellular Biology*, vol. 19, no. 3, pp. 1720–1730, 1999.

[26] T. Maier, M. Güell, and L. Serrano, "Correlation of mRNA and protein in complex biological samples," *FEBS Letters*, vol. 583, no. 24, pp. 3966–3973, 2009.

[27] R. Herzog, T. O. Bender, A. Vychytil, K. Bialas, C. Aufricht, and K. Kratochwill, "Dynamic O-linked N-acetylglucosamine modification of proteins affects stress responses and survival of mesothelial cells exposed to peritoneal dialysis fluids," *Journal of the American Society of Nephrology*, vol. 25, no. 12, pp. 2778–2788, 2014.

[28] M. Lechner, K. Kratochwill, A. Lichtenauer et al., "A proteomic view on the role of glucose in peritoneal dialysis," *Journal of Proteome Research*, vol. 9, no. 5, pp. 2472–2479, 2010.

[29] M. V. Ursini, A. Parrella, G. Rosa, S. Salzano, and G. Martini, "Enhanced expression of glucose-6-phosphate dehydrogenase in human cells sustaining oxidative stress," *Biochemical Journal*, vol. 323, no. 3, pp. 801–806, 1997.

[30] W.-N. Tian, L. D. Braunstein, K. Apse et al., "Importance of glucose-6-phosphate dehydrogenase activity in cell death," *The American Journal of Physiology—Cell Physiology*, vol. 276, no. 5, pp. C1121–C1131, 1999.

[31] M. Brownlee, "Biochemistry and molecular cell biology of diabetic complications," *Nature*, vol. 414, no. 6865, pp. 813–820, 2001.

[32] M. A. Queisser, D. Yao, S. Geisler et al., "Hyperglycemia impairs proteasome function by methylglyoxal," *Diabetes*, vol. 59, no. 3, pp. 670–678, 2010.

[33] F. Salvemini, A. Franzé, A. Iervolino, S. Filosa, S. Salzano, and M. V. Ursini, "Enhanced glutathione levels and oxidoresistance mediated by increased glucose-6-phosphate dehydrogenase expression," *The Journal of Biological Chemistry*, vol. 274, no. 5, pp. 2750–2757, 1999.

[34] M. Ni and A. S. Lee, "ER chaperones in mammalian development and human diseases," *FEBS Letters*, vol. 581, no. 19, pp. 3641–3651, 2007.

[35] D. Xu, R. E. Perez, M. H. Rezaiekhaligh, M. Bourdi, and W. E. Truog, "Knockdown of ERp57 increases BiP/GRP78 induction and protects against hyperoxia and tunicamycin-induced apoptosis," *The American Journal of Physiology—Lung Cellular and Molecular Physiology*, vol. 297, no. 1, pp. L44–L51, 2009.

[36] A.-P. Arrigo, W. J. J. Firdaus, G. Mellier et al., "Cytotoxic effects induced by oxidative stress in cultured mammalian cells and protection provided by Hsp27 expression," *Methods*, vol. 35, no. 2, pp. 126–138, 2005.

[37] A. L. Bryantsev, S. Y. Kurchashova, S. A. Golyshev et al., "Regulation of stress-induced intracellular sorting and chaperone function of Hsp27 (HspB1) in mammalian cells," *Biochemical Journal*, vol. 407, no. 3, pp. 407–417, 2007.

[38] J. L. Kofron, P. V. Kuzmic, E. Kishore, E. Colon-Bonilla, and D. H. Rich, "Determination of kinetic constants for peptidyl prolyl cis-trans isomerases by an improved spectrophotometric assay," *Biochemistry*, vol. 30, no. 25, pp. 6127–6134, 1991.

[39] A. Galat, "Peptidylproline cis-trans-isomerases: immunophilins," *European Journal of Biochemistry*, vol. 216, no. 3, pp. 689–707, 1993.

[40] D. A. Fruman, P. E. Mather, S. J. Burakoff, and B. E. Bierer, "Correlation of calcineurin phosphatase activity and programmed cell death in murine T cell hybridomas," *European Journal of Immunology*, vol. 22, no. 10, pp. 2513–2517, 1992.

[41] J. Liu, J. O. Farmer Jr., W. S. Lane, J. Friedman, I. Weissman, and S. L. Schreiber, "Calcineurin is a common target of cyclophilin-cyclosporin A and FKBP-FK506 complexes," *Cell*, vol. 66, no. 4, pp. 807–815, 1991.

[42] L. Gotloib, A. Shostak, V. Wajsbrot, and R. Kushnier, "High glucose induces a hypertrophic, senescent mesothelial cell phenotype after long in vivo exposure," *Nephron*, vol. 82, no. 2, pp. 164–173, 1999.

[43] J. Witowski, A. Jörres, K. Korybalska et al., "Glucose degradation products in peritoneal dialysis fluids: do they harm?" *Kidney International, Supplement*, vol. 63, no. 84, pp. S148–S151, 2003.

[44] J. D. Williams, K. J. Craig, N. Topley et al., "Morphologic changes in the peritoneal membrane of patients with renal disease," *Journal of the American Society of Nephrology*, vol. 13, no. 2, pp. 470–479, 2002.

[45] M. N. Schilte, J. W. A. M. Celie, P. M. Ter Wee, R. H. J. Beelen, and J. van den Born, "Factors contributing to peritoneal tissue remodeling in peritoneal dialysis," *Peritoneal Dialysis International*, vol. 29, no. 6, pp. 605–617, 2009.

Hindawi Publishing Corporation
BioMed Research International
Volume 2015, Article ID 595030, 12 pages
http://dx.doi.org/10.1155/2015/595030

Research Article

Vitamin D Can Ameliorate Chlorhexidine Gluconate-Induced Peritoneal Fibrosis and Functional Deterioration through the Inhibition of Epithelial-to-Mesenchymal Transition of Mesothelial Cells

Yi-Che Lee,[1,2] Shih-Yuan Hung,[1,3] Hung-Hsiang Liou,[4] Tsun-Mei Lin,[5] Chu-Hung Tsai,[2] Sheng-Hsiang Lin,[2] Yau-Sheng Tsai,[2] Min-Yu Chang,[1] Hsi-Hao Wang,[1] Li-Chun Ho,[1,2] Yi-Ting Chen,[1] Ching-Fang Wu,[1] Ho-Ching Chen,[1] Hsin-Pao Chen,[6] Kuang-Wen Liu,[6] Chih-I. Chen,[6] Kuan Min She,[6] Hao-Kuang Wang,[7] Chi-Wei Lin,[8] and Yuan-Yow Chiou[2,9]

[1]*Division of Nephrology, Department of Internal Medicine, E-DA Hospital, I-Shou University, Kaohsiung, Taiwan*
[2]*Institute of Clinical Medicine, National Cheng Kung University, Tainan, Taiwan*
[3]*School of Medicine for International Students, I-Shou University, Kaohsiung, Taiwan*
[4]*Division of Nephrology, Department of Medicine, Hsin-Jen Hospital, New Taipei City, Taiwan*
[5]*Department of Laboratory Medicine, E-DA Hospital, I-Shou University, Kaohsiung, Taiwan*
[6]*Division of Colorectal Surgery, Department of Surgery, E-DA Hospital, I-Shou University, Kaohsiung, Taiwan*
[7]*Department of Neurosurgery, E-DA Hospital, I-Shou University, Kaohsiung, Taiwan*
[8]*Department of Medical Education, I-Shou University, Kaohsiung, Taiwan*
[9]*Department of Pediatrics, National Cheng Kung University Hospital, Tainan, Taiwan*

Correspondence should be addressed to Yuan-Yow Chiou; yuanyow@mail.ncku.edu.tw

Received 29 March 2015; Accepted 12 July 2015

Academic Editor: Robert Beelen

Background. Peritoneal dialysis (PD) can induce fibrosis and functional alterations in PD patients' peritoneal membranes, due to long-term unphysiological dialysate exposure, partially occurring via triggering of epithelial-to-mesenchymal transition (EMT) in peritoneal mesothelial cells (MCs). Vitamin D can ameliorate these negative effects; however, the mechanism remains unexplored. Therefore, we investigated its possible links to MCs EMT inhibition. *Methods*. Peritoneal fibrosis was established in Sprague-Dawley rats by chlorhexidine gluconate (CG) intraperitoneal injection for 21 days, with and without $1\alpha,25(OH)_2D_3$ treatment. Morphological and functional evaluation and western blot analysis of EMT marker were performed upon peritoneum tissue. *In vitro* study was also performed in a primary human peritoneal MC culture system; MCs were incubated with transforming growth factor-β1 (TGF-β1) in the absence or presence of $1\alpha,25(OH)_2D_3$. EMT marker expression, migration activities, and cytoskeleton redistribution of MCs were determined. *Results*. $1\alpha,25(OH)_2D_3$ ameliorated CG-induced morphological and functional deterioration in animal model, along with CG-induced upregulation of α-SMA and downregulation of E-cadherin expression. Meanwhile, $1\alpha,25(OH)_2D_3$ also ameliorated TGF-β1-induced decrease in E-cadherin expression, increase in Snai1 and α-SMA expression, intracellular F-actin redistribution, and migration activity *in vitro*. *Conclusion*. $1\alpha,25(OH)_2D_3$ can ameliorate CG-induced peritoneal fibrosis and attenuate functional deterioration through inhibiting MC EMT.

1. Introduction

Peritoneal dialysis (PD) has become an important renal replacement therapy in recent decades in end-stage renal disease (ESRD) patients as hemodialysis (HD) [1–4]. However, the biggest limitation of PD therapy is that many patients have to shift to HD after several years due to treatment failure [5–9]. This failure is mainly attributed to inadequate dialysis, recurrent peritonitis, or peritoneal fibrosis [5, 6, 10, 11]. Patients' peritonitis rate and solute clearance have

been greatly improved in recent years; however, PD-related peritoneal damage and fibrosis have become a major cause of treatment failure [11–13].

Under PD therapy, conventional bioincompatible dialysate, characterized by possessing acidic PH, hypertonicity, high glucose, and containing lactate, glucose degradation products (GDPs) induce mesothelial cell (MC) injury and promote pathological changes including induction of the epithelial-to-mesenchymal transition (EMT) process [14–16]. Subsequently, the peritoneal membrane undergoes several structural and functional changes, including fibrosis and neoangiogenesis, resulting in the promotion of peritoneal membrane failure [14, 15, 17, 18].

EMT plays a role in PD-related peritoneal membrane morphological and functional alterations [19, 20]. The EMT begins with the downregulation of selected adhesion molecules, such as E-cadherin, and dissociation of the intercellular junctions of MCs. Then, the cell cytoskeleton undergoes reorganization, and MCs acquire mesenchymal markers such as Snail and α-smooth muscle actin (α-SMA) [19]. Through this process, MCs gain higher invasive and migration capacities and promote peritoneal membrane fibrosis and functional changes [21, 22].

Recently, several studies have proven a protective effect of vitamin D against peritoneal fibrosis [23–27]. Furthermore, studies in the field of cancer research also found that vitamin D can ameliorate cancer cell EMT through the promotion of E-cadherin expression [28]. Therefore, in our study we aimed to investigate whether inhibition of the EMT process in MCs plays a role in the protective effects of vitamin D, both *in vitro* and *in vivo*.

2. Materials and Methods

2.1. Human Primary Mesothelial Cells. Omentum-derived MCs were obtained from nonuremic patients undergoing abdominal surgery; the omentum samples were digested in 0.05% trypsin and 0.02% EDTA to isolate MCs [14, 29]. All MCs isolated from the omentum were then incubated in culture medium consisting of Earle M199 medium (Gibco, NY, USA) supplemented with 10% fetal calf serum (Biological Industries, Kibbutz Beit-Haemek, Israel), insulin-transferrin-selenium-sodium pyruvate (ITS-A) (Gibco), 100 μg/mL of streptomycin (MDBio, Inc., Taipei, Taiwan), 63.6 μg/mL of penicillin G (Sigma-Aldrich, MO, USA), and 250 ng/mL Fungizone (MDBio, Inc.).

2.2. In Vitro Study Design. To investigate the effects of vitamin D on MC EMT process, omentum-derived MCs were treated with human recombinant transforming growth factor-β1 1 ng/mL (TGF-β1) (PeproTech, Rehovot, Israel) in culture medium with or without 1α,25(OH)$_2$D$_3$ (10^{-6} mol/L, Sigma-Aldrich), the active form of vitamin D$_3$.

2.3. Flow Cytometry and Immunofluorescence. To validate the purity of isolated MCs, omentum-derived cells were verified by ICAM-1 expression (anti-ICAM-1; eBioscience, CA, USA), determined according to a previously published protocol [14]. To validate changes in the EMT process, phalloidin-labeled staining (Life Technologies, NY, USA) and α-SMA staining (Sigma-Aldrich) were carried out [30]. DAPI staining was conducted for visualization of cell nuclei (Sigma-Aldrich).

2.4. Reverse Transcription-Polymerase Chain Reaction (RT-PCR). Total RNA was extracted by using TRIzol method (Invitrogen, NY, USA) and complementary DNA was subsequently acquired from 1 μg of total RNA by reverse transcription as per the manufacturer's instructions (Bio-Rad, CA, USA). E-cadherin mRNA was amplified by a Light Cycler using an SYBR Green Kit (Bio-Rad) and the specific primer set: 5′-GCATTGCCACATACACTCTCTTCT-3′ and 5′-CATTCTGATCGGTTACCGTGATC-3′. Snail mRNA was amplified using the primers 5′-GCAAATACT-GCAACAAGG-3′ and 5′-GCACTGGTACTTCTTGACA-3′ under similar conditions. GAPDH was amplified using commercially produced primers: 5′-TGAACGGGAAGC-TCACTGG-3′ and 5′-TCCACCACCCTGTTGCTGTA-3′. The annealing temperature used for all targets was 60°C. All samples were normalized to GAPDH.

2.5. Western Blotting for E-Cadherin and Snail. To investigate changes in MC EMT, primary antibodies to the epithelial marker, E-cadherin (mouse anti-E-cadherin, diluted 1 : 500; BD Bioscience, MA, USA), and the mesenchymal marker, Snail (rabbit anti-Snail; diluted 1 : 2000; Cell Signaling Technology Inc., MA, USA), were used [31, 32]. Each of the primary antibody blots was incubated with goat anti-mouse IgG (H+L) secondary antibody-HRP conjugate, diluted 1 : 5000 (Pierce, IL, USA), or goat anti-rabbit IgG (H+L) secondary antibody-HRP conjugate, diluted 1 : 5000 (KPL # 4741516), and visualized using enhanced chemiluminescence (Merck Millipore, Darmstadt, Germany).

2.6. Cell Migration Assay. MCs undergoing EMT show increased migration capacity; therefore, a wound-healing assay was performed to validate the response and change in EMT to 1α,25(OH)$_2$D$_3$. MCs were seeded at a concentration of 5×10^5 in 6 cm culture dish. A scratch was made in the MC cell monolayer using a 200 μL plastic pipette tip. MCs were then washed with PBS to remove the dead cells. The width of cell-free space was measured after the initial scratch at 0, 3, 6, 9, and 12 hours using a microscope (ZEISS; Primo Vert).

2.7. Quantification of α-SMA Positive Cells by Immunofluorescence. The α-SMA positive MCs were measured and expressed as mean ± standard deviation (S.D.). Each treatment group was measured at 10 random sites (magnification ×200) by blinded researchers using microscope analysis with a metric ocular.

2.8. Peritoneal Fibrosis-Model Experimental Protocol. To investigate the protective effects of 1α,25(OH)$_2$D$_3$ on peritoneal fibrosis, a total of 30 male Sprague-Dawley (SD) rats weighing 200 to 250 g were used. In the control group, rats received intraperitoneal (IP) injection of 1 mL/kg PBS in the first 7 days and then 1 mL/kg PBS followed by an additional 2 mL saline IP injection daily for a further 21 days

($N = 6$). Peritoneal fibrosis was induced by chlorhexidine gluconate (CG), as described previously by Coles and Topley [33]. Briefly, CG group rats received an IP injection of PBS (1 mL/kg) in the first 7 days and then PBS (1 mL/kg) followed by IP injection of 0.1% CG in ethanol (15%) dissolved in 2 mL saline daily for another 21 days ($N = 6$). In the group receiving CG with low dose vitamin D, rats received daily IP injections of 500 ng/kg vitamin D (Nang Kuang; Taiwan) in the first 7 days and then 500 ng/kg vitamin D followed by CG IP injection daily for another 21 days ($N = 6$). In the CG-receiving group with middle or high dose vitamin D, rats received IP injection of 750 ng/kg or 1 μg/kg vitamin D, respectively, daily in the first 7 days and then the same dosage of vitamin D followed by CG IP injection daily for another 21 days (each groups $N = 6$). Finally, a modified peritoneal equilibration test was performed 29 days after the first IP injection and a blood sample was obtained by cardiac puncture [34]. The peritoneum and aorta were then removed by dissection.

2.9. Modified 4-Hour Peritoneal Equilibration Test. For evaluation of the peritoneal ultrafiltration rate, rats were anesthetized (Zoletil 50: Rompun 2% injection = 1 : 2; 100 μL/100 g; intramuscular injection) and instilled with 90 mL/kg commercial dialysis solution containing 4.25% glucose (Dianeal; Baxter International, Inc., IL, USA), and 4 hr later, the rats were sacrificed by cervical dislocation to record the residual intraperitoneal volumes. Net ultrafiltration was calculated using the following formula: (final dialysate volume − initial dialysate volume)/initial dialysate volume. Glucose transport was obtained using the following formula: (initial dialysate glucose × initial volume) − (final dialysate glucose × final volume) [34].

2.10. Histopathological Examination. For histological analysis, 3 μm thick paraffin sections of the rats' abdominal wall were stained by Masson's trichrome. The thickness of submesothelial tissue of the peritoneum was then measured and expressed as the mean ± S.D. For each rat, corresponding samples were measured at 6 random sites by blinded researchers performing microscope analysis with a metric ocular.

2.11. Quantification of Aortic Calcium and Phosphate. Aortic segments were lyophilized and decalcified with 0.6 N HCl and incubated at 37°C for 1 day. The o-cresolphthalein complexone kit (Teco Diagnostics, CA, USA) was used for determining the calcium content of the supernatant. The inorganic phosphorus reacted with ammonium molybdate in the sulfuric acid to form an unreduced phosphomolybdate complex. Then the complex absorbs light and was quantified photometrically in ultraviolet light. Light absorbance of the sample was directly proportional to the phosphorus concentration. Aortic calcium and phosphate content were normalized to the tissue dry weight (mg/g dry weight) [35].

2.12. Statistical Analysis. All data were expressed as mean ± S.D. and statistical significance was analyzed with a one-way analysis of variance. A significant result was defined as $P < 0.05$.

2.13. Ethics Statement. This study was approved by the ethics committee/institutional review board of E-Da Hospital, and written informed consent was obtained from all patients (IRB number: EMRP18100N).

3. Results

3.1. The Effect of Different Dosages of Vitamin D on Serum and Aortic Calcium and Phosphate Content. Vitamin D is well known to regulate serum calcium and phosphate and also vascular calcification. We therefore investigated the serum and aortic calcium and phosphate content in the rats under varying vitamin D dosage. $1\alpha,25(OH)_2D_3$ induced mild hypercalcemia in the low and middle dose groups but induced severe hypercalcemia (>15 mg/dL) in the high dose group, as shown in Figure 1(a). However, no significant difference was found in the serum phosphate content of the different groups (Figure 1(b)). High dose vitamin D also induced severe aortic calcium and phosphate deposition, as illustrated in Figures 1(c) and 1(d). Further, we analyzed serum 25(OH)D levels, and the results indicated that endogenous 25(OH)D was significantly suppressed after $1\alpha,25(OH)_2D_3$ treatment (Figure 1(e)).

3.2. Vitamin D Ameliorates CG-Induced Peritoneal Fibrosis in a Rat Model. We then investigated whether vitamin D could ameliorate the structural deterioration of the peritoneal membrane in a peritoneal fibrosis animal model. As high dose vitamin D was demonstrated to induce severe hypercalcemia and aortic calcium and phosphate deposition, we postulated that 500 ng/kg (L) or 750 ng/kg (M) would be an ideal therapeutic dosage without apparent significant side effects. IP administration of $1\alpha,25(OH)_2D_3$ significantly ameliorated the peritoneal thickening in a dose-dependent manner as visualized by Masson's trichrome stain, shown in Figure 2.

3.3. Vitamin D Ameliorates CG-Induced Functional Deterioration of the Peritoneum in a Rat Model. To further investigate the functional relevance of the peritoneum, a modified peritoneal equilibration test was performed on the final treatment day. The ultrafiltration volumes from the CG-exposed group were significantly lower than those from the saline group; and vitamin D was able to ameliorate CG-induced decrease in ultrafiltration, illustrated in Figure 3(a). In addition, the mass transport of glucose also indicated that vitamin D could ameliorate CG-induced increase in peritoneal permeability in a dose-dependent manner (Figure 3(b)).

3.4. Vitamin D Treatment Decreases CG-Induced EMT in a Rat Model. We investigated the inhibitory effect of vitamin D on the EMT process *in vivo.* Western blot analysis showed that vitamin D inhibited CG-induced upregulation of α-SMA and downregulation of E-cadherin in rat visceral peritoneum (Figure 4).

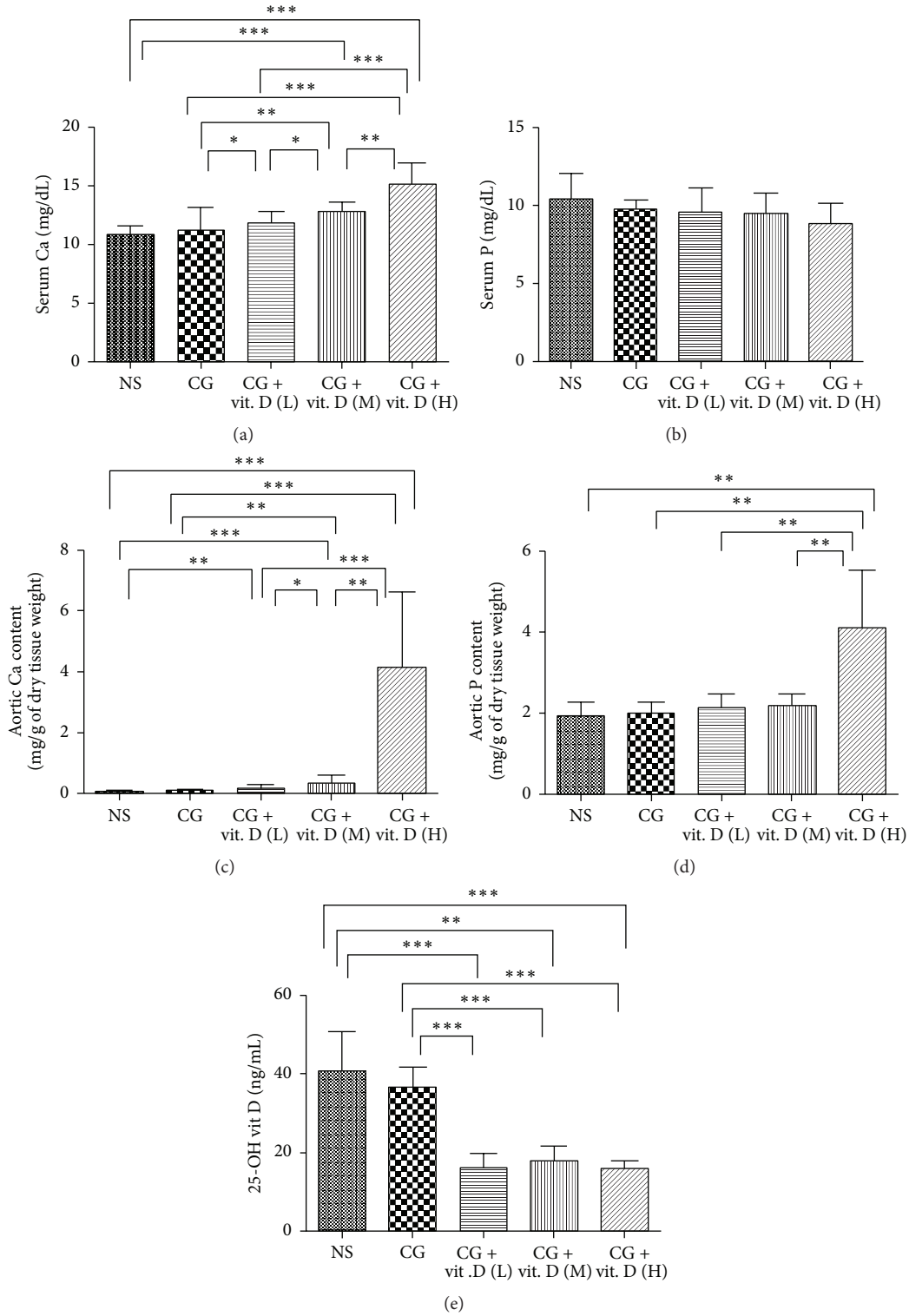

Figure 1: Effect of vitamin D on serum and aortic calcium and phosphate content. Sprague-Dawley rats received intraperitoneal (IP) injection of chlorhexidine gluconate (CG) daily with or without administration of low (L, 500 ng/kg), middle (M, 750 ng/kg), or high (H, 1 μg/kg) dose $1\alpha,25(OH)_2D_3$ (vit. D). Rats also received daily intraperitoneal instillation of normal saline (NS) as a control. Blood samples and aorta tissue samples were taken 29 days after the first IP injection. (a) $1\alpha,25(OH)_2D_3$ induced mild hypercalcemia in the low and middle dose groups but induced severe hypercalcemia (>15 mg/dL) in the high dose group. (b) However, no significant difference was found in the serum phosphate content of the different groups. (c and d) High dose vitamin D also induced severe aortic calcium and phosphate deposition. (e) Further, we analyzed serum 25(OH)D levels, and the results indicated that endogenous 25(OH)D was significantly suppressed after $1\alpha,25(OH)_2D_3$ treatment. Data are represented as mean ± S.D. ($^*P < 0.05$; $^{**}P < 0.01$; $^{***}P < 0.005$).

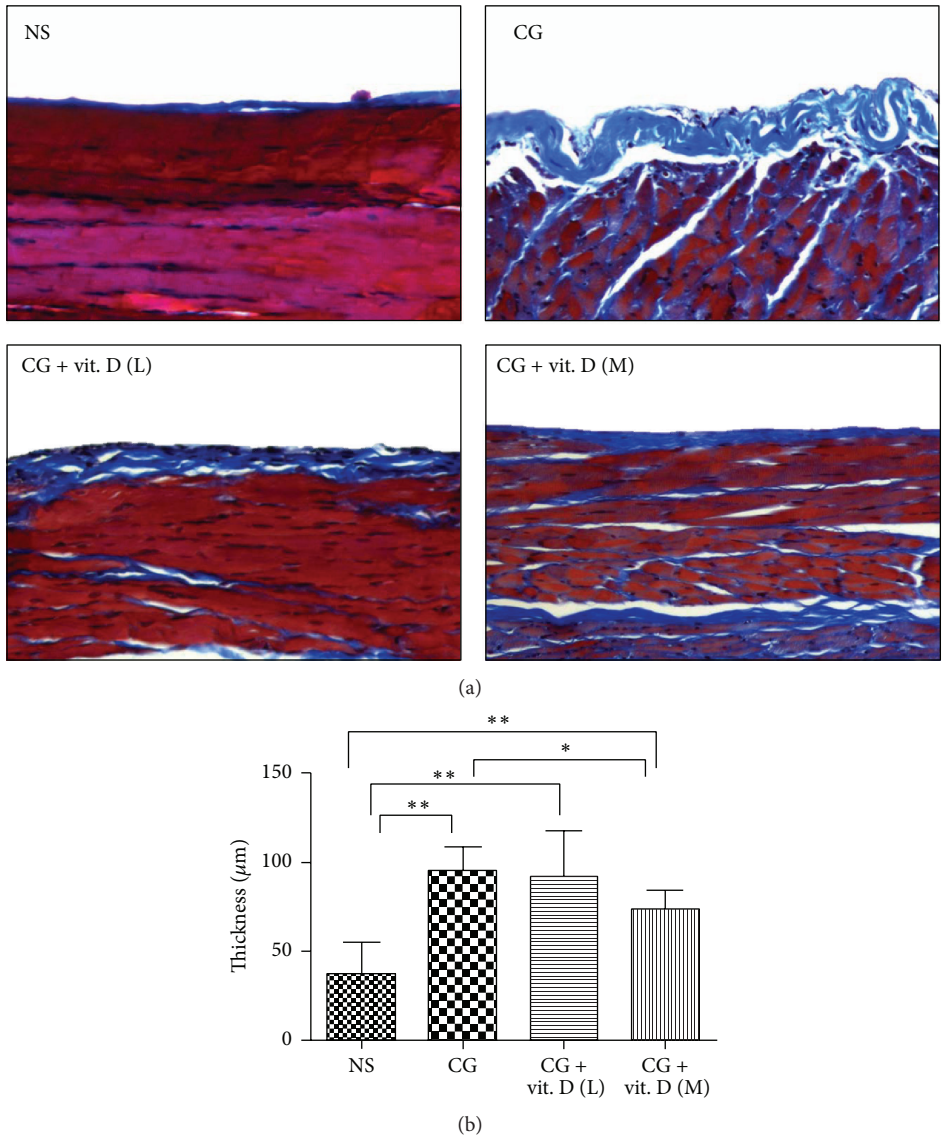

Figure 2: Vitamin D treatment decreased chlorhexidine gluconate- (CG-) induced peritoneal membrane fibrosis in a rat model. Sprague-Dawley rats received a daily intraperitoneal (IP) injection of chlorhexidine gluconate (CG) with or without administration of low (L, 500 ng/kg) or middle (M, 750 ng/kg) dose $1\alpha,25(OH)_2D_3$ (vit. D). Control rats received a daily IP instillation of normal saline (NS). (a) Representative images of peritoneum samples extracted 29 days after initial IP injection, stained with Masson's trichrome. CG instillation induced matrix deposition and thickening of the peritoneal membrane, while vitamin D treatment ameliorated these effects. Magnification ×200. (b) Quantification of the peritoneal membrane thickness. The antifibrotic effects of vitamin D were dose-dependent. Data represent mean ± S.D. ($n = 6$) ($^*P < 0.05$; $^{**}P < 0.01$).

3.5. Vitamin D Attenuates TGF-β-Induced EMT and Migration Activity In Vitro. To further confirm that vitamin D exerts its antifibrotic effect through inhibition of the EMT process of MCs, primary human MCs were incubated with TGF-β1 in the absence or the presence of vitamin D. RT-PCR and western blot analysis both verified that $1\alpha,25(OH)_2D_3$ significantly ameliorated TGF-β1-induced EMT (Figure 5). We subsequently investigated the effect of vitamin D on cell migration activity as cells gain greater migration ability after undergoing EMT. The results showed that $1\alpha,25(OH)_2D_3$ significantly inhibited TGF-β1 promoted cell migrating activity (Figure 6). Furthermore, we also verified the change in the EMT process by phalloidin-labeled staining to visualize cytoskeletal actin expression changes in MCs. As evidenced in Figure 7, $1\alpha,25(OH)_2D_3$ inhibited TGF-β1-induced intracellular F-actin redistribution. TGF-β1 promoted upregulation of α-SMA in MCs was also demonstrated (Figure 8) and it was found that vitamin D could inhibit this effect.

4. Discussion

Our data showed that $1\alpha,25(OH)_2D_3$ ameliorates CG-induced morphological and functional deterioration of the peritoneal membrane in a dose-dependent manner and that

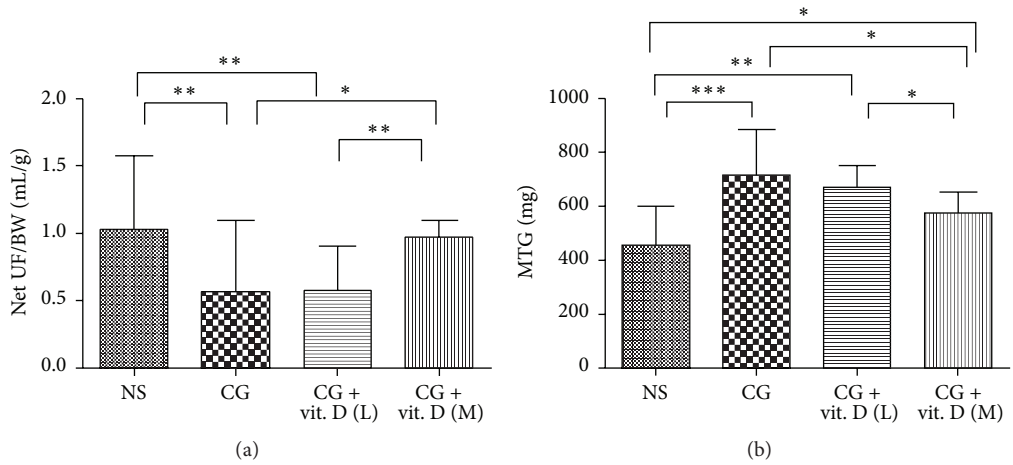

Figure 3: Vitamin D treatment prevented loss of peritoneal function caused by chlorhexidine gluconate (CG) exposure in a rat model. Sprague-Dawley rats received a daily intraperitoneal injection of chlorhexidine gluconate (CG) with or without administration of low (L, 500 ng/kg) or middle (M, 750 ng/kg) dose 1α,25$(OH)_2D_3$ (vit. D). Rats received a daily intraperitoneal instillation of normal saline (NS) as a control. Peritoneal function was assessed by (a) net ultrafiltration divided from body weight (UF/BW) and (b) mass transfer of glucose (MTG). CG instillation induced peritoneal function impairment, while vitamin D treatment significantly ameliorated this phenomenon. Data represent mean ± S.D. ($n = 6$) ($^*P < 0.05$; $^{**}P < 0.01$; $^{***}P < 0.005$).

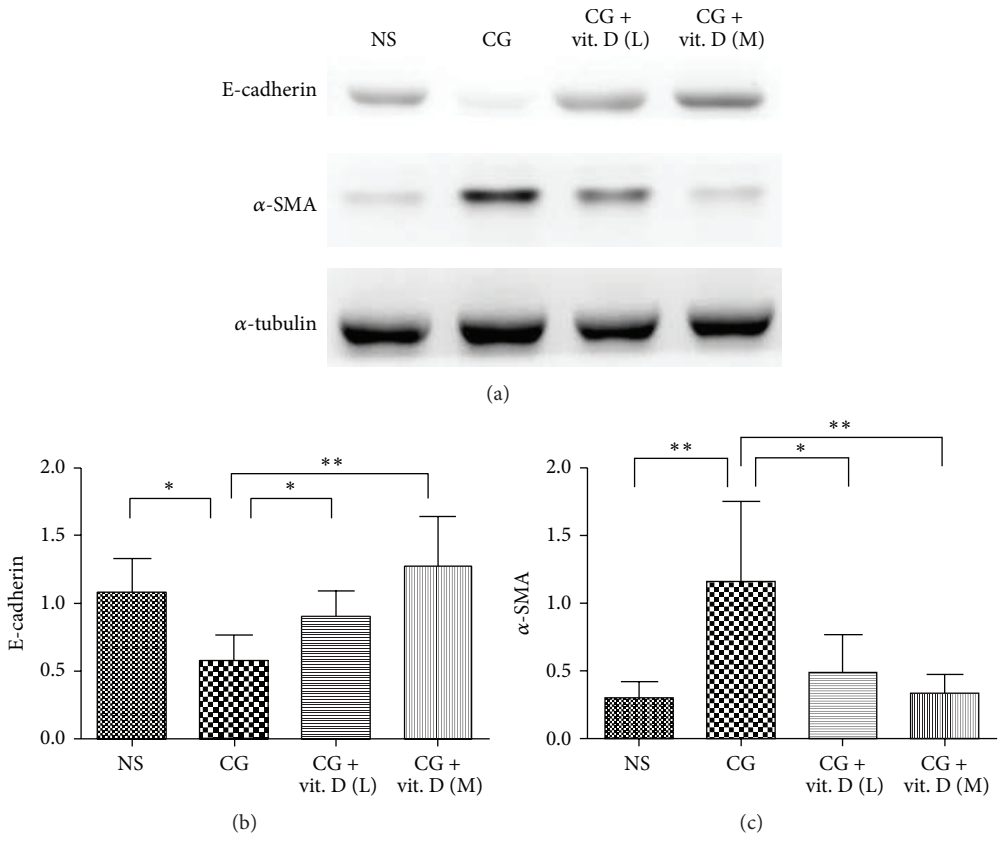

Figure 4: Vitamin D treatment decreased chlorhexidine gluconate- (CG-) induced peritoneal epithelial-to-mesenchymal transition in a rat model. Sprague-Dawley rats received a daily intraperitoneal injection of chlorhexidine gluconate (CG) with or without administration of low (L, 500 ng/kg) or middle (M, 750 ng/kg) dose 1α,25$(OH)_2D_3$ (vit. D). As a control, rats received daily intraperitoneal instillation of normal saline (NS). (a) Western blot analysis showed that vitamin D inhibited chlorhexidine gluconate- (CG-) induced downregulation of (b) E-cadherin and upregulation of (c) α-smooth muscle actin (α-SMA) in rat visceral peritoneum. Protein levels are represented semiquantitatively by the corresponding graphs and were measured on an arbitrary scale in both graphs. Data represent mean ± S.D. ($n = 6$) ($^*P < 0.05$; $^{**}P < 0.01$).

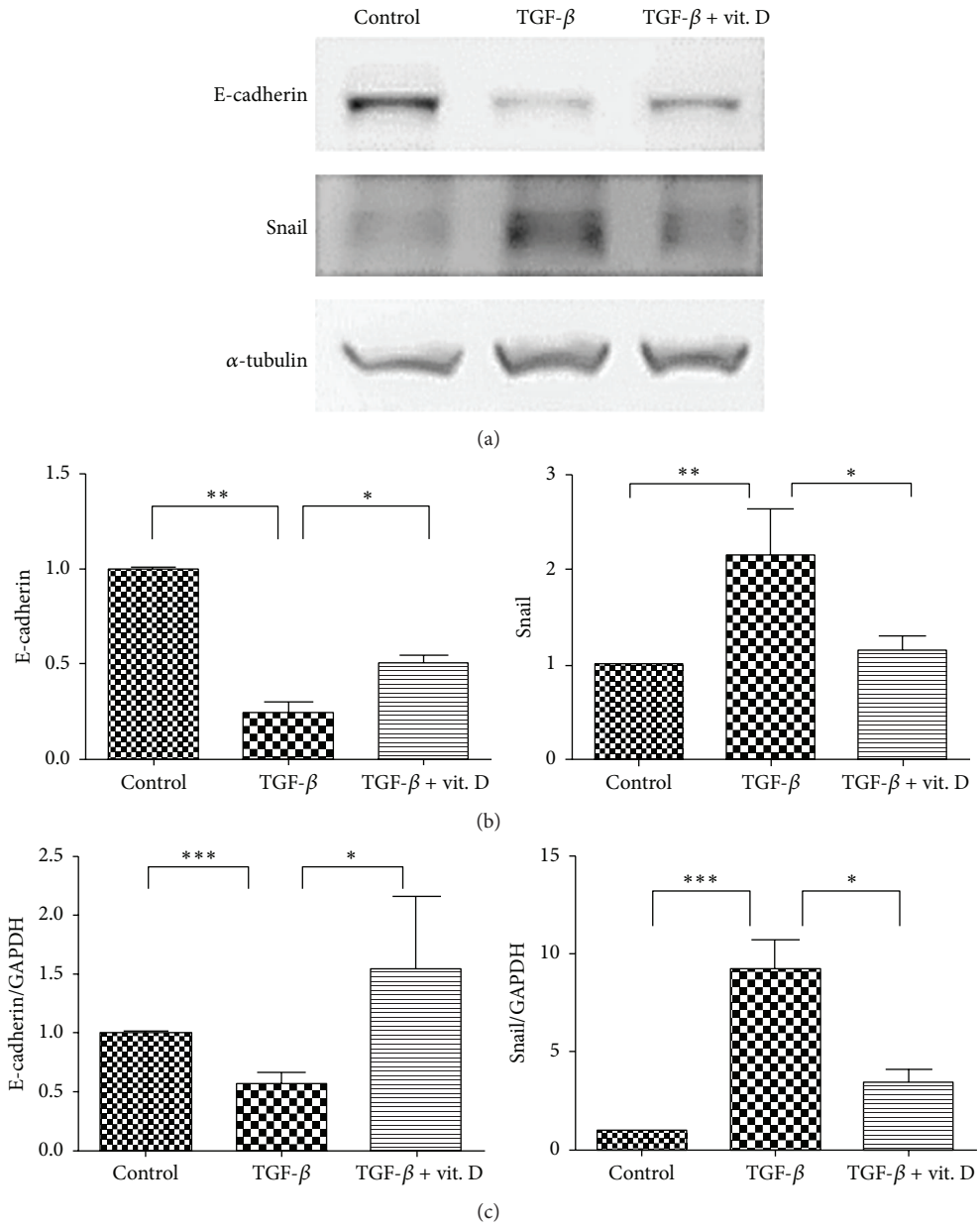

Figure 5: Vitamin D3 inhibited transforming growth factor-β1- (TGF-β1-) induced epithelial-to-mesenchymal transition (EMT) of mesothelial cells (MCs) *in vitro*. (a) Primary human peritoneal MCs were incubated with TGF-β1 *in vitro*. Western blot analysis showed that addition of $1\alpha,25(OH)_2D_3$ (vit. D, 10^{-6} mol/L) inhibited TGF-β1-induced EMT (epithelial marker: E-cadherin; mesenchymal marker: Snail). (b) Semiquantitative data of protein levels of E-cadherin and Snail. ($N = 6$) (c) Vitamin D inhibited TGF-β1-induced downregulation of E-cadherin and upregulation of Snail mRNA (normalized with GAPDH). Protein levels were measured on an arbitrary scale in all graphs (protein level from Western blots was performed using AlphaImager 2200). Data are represented as mean ± S.D. ($N = 3$) ($^{*}P < 0.05$; $^{**}P < 0.01$; $^{***}P < 0.005$).

vitamin D could inhibit the CG-induced EMT process *in vivo*. In addition, our *in vitro* study also proved that vitamin D inhibited TGF-β1-induced EMT marker change, migrating activities, and cytoskeleton redistribution in MCs. Taken together, our study demonstrated that inhibition of the EMT process of MCs plays a role in the peritoneum-protective effect of vitamin D.

Several studies have previously investigated the protective effect of vitamin D on peritoneal membranes. Coronel et al. reported a preliminary study showing that paricalcitol decreased peritoneal membrane permeability, with diminished peritoneal protein loss and increased ultrafiltration in PD patients [23]. Lee et al. proved that calcitriol could decrease peritoneal fibrosis in a rat model of acute CG exposure. Further, expression of TGF-β1 and angiotensin II induced by CG were also reduced [27]. González-Mateo et al. reported that paricalcitol could ameliorate peritoneal fibrosis in a murine PD model through the activation of

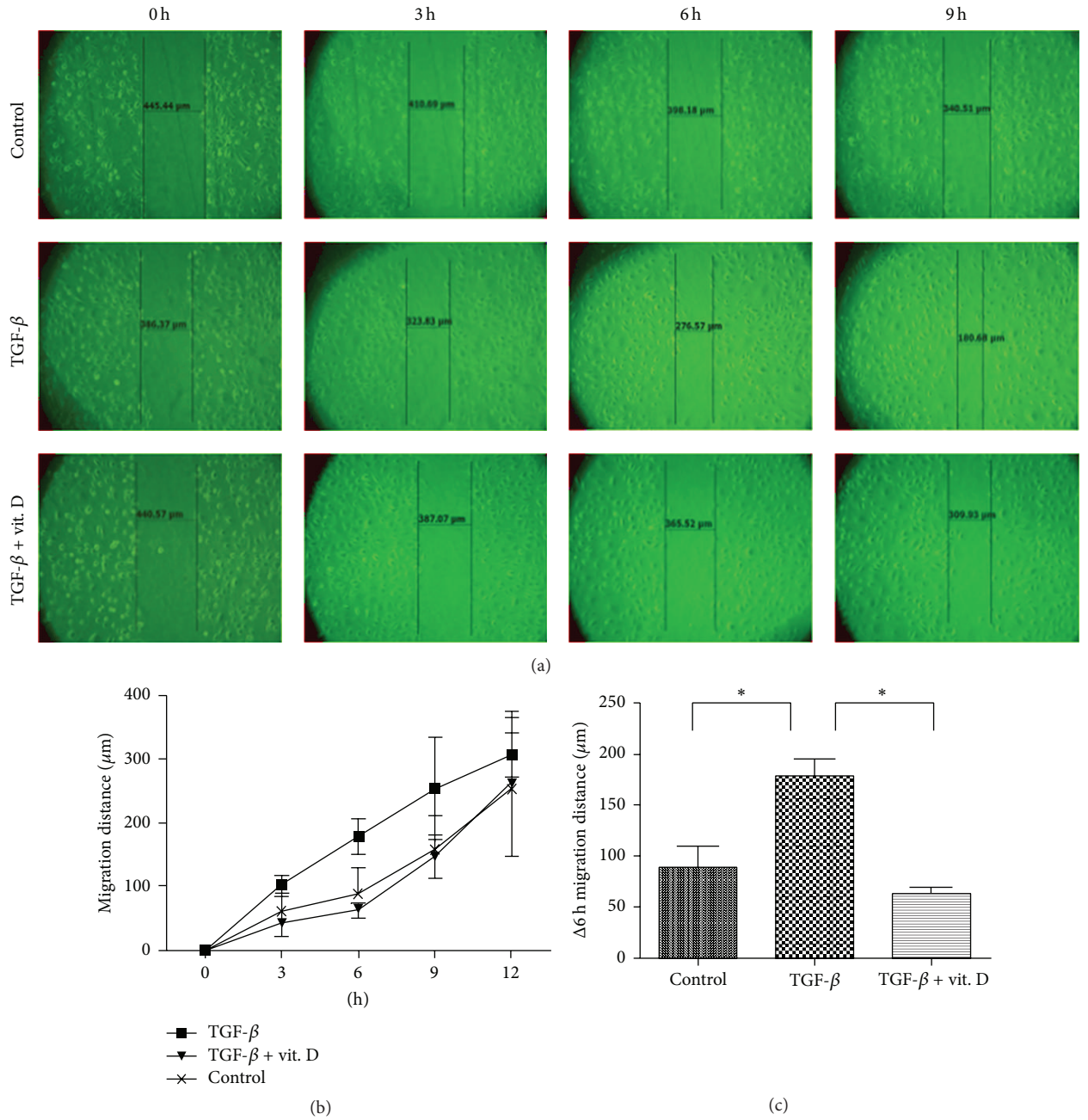

FIGURE 6: Vitamin D3 inhibited transforming growth factor-β1- (TGF-β1-) induced migration activity of mesothelial cells (MCs) *in vitro*. (a) Representative images of MCs in the wound-healing assay. MCs were treated with TGF-β1 (1 ng/mL) with or without 1α,25$(OH)_2D_3$ (vit. D, 10^{-6} mol/L). (b) Quantitative analysis of the width of the postscratch cell-free space at each follow-up time point. (c) The difference in the migration distance at 6 hr (Δ6 hr) is represented in (c). TGF-β1 promoted MCs migration activity was inhibited by vitamin D3. ($N = 4$) Graphical data represent mean ± S.D. ($^*P < 0.05$).

regulatory T cells and reduction in IL-17 production [25]. Recently, Kang et al. showed that paricalcitol affected EMT [26]. However, there were some limitations to their study. First, the *in vitro* study did not completely validate the EMT process. They only investigated the expression of EMT markers but not the migration capacity and cytoskeletal redistribution of MCs. Second, in their *in vivo* study, they only investigated the kinetics of glucose mass transfer but not of ultrafiltration. In addition, they only examined the expression of the mesenchymal marker α-SMA in the peritoneum; no epithelial marker was analyzed. Finally, the study lacked information about the influence of their therapeutic dose of vitamin D on serum calcium and phosphate levels and vascular calcification and the dose-dependent effects of therapeutic vitamin D were also unknown.

TGF-β1 is a key cytokine for the promotion of EMT in peritoneal MCs and of peritoneal fibrosis [36]. TGF-β1 binds to its receptor and exerts its biological and pathological

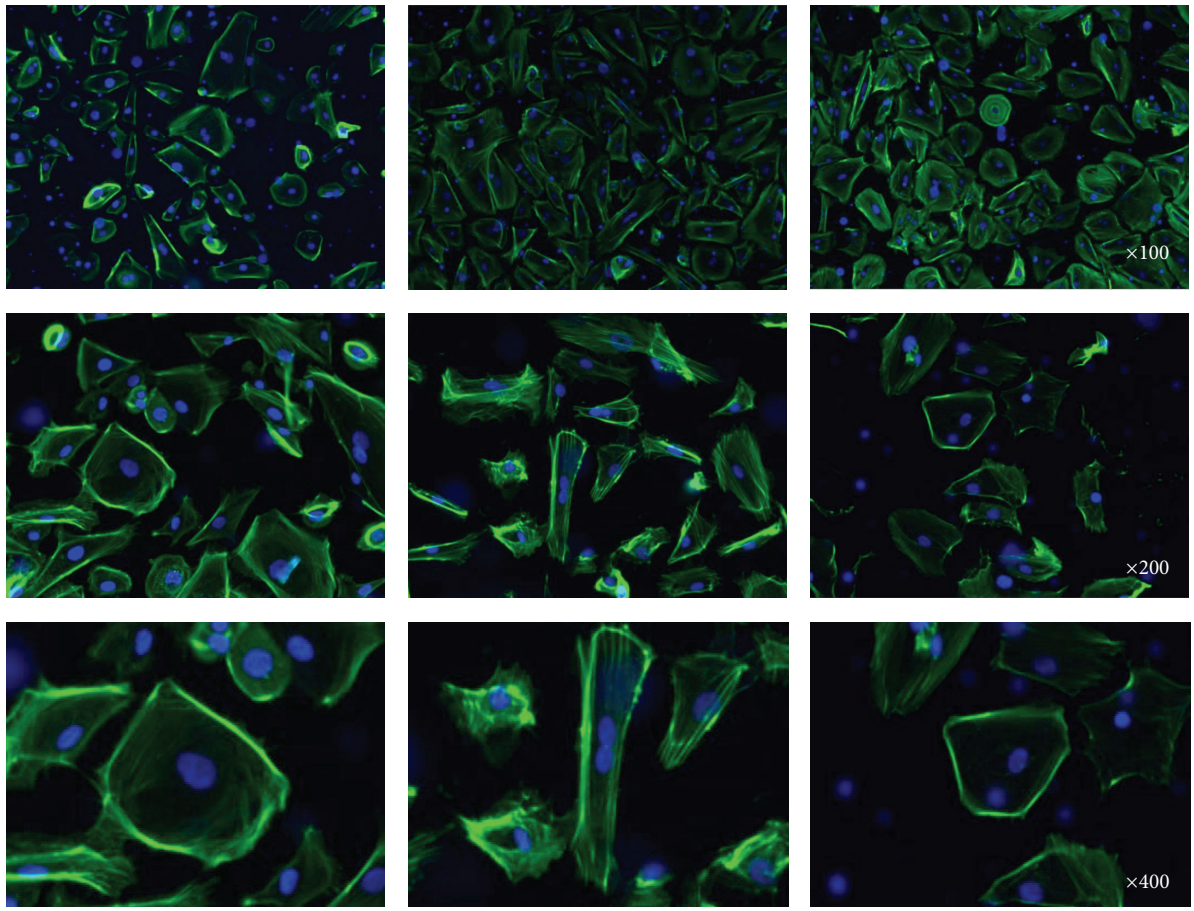

Figure 7: Vitamin D3 inhibited transforming growth factor-β1- (TGF-β1-) induced mesothelial cell (MC) cytoskeleton redistribution *in vitro*. MCs were cultured with TGF-β1 with or without addition of 1α,25$(OH)_2D_3$ (vit. D). MC cytoskeletons were stained with anti-F-actin antibodies. In normal culture medium, the actin cytoskeleton (green) was in the cortical band and TGF-β1 promoted cytoskeleton redistribution (fibroblast-like cytoskeleton). Vitamin D inhibited TGF-β1-induced cytoskeleton redistribution. Nuclei were stained with DAPI (blue). Magnification ×400.

activities via activation of Smad and non-Smad signaling pathways [37]. The Smad-dependent signaling pathway is the major mechanism of EMT and fibrosis through promotion of mesenchymal marker overexpression, such as α-SMA and Snail, and suppression of epithelial markers, such as E-cadherin and cytokeratin. There are several possible mechanisms that explain how vitamin D inhibits MC EMT. Firstly, downregulation of E-cadherin is an important step in EMT and vitamin D has been proven to promote E-cadherin expression in some cancer studies [28]. Secondly, under MC injury conditions, MCs will express and secrete TGF-β1; TGF-β1 then channels back to induce MC EMT. At least one study had proven that vitamin D can inhibit TGF-β1 expression and secretion during MC damage [27]. Besides, inhibition of MC EMT by vitamin D may be also attributed to the inhibitory effects on TGF-β dependent pathways. For example, Nolan et al. report that vitamin D significantly attenuated TGF-β1-induced renal epithelial injury *in vitro* through attenuating Smad2 phosphorylation [38]. Zerr et al. also proved that vitamin D receptor regulates Smad3-dependent transcription [39].

Our study had several limitations. The first was the use of CG as a chemical irritant and not dialysate to induce peritoneal fibrosis and functional deterioration in our animal model. Furthermore, our model did not contain uremic rats; uremic toxins effect on peritoneum could therefore not be measured here. The CG model of peritoneal fibrosis is a simple model and is easy to use but certainly may not be an ideal substitute for PD fluid installation [40]. It should be emphasized that results obtained in CG models may not translate to PD fluid models of fibrosis as in the latter the changes are more subtle and may follow different pathways of fibrosis. However, previous studies have proved that it is a feasible model for studying peritoneal fibrosis [41–43]. Second, although our data suggest that vitamin D can ameliorate peritoneal membrane morphological and functional deterioration, the results also showed that vitamin D may induce a mild degree of vascular calcification

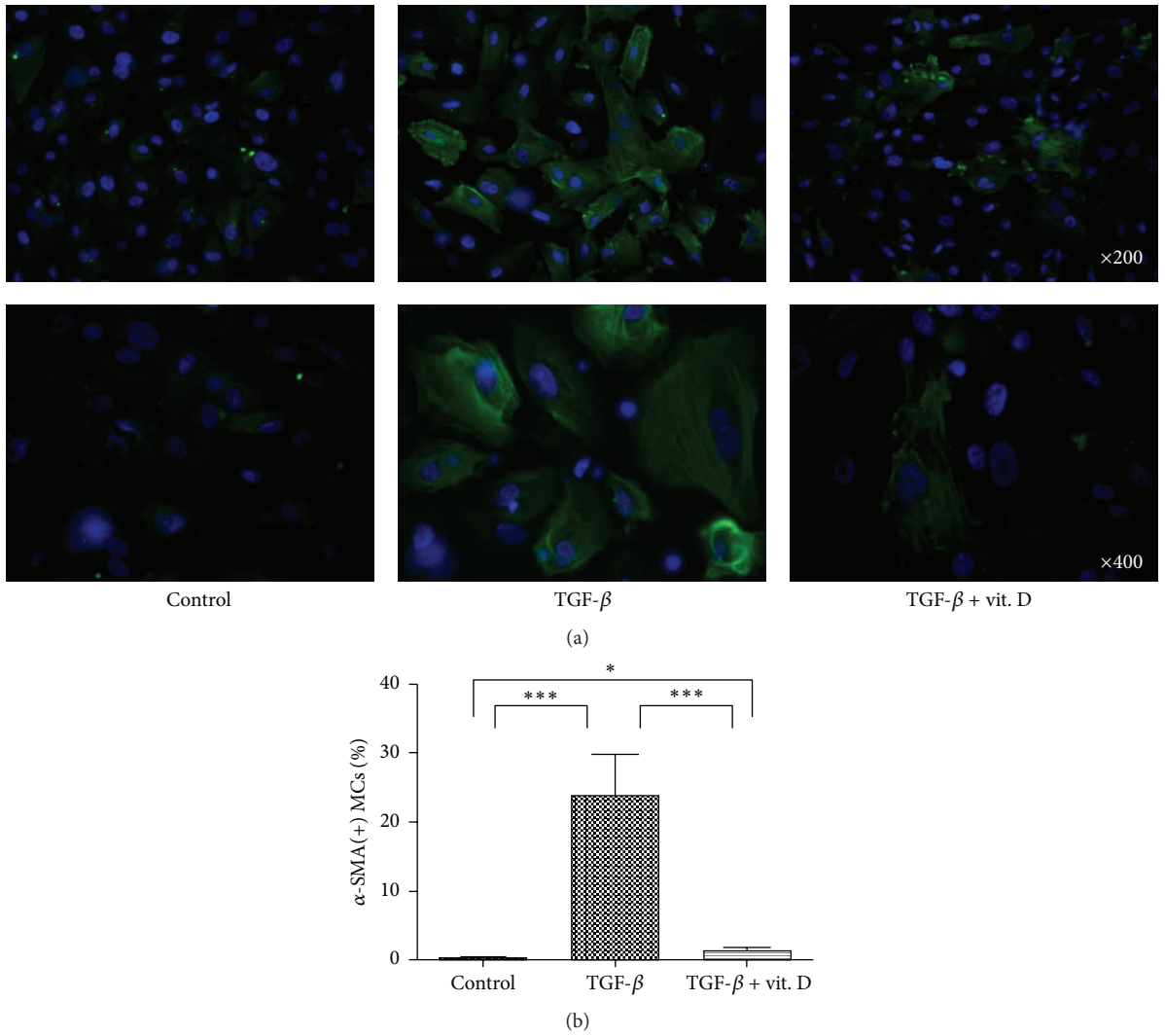

FIGURE 8: Vitamin D3 inhibits transforming growth factor-β1- (TGF-β1-) induced α-smooth muscle actin (α-SMA) upregulation of mesothelial cells (MCs) *in vitro*. MCs were treated with TGF-β1 with or without addition of $1\alpha,25(OH)_2D_3$ (vit. D). Immunofluorescence analysis showed that TGF-β1 promoted upregulation of α-SMA (green) in MCs and vitamin D inhibited this phenomenon. Nuclei are stained with DAPI (blue). This inhibition effect is quantified in (b) where the positive staining for α-SMA was calculated as a percentage of MCs present. Data represent mean ± S.D. ($^{*}P < 0.05$; $^{***}P < 0.005$).

and hypercalcemia under our therapeutic dosage. Besides, in the human setting, 1-2 μg of $1\alpha,25(OH)_2D_3$ in a daily dose is considered a high dose and may already induce hypercalcemia. But in our experimental model, the dosage was at least ten times more than human setting and really a supraphysiological dose. Further study is required to resolve this problem and we postulate that a tissue-specific drug delivery system may be an ideal solution [44]. Finally, many previous studies have shown MCs to be an important source of myofibroblasts via the EMT process [14, 19, 45]; however, one recent *in vivo* study did suggest that MCs may not be the main source of submesothelial fibroblasts [46]. Additional study is needed to confirm this result; but we hypothesize that even if EMT MCs are not the main source of submesothelial fibroblasts, they will still play a role in the process of fibrosis.

5. Conclusions

The present study demonstrates that vitamin D can ameliorate EMT process in MCs, improve peritoneal fibrosis, and attenuate functional deterioration. We propose that vitamin D may be an advantageous addition to PD therapy, preserving peritoneum function during long-term PD and preventing technique failure.

Abbreviations

α-SMA: α-smooth muscle actin
CG: Chlorhexidine gluconate
EMT: Epithelial-to-mesenchymal transition
ESRD: End-stage renal disease

GDPs: Glucose degradation products
HD: Hemodialysis
ICAM-1: Intercellular adhesion molecule-1
IP: Intraperitoneal
MCs: Mesothelial cells
PBS: Phosphate buffered saline
PD: Peritoneal dialysis
SD: Sprague-Dawley
S.D.: Standard deviation
TGF-β1: Transforming growth factor-β1.

Conflict of Interests

The authors declare that they have no conflict of interests.

Authors' Contribution

Yi-Che Lee, Shih-Yuan Hung, Hung-Hsiang Liou, Tsun-Mei Lin, Yau-Sheng Tsai, and Yuan-Yow Chiou contributed to study conception, participated in its design and coordination, and helped to draft this paper; Sheng-Hsiang Lin performed the statistical analysis; Chu-Hung Tsai, Min-Yu Chang, Hsi-Hao Wang, Li-Chun Ho, Yi-Ting Chen, Ching-Fang Wu, Ho-Ching Chen, Hsin-Pao Chen, Kuang-Wen Liu, Chih-I. Chen, Kuan Min She, Hao-Kuang Wang, and Chi-Wei Lin participated in the collection of study material. All authors read and approved the final paper. Hung-Hsiang Liou and Tsun-Mei Lin contributed equally to this work.

Acknowledgments

The authors are indebted to Shin-Hann Tseng, Chih-ting Huang, Chiung-Wen Tu, and Yi-Chun Teng for critical discussion and partial execution of the study. This study was supported by EDAHP-103035, EDAHP-103050, NCKUEDA-10302 and NCKUEDA-10402 from the Research Foundation of E-DA Hospital and National Cheng Kung University, Taiwan.

References

[1] C.-C. Huang, K.-F. Cheng, and H.-D. I. Wu, "Survival analysis: comparing peritoneal dialysis and hemodialysis in Taiwan," *Peritoneal Dialysis International*, vol. 28, no. 3, pp. S15–S20, 2008.

[2] E. F. Vonesh, J. J. Snyder, R. N. Foley, and A. J. Collins, "Mortality studies comparing peritoneal dialysis and hemodialysis: what do they tell us?" *Kidney International*, vol. 70, no. 103, pp. S3–S11, 2006.

[3] S. S. A. Fenton, D. E. Schaubel, M. Desmeules et al., "Hemodialysis versus peritoneal dialysis: a comparison of adjusted mortality rates," *American Journal of Kidney Diseases*, vol. 30, no. 3, pp. 334–342, 1997.

[4] R. Mehrotra, Y.-W. Chiu, K. Kalantar-Zadeh, J. Bargman, and E. Vonesh, "Similar outcomes with hemodialysis and peritoneal dialysis in patients with end-stage renal disease," *Archives of Internal Medicine*, vol. 171, no. 2, pp. 110–118, 2011.

[5] Y. Kawaguchi, T. Hasegawa, M. Nakayama, H. Kubo, and T. Shigematu, "Issues affecting the longevity of the continuous peritoneal dialysis therapy," *Kidney International, Supplement*, vol. 51, no. 62, pp. S105–S107, 1997.

[6] F. Schaefer, G. Klaus, D. E. Müller-Wiefel, and O. Mehls, "Current practice of peritoneal dialysis in children: results of a longitudinal survey. Mid European Pediatric Peritoneal Dialysis Study Group (MEPPS)," *Peritoneal Dialysis International*, vol. 19, supplement 2, pp. S445–S449, 1999.

[7] S. H. Han, S. C. Lee, S. V. Ahn et al., "Improving outcome of CAPD: twenty-five years' experience in a single Korean center," *Peritoneal Dialysis International*, vol. 27, no. 4, pp. 432–440, 2007.

[8] G. Woodrow, J. H. Turney, and A. M. Brownjohn, "Technique failure in peritoneal dialysis and its impact on patient survival," *Peritoneal Dialysis International*, vol. 17, no. 4, pp. 360–364, 1997.

[9] H. Nakamoto, Y. Kawaguchi, and H. Suzuki, "Is technique survival on peritoneal dialysis better in Japan?" *Peritoneal Dialysis International*, vol. 26, no. 2, pp. 136–143, 2006.

[10] S. P. Andreoli, C. D. Langefeld, S. Stadler, P. Smith, A. Sears, and K. West, "Risks of peritoneal membrane failure in children undergoing long-term peritoneal dialysis," *Pediatric Nephrology*, vol. 7, no. 5, pp. 543–547, 1993.

[11] S. J. Davies, L. Phillips, A. M. Griffiths, L. H. Russell, P. F. Naish, and G. I. Russell, "What really happens to people on long-term peritoneal dialysis?" *Kidney International*, vol. 54, no. 6, pp. 2207–2217, 1998.

[12] R. T. Krediet, "The peritoneal membrane in chronic peritoneal dialysis," *Kidney International*, vol. 55, no. 1, pp. 341–356, 1999.

[13] S. J. Davies, L. Phillips, P. F. Naish, and G. I. Russell, "Peritoneal glucose exposure and changes in membrane solute transport with time on peritoneal dialysis," *Journal of the American Society of Nephrology*, vol. 12, no. 5, pp. 1046–1051, 2001.

[14] M. Yáñez-Mó, E. Lara-Pezzi, R. Selgas et al., "Peritoneal dialysis and epithelial-to-mesenchymal transition of mesothelial cells," *The New England Journal of Medicine*, vol. 348, no. 5, pp. 403–413, 2003.

[15] A. H. Yang, J. Y. Chen, Y. P. Lin, T. P. Huang, and C. W. Wu, "Peritoneal dialysis solution induces apoptosis of mesothelial cells," *Kidney International*, vol. 51, no. 4, pp. 1280–1288, 1997.

[16] Z. Zheng, R. Ye, X. Yu, J. Bergström, and B. Lindholm, "Peritoneal dialysis solutions disturb the balance of apoptosis and proliferation of peritoneal cells in chronic dialysis model," *Advances in Peritoneal Dialysis*, vol. 17, pp. 53–57, 2001.

[17] R. Selgas, M. A. Bajo, A. Aguilera et al., "Epithelial-mesenchymal transition in fibrosing processes. Mesothelial cells obtained ex vivo from patients treated with peritoneal dialysis as transdifferentiation model," *Nefrologia*, vol. 24, no. 1, pp. 34–39, 2004.

[18] A. Aguilera, M. Yáñez-Mo, R. Selgas, F. Sánchez-Madrid, and M. López-Cabrera, "Epithelial to mesenchymal transition as a triggering factor of peritoneal membrane fibrosis and angiogenesis in peritoneal dialysis patients," *Current Opinion in Investigational Drugs*, vol. 6, no. 3, pp. 262–268, 2005.

[19] L. S. Aroeira, A. Aguilera, J. A. Sánchez-Tomero et al., "Epithelial to mesenchymal transition and peritoneal membrane failure in peritoneal dialysis patients: pathologic significance and potential therapeutic interventions," *Journal of the American Society of Nephrology*, vol. 18, no. 7, pp. 2004–2013, 2007.

[20] Y.-C. Lee, Y.-S. Tsai, S.-Y. Hung et al., "Shorter daily dwelling time in peritoneal dialysis attenuates the epithelial-to-mesenchymal transition of mesothelial cells," *BMC Nephrology*, vol. 15, no. 1, article 35, 2014.

[21] J. Liu, X. Wu, Y. Liu et al., "High-glucose-based peritoneal dialysis solution induces the upregulation of VEGF expression in human peritoneal mesothelial cells: the role of pleiotrophin," *International Journal of Molecular Medicine*, vol. 32, no. 5, pp. 1150–1158, 2013.

[22] T. Ito, N. Yorioka, M. Yamamotcv, K. Kataoka, and M. Yamakido, "Effect of glucose on intercellular junctions of cultured human peritoneal mesothelial cells," *Journal of the American Society of Nephrology*, vol. 11, no. 11, pp. 1969–1979, 2000.

[23] F. Coronel, S. Cigarran, A. Gomis et al., "Changes in peritoneal membrane permeability and proteinuria in patients on peritoneal dialysis after treatment with paricalcitol—a preliminary study," *Clinical Nephrology*, vol. 78, no. 2, pp. 93–99, 2012.

[24] M. Hirose, T. Nishino, Y. Obata et al., "22-oxacalcitriol prevents progression of peritoneal fibrosis in a mouse model," *Peritoneal Dialysis International*, vol. 33, no. 2, pp. 132–142, 2013.

[25] G. T. González-Mateo, V. Fernández-Míllara, T. Bellón et al., "Paricalcitol reduces peritoneal fibrosis in mice through the activation of regulatory T cells and reduction in IL-17 production," *PLoS ONE*, vol. 9, no. 10, Article ID e108477, 2014.

[26] S. H. Kang, S. O. Kim, K. H. Cho, J. W. Park, K. W. Yoon, and J. Y. Do, "Paricalcitol ameliorates epithelial-to-mesenchymal transition in the peritoneal mesothelium," *Nephron—Experimental Nephrology*, vol. 126, no. 1, pp. 1–7, 2014.

[27] C.-J. Lee, Y.-M. Subeq, R.-P. Lee, H.-H. Liou, and B.-G. Hsu, "Calcitriol decreases TGF-beta1 and angiotensin II production and protects against chlorhexide digluconate-induced liver peritoneal fibrosis in rats," *Cytokine*, vol. 65, no. 1, pp. 105–118, 2014.

[28] K. K. Deeb, D. L. Trump, and C. S. Johnson, "Vitamin D signalling pathways in cancer: potential for anticancer therapeutics," *Nature Reviews Cancer*, vol. 7, no. 9, pp. 684–700, 2007.

[29] C. Díaz, R. Selgas, M. A. Castro et al., "Ex vivo proliferation of mesothelial cells directly obtained from peritoneal effluent: its relationship with peritoneal antecedents and functional parameters," *Advances in Peritoneal Dialysis*, vol. 14, pp. 19–24, 1998.

[30] M. Yáñez-Mó, A. Alfranca, C. Cabañas et al., "Regulation of endothelial cell motility by complexes of tetraspan molecules CD81/TAPA-1 and CD151/PETA-3 with $\alpha 3\beta 1$ integrin localized at endothelial lateral junctions," *The Journal of Cell Biology*, vol. 141, no. 3, pp. 791–804, 1998.

[31] A. Cano, M. A. Pérez-Moreno, I. Rodrigo et al., "The transcription factor snail controls epithelial-mesenchymal transitions by repressing E-cadherin expression," *Nature Cell Biology*, vol. 2, no. 2, pp. 76–83, 2000.

[32] C. Li, Y. Ren, X. Jia et al., "Twist overexpression promoted epithelial-to-mesenchymal transition of human peritoneal mesothelial cells under high glucose," *Nephrology Dialysis Transplantation*, vol. 27, no. 11, pp. 4119–4124, 2012.

[33] G. A. Coles and N. Topley, "Long-term peritoneal membrane changes," *Advances in Renal Replacement Therapy*, vol. 7, no. 4, pp. 289–301, 2000.

[34] F. Zhu, T. Li, F. Qiu et al., "Preventive effect of Notch signaling inhibition by a γ-secretase inhibitor on peritoneal dialysis fluid-induced peritoneal fibrosis in rats," *The American Journal of Pathology*, vol. 176, no. 2, pp. 650–659, 2010.

[35] S. Jono, M. D. McKee, C. E. Murry et al., "Phosphate regulation of vascular smooth muscle cell calcification," *Circulation Research*, vol. 87, no. 7, pp. E10–E17, 2000.

[36] P. J. Margetts, P. Bonniaud, L. Liu et al., "Transient overexpression of TGF-β1 induces epithelial mesenchymal transition in the rodent peritoneum," *Journal of the American Society of Nephrology*, vol. 16, no. 2, pp. 425–436, 2005.

[37] R. Derynck and Y. E. Zhang, "Smad-dependent and Smad-independent pathways in TGF-beta family signalling," *Nature*, vol. 425, no. 6958, pp. 577–584, 2003.

[38] K. A. Nolan, E. P. Brennan, C. C. Scholz et al., "Paricalcitol protects against TGF-β1-induced fibrotic responses in hypoxia and stabilises HIF-α in renal epithelia," *Experimental Cell Research*, vol. 330, no. 2, pp. 371–381, 2015.

[39] P. Zerr, S. Vollath, K. Palumbo-Zerr et al., "Vitamin D receptor regulates TGF-β signalling in systemic sclerosis," *Annals of the Rheumatic Diseases*, vol. 74, no. 3, article e20, 2015.

[40] A. Vlijm, D. E. Sampimon, M. de Graaff, D. G. Struijk, and R. T. Krediet, "Experimental peritoneal sclerosis models should not be based on chlorhexidine gluconate anymore," *Nephron—Experimental Nephrology*, vol. 117, no. 1, pp. e1–e8, 2010.

[41] T. Nishino, M. Miyazaki, K. Abe et al., "Antisense oligonucleotides against collagen-binding stress protein HSP47 suppress peritoneal fibrosis in rats," *Kidney International*, vol. 64, no. 3, pp. 887–896, 2003.

[42] Y. Mishima, M. Miyazaki, K. Abe et al., "(CG)enhanced expression of heat shock protein 47 in rat model of peritoneal fibrosis," *Peritoneal Dialysis International*, vol. 23, no. 1, pp. 14–22, 2003.

[43] Y. Yoshio, M. Miyazaki, K. Abe et al., "TNP-470, an angiogenesis inhibitor, suppresses the progression of peritoneal fibrosis in mouse experimental model," *Kidney International*, vol. 66, no. 4, pp. 1677–1685, 2004.

[44] E. Almouazen, S. Bourgeois, L. P. Jordheim, H. Fessi, and S. Briançon, "Nano-encapsulation of vitamin D3 active metabolites for application in chemotherapy: formulation study and *in vitro* evaluation," *Pharmaceutical Research*, vol. 30, no. 4, pp. 1137–1146, 2013.

[45] L. S. Aroeira, E. Lara-Pezzi, J. Loureiro et al., "Cyclooxygenase-2 mediates dialysate-induced alterations of the peritoneal membrane," *Journal of the American Society of Nephrology*, vol. 20, no. 3, pp. 582–592, 2009.

[46] Y. T. Chen, Y. T. Chang, S. Y. Pan et al., "Lineage tracing reveals distinctive fates for mesothelial cells and submesothelial fibroblasts during peritoneal injury," *Journal of the American Society of Nephrology*, vol. 25, no. 12, pp. 2847–2858, 2014.

Hindawi Publishing Corporation
BioMed Research International
Volume 2015, Article ID 929806, 9 pages
http://dx.doi.org/10.1155/2015/929806

Review Article

microRNA Regulation of Peritoneal Cavity Homeostasis in Peritoneal Dialysis

Melisa Lopez-Anton, Timothy Bowen, and Robert H. Jenkins

Department of Nephrology, School of Medicine, College of Biomedical & Life Sciences, Cardiff University, Heath Park Campus, Cardiff CF14 4XN, UK

Correspondence should be addressed to Robert H. Jenkins; jenkinsrh2@cardiff.ac.uk

Received 22 June 2015; Accepted 9 August 2015

Academic Editor: Janusz Witowski

Preservation of peritoneal cavity homeostasis and peritoneal membrane function is critical for long-term peritoneal dialysis (PD) treatment. Several microRNAs (miRNAs) have been implicated in the regulation of key molecular pathways driving peritoneal membrane alterations leading to PD failure. miRNAs regulate the expression of the majority of protein coding genes in the human genome, thereby affecting most biochemical pathways implicated in cellular homeostasis. In this review, we report published findings on miRNAs and PD therapy, with emphasis on evidence for changes in peritoneal miRNA expression during long-term PD treatment. Recent work indicates that PD effluent- (PDE-) derived cells change their miRNA expression throughout the course of PD therapy, contributing to the loss of peritoneal cavity homeostasis and peritoneal membrane function. Changes in miRNA expression profiles will alter regulation of key molecular pathways, with the potential to cause profound effects on peritoneal cavity homeostasis during PD treatment. However, research to date has mainly adopted a literature-based miRNA-candidate methodology drawing conclusions from modest numbers of patient-derived samples. Therefore, the study of miRNA expression during PD therapy remains a promising field of research to understand the mechanisms involved in basic peritoneal cell homeostasis and PD failure.

1. Introduction

Peritoneal dialysis (PD) therapy involves constant exposure of the peritoneal membrane to bioincompatible PD solutions and a high basal inflammatory state. This results in an alteration of the peritoneal cavity homeostasis characterized by progressive fibrosis, angiogenesis, and ultrafiltration failure [1]. The success of long-term PD therapy depends on the maintenance of the structural and functional integrity of the peritoneal membrane, across which solute transfer occurs. Although different cell types are involved in the loss of peritoneal membrane homeostasis there is particular interest in peritoneal mesothelial cells (MCs), one of the most numerous cell types of the peritoneal cavity, 1×10^9 cells. PD failure has been largely associated with the conversion of MCs to myofibroblasts, via mesothelial-to-mesenchymal transition (MMT) and mesothelial cell loss [2]. This phenotypic conversion leads to increased synthesis of extracellular matrix components and release of proinflammatory and proangiogenic factors [3] (Figure 1(b)). Therefore, PD treatment directs the fate of peritoneal homeostasis through the modulation of cell type specific signal transduction networks. The dysregulation of different molecules has been observed to play a causative role in the etiology of PD therapy. Accordingly, the determination of the upstream pathways that control the expression and/or activity of specific peritoneal cell types has turned into an important field of research.

microRNAs (miRNAs) were initially discovered in *C. elegans* as critical developmental regulators over a decade ago [4, 5]. Alterations in miRNA expression have been described in a wide range of *in vitro* and *in vivo* disease models [6]. miRNAs are short noncoding RNAs that regulate gene expression at the posttranscriptional level. Broadly, miRNAs are transcribed by RNA polymerase (Pol II) or Pol III enzymes [7, 8] as long, polyadenylated primary miRNA (pri-miRNA) molecules [9]. The pri-miRNA transcripts are processed by Drosha, a nuclear RNase III endonuclease, generating precursor miRNAs (pre-miRNA) [10]. Pre-miRNAs are

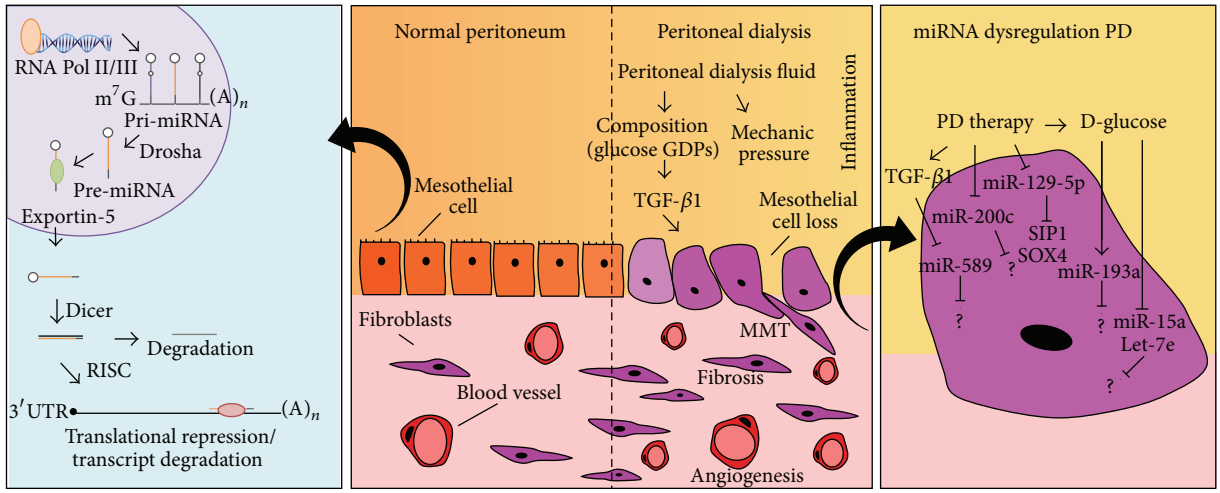

Figure 1: miRNA dysregulation in peritoneal dialysis. (a) miRNA biogenesis pathway. miRNAs are transcribed by RNA polymerase (Pol II) or Pol III as primary miRNA (pri-miRNA) transcripts that are processed by Drosha to generate precursor miRNAs (pre-miRNAs). Pre-miRNA hairpins are transported by Exportin-5 to the cytoplasm, where mature miRNAs are generated by Dicer, and incorporated into the RNA-induced silencing complex (RISC). miRNA-RISC complexes bind to the 3′ untranslated regions (3′ UTRs) of target mRNAs by partial complementarity, resulting in repression of translation and/or mRNA degradation. (b) Peritoneal mesothelial-to-mesenchymal transition (MMT) is associated with PD therapy. Healthy peritoneal mesothelial cells (PMCs; left hand side) undergo morphological changes during PD-driven MMT, invading the submesothelium where they contribute to angiogenesis and fibrosis and increase extracellular matrix (ECM) components deposition during PD therapy (right hand side). (c) Dysregulated miRNA expression resulting from PD therapy. Only miRNAs for which specific evidence in HPMCs exists are shown.

60–70 nt stem-loop hairpin molecules that are transported to the cytoplasm by Exportin-5 [11, 12]. Mature miRNAs (22–25 nt) are generated by Dicer, a cytoplasmic RNase III, and incorporated into the RNA-induced silencing complex (RISC) [13]. miRNA-RISC complex binds to 3′ untranslated regions (3′ UTRs) of specific target genes by partial complementarity, which results in repression of translation and/or degradation of the target mRNA [14]. miRNAs control the expression of the majority of protein coding genes in the human genome, thereby affecting most biochemical pathways implicated in cellular homeostasis. Additionally, one miRNA may regulate the expression of hundreds of target mRNAs, profoundly affecting cell phenotype and function. Studies on miRNA expression in different model systems and body fluids have also emphasized their potential as therapeutic targets and disease biomarkers [15–18] (Figure 1(a)).

Aberrant miRNA levels associated with PD therapy may affect the regulation of a multitude of mRNA species resulting in significant cellular effects. In the context of PD, continuous dialysis fluid exchange allows easy access to monitor peritoneal cells and miRNA expression in PD effluent (PDE), presenting the enticing possibility of monitoring peritoneal cavity homeostasis during PD treatment. In this review, we comment on published findings describing miRNAs in PD therapy, with emphasis on evidence for changes in peritoneal miRNA expression during long-term PD treatment. Compelling data suggest that miRNAs are implicated in the regulation of key molecular pathways driving peritoneal membrane alterations leading to PD failure. Additionally, miRNAs implicated in epithelial-to-mesenchymal transition (EMT) in other contexts have been associated with MCs MMT during PD therapy [19, 20]. These results have important implications for understanding peritoneal cavity alterations associated with PD therapy. However, research to date has mainly adopted a literature-based miRNA-candidate methodology drawing conclusions from modest numbers of patient-derived samples. Therefore, the study of miRNA expression during PD therapy remains a promising field of research to understand the mechanisms involved in basic peritoneal cell homeostasis and PD failure (Figure 1(c)).

2. miRNA-Changes during PD Therapy

miRNAs are dysregulated in a broad range of diseases. The cellular homeostasis of the peritoneal cavity is dramatically affected during long-term peritoneal dialysis (PD) therapy [21, 22]. PD treatment induces several structural and functional changes in the peritoneal cavity including cellular percentage [21, 22] and phenotypic [23] changes that may potentially be controlled by specific miRNA expression profiles. The development of micro-sample analysis techniques, together with structural and functional similarities of human peritoneal physiology compared with mouse and rat models, allowed the development of PD *in vivo* studies [24]. The establishment of competent animal models has been decisive for *in vivo* scrutiny of PD characteristics that cannot be appraised by *in vitro* models [25].

Rat PD models allow the study of long-term PD effects while being relatively economical and easy to maintain.

Models based on daily intraperitoneal injections of 4.25% dextrose PD solution showed impaired peritoneal function accompanied by morphological peritoneal changes characterized by a fibroblast-like phenotype acquisition of mesothelial cells after 4 weeks [19, 26]. Total rat peritoneal RNA from this model has been analyzed by miRNA array [19, 26]. Lin et al. found robust and significant downregulation of 8 miRNAs in the hypertonic dialysate group (miR-31, miR-93, miR-100, miR-152, miR-497, miR-192, miR-194, and miR-200b) and increased expression of miR-122 was observed in the hypertonic dialysate group compared with the saline and control groups [26]. All results were RT-qPCR confirmed [26]. When the same model was analyzed by Zhou et al. [19], peritoneal fibrotic tissues displayed upregulation in 8 miRNAs (miR-205, miR-664, miR-352, miR-146b-5p, predicted miR-160, miR-132, miR-15b, and let-7d) while 15 were downregulated (miR-335, miR-923, miR-801, miR-200a, miR-801, miR-30a, miR-193a-3p, miR-193b, miR-29b, miR-203, miR-148a, miR-709, miR-192, miR-15a, and miR-26b) [19]. Among them, only miR-192 overlapped with the miRNAs described by Lin et al. [19, 26]. The authors found miR-30a downregulation particularly interesting as it is known to target EMT-related genes, such as Snail and vimentin [19, 27, 28]. Using RT-qPCR, Zhou et al. [19] validated miR-30a downregulation in total peritoneum from the rat PD model, in PD patients undergoing therapy for 3.5–66 months and following addition of TGF-β1 to rat primary peritoneal mesothelial cells and to human peritoneal mesothelial cell line HMrSV5 [19]. miR-30a downregulation was associated with Snail upregulation in HMrSV5 cells, in which miR-30a stable overexpression blocked TGF-β1-induced Snail expression resulting in inhibition of EMT [19].

A rat EMT model based on repeated exposure to glucose degradation products (GDPs) during 1-2 weeks, using methylglyoxal (MGO), has been investigated by Liu et al. [29]. Total RNA from the peritoneum of rats subjected to this model was analyzed by miRNA array [29]. Liu et al. [29] found that expression of 4 miRNAs was significantly upregulated (miR-136, miR-703, miR-30b, and miR-107), while miR-653 and miR-598 were significantly downregulated. None of these findings overlapped with the miRNAs identified by Lin et al. and Zhou et al. [19, 26, 29]. All array data were confirmed by RT-qPCR analysis, with miR-30b showing the greatest increase in the PMs of rats injected with MGO [29]. Intraperitoneal injection of miR-30b chemically modified antisense RNA oligonucleotide (ASO) in week 2 counteracted MGO-induced EMT of PMCs in rats [29]. This effect was associated with bone morphogenetic protein-7 (BMP-7), a member of the transforming growth factor-β1 (TGF-β1) superfamily that negatively regulates EMT and prevents fibrosis [30, 31]. BMP-7 was significantly downregulated after 4 weeks of MGO injection and this effect was reversed by intraperitoneal miR-30b ASO injection [29]. Finally, this group demonstrated that miR-30b directly targets BMP-7 in PMs of rats, which could antagonize the effects of TGF-β1 [29].

Due to significant benefits such as low cost, quick turnover, simple breeding, and multiple potential genetic manipulations, mouse PD models have become increasingly popular. Liu et al. [32] studied the expression profiles of long noncoding RNA (lncRNAs), miRNAs, and mRNAs comparing total peritoneal tissue from a mouse model of peritoneal fibrosis induced by daily intraperitoneal injection of 4.25% dextrose PD fluid (PDF) or saline solution for 4 weeks [32]. Array data showed that 14 miRNAs were upregulated and 1 miRNA was downregulated compared to normal peritoneal tissue [32]. Subsequent RT-qPCR validated upregulated expression of miR-182, miR-488, miR-292, and miR-296, while miR-200a was downregulated in the model group compared to controls [32]. Despite use of integrative pathway and coexpression network analyses, the mechanisms and functions of these miRNAs remain unclear [32].

Continuous dialysis fluid exchange offers the possibility to assess the integrity of the peritoneal membrane and characterize the functionality of the cellular components derived from PDE of patients [33, 34]. Analysis of miRNA expression profiles in total PDE cells from patients having undergone PD therapy for less than 6 months versus long-term PD patients identified downregulation of miR-129-5p, a potent downstream inhibitor of TGF-β1 in renal fibrosis [33]. The authors confirmed miR-129-5p downregulation by RT-qPCR and northern blot analysis and found that miR-129-5p modulated E-cadherin and vimentin expression by targeting SIP1 and SOX4 3′UTRs and modulating E-cadherin and vimentin promoter activity via the TGF-β1/SIP1 pathway [33]. These data suggest that miR-129-5p protects MCs undergoing MMT transformation induced by TGF-β1 during PD through direct targeting of SIP1 and SOX4 [33]. By contrast, Zhang et al. [34] used their unpublished data of miRNA expression profiles in HPMCs of PD patients and HMrSV5 cells treated with TGF-β1 to focus their studies on miR-589 [34]. miR-589 downregulation was confirmed in HPMCs from PD patients and HMrSV5 cells treated with TGF-β1, in which overexpression of miR-589 attenuated the EMT changes induced by TGF-β1 [34].

Most PD-related miRNA studies have taken a literature-based approach to the identification of candidate miRNAs for further analysis [20, 35–37]. The miR-29 family is known to be a potent downstream inhibitor of TGF-β1/Smad3 in heart, liver, lung, and kidney fibrosis [38–41]. Yu et al. [20] examined the therapeutic potential of miR-29b in a mouse model of PD induced fibrosis by daily infusion of 4.25% dextrose solution by miR-29b delivery before and at day 14 of therapy [20]. miR-29b overexpression showed a protective effect on peritoneal fibrosis including EMT and not only prevented peritoneal dysfunction when delivered before starting the therapy, but also altered the progression of the fibrosis when delivered after fibrosis establishment (day 14) [20]. Although there are several mechanisms by which miR-29b might inhibit peritoneal fibrosis, the authors focused on the transcription factor specificity protein 1 (Sp1), which is a putative target of miR-29b that plays an important role in TGF-β1/Smad3 pathway and may be a mechanism by which miR-29b inhibited peritoneal fibrosis [20, 42, 43].

The miR-200 family of miRNAs has been closely associated with a variety of fibrotic diseases including lung

and kidney fibrosis [44, 45]. Zhang et al. [35] showed miRNA-200c downregulation when comparing PDE-derived MCs from patients that had recently started PD therapy with those undergoing PD for more than 6 months [35]. miR-200c expression also correlated with morphological changes in HPMCs suggesting that it may be associated with the EMT process [35]. Chen et al. [36] selected the following candidate miRNAs based on a report on EMT and kidney disease [46]: miR-15a, miR-17-92, miR-21, miR-30, miR-192, miR-216a, miR-217, and miR-377 [36]. Total PDE-derived cells from 110 PD patients (82 new, 28 prevalent) showed significant miRNA upregulation of miR-15a, miR-21, and miR-192 when comparing new, prevalent and UF groups, while miR-17, miR-30, and miR-377 expression was similar between groups [36]. miR-30 significantly correlated with GFR and no detectable expression of miR-216a and miR-217 was found in patient samples [36].

Bao et al. [37] studied a set of miRNAs related to kidney development and diseases (miR-193a, miR-21, miR-15a, miR-16, and let-7e) in a model of high-glucose EMT in HPMCs and found miR-193 upregulation, miR-15a and let-7e downregulation, and no significant changes for miR-16 and miR-21 [37]. miR-193a increase correlated with stimulus duration, suggesting to the authors that miR-193a may play an important role in the EMT of the PMCs and regulate peritoneal fibrosis [37].

3. Relevance of miRNA-Mediated Regulation of Peritoneal Cell Maintenance and Characteristics during PD Therapy

Several risk factors for PD therapy failure and/or the development of peritoneal fibrosis in PD patients have been described including biocompatibility of PD solutions, repeat peritonitis, and elevated expression of growth factors [26]. There is a continuous need to improve and promote large and well-documented multinational and multicenter PD registries which would allow research of appropriately sized cohort studies like the Global Fluid Study (GFS) and the balANZ study to overcome control group limitations [47, 48].

Animal models offer an accurate replication of PD therapy but may also increase the complexity of the study [24, 25]. The use of intraperitoneal injection of dialysate as PD model has many advantages including low cost, high practicality, and low infection risk [19, 20, 26, 29, 32]. Nevertheless, better PD models, in which a catheter is permanently inserted into the peritoneal cavity of the animals, have been already described with a minimum risk of developing exit site infection [25]. It is also important to remember that miRNA sequences are not always conserved between humans and animals [49], and analyzing their relevance in humans is, therefore, highly important (Table 1, [26, 29, 32]).

Several articles have based their miRNA microarray analysis on total peritoneal RNA samples (Table 1 [19, 26, 29, 32]). Nevertheless, it is well accepted that PD treatment induces several structural and functional changes in the peritoneal cavity including changes in the percentages of constituent cell types and phenotype [22]. miRNA expression profiles will change with each defined cell phenotype and context. Therefore, the study of miRNAs from total peritoneal samples has important associated challenges defining the specific cell type contribution and validating the changes in different, cell-specific models where mechanistic studies can be performed.

Indeed, CAPD patient PDE cell populations have been previously described as composed principally of macrophages (78%), followed by lymphocytes (12.3%), neutrophils (4.9%), eosinophils (2.6%), mesothelial cells (1.9%), and mast cells (0.3%) [21]. Therefore, although the study patients would be free of peritonitis, macrophages will still have an important contribution to the miRNA profile measured by total PDE-derived cells miRNA array. Consequently, miRNA arrays based on all PDE-derived cells and/or full membrane digests [19, 26, 29, 32] may not be a good model for mesothelial cell changes associated with PD therapy as suggested by some of the reviewed articles. Similarly, when the studied miRNAs are chosen from the existing literature, the choice of an appropriate model of study remains essential [20, 36, 37]. *In vitro* models, although more simplistic, may be critical to understand the specific pattern of miRNA expression in response to a known stimulus in a specific cell type where mechanistic research can be pursued. Further *in vitro* research is required to elucidate specific changes in cellular miRNA expression and their downstream mechanistic events (Figure 1(c)).

Under normal conditions basal peritoneal fluid (PF) is maintained within the body to serve as a lubricant and a protective barrier between organs. The median total RNA concentration of PF was 775 μg/L and 345 μg/L interquartile range, and the number of detectable miRNAs was 397 [50]. When compared with other 11 body fluids (amniotic fluid, breast milk, bronchial lavage, cerebrospinal fluid, colostrum, plasma, pleural fluid, saliva, seminal fluid, tears, and urine), PF had the fifth highest RNA content and the fourth highest miRNAs content [50]. The 20 miRNAs with the highest concentrations in PF were miR-515-3p, miR-892a, miR-518e, miR-134, miR-509-5p, miR-223*, miR-515-5p, miR-616, miR-302d, miR-873, miR-483-5p, miR-923, miR-374a, miR-598, miR-548b-3p, miR-1238, miR-92b, miR-498, miR-937, and miR-377*, while those uniquely detected in peritoneal fluid were miR-129*, miR-583, miR-223, miR-627, and miR-29b-1* [50]. Of the above, only miR-598 has been described to be downregulated by miRNA array data from total peritoneum in a rat model of MGO-induced EMT [29]. The authors measured miRNAs from PF supernatant for the first time, raising the possibility of using PDE from PD patients as a source of miRNAs that could be used as biomarkers to monitor PD therapy [50]. Of note, the measurement of miRNAs from patient PDE supernatant may be an important challenge due to the relatively short duration of the PD exchanges (4 h peritoneal equilibration test, PET) and the large fluid volume involved.

Table 1: miRNAs implicated in the regulation of peritoneal cavity homeostasis during peritoneal dialysis therapy.

miRNA	Study selection	Model(s)	Target(s)	Downstream signaling	References
Downregulation: miR-31*, miR-93, miR-100, miR-152, miR-497*, miR-192, miR-194, and miR-200b* *Upregulation*: miR-122	Microarray analysis (rat PD model, 4 weeks, total peritoneal tissue)	Rat PD model (4 weeks, total peritoneal tissue)	No	No	[26]
Downregulation: miR-30a	Microarray analysis (rat PD model, 4 weeks, total peritoneal tissue)	Rat PD model (4 weeks, total peritoneal tissue) HMrSV5 and primary rat PMCs TGF-β1 stimulated Total peritoneal tissue from PD patients miR-30a stable overexpression in HMrSV5	Snail1[&]	miR-30a acts as a negative regulator of TGF-β1 and induces Snail1-dependent EMT during peritoneal fibrosis	[19]
Downregulation: miR-653*, miR-598* *Upregulation*: miR-136, miR-703#, miR-30b, and miR-107	Microarray analysis (rat PD model, MGO-induced EMT, 1-2 weeks, total peritoneal tissue)	Rat MGO-induced EMT PD model (1-2 weeks, total peritoneal tissue) Rat MGO-induced EMT PD model with miR-30b-ASO *Ex vivo* rat PMCs cultured *in vitro*	BMP7 (miR-30b)	BMP-7 is downregulated in rat MGO-induced EMT PD model, reverted by miR-30b-ASO, and directly targeted by miR-30b, which could antagonize TGF-β1 effects	[29]
Downregulation: miR-200a-3p *Upregulation*: miR-182-5p*, miR-488-5p, miR-296-3p, and miR-292-5p*	Microarray analysis (mouse PD model, 4 weeks, total peritoneal tissue)	Mouse PD model (4 weeks, total peritoneal tissue)	No	No	[32]
Downregulation: miR-129-5p	Microarray analysis (PDE-derived HPMCs from PD patients)	PDE-derived HPMCs from PD patients HMrSV5 TGF-β1 stimulated miR-129-5p overexpression and SIP1/SOX4 knockdown in HMrSV5 TGF-β1 stimulated	SIP1, SOX4	miR-129-5p modulates E-cadherin and vimentin expression by targeting SIP1 and SOX4 genes or by modulating the promoter activity of E-cadherin and vimentin by the TGF-β1/SIP1 pathway. miR-125-5p protects MCs undergoing MMT TGF-β1-induced during PD and may exert protective effect targeting SIP1 and SOX4	[33]
Downregulation: miR-589	Unpublished (preexperiment CAPD profile miRNAs)	PDE-derived HPMCs from PD patients PDE-derived HPMCs and HMrSV5 TGF-β1 stimulated miR-589 overexpression in HMrSV5	No	No	[34]
Downregulation: miR-29b	Literature-based: studies on TGF-β1-mediated fibrosis	Mouse PD model with miR-29b overexpression (total omentum and peritoneal tissue)	SP1[&]	Blockade of the Sp1/TGF-β1/Smad3 pathway may be a mechanism by which miR-29b inhibited peritoneal fibrosis	[20]
Downregulation: miRNA-200c	Literature-based	PDE-derived HPMCs from PD patients	No	No	[35]
Upregulation: miR-15, miR-21, and miR-192 *No-changes*: miR-377, miR-30, and miR-17 *No-detection*: miR-216a, miR-217	Literature-based: studies on potential EMT miRNAs	PDE-derived cells from PD patients	No	No	[36]
Downregulation: miR-15a, let-7e *Upregulation*: miR-193a *No-changes*: miR-16, miR-21	Literature-based: studies related to kidney development and diseases	Cultured HPMCs stimulated by D-glucose (time course, 48 h) as a EMT model	No	No	[37]

*miRNA sequence is not conserved between the model of study and human.
#miRNA sequence is not present in miRBase (v21, June 2014) for rat or human.
[&]Putative targets already described [19, 20].

4. miRNAs as Biomarkers of the PD Cavity during PD Therapy

The National Institutes of Health (NIH) defines a biomarker as "*a characteristic that is objectively measured and evaluated as an indication of normal biological processes, pathogenic processes, or pharmacologic responses to a therapeutic intervention*" [51]. The prototypical biomarker must be well characterized and easily and effectively translated from basic research to routine clinical laboratories or point-of-care test. The best biomarker development practice can be achieved by the use of the Bradford Hill criteria: (A) strength, robust biomarker-outcome association; (B) consistency, persistence in different individuals, places, circumstances, and times; (C) specificity, diseases-explicit association; (D) temporality, the time course of changes in the biomarker and outcome occurring in parallel; (E) plausibility, reliable biomarker-pathogen connection; and (F) experimental evidence, biological biomarker understanding [51–53]. The evaluation of biomarker consistency is especially challenging as it requires the collection of large number of well-characterized clinical samples, and PD multinational and multicenter collections include the GFS and balANZ [47, 48].

Long-term PD therapy is characterized by the loss of the structural and functional integrity of the peritoneal membrane which leads to a progressive fibrosis, angiogenesis, and ultrafiltration failure resulting in a discontinuation of the therapy and, ultimately, transition to hemodialysis [1, 54, 55]. PET can provide therapy functional information but continuous morphological biopsy analysis is impractical. In PD patients, continuous dialysis fluid exchanges allow easy access to monitor potential peritoneal biomarkers for structural and functional peritoneal membrane changes. PDE contains several intraperitoneal and leukocyte-derived macromolecules, proteins, and RNA species, which may serve as potential biomarkers.

Cancer antigen 125 (CA-125) and interleukin-6 (IL-6) are the most highly studied PDE biomarkers. CA-125 is a high molecular weight glycoprotein and a significant body of work hypothesizes that the level of CA-125 in PDE correlates with mesothelial cell mass and a decline is indicative of mesothelial cell damage, EMT, and fibrosis [56–58]. However, recent evidence challenges this view and rather PDE CA-125 may instead reflect mesothelial cell damage, death, and detachment [59, 60]. Therefore, further research is needed to clarify CA-125 function, regulation of expression, and secretion/shedding. Pleiotropic cytokine IL-6 has essential roles in homeostasis including glucose metabolism, hypothalamic-pituitary-adrenal axis, acute inflammation, and wound healing [61]. IL-6 has been implicated in bacterial clearance during peritonitis and development of peritoneal fibrosis [61]. Plasma IL-6 correlates with comorbidity and survival of hemodialysis and PD patients while PDE IL-6 associates with peritoneal solute transport rate (PSTR) [47, 62]. However, the potential of IL-6 as a biomarker is hindered by intra- and interindividual variability [63]. No PDE-derived biomarker is currently used in clinical routine to monitor the homeostatic maintenance of the peritoneal cavity. Further research to identify PDE-miRNAs as biomarkers may contribute to individualizing PD therapy by indicating the adequacy of switching therapy, interrogating and discriminating clinical trials competence, and guiding the development of therapy innovations.

miRNAs have shown a sound potential as biomarkers in several fields and are easy to detect in different body fluids in which they may associate with proteins, microvesicles, exosomes, or necrotic bodies [64]. PDE-derived miRNAs may be particularly suitable as biomarkers due to their specific pattern of expression, easy detection, stability, and reliability [65–68]. PD-miRNA research is in early stage but there is a particular interest regarding miRNA as biomarkers to help individualizing PD treatment. Several studies have investigated the role of specific microRNAs in the peritoneum as discussed previously (Table 1), primarily associated with mesothelial EMT. These *in vitro* and *murine* models provide some association [26, 32, 34–37] and functional data [19, 20, 29, 33], but their utility as PDE biomarkers has yet to be established. Ultimately, unbiased multicenter miRNA expression analysis of PDE samples combined with robust function data would be essential for the establishment of miRNA-biomarkers associated with PD therapy.

The development of biomarkers in complex multifactorial disease, such as PD therapy, is especially challenging. Peritoneal therapy may require multiple biomarkers to achieve the degree of accuracy needed and different biomarkers may be required to address distinct specific questions. In this respect miRNAs are convenient as biomarkers due to easy, cost-effective, multiple-detection methods that have been recently developed.

5. Conclusion

Collectively, these studies suggest that miRNAs are likely to be important in the regulation of mesothelial cell phenotype and homeostasis in the peritoneal cavity during PD therapy. Measurement of miRNAs in PDE may therefore be valuable in predicting the clinical course of PD patients. However, previous studies have had significant design weaknesses. To maximize the success of identifying miRNA biomarkers for PD therapy it is important to adhere to the Bradford Hill criteria, develop a thorough mechanistic understanding of the biomarker, and ensure the clinical evaluation of independent cohorts is sufficiently powered. Collaboration between basic and clinical researchers is essential to develop robust data that can be transferred into diagnostics for clinical laboratories. Further research to identify PDE-miRNAs as biomarkers may contribute to individualizing PD therapy by indicating the adequacy of switching therapy, interrogating and discriminating clinical trial competence, and guiding the development of therapeutic innovations.

Conflict of Interests

The authors declare that there is no conflict of interests regarding the publication of this paper.

References

[1] L. S. Aroeira, A. Aguilera, J. A. Sánchez-Tomero et al., "Epithelial to mesenchymal transition and peritoneal membrane failure in peritoneal dialysis patients: Pathologic significance and potential therapeutic interventions," *Journal of the American Society of Nephrology*, vol. 18, no. 7, pp. 2004–2013, 2007.

[2] R. Selgas, A. Bajo, J. A. Jiménez-Heffernan et al., "Epithelial-to-mesenchymal transition of the mesothelial cell—its role in the response of the peritoneum to dialysis," *Nephrology Dialysis Transplantation*, vol. 21, no. 2, pp. ii2–ii7, 2006.

[3] J. Loureiro, A. Aguilera, R. Selgas et al., "Blocking TGF-β1 protects the peritoneal membrane from dialysate-induced damage," *Journal of the American Society of Nephrology*, vol. 22, no. 9, pp. 1682–1695, 2011.

[4] B. Wightman, I. Ha, and G. Ruvkun, "Posttranscriptional regulation of the heterochronic gene lin-14 by lin-4 mediates temporal pattern formation in *C. elegans*," *Cell*, vol. 75, no. 5, pp. 855–862, 1993.

[5] R. C. Lee, R. L. Feinbaum, and V. Ambros, "The *C. elegans* heterochronic gene lin-4 encodes small RNAs with antisense complementarity to lin-14," *Cell*, vol. 75, no. 5, pp. 843–854, 1993.

[6] P. Landgraf, M. Rusu, R. Sheridan et al., "A mammalian microRNA expression atlas based on small RNA library sequencing," *Cell*, vol. 129, no. 7, pp. 1401–1414, 2007.

[7] G. M. Borchert, W. Lanier, and B. L. Davidson, "RNA polymerase III transcribes human microRNAs," *Nature Structural and Molecular Biology*, vol. 13, no. 12, pp. 1097–1101, 2006.

[8] Y. Lee, M. Kim, J. Han et al., "MicroRNA genes are transcribed by RNA polymerase II," *The EMBO Journal*, vol. 23, no. 20, pp. 4051–4060, 2004.

[9] Y. Lee, K. Jeon, J.-T. Lee, S. Kim, and V. N. Kim, "MicroRNA maturation: stepwise processing and subcellular localization," *The EMBO Journal*, vol. 21, no. 17, pp. 4663–4670, 2002.

[10] Y. Lee, C. Ahn, J. Han et al., "The nuclear RNase III Drosha initiates microRNA processing," *Nature*, vol. 425, no. 6956, pp. 415–419, 2003.

[11] R. Yi, Y. Qin, I. G. Macara, and B. R. Cullen, "Exportin-5 mediates the nuclear export of pre-microRNAs and short hairpin RNAs," *Genes and Development*, vol. 17, no. 24, pp. 3011–3016, 2003.

[12] A. Grishok, A. E. Pasquinelli, D. Conte et al., "Genes and mechanisms related to RNA interference regulate expression of the small temporal RNAs that control *C. elegans* developmental timing," *Cell*, vol. 106, no. 1, pp. 23–34, 2001.

[13] E. Bernstein, A. A. Caudy, S. M. Hammond, and G. J. Hannon, "Role for a bidentate ribonuclease in the initiation step of RNA interference," *Nature*, vol. 409, no. 6818, pp. 363–366, 2001.

[14] A. E. Pasquinelli, "MicroRNAs and their targets: recognition, regulation and an emerging reciprocal relationship," *Nature Reviews Genetics*, vol. 13, no. 4, pp. 271–282, 2012.

[15] B. D. Brown and L. Naldini, "Exploiting and antagonizing microRNA regulation for therapeutic and experimental applications," *Nature Reviews Genetics*, vol. 10, no. 8, pp. 578–585, 2009.

[16] M. A. Cortez, C. Bueso-Ramos, J. Ferdin, G. Lopez-Berestein, A. K. Sood, and G. A. Calin, "MicroRNAs in body fluids-the mix of hormones and biomarkers," *Nature Reviews Clinical Oncology*, vol. 8, no. 8, pp. 467–477, 2011.

[17] J. Kota, R. R. Chivukula, K. A. O'Donnell et al., "Therapeutic microRNA delivery suppresses tumorigenesis in a murine liver cancer model," *Cell*, vol. 137, no. 6, pp. 1005–1017, 2009.

[18] A. Turchinovich, L. Weiz, A. Langheinz, and B. Burwinkel, "Characterization of extracellular circulating microRNA," *Nucleic Acids Research*, vol. 39, no. 16, pp. 7223–7233, 2011.

[19] Q. Zhou, M. Yang, H. Lan, and X. Yu, "MiR-30a negatively regulates TGF-β1-induced epithelial-mesenchymal transition and peritoneal fibrosis by targeting snail," *American Journal of Pathology*, vol. 183, no. 3, pp. 808–819, 2013.

[20] J.-W. Yu, W.-J. Duan, X.-R. Huang, X.-M. Meng, X.-Q. Yu, and H.-Y. Lan, "MicroRNA-29b inhibits peritoneal fibrosis in a mouse model of peritoneal dialysis," *Laboratory Investigation*, vol. 94, no. 9, pp. 978–990, 2014.

[21] H. J. Bos, D. G. Struijk, C. W. Tuk et al., "Peritoneal dialysis induces a local sterile inflammatory state and the mesothelial cells in the effluent are related to the bacterial peritonitis incidence," *Nephron*, vol. 59, no. 3, pp. 508–509, 1991.

[22] M. F. de Castro, R. Selgas, C. Jimenez et al., "Cell populations present in the nocturnal peritoneal effluent of patients on continuous ambulatory peritoneal dialysis and their relationship with peritoneal function and incidence of peritonitis," *Peritoneal Dialysis International*, vol. 14, no. 3, pp. 265–270, 1994.

[23] M. Yáñez-Mó, E. Lara-Pezzi, R. Selgas et al., "Peritoneal dialysis and epithelial-to-mesenchymal transition of mesothelial cells," *The New England Journal of Medicine*, vol. 348, no. 5, pp. 403–413, 2003.

[24] N. Lameire, W. Van Biesen, M. Van Landschoot et al., "Experimental models in peritoneal dialysis: a European experience," *Kidney International*, vol. 54, no. 6, pp. 2194–2206, 1998.

[25] G. T. González-Mateo, J. Loureiro, J. A. Jiménez-Hefferman et al., "Chronic exposure of mouse peritoneum to peritoneal dialysis fluid: structural and functional alterations of the peritoneal membrane," *Peritoneal Dialysis International*, vol. 29, no. 2, pp. 227–230, 2009.

[26] F. Lin, X. Wu, H. Zhang et al., "A microrna screen to identify regulators of peritoneal fibrosis in a rat model of peritoneal dialysis," *BMC Nephrology*, vol. 16, article 48, 2015.

[27] C.-W. Cheng, H.-W. Wang, C.-W. Chang et al., "microRNA-30a inhibits cell migration and invasion by downregulating vimentin expression and is a potential prognostic marker in breast cancer," *Breast Cancer Research and Treatment*, vol. 134, no. 3, pp. 1081–1093, 2012.

[28] R. Kumarswamy, G. Mudduluru, P. Ceppi et al., "MicroRNA-30a inhibits epithelial-to-mesenchymal transition by targeting Snai1 and is downregulated in non-small cell lung cancer," *International Journal of Cancer*, vol. 130, no. 9, pp. 2044–2053, 2012.

[29] H. Liu, N. Zhang, and D. Tian, "MiR-30b is involved in methylglyoxal-induced epithelial-mesenchymal transition of peritoneal mesothelial cells in rats," *Cellular and Molecular Biology Letters*, vol. 19, no. 2, pp. 315–329, 2014.

[30] S. Wang, Q. Chen, T. C. Simon et al., "Bone morphogenic protein-7 (BMP-7), a novel therapy for diabetic nephropathy," *Kidney International*, vol. 63, no. 6, pp. 2037–2049, 2003.

[31] M. Zeisberg, J.-I. Hanai, H. Sugimoto et al., "BMP-7 counteracts TGF-β1-induced epithelial-to-mesenchymal transition and reverses chronic renal injury," *Nature Medicine*, vol. 9, no. 7, pp. 964–968, 2003.

[32] Y. Liu, R. Guo, G. Hao et al., "The expression profiling and ontology analysis of noncoding rnas in peritoneal fibrosis induced by peritoneal dialysis fluid," *Gene*, vol. 564, pp. 210–219, 2015.

[33] L. Xiao, X. Zhou, F. Liu et al., "MicroRNA-129-5p modulates epithelial-to-mesenchymal transition by targeting SIP1 and SOX4 during peritoneal dialysis," *Laboratory Investigation*, vol. 95, no. 7, pp. 817–832, 2015.

[34] K. Zhang, H. Zhang, X. Zhou et al., "miRNA589 regulates epithelial-mesenchymal transition in human peritoneal mesothelial cells," *Journal of Biomedicine and Biotechnology*, vol. 2012, Article ID 673096, 6 pages, 2012.

[35] L. Zhang, F. Liu, Y. Peng, L. Sun, and G. Chen, "Changes in expression of four molecular marker proteins and one microRNA in mesothelial cells of the peritoneal dialysate effluent fluid of peritoneal dialysis patients," *Experimental and Therapeutic Medicine*, vol. 6, no. 5, pp. 1189–1193, 2013.

[36] J. Chen, P. Kam-Tao, B. C.-H. Kwan et al., "Relation between microRNA expression in peritoneal dialysis effluent and peritoneal transport characteristics," *Disease Markers*, vol. 33, no. 1, pp. 35–42, 2012.

[37] J. F. Bao, J. Hao, J. Liu, W. J. Yuan, and Q. Yu, "The abnormal expression level of microrna in epithelial-mesenchymal transition of peritoneal mesothelial cells induced by high glucose," *European Review for Medical and Pharmacological Sciences*, vol. 19, pp. 289–292, 2015.

[38] Y. Zhang, X.-R. Huang, L.-H. Wei, A. C. Chung, C.-M. Yu, and H.-Y. Lan, "miR-29b as a therapeutic agent for angiotensin II-induced cardiac fibrosis by targeting TGF-β/Smad3 signaling," *Molecular Therapy*, vol. 22, no. 5, pp. 974–985, 2014.

[39] C. Roderburg, G.-W. Urban, K. Bettermann et al., "Micro-RNA profiling reveals a role for miR-29 in human and murine liver fibrosis," *Hepatology*, vol. 53, no. 1, pp. 209–218, 2011.

[40] L. Cushing, P. P. Kuang, J. Qian et al., "miR-29 is a major regulator of genes associated with pulmonary fibrosis," *American Journal of Respiratory Cell and Molecular Biology*, vol. 45, no. 2, pp. 287–294, 2011.

[41] W. Qin, A. C. K. Chung, X. R. Huang et al., "TGF-β/Smad3 signaling promotes renal fibrosis by inhibiting miR-29," *Journal of the American Society of Nephrology*, vol. 22, no. 8, pp. 1462–1474, 2011.

[42] A.-C. Poncelet and H. W. Schnaper, "Sp1 and smad proteins cooperate to mediate transforming growth factor-beta 1-induced alpha 2(i) collagen expression in human glomerular mesangial cells," *The Journal of Biological Chemistry*, vol. 276, no. 10, pp. 6983–6992, 2001.

[43] S. Liu, L.-C. Wu, J. Pang et al., "Sp1/NFκB/HDAC/*miR-29b* regulatory network in KIT-driven myeloid leukemia," *Cancer Cell*, vol. 17, no. 4, pp. 333–347, 2010.

[44] B. Wang, P. Koh, C. Winbanks et al., "miR-200a prevents renal fibrogenesis through repression of TGF-β2 expression," *Diabetes*, vol. 60, no. 1, pp. 280–287, 2011.

[45] S. Yang, S. Banerjee, A. de Freitas et al., "Participation of miR-200 in pulmonary fibrosis," *The American Journal of Pathology*, vol. 180, no. 2, pp. 484–493, 2012.

[46] J. Y. Z. Li, T. Y. Yong, M. Z. Michael, and J. M. Gleadle, "Review: the role of microRNAs in kidney disease," *Nephrology*, vol. 15, no. 6, pp. 599–608, 2010.

[47] M. Lambie, J. Chess, K. L. Donovan et al., "Independent effects of systemic and peritoneal inflammation on peritoneal dialysis survival," *Journal of the American Society of Nephrology*, vol. 24, no. 12, pp. 2071–2080, 2013.

[48] D. W. Johnson, M. Clarke, V. Wilson, F. Woods, and F. G. Brown, "Rationale and design of the balANZ trial: a randomised controlled trial of low GDP, neutral pH versus standard peritoneal dialysis solution for the preservation of residual renal function," *BMC Nephrology*, vol. 11, no. 1, article 25, 2010.

[49] A. Kozomara and S. Griffiths-Jones, "miRBase: annotating high confidence microRNAs using deep sequencing data," *Nucleic Acids Research*, vol. 42, no. 1, pp. D68–D73, 2014.

[50] J. A. Weber, D. H. Baxter, S. Zhang et al., "The microRNA spectrum in 12 body fluids," *Clinical Chemistry*, vol. 56, no. 11, pp. 1733–1741, 2010.

[51] Biomarkers Definitions Working Group, "Biomarkers and surrogate endpoints: preferred definitions and conceptual framework," *Clinical Pharmacology and Therapeutics*, vol. 69, no. 3, pp. 89–95, 2001.

[52] J. K. Aronson, "Biomarkers and surrogate endpoints," *British Journal of Clinical Pharmacology*, vol. 59, no. 5, pp. 491–494, 2005.

[53] C. Sturgeon, R. Hill, G. L. Hortin, and D. Thompson, "Taking a new biomarker into routine use—a perspective from the routine clinical biochemistry laboratory," *Proteomics—Clinical Applications*, vol. 4, no. 12, pp. 892–903, 2010.

[54] J. D. Williams, K. J. Craig, N. Topley et al., "Morphologic changes in the peritoneal membrane of patients with renal disease," *Journal of the American Society of Nephrology*, vol. 13, no. 2, pp. 470–479, 2002.

[55] S. J. Davies, L. Phillips, A. M. Griffiths, L. H. Russell, P. F. Naish, and G. I. Russell, "What really happens to people on long-term peritoneal dialysis?" *Kidney International*, vol. 54, no. 6, pp. 2207–2217, 1998.

[56] C. E. Visser, J. J. E. Brouwer-Steenbergen, M. G. H. Betjes, G. C. M. Koomen, R. H. J. Beelen, and R. T. Krediet, "Cancer antigen 125: a bulk marker for the mesothelial mass in stable peritoneal dialysis patients," *Nephrology Dialysis Transplantation*, vol. 10, no. 1, pp. 64–69, 1995.

[57] M. M. Ho-Dac-Pannekeet, J. K. Hiralall, D. G. Struijk, and R. T. Krediet, "Longitudinal follow-up of CA125 in peritoneal effluent," *Kidney International*, vol. 51, no. 3, pp. 888–893, 1997.

[58] D. Lopes Barreto and R. T. Krediet, "Current status and practical use of effluent biomarkers in peritoneal dialysis patients," *The American Journal of Kidney Diseases*, vol. 62, no. 4, pp. 823–833, 2013.

[59] K. N. Lai, K. B. Lai, C. C. Szeto et al., "Dialysate cell population and cancer antigen 125 in stable continuous ambulatory peritoneal dialysis patients: their relationship with transport parameters," *American Journal of Kidney Diseases*, vol. 29, no. 5, pp. 699–705, 1997.

[60] A. Bręborowicz, M. Bręborowicz, M. Pyda, A. Połubinska, and D. Oreopoulos, "Limitations of CA125 as an index of peritoneal mesothelial cell mass," *Nephron. Clinical Practice*, vol. 100, no. 2, pp. c46–c51, 2005.

[61] S. A. Jones, D. J. Fraser, C. A. Fielding, and G. W. Jones, "Interleukin-6 in renal disease and therapy," *Nephrology, Dialysis, Transplantation*, vol. 30, no. 4, pp. 564–574, 2015.

[62] Y. Cho, D. W. Johnson, D. A. Vesey et al., "Dialysate interleukin-6 predicts increasing peritoneal solute transport rate in incident peritoneal dialysis patients," *BMC Nephrology*, vol. 15, article 8, 2014.

[63] D. Lopes Barreto, A. M. Coester, M. Noordzij et al., "Variability of effluent cancer antigen 125 and interleukin-6 determination in peritoneal dialysis patients," *Nephrology, Dialysis, Transplantation*, vol. 26, pp. 3739–3744, 2011.

[64] N. Kosaka, H. Iguchi, and T. Ochiya, "Circulating microRNA in body fluid: a new potential biomarker for cancer diagnosis and prognosis," *Cancer Science*, vol. 101, no. 10, pp. 2087–2092, 2010.

[65] Y. Liang, D. Ridzon, L. Wong, and C. Chen, "Characterization of microRNA expression profiles in normal human tissues," *BMC Genomics*, vol. 8, article 166, 2007.

[66] J. M. Lorenzen, R. Kumarswamy, S. Dangwal, and T. Thum, "microRNAs in diabetes and diabetes-associated complications," *RNA Biology*, vol. 9, no. 6, pp. 820–827, 2012.

[67] K. M. Akat, D. Moore-McGriff, P. Morozov et al., "Comparative RNA-sequencing analysis of myocardial and circulating small RNAs in human heart failure and their utility as biomarkers," *Proceedings of the National Academy of Sciences of the United States of America*, vol. 111, no. 30, pp. 11151–11156, 2014.

[68] G. Di Leva, M. Garofalo, and C. M. Croce, "MicroRNAs in cancer," *Annual Review of Pathology*, vol. 9, pp. 287–314, 2014.

Hindawi Publishing Corporation
BioMed Research International
Volume 2015, Article ID 134708, 7 pages
http://dx.doi.org/10.1155/2015/134708

Review Article

New Developments in Peritoneal Fibroblast Biology: Implications for Inflammation and Fibrosis in Peritoneal Dialysis

Janusz Witowski,[1,2] Edyta Kawka,[1,2] Andras Rudolf,[1] and Achim Jörres[2]

[1]*Department of Pathophysiology, Poznan University of Medical Sciences, Medical Biology Centre, Rokietnicka 8, 60-806 Poznan, Poland*
[2]*Department of Nephrology and Medical Intensive Care, Charité-Universitätsmedizin Berlin, Campus Virchow-Klinikum, Augustenburger Platz 1, 13353 Berlin, Germany*

Correspondence should be addressed to Janusz Witowski; jwitow@ump.edu.pl

Received 22 June 2015; Revised 11 August 2015; Accepted 25 August 2015

Academic Editor: Gang Liu

Uraemia and long-term peritoneal dialysis (PD) can lead to fibrotic thickening of the peritoneal membrane, which may limit its dialytic function. Peritoneal fibrosis is associated with the appearance of myofibroblasts and expansion of extracellular matrix. The extent of contribution of resident peritoneal fibroblasts to these changes is a matter of debate. Recent studies point to a significant heterogeneity and complexity of the peritoneal fibroblast population. Here, we review recent developments in peritoneal fibroblast biology and summarize the current knowledge on the involvement of peritoneal fibroblasts in peritoneal inflammation and fibrosis.

1. Introduction

Fibroblasts are the commonest connective tissue cells and the main source of extracellular matrix. Until recently, fibroblasts have been viewed as cells providing only structural framework for tissues. Now it is clear that fibroblasts are at the center of tissue homeostasis and serve specialized functions in different organs. Impressive versatility of fibroblasts is reflected by differences in gene expression patterns according to anatomic location [1]. Moreover, even the same tissue can be populated with several fibroblast subsets with distinct functions [2]. The phenotype of fibroblasts may change further during wound healing or fibrosis, when cells become activated and termed "myofibroblasts." When analyzing fibroblasts, it is therefore essential to take the exact physiological and clinical context into account. Here, we review new developments in our understanding of the role of fibroblasts in the peritoneum, especially their involvement in peritoneal dialysis- (PD-) associated fibrosis.

2. Fibroblast Identity and Phenotype

Normal resident tissue fibroblasts are identified by their spindle-shape appearance and location within the connective tissue. They may also express fibroblast-specific protein-1 (FSP-1), but not molecular markers for other cell types. In response to tissue injury and stimulation with growth factors (e.g., TGF-β), fibroblasts can adopt an activated phenotype resembling that of smooth muscle cells and characterized by the expression of smooth muscle actin (α-SMA). The resulting myofibroblasts have increased contractile capacity and show increased proliferation and motility. They produce more extracellular matrix (ECM) components and more regulators of the ECM turnover. The origin of myofibroblasts in different tissues (including the peritoneum) is a matter of intensive research and some controversy. Classically, myofibroblasts were thought to derive from resident tissue fibroblasts. However, there are other potential precursors of myofibroblasts, including epithelial, mesothelial, and endothelial cells, as well as bone marrow-derived fibrocytes.

Introduction of new fibroblast biomarkers and great advances in lineage tracing techniques allowed us to better define the contribution of these cells to adverse tissue remodeling.

The analysis of peritoneal membrane biopsies from patients treated with PD has clearly demonstrated that the thickness of the submesothelial compact zone, a layer of mature fibrous tissue containing collagen and elastin fibers, progressively increases with duration of PD [3]. This is particularly evident in the parietal peritoneum [4]. Thickening of the peritoneum reflects the expansion of ECM, which is deposited primarily by myofibroblasts. To determine the origin of myofibroblasts, it is necessary to identify first resident fibroblasts and mesothelial cells. This has not always been an easy task, either in vivo or in culture (see [5] for a review). Mesothelial cells display typically an epithelial-like appearance and form a monolayer covering the peritoneal surface, while fibroblasts are fusiform cells embedded in the submesothelial interstitium. In the course of mesenchymal transition, however, mesothelial cells acquire a fibroblast-like phenotype, become motile, and invade the underlying stroma. Moreover, both fibroblasts and mesothelial arise from the mesoderm and can share rather than differ in certain biomarkers, for example, vimentin. Therefore, the identification of FSP-1, a calcium-binding protein of the S100 family, as providing better specificity for fibroblasts [6, 7] was viewed as a great step forward in tracking fibroblasts. However, the validity of FSP-1 as the specific fibroblast marker has been questioned. It turned out that FSP-1 might be absent in a proportion of normal interstitial fibroblasts and some FSP-1-positive cells in diseased tissues might be, in fact, mononuclear or endothelial cells [8]. Despite these uncertainties, FSP-1 in combination with other biomarkers is still used in studies on the origin of peritoneal myofibroblasts [9, 10]. In cell culture, antibodies against FSP-1 can help purify peritoneal fibroblasts from contaminating mesothelial cells [11] (Figure 1).

3. Fibroblast Subsets

In addition to FSP-1, further fibroblast subsets can be identified using other criteria. Thy-1 (CD90), a glycophosphatidylinositol-linked outer cell membrane protein, is expressed by many cell types, but it can separate fibroblasts into Thy-1^+ and Thy-1^- subpopulations with different phenotypic and functional features [12–15]. The significance of this trait may differ according to the origin of fibroblasts. Normal lung fibroblasts, both in mice and in humans, are predominantly Thy-1-positive and their presence appears to limit pulmonary fibrosis [15–18]. It has been demonstrated that the absence of Thy-1 on lung fibroblasts is associated with their myofibroblastic phenotype and enhanced proliferative response to fibrogenic stimuli. Mice deficient in Thy-1 show exaggerated fibrosis and myofibroblastic differentiation after bleomycin-induced pulmonary injury. In humans with idiopathic pulmonary fibrosis, no Thy-1 staining was seen in fibroblastic foci. These results suggest that the loss of lung fibroblast Thy-1 expression after injury promotes enhanced fibrogenesis. In contrast to lung fibroblasts, however, the myofibroblastic conversion of orbital and myometrial fibroblasts in response to TGF-β appears to be favored by the presence rather than the absence of Thy-1 [12].

Little is known about the role of Thy-1 in peritoneal cells. A small population of Thy-1^+ ($CD90^+$) mesothelial-like cells has recently been detected in ascites drained from patients with gastrointestinal cancers [19]. These cells were defined as mesenchymal stem cells and showed a distinct myofibroblastic phenotype after stimulation with TGF-β. We have examined Thy-1 expression patterns in apparently normal human peritoneal fibroblasts (HPFB) in culture. Indeed, it appears that both Thy-1^+ and Thy-1^- subsets of HPFB exist in the peritoneum and differ in morphology and the ability to acquire a myofibroblastic phenotype (Kawka E. et al., personal observations).

4. Resident Peritoneal Fibroblasts

Fibroblasts of the normal peritoneum are scattered in the submesothelial connective tissue. Electron microscopy shows large multipolar cells embedded between collagen and elastic fibers [20]. These cells express neither myofibroblastic nor mesothelial markers [21]. Also, the expression of FSP-1 is not evident [9, 22] (Kawka E. et al., personal observations), which adds to the reservations about FSP-1 marking resident fibroblasts in the normal peritoneum [8]. On the other hand, the cells may bear platelet-derived growth factor receptor-β (PDGFRβ, CD140b) [23], which is sometimes used as a marker of resident fibroblasts. However, PDGFRβ is also expressed by pericytes and the exact relationship between pericytes and perivascular fibroblasts is not clear [24].

The cells identified as submesothelial fibroblasts occasionally express hematopoietic cell surface marker CD34 [21], which may indicate that they are derived from blood-borne fibrocytes. But they do not usually express other fibrocyte markers (CD45, CD11b, and MHC class II), suggesting that they are rather primal mesenchymal cells [25] residing in the peritoneum.

The thickness of the submesothelial compact zone in uremic patients is already increased before the commencement of dialysis, pointing to a detrimental impact of uraemia itself [3, 26]. Nevertheless, the phenotype of resident fibroblasts and their biomarker expression patterns do not seem to be altered significantly [21]. PD exposure leads to further thickening of the compact zone and distinct changes in peritoneal fibroblasts. The presence of FSP-1 expression becomes evident [9, 10], although it is not clear whether this comes from resident fibroblasts or other cell types transitioning into fibroblasts (see below). Soon after the initiation of PD many fibroblasts acquire a myofibroblastic phenotype as evidenced by α-SMA expression [21, 27, 28]. They often form clusters and localize immediately beneath the mesothelial surface. They may also lose CD34 expression and show cytokeratin and E-cadherin expression instead [21]. The significance of CD34 loss is unclear, although it has been observed in fibrotic lesions in other tissues [29]. On the other hand, the expression of cytokeratin and E-cadherin by myofibroblasts is viewed as an indication of their origin from mesothelial cells [30].

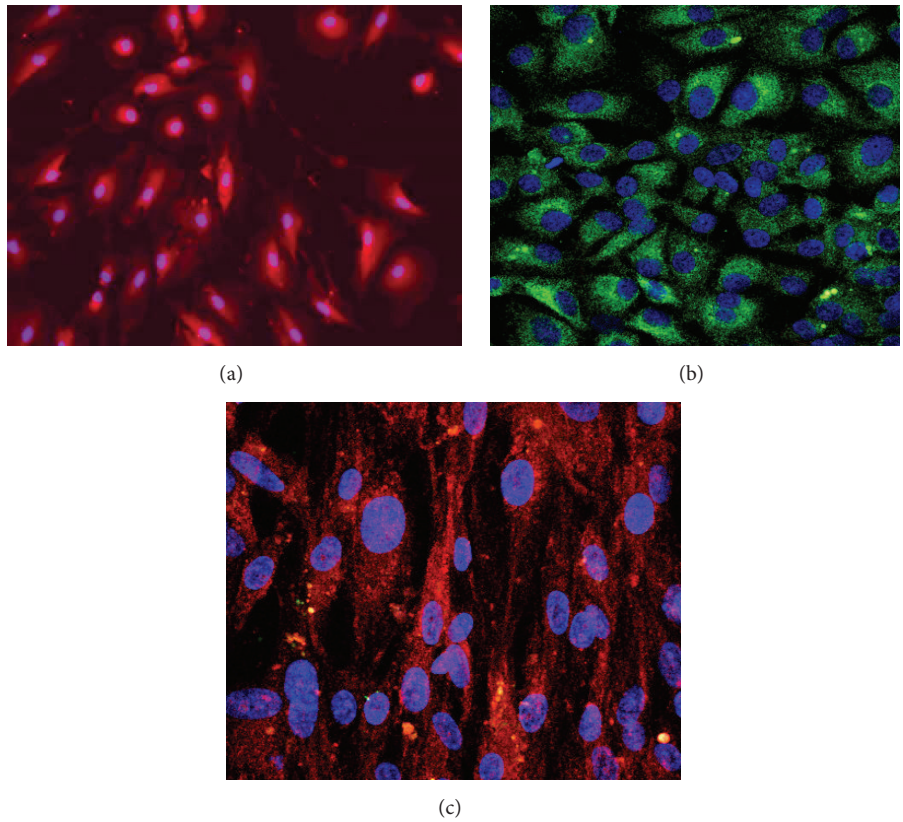

Figure 1: Expression of FSP-1 by human peritoneal fibroblasts and mesothelial cells. Human peritoneal mesothelial cells and peritoneal resident fibroblasts were isolated from apparently normal omentum by enzymatic digestion, as described [5]. Populations of mesothelial cells and fibroblasts were immunostained for FSP-1 (red) and cytokeratin (green). Nuclei were counterstained with DAPI (blue). Magnification 200x. (a) Human peritoneal fibroblasts express FSP-1 but not cytokeratin. (b) Human peritoneal mesothelial cells express cytokeratin but not FSP-1. (c) Stimulation of mesothelial cells with TGF-β1 (1 ng/mL; 72 hours) leads to mesenchymal transition that is associated with loss of cytokeratin expression and de novo FSP-1 expression.

5. Epithelial-to-Mesenchymal Transition as a Source of Peritoneal Fibroblasts

The concept of peritoneal myofibroblasts arising from the mesothelium through epithelial-to-mesenchymal transition (EMT) received a lot of attention over the past decade (see [25, 31–33] for excellent reviews). It appears that in the course of PD mesothelial cells upregulate transcription factors of the snail, ZEB, and Twist families, which control molecular reprogramming of EMT [34]. The whole process can be induced by a number of growth factors, including transforming growth factor-β (TGF-β), which has been identified as a key mediator of mesothelial EMT both in vitro [35] (Figure 1) and in vivo [36]. TGF-β exerts its effects by engaging various members of the family of mitogen-activated protein kinases (MAPKs), including TGF-β-activated kinase-1 (TAK-1) [37], p38 [38], and JNK kinase [39]. Inhibition of MAPK phosphorylation with glucocorticoids can block TGF-β-induced EMT of mesothelial cells in culture [40]. In addition to MAPKs, the involvement of the nuclear transcription factor-κB (NF-κB) in mesothelial cell transition has been postulated [41]. In vivo, adenovirus-mediated overexpression of TGF-β in the rat peritoneum results in the upregulation of several genes involved in EMT (snail, collagen 1, and α-SMA) [36]. In this setting the cytokeratin/α-SMA double-positive cells appear first in the mesothelial monolayer and later in the reorganized submesothelial matrix [36]. These effects are mediated by both SMAD3-dependent and SMAD3-independent mechanisms [42]. The fibroblast-like phenotype of mesothelial cells isolated from PD patients or treated in vitro with TGF-β could be reversed by bone morphogenic protein-7 (BMP-7) [43] or by TAK-1 inhibitors [37]. Of particular interest in the context of PD is the observation that exposure of mesothelial cells in vitro to high glucose can induce Twist, a key EMT-controlling transcription factor [44], and increase the expression of α-SMA [45]. These effects could be related to upregulation of TGF-β by high glucose [46], but they can also be attributed to decreased expression of BMP-7 [45] or heme oxygenase-1 (HO-1) [47]. Indeed, experimental upregulation of BMP-7 or HO-1 could partly reduce high glucose-induced EMT of mesothelial cells. In an animal model of PD, adenovirus-mediated transfection of BMP-7 was found to inhibit EMT in mesothelial cells and decrease subsequent peritoneal thickening [45].

What still remains unclear is the mechanism by which PD exposure initiates EMT. The analysis of peritoneal membrane

biopsies revealed that the loss of mesothelial cells from the peritoneal surface and the appearance of submesothelial cytokeratin staining occur relatively often and early during PD [49]. The observation that the number of fibroblast-like mesothelial cells isolated from spent dialysate effluent increases with the duration of therapy [30] points to the role of cumulative exposure to PD fluids and/or occasional episodes of peritonitis. In this respect, it has been demonstrated that key proinflammatory cytokines IL-1β and TNFα induce increased peritoneal TGF-β expression in animal models [50]. Moreover, there exists data to suggest a link between EMT and biocompatibility of PD solutions. It has been observed that PD fluids with high concentration of glucose degradation products (GDP) can induce EMT in mesothelial cells both during short-term direct exposure in culture and—to lesser extent—after chronic PD exposure in vivo [51, 52]. This finding is in line with earlier observations of EMT in the peritoneal membrane of rats treated with chronic intraperitoneal administration of GDP [53].

Loureiro and colleagues have assessed the exact contribution of various precursors to the pool of peritoneal fibroblasts that accumulate in the peritoneum of mice during chronic PD [9]. They found no FSP-1$^+$ cells in the normal peritoneum. However, such cells did appear after exposure to PD fluids and could be further characterized by dual-immunolabeling using an anti-FSP-1 antibody in conjunction with antibodies against cytokeratin, CD45, or CD31. Approximately 37% FSP-1$^+$ cells were identified as derived from mesothelial cells (FSP-1$^+$/cytokeratin$^+$), 34% from fibrocytes (FSP-1$^+$/CD45$^+$), and 5% from endothelial cells (FSP-1$^+$/CD31$^+$). The remaining 24% cells stained singly for FSP-1 and their origin was not defined. Interestingly, by using three-color immunofluorescence it has been estimated that approximately 50% of FSP-1$^+$/cytokeratin$^+$ cells coexpressed α-SMA, which pointed to their myofibroblastic phenotype. Importantly, the administration of TGF-β-blocking peptides significantly reduced the extent of PD fluid-induced peritoneal fibrosis and the number of FSP-1$^+$ cells, especially of the FSP-1$^+$/cytokeratin$^+$ subpopulation. More recently, the same group have demonstrated that TGF-β can be also involved in mesenchymal transition of mesothelial cells induced by endothelin-1 [54]. These data support the concept that peritoneal fibrosis in PD is largely related to TGF-β-driven conversion of mesothelial cells into myofibroblasts.

The potential of mesothelial cells to undergo EMT and to contribute to other cell lineages has been well documented during development. In particular, it has been demonstrated that the pleural mesothelium is a source of peribronchiolar fibroblasts in the foetal lung and that the process of mesothelial cell migration into the lung parenchyma is controlled by the hedgehog signaling pathway [55]. Moreover, it appears that such a process may also occur in adult tissues. In this respect, mesothelial cells covering the liver were found to differentiate into hepatic myofibroblasts during liver injury and fibrosis [56]. Similarly, EMT in pleural mesothelial cells was found to be contributing to idiopathic pulmonary fibrosis [57]. Interestingly, several of the above studies employed the Cre recombinase technology to trace the fate of mesothelial cells that expressed the Wilms tumor-1 (Wt-1) transcription factor as a biomarker. Genetic mapping of Wt-1$^+$ cells has also been used recently by Chen and colleagues to identify the cellular origin of myofibroblasts during peritoneal fibrosis [58]. The results of their study posed a challenge to the relevance of mesothelial cells as a source of peritoneal myofibroblasts. In contrast to earlier studies, they have observed that these were submesothelial resident fibroblasts rather than mesothelial cells that gave rise to collagen-producing myofibroblasts after injury induced by sodium hypochlorite (and to lesser extent by PD solutions or by adenovirus-mediated TGF-β1 overexpression). Resident fibroblasts were defined as cytokeratin$^-$, vimentin$^+$, and PDGFβ^+ cells located beneath mesothelial cell basement membrane. Interestingly, the use of PDGFR inhibitor after injury significantly attenuated the accumulation of αSMA$^+$ myofibroblasts and peritoneal fibrosis. Obviously, the results of this study will need to be independently confirmed, given the limitations of current lineage tracing techniques. As correctly pointed out in a recent review [32], these technical shortcomings do not permit the possibility of mesothelial cell transition in vivo to be ruled out entirely. Moreover, mesothelial cells may still contribute to peritoneal fibrosis through their capacity for producing collagen [58]. They can also act indirectly by affecting peritoneal fibroblasts in a paracrine manner. In this respect, it has been demonstrated that lysophosphatidic acid signaling through LPA_1, a G protein-coupled receptor, stimulates mesothelial cells to produce connective tissue growth factor (CTGF) that subsequently drives peritoneal fibrosis by inducing peritoneal fibroblast proliferation and collagen synthesis [59].

6. Fibroblast Involvement in Peritoneal Inflammation

Persistent tissue irritation, inflammation, and fibroblast activation are key features of fibrosis [60]. In this setting fibroblasts not only are effector cells but also contribute signals that control the function of other cell types. Peritonitis is the commonest PD-associated insult to the peritoneum, which is characterized by massive leukocyte infiltration. It is now recognized that the sequence at which different leukocyte subsets arrive in the peritoneum is controlled by a complex intraperitoneal network of chemokines [31]. These chemokines are thought to be produced primarily by mesothelial cells. However, peritoneal fibroblasts are also capable of synthesizing some chemokines and can be as potent in this respect as the mesothelium [61–63]. This activity of peritoneal fibroblasts can help recruit leukocytes during those episodes of severe peritonitis that are associated with extensive mesothelial cell damage and exfoliation [64, 65]. We have demonstrated that HPFB release chemokines MCP-1/CCL2 and IL-8/CXCL8 either constitutively or after stimulation with IL-1β and TNFα. The response to these macrophage-derived proinflammatory cytokines is mediated through transcription factors of the NF-κB family [61]. The production of neutrophil-targeting cytokines by HPFB is triggered predominantly by IL-1β [62]. We have demonstrated that it stimulates the secretion of CXCL1 and CXCL8, classic chemokines for neutrophils, but also of granulocyte

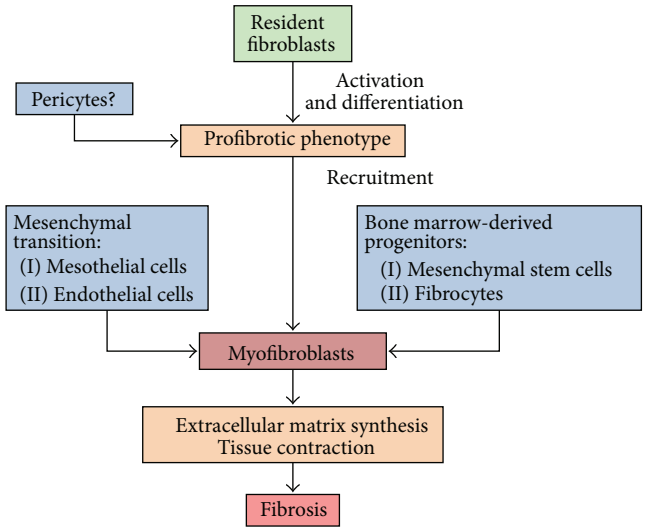

Figure 2: Potential myofibroblast precursors contributing to peritoneal fibrosis in PD. In response to peritoneal irritation or injury, myofibroblasts accumulate in the peritoneum as a result of (i) resident peritoneal fibroblasts activation and proliferation; (ii) transformation of local pericytes; (iii) proliferation and infiltration by resident and circulating fibrocytes; (iv) differentiation of local mesenchymal stem cells; (v) dedifferentiation and mesenchymal transition of peritoneal mesothelial cells; and (vi) dedifferentiation and mesenchymal transition of endothelial cells (adapted from [32, 48]).

colony-stimulating factor (G-CSF) that mobilizes neutrophils from the bone marrow and promotes their survival. On the other hand, we have demonstrated that HPFB can also produce CCL5, a strong chemoattractant for mononuclear leukocytes [63]. The process is critically controlled by IFN-γ, which does not stimulate CCL5 itself but synergistically amplifies the effect of TNFα. Moreover, by inducing CD40 expression it allows HPFB to synthesize CCL5 in response to CD40 ligand (CD40L) present primarily on T cells.

HPFB can also generate chemokines in response to high glucose exposure. It has recently been observed that the incubation of HPFB with glucose led to a dose-dependent increase in CCL2 mRNA expression [66]. It was preceded by a short-lived increase in the expression of the osmosensitive transcription factor, nuclear factor of activated T cells 5 (NFAT5). However, it is uncertain whether this glucose-induced increase in CCL2 mRNA is mediated by NFAT5. The analysis of peritoneal biopsies revealed no difference in the expression of NFAT5 but still increased expression of CCL2 in the peritoneum of patients undergoing PD compared to those with uraemia but not requiring dialysis.

Taken together, all these observations are in line with the concept of resident tissue fibroblasts acting as sentinel cells that control inflammatory response to tissue injury or infection [67]. In this respect, HPFB can add significantly to transperitoneal chemotactic gradients during peritonitis.

7. Conclusions

Increasing data suggests that collagen-producing myofibroblasts that accumulate in the peritoneum in the course of PD are derived from various precursors (Figure 2). The exact contribution of these cellular sources remains to be established. Of those, resident peritoneal fibroblasts still need to be considered as important predecessors of myofibroblasts. However, given unique immune environment of the peritoneal cavity, site-specific variation in fibroblast transcriptional profiles, and internal heterogeneity, it is essential to better understand the basics of peritoneal fibroblast biology. This is the prerequisite for interventional therapies targeting PD-associated peritoneal fibrosis.

Conflict of Interests

The authors declare that there is no conflict of interests regarding the publication of this paper.

References

[1] J. L. Rinn, C. Bondre, H. B. Gladstone, P. O. Brown, and H. Y. Chang, "Anatomic demarcation by positional variation in fibroblast gene expression programs," *PLoS Genetics*, vol. 2, no. 7, article e119, 2006.

[2] R. R. Driskell and F. M. Watt, "Understanding fibroblast heterogeneity in the skin," *Trends in Cell Biology*, vol. 25, no. 2, pp. 92–99, 2015.

[3] J. D. Williams, K. J. Craig, N. Topley et al., "Morphologic changes in the peritoneal membrane of patients with renal disease," *Journal of the American Society of Nephrology*, vol. 13, no. 2, pp. 470–479, 2002.

[4] J. D. Williams, K. J. Craig, C. Von Ruhland, N. Topley, and G. T. Williams, "The natural course of peritoneal membrane biology during peritoneal dialysis," *Kidney International, Supplement*, vol. 64, no. 88, pp. S43–S49, 2003.

[5] J. Witowski and A. Jörres, "Peritoneal cell culture: fibroblasts," *Peritoneal Dialysis International*, vol. 26, no. 3, pp. 292–299, 2006.

[6] F. Strutz, H. Okada, C. W. Lo et al., "Identification and characterization of a fibroblast marker: FSP1," *Journal of Cell Biology*, vol. 130, no. 2, pp. 393–405, 1995.

[7] R. Kalluri and E. G. Neilson, "Epithelial-mesenchymal transition and its implications for fibrosis," *The Journal of Clinical Investigation*, vol. 112, no. 12, pp. 1776–1784, 2003.

[8] M. Le Hir, I. Hegyi, D. Cueni-Loffing, J. Loffing, and B. Kaissling, "Characterization of renal interstitial fibroblast-specific protein 1/S100A4-positive cells in healthy and inflamed rodent kidneys," *Histochemistry and Cell Biology*, vol. 123, no. 4-5, pp. 335–346, 2005.

[9] J. Loureiro, A. Aguilera, R. Selgas et al., "Blocking TGF-β1 protects the peritoneal membrane from dialysate-induced damage," *Journal of the American Society of Nephrology*, vol. 22, no. 9, pp. 1682–1695, 2011.

[10] J. Loureiro, M. Schilte, A. Aguilera et al., "BMP-7 blocks mesenchymal conversion of mesothelial cells and prevents peritoneal damage induced by dialysis fluid exposure," *Nephrology Dialysis Transplantation*, vol. 25, no. 4, pp. 1098–1108, 2010.

[11] R. Catar, J. Witowski, P. Wagner et al., "The proto-oncogene C-Fos transcriptionally regulates VEGF production during peritoneal inflammation," *Kidney International*, vol. 84, no. 6, pp. 1119–1128, 2013.

[12] L. Koumas, T. J. Smith, S. Feldon, N. Blumberg, and R. P. Phipps, "Thy-1 expression in human fibroblast subsets defines myofibroblastic or lipofibroblastic phenotypes," *American Journal of Pathology*, vol. 163, no. 4, pp. 1291–1300, 2003.

[13] L. Koumas and R. P. Phipps, "Differential COX localization and PG release in Thy-1^+ and Thy-1^- human female reproductive tract fibroblasts," *The American Journal of Physiology: Cell Physiology*, vol. 283, no. 2, pp. C599–C608, 2002.

[14] T. J. Smith, L. Koumas, A. Gagnon et al., "Orbital fibroblast heterogeneity may determine the clinical presentation of thyroid-associated ophthalmopathy," *Journal of Clinical Endocrinology and Metabolism*, vol. 87, no. 1, pp. 385–392, 2002.

[15] Y. Zhou, J. S. Hagood, and J. E. Murphy-Ullrich, "Thy-1 expression regulates the ability of rat lung fibroblasts to activate transforming growth factor-beta in response to fibrogenic stimuli," *American Journal of Pathology*, vol. 165, no. 2, pp. 659–669, 2004.

[16] Y. Y. Sanders, P. Kumbla, and J. S. Hagood, "Enhanced myofibroblastic differentiation and survival in thy-1(−) lung fibroblasts," *American Journal of Respiratory Cell and Molecular Biology*, vol. 36, no. 2, pp. 226–235, 2007.

[17] G. Ramírez, J. S. Hagood, Y. Sanders et al., "Absence of Thy-1 results in TGF-β induced MMP-9 expression and confers a profibrotic phenotype to human lung fibroblasts," *Laboratory Investigation*, vol. 91, no. 8, pp. 1206–1218, 2011.

[18] J. S. Hagood, P. Prabhakaran, P. Kumbla et al., "Loss of fibroblast Thy-1 expression correlates with lung fibrogenesis," *American Journal of Pathology*, vol. 167, no. 2, pp. 365–379, 2005.

[19] J. Kitayama, S. Emoto, H. Yamaguchi, H. Ishigami, and T. Watanabe, "CD90(+) mesothelial-like cells in peritoneal fluid promote peritoneal metastasis by forming a tumor permissive microenvironment," *PLoS ONE*, vol. 9, no. 1, Article ID e86516, 2014.

[20] N. Jovanović, S. Zunić-Bozinovski, D. Trpinac et al., "Ultrastructural changes of the peritoneum in a rabbit model of peritoneal dialysis," *Vojnosanitetski Pregled*, vol. 70, no. 11, pp. 1023–1028, 2013.

[21] J. A. Jiménez-Heffernan, A. Aguilera, L. S. Aroeira et al., "Immunohistochemical characterization of fibroblast subpopulations in normal peritoneal tissue and in peritoneal dialysis-induced fibrosis," *Virchows Archiv*, vol. 444, no. 3, pp. 247–256, 2004.

[22] J. Loureiro, P. Sandoval, G. del Peso et al., "Tamoxifen ameliorates peritoneal membrane damage by blocking mesothelial to mesenchymal transition in peritoneal dialysis," *PLoS ONE*, vol. 8, no. 4, Article ID e61165, 2013.

[23] H. Seeger, N. Braun, J. Latus et al., "Platelet-derived growth factor receptor-beta expression in human peritoneum," *Nephron Clinical Practice*, vol. 128, no. 1-2, pp. 178–184, 2014.

[24] M. Mack and M. Yanagita, "Origin of myofibroblasts and cellular events triggering fibrosis," *Kidney International*, vol. 87, pp. 297–307, 2015.

[25] L. S. Aroeira, A. Aguilera, J. A. Sánchez-Tomero et al., "Epithelial to mesenchymal transition and peritoneal membrane failure in peritoneal dialysis patients: pathologic significance and potential therapeutic interventions," *Journal of the American Society of Nephrology*, vol. 18, no. 7, pp. 2004–2013, 2007.

[26] K. Honda, C. Hamada, M. Nakayama et al., "Impact of uremia, diabetes, and peritoneal dialysis itself on the pathogenesis of peritoneal sclerosis: a quantitative study of peritoneal membrane morphology," *Clinical Journal of the American Society of Nephrology*, vol. 3, no. 3, pp. 720–728, 2008.

[27] K. Shioshita, M. Miyazaki, Y. Ozono et al., "Expression of heat shock proteins 47 and 70 in the peritoneum of patients on continuous ambulatory peritoneal dialysis," *Kidney International*, vol. 57, no. 2, pp. 619–631, 2000.

[28] M. A. M. Mateijsen, A. C. van der Wal, P. M. E. M. Hendriks et al., "Vascular and interstitial changes in the peritoneum of CAPD patients with peritoneal sclerosis," *Peritoneal Dialysis International*, vol. 19, no. 6, pp. 517–525, 1999.

[29] L. Díaz-Flores, R. Gutiérrez, M. P. García et al., "$CD34^+$ stromal cells/fibroblasts/fibrocytes/telocytes as a tissue reserve and a principal source of mesenchymal cells. Location, morphology, function and role in pathology," *Histology and Histopathology*, vol. 29, no. 7, pp. 831–870, 2014.

[30] M. Yáñez-Mó, E. Lara-Pezzi, R. Selgas et al., "Peritoneal dialysis and epithelial-to-mesenchymal transition of mesothelial cells," *The New England Journal of Medicine*, vol. 348, no. 5, pp. 403–413, 2003.

[31] O. Devuyst, P. J. Margetts, and N. Topley, "The pathophysiology of the peritoneal membrane," *Journal of the American Society of Nephrology*, vol. 21, no. 7, pp. 1077–1085, 2010.

[32] Y. Liu, Z. Dong, H. Liu, J. Zhu, F. Liu, and G. Chen, "Transition of mesothelial cell to fibroblast in peritoneal dialysis: EMT, stem cell or bystander?" *Peritoneal Dialysis International*, vol. 35, no. 1, pp. 14–25, 2015.

[33] S. E. Mutsaers, K. Birnie, S. Lansley, S. E. Herrick, C. Lim, and C. M. Prele, "Mesothelial cells in tissue repair and fibrosis," *Frontiers in Pharmacology*, vol. 6, article 113, 2015.

[34] E. Sánchez-Tilló, Y. Liu, O. de Barrios et al., "EMT-activating transcription factors in cancer: beyond EMT and tumor invasiveness," *Cellular and Molecular Life Sciences*, vol. 69, no. 20, pp. 3429–3456, 2012.

[35] A. H. Yang, J. Y. Chen, and J. K. Lin, "Myofibroblastic conversion of mesothelial cells," *Kidney International*, vol. 63, no. 4, pp. 1530–1539, 2003.

[36] P. J. Margetts, P. Bonniaud, L. Liu et al., "Transient overexpression of TGF-beta1 induces epithelial mesenchymal transition in the rodent peritoneum," *Journal of the American Society of Nephrology*, vol. 16, no. 2, pp. 425–436, 2005.

[37] R. Strippoli, I. Benedicto, M. L. P. Lozano et al., "Inhibition of transforming growth factor-activated kinase 1 (TAK1) blocks and reverses epithelial to mesenchymal transition of mesothelial cells," *PLoS ONE*, vol. 7, no. 2, Article ID e31492, 2012.

[38] R. Strippoli, I. Benedicto, M. Foronda et al., "p38 maintains E-cadherin expression by modulating TAK1-NF-κB during epithelial-to-mesenchymal transition," *Journal of Cell Science*, vol. 123, no. 24, pp. 4321–4331, 2010.

[39] Q. Liu, Y. Zhang, H. Mao et al., "A crosstalk between the Smad and JNK signaling in the TGF-β-induced epithelial-mesenchymal transition in rat peritoneal mesothelial cells," *PLoS ONE*, vol. 7, no. 2, Article ID e32009, 2012.

[40] Y.-H. Jang, H.-S. Shin, H. Sun Choi et al., "Effects of dexamethasone on the TGF-beta1-induced epithelial-to-mesenchymal transition in human peritoneal mesothelial cells," *Laboratory Investigation*, vol. 93, no. 2, pp. 194–206, 2013.

[41] R. Strippoli, I. Benedicto, M. L. P. Lozano, A. Cerezo, M. López-Cabrera, and M. A. Del Pozo, "Epithelial-to-mesenchymal transition of peritoneal mesothelial cells is regulated by an ERK/NF-kappaB/Snail1 pathway," *Disease Models and Mechanisms*, vol. 1, no. 4-5, pp. 264–274, 2008.

[42] P. Patel, Y. Sekiguchi, K.-H. Oh, S. E. Patterson, M. R. J. Kolb, and P. J. Margetts, "Smad3-dependent and -independent

pathways are involved in peritoneal membrane injury," *Kidney International*, vol. 77, no. 4, pp. 319–328, 2010.

[43] R. Vargha, M. Endemann, K. Kratochwill et al., "Ex vivo reversal of in vivo transdifferentiation in mesothelial cells grown from peritoneal dialysate effluents," *Nephrology Dialysis Transplantation*, vol. 21, no. 10, pp. 2943–2947, 2006.

[44] C. Li, Y. Ren, X. Jia et al., "Twist overexpression promoted epithelial-to-mesenchymal transition of human peritoneal mesothelial cells under high glucose," *Nephrology Dialysis Transplantation*, vol. 27, no. 11, pp. 4119–4124, 2012.

[45] M.-A. Yu, K.-S. Shin, J. H. Kim et al., "HGF and BMP-7 ameliorate high glucose-induced epithelial-to-mesenchymal transition of peritoneal mesothelium," *Journal of the American Society of Nephrology*, vol. 20, no. 3, pp. 567–581, 2009.

[46] T. Y. H. Wong, A. O. Phillips, J. Witowski, and N. Topley, "Glucose-mediated induction of TGF-beta1 and MCP-1 in mesothelial cells in vitro is osmolality and polyol pathway dependent," *Kidney International*, vol. 63, no. 4, pp. 1404–1416, 2003.

[47] K. Bang, J. Jeong, J. H. Shin et al., "Heme oxygenase-1 attenuates epithelial-to-mesenchymal transition of human peritoneal mesothelial cells," *Clinical and Experimental Nephrology*, vol. 17, no. 2, pp. 284–293, 2013.

[48] D. J. Abraham, B. Eckes, V. Rajkumar, and T. Krieg, "New developments in fibroblast and myofibroblast biology: implications for fibrosis and scleroderma," *Current Rheumatology Reports*, vol. 9, no. 2, pp. 136–143, 2007.

[49] G. del Peso, J. A. Jimenez-Heffernan, M. A. Bajo et al., "Epithelial-to-mesenchymal transition of mesothelial cells is an early event during peritoneal dialysis and is associated with high peritoneal transport," *Kidney International Supplements*, vol. 73, no. 108, pp. S26–S33, 2008.

[50] P. J. Margetts, M. Kolb, L. Yu et al., "Inflammatory cytokines, angiogenesis, and fibrosis in the rat peritoneum," *The American Journal of Pathology*, vol. 160, no. 6, pp. 2285–2294, 2002.

[51] M. A. Bajo, M. L. Príez-Lozano, P. Albar-Vizcaino et al., "Low-GDP peritoneal dialysis fluid ('balance') has less impact in vitro and ex vivo on epithelial-to-mesenchymal transition (EMT) of mesothelial cells than a standard fluid," *Nephrology Dialysis Transplantation*, vol. 26, no. 1, pp. 282–291, 2011.

[52] A. Fernández-Perpén, M. L. Pérez-Lozano, M.-A. Bajo et al., "Influence of bicarbonate/low-GDP peritoneal dialysis fluid (Bicavera) on *in vitro* and *ex vivo* epithelial-to-mesenchymal transition of mesothelial cells," *Peritoneal Dialysis International*, vol. 32, no. 3, pp. 292–304, 2012.

[53] I. Hirahara, Y. Ishibashi, S. Kaname, E. Kusano, and T. Fujita, "Methylglyoxal induces peritoneal thickening by mesenchymal-like mesothelial cells in rats," *Nephrology Dialysis Transplantation*, vol. 24, no. 2, pp. 437–447, 2009.

[54] O. Busnadiego, J. Loureiro-Alvarez, P. Sandoval et al., "A pathogenetic role for endothelin-1 in peritoneal dialysis-associated fibrosis," *Journal of the American Society of Nephrology*, vol. 26, no. 1, pp. 173–182, 2015.

[55] R. Dixit, X. Ai, and A. Fine, "Derivation of lung mesenchymal lineages from the fetal mesothelium requires hedgehog signaling for mesothelial cell entry," *Development*, vol. 140, no. 21, pp. 4398–4406, 2013.

[56] Y. Li, J. Wang, and K. Asahina, "Mesothelial cells give rise to hepatic stellate cells and myofibroblasts via mesothelial-mesenchymal transition in liver injury," *Proceedings of the National Academy of Sciences of the United States of America*, vol. 110, no. 6, pp. 2324–2329, 2013.

[57] S. Karki, R. Surolia, T. D. Hock et al., "Wilms' tumor 1 (Wt1) regulates pleural mesothelial cell plasticity and transition into myofibroblasts in idiopathic pulmonary fibrosis," *The FASEB Journal*, vol. 28, no. 3, pp. 1122–1131, 2014.

[58] Y.-T. Chen, Y.-T. Chang, S.-Y. Pan et al., "Lineage tracing reveals distinctive fates for mesothelial cells and submesothelial fibroblasts during peritoneal injury," *Journal of the American Society of Nephrology*, vol. 25, no. 12, pp. 2847–2858, 2014.

[59] N. Sakai, J. Chun, J. S. Duffield, T. Wada, A. D. Luster, and A. M. Tager, "LPA1-induced cytoskeleton reorganization drives fibrosis through CTGF-dependent fibroblast proliferation," *The FASEB Journal*, vol. 27, no. 5, pp. 1830–1846, 2013.

[60] T. A. Wynn and T. R. Ramalingam, "Mechanisms of fibrosis: therapeutic translation for fibrotic disease," *Nature Medicine*, vol. 18, no. 7, pp. 1028–1040, 2012.

[61] J. Witowski, A. Thiel, R. Dechend et al., "Synthesis of C-X-C and C-C chemokines by human peritoneal fibroblasts: induction by macrophage-derived cytokines," *American Journal of Pathology*, vol. 158, no. 4, pp. 1441–1450, 2001.

[62] J. Witowski, H. Tayama, K. Ksiek, M. Wanic-Kossowska, T. O. Bender, and A. Jörres, "Human peritoneal fibroblasts are a potent source of neutrophil-targeting cytokines: a key role of IL-1β stimulation," *Laboratory Investigation*, vol. 89, no. 4, pp. 414–424, 2009.

[63] E. Kawka, J. Witowski, N. Fouqet et al., "Regulation of chemokine CCL5 synthesis in human peritoneal fibroblasts: a key role of IFN-γ," *Mediators of Inflammation*, vol. 2014, Article ID 590654, 9 pages, 2014.

[64] C. Verger, A. Luger, H. L. Moore, and K. D. Nolph, "Acute changes in peritoneal morphology and transport properties with infectious peritonitis and mechanical injury," *Kidney International*, vol. 23, no. 6, pp. 823–831, 1983.

[65] B. Haslinger-Löffler, B. Wagner, M. Brück et al., "*Staphylococcus aureus* induces caspase-independent cell death in human peritoneal mesothelial cells," *Kidney International*, vol. 70, no. 6, pp. 1089–1098, 2006.

[66] D. Kitterer, J. Latus, C. Ulmer et al., "Activation of nuclear factor of activated T cells 5 in the peritoneal membrane of uremic patients," *The American Journal of Physiology—Renal Physiology*, vol. 308, no. 11, pp. F1247–F1258, 2015.

[67] R. S. Smith, T. J. Smith, T. M. Blieden, and R. P. Phipps, "Fibroblasts as sentinel cells. Synthesis of chemokines and regulation of inflammation," *The American Journal of Pathology*, vol. 151, no. 2, pp. 317–322, 1997.